

Characterisation of Some Fractured-Rock Aquifers in Limpopo Province, South Africa: Review and Case Study

**Submitted in full requirement for the degree
M.Sc. Engineering- and Environmental Geology**

To:

Department of Geology
School of Physical Sciences
Faculty of Natural and Agricultural Sciences
University of Pretoria

By:

Matthys Alois Dippenaar
Student Number 99139813

October 2008

Declaration and Acknowledgements:

I, Matthys Alois Dippenaar, student number 99139813, submit this dissertation to the Department of Geology, University of Pretoria, in accordance with the full requirements and prerequisites for the degree Masters in Sciences (M.Sc. Engineering and Environmental Geology). I declare that everything contained in this dissertation is my own work unless noted otherwise. All external sources have been referenced diligently and all credit for previously published work is acknowledged to the respective authors.

I furthermore acknowledge the following people and/or institutions:

- Dr K. T. Witthüser and the University of Pretoria (UP) for mentorship and valuable input.
- Prof J. L. van Rooy and UP for mentorship and valuable input.
- Dr. A. Bumby (UP) for his input on the structural aspects of this dissertation.
- Mr T. G. Rossouw for his help with the GIS and compilation of the maps.
- Dr S. Adams and the Water Research Commission for funding.
- The Department of Water Affairs and Forestry (DWAF) for granting me permission to use the data.
- Mr C. J. Haupt and WSM Leshika Consulting for readily sharing data and expertise gained from working on the GRIP project.
- Mr R. Weidemann and VSA Leboa Consulting for readily sharing data and expertise gained from working on the GRIP project.

Signed:



M. A. Dippenaar

06 October 2008

Date

ABSTRACT

This dissertation collates all available data from the Department of Water Affairs and Forestry's (DWAFF's) National Groundwater Database (NGDB), DWAFF's Groundwater Resource Information Project (GRIP) and tests conducted during the progress of this project in order to evaluate Basement aquifers. The project was commenced at the request of the Water Research Commission (WRC), situated in Pretoria, South Africa. The study area (Limpopo and Luvuvhu-Letaba Water Management Areas, WMA1 and WMA2 respectively) is underlain by fractured, crystalline Basement terrain. The influences of structures (i.e. joints, faults and shear zones) and the neotectonic stress conditions were also studied to address the influence on groundwater flow and occurrence. The aim of the project was to address the determination of the aquifer parameters (essentially transmissivity and sustainable yield) in Basement terrane. Pumping test data was used and analysed via the Flow Characteristic Programme (Institute for Groundwater Studies, University of Free State). The methods of Logan (1964), Theis (1935), Cooper-Jacob (1946) and Birsoy-Summers (1980) were applied for comparative purposes. Statistically, all four methods supplied results within the same order of magnitude, with Theis and Cooper-Jacob correlating extremely well. Results from the Logan and Birsoy-Summers methods correlated very well too, but the T-values calculated via Logan's method were almost double those obtained from the step-drawdown data analysed via the Birsoy-Summers method. The combined results adhered to a developed model-setting-scenario approach where each borehole can be evaluated based on three parameters. Firstly, the model refers to the potential water-bearing and/or water-barring features. In the study area, it was found that water predominates in the Hout River Shear Zone, and that the neotectonic stress fields have little influence on determining the orientation of favourable water-bearing structures. Geological contacts often resulted in higher yielding boreholes than geological structures. Secondly, the setting refers to the climatic and tectonic setting of the site. This determines the recharge and the orientation of structures. Based on this, supposedly closed structures (due to prevailing neotectonic stress fields) often supplied higher yielding boreholes than the supposedly open structures. Rainfall and climate however had little influence on the results. Finally, the scenario ranks a borehole in terms of high, intermediate or low transmissivity and subsequently potential yield. High T-values typically exceeded 100 m²/d whereas low T-values were generally below 5 m²/d. Significantly low yielding boreholes therefore formed part of the Low T Scenario, and high yielding boreholes of the High T Scenario.

CONTENTS

	Page
1. INTRODUCTION.....	1
1.1. Project Background.....	1
1.2. Objectives.....	1
1.3. Methodology.....	2
1.3.1. Acquisition.....	2
1.3.2. Analysis.....	2
1.3.3. Appraisal.....	3
2. LITERATURE REVIEW.....	4
2.1. Fracture Flow.....	4
2.1.1. The influence of fractures.....	4
2.1.2. Flow through fractures.....	8
2.1.3. Basement aquifers.....	14
2.1.4. Neotectonics and its influence on fracture flow.....	15
2.1.5. Geomorphological history and erosion cycles.....	16
2.2. Modelling Aquifers.....	16
2.3. Hydraulic Testing.....	17
2.3.1. Pumping tests.....	18
2.3.2. Diagnostic and derivative plots.....	20
2.3.3. Interpreting pumping test data.....	20
2.3.4. Problems pertaining to pumping tests.....	28
2.4. Sustainable Yield.....	30
2.5. Flow Characteristic (FC) Programme.....	31
3. CASE STUDY.....	32
3.1. Study Area.....	32
3.1.1. Limpopo Water Management Area.....	33
3.1.2. Luvuvhu-Letaba Water Management Area.....	34
3.2. Geology of the Study Area.....	35
3.3. Terrane Settings (Sub-areas).....	40
3.4. Pumping Tests.....	40
3.5. Map Compilation.....	41
4. ANALYSIS.....	42
4.1. Pumping Test Results.....	42
4.1.1. High T Scenario: H04-0306.....	42
4.1.2. Intermediate T Scenario: H10-0084.....	44
4.1.3. Low T Scenario: H07-0841.....	46

4.1.4.	Derivative and diagnostic plots.....	48
4.2.	Results	54
4.2.1.	Discussion of T-values	54
4.2.2.	Discussion of static water levels.....	56
4.2.3.	Discussion of sustainable yields.....	56
4.2.4.	Geological, structural, tectonic and geomorphologic influences.....	56
4.3.	Site Characterisation	59
4.3.1.	Hout River Shear Zone (HRSZ Model).....	61
4.3.2.	Open structure parallel to compression (Open Structure Model)	62
4.3.3.	Closed structure perpendicular to compression (Closed Structure Model)	62
4.3.4.	Geological Contact Model	62
4.3.5.	Weathered Aquifer Model.....	63
5.	CONCLUSIONS.....	64
6.	REFERENCES.....	66
7.	APPENDICES	72

FIGURES

Figure 2-1:	Variation in porosity in the vicinity of a point as a function of the averaging volume (after Bear & Bachman, 1990 in Bear, 1993).....	7
Figure 2-2:	Very small volumes can result in a porosity of either zero or one ($n = \text{porosity}$). ..	7
Figure 2-3:	Relative roughness variables (a) and types of flow (b) (after Wittke, 1990).	9
Figure 2-4:	Flow dimensions and concept of fracture continuity (Barker, 1988 in Black, 1994).	10
Figure 2-5:	Different flow phases with increasing pumping from a borehole, Q	12
Figure 2-6:	Radial flow towards a borehole in a cylindrical confined aquifer (after Li, 2007) .	12
Figure 2-7:	Typical pumping test set-up.....	19
Figure 2-8:	Some factors influencing pumping test data.....	28
Figure 2-9:	Skin effects influencing early pumping test data.....	29
Figure 3-1:	Topography of study area.....	32
Figure 3-2:	Geology of the study area (adapted from Robb <i>et al</i> , 2006).....	36
Figure 3-3:	Quartz (Q) – Alkali feldspar (A) – Plagioclase (P) – Foid (F) diagram depicting igneous rock composition (after: Blatt & Tracy, 1997).	37
Figure 3-4:	Sketch map of the Limpopo Complex showing the Hout River Shear Zone (after Van Reenen <i>et al</i> , 1990 and Boshoff, 2004 in Boshoff <i>et al</i> , 2006).....	39
Figure 3-5:	Schematic diagram depicting the current compressive stress conditions in Limpopo Province, southern Africa (adapted from Bird <i>et al</i> , 2006).	39
Figure 4-1:	Constant discharge test results of borehole H04-0306.....	42
Figure 4-2:	Cooper-Jacob fitting for borehole H04-0306.....	43
Figure 4-3:	Theis fitting for borehole H04-0306.	43
Figure 4-4:	Step-drawdown test results of borehole H04-0306.....	44
Figure 4-5:	Constant discharge test results of borehole H10-0084.....	45
Figure 4-6:	Cooper-Jacob fitting for borehole H10-0084.....	45
Figure 4-7:	Theis fitting for borehole H10-0084.	45
Figure 4-8:	Step-drawdown test results of borehole H10-0084.....	46
Figure 4-9:	Constant discharge test results of borehole H07-0841.....	46
Figure 4-10:	Cooper-Jacob fitting for borehole H07-0841.....	47
Figure 4-11:	Theis fitting for borehole H07-0841.	47
Figure 4-12:	Step-drawdown test results of borehole H07-0841.....	48
Figure 4-13:	High T Scenario: derivative plots for constant discharge test, borehole H04-0306.	48
Figure 4-14:	Intermediate T Scenario: derivative plots for constant discharge test, borehole H10-0084.	49

Figure 4-15: Low T Scenario: derivative plots for constant discharge test, borehole H07-0841.	49
Figure 4-16: High T Scenario: semi-log plot for constant discharge test, borehole H04-0306.	50
Figure 4-17: Intermediate T Scenario: semi-log plot for constant discharge test, borehole H10-0084.	50
Figure 4-18: Low T Scenario: semi-log plot for constant discharge test, borehole H07-0841.	50
Figure 4-19: High T Scenario: log-log plot for constant discharge test, borehole H04-0306.	51
Figure 4-20: Intermediate T Scenario: log-log plot for constant discharge test, borehole H10-0084.	51
Figure 4-21: Low T Scenario: log-log plot for constant discharge test, borehole H07-0841.	51
Figure 4-22: High T Scenario: square root of time plot for constant discharge test, borehole H04-0306.	52
Figure 4-23: Intermediate T Scenario: square root of time plot for constant discharge test, borehole H10-0084.	52
Figure 4-24: Low T Scenario: square root of time plot for constant discharge test, borehole H07-0841.	53
Figure 4-25: Schematic Basement granite profile in high-rainfall areas of decomposition, South Africa.	58
Figure 4-26: Schematic Basement granite profile in low-rainfall areas of disintegration, South Africa.	59
Figure 4-27: Classification of settings and relevance of different models per setting.	61

TABLES

Table 2-1:	Components of a Basement aquifer system (after Dewandel et al, 2006).....	15
Table 2-2:	Information obtained from diagnostic and derivative plots (after Bäumlé, 2003).	21
Table 3-1:	Definition of the four settings.	40
Table 3-2:	H-numbers and amount of boreholes used in the investigation.....	41
Table 4-1:	Comparison of pumping test outcomes.	53
Table 4-2:	Statistical summary of results – transmissivity (T), static water level prior to test (swl) and sustainable yield (Sust Q).	55
Table 4-3:	Coefficient of determination (r^2) values for comparison of T-value estimates.....	55

APPENDICES

APPENDIX A: FIGURES	1
APPENDIX B: DATA	2

1. INTRODUCTION

1.1. Project Background

The work contained in this dissertation, including the full literature review and the case studies, forms part of a project funded by the Water Research Commission (WRC), situated in Pretoria, South Africa. The project title is *Determining sustainable yields of potential productive well fields in the Basement aquifers of the Limpopo Province (with special emphasis on the Limpopo (WMA 1) and Luvuvhu/Letaba (WMA 2) Water Management Areas)*, WRC project number K5/1693/1.

These case studies address the determination of the aquifer parameters (essentially transmissivity and sustainable yield) in fractured, crystalline Basement terrain. The influences of structures (i.e. joints, faults and shear zones) and the neotectonic stress conditions on groundwater flow and occurrence were also investigated.

All pumping test data (unless noted otherwise) were obtained from the Department of Water Affairs and Forestry's (DWA's) National Groundwater Database (NGDB), DWA's Groundwater Resource Information Project (GRIP) and tests conducted during this project.

1.2. Objectives

The main objectives were to:

- address groundwater occurrence in Basement aquifers;
- grasp a clearer understanding of fractured aquifer systems;
- evaluate pumping tests as a tool for groundwater characterisation;
- correlate between transmissivities obtained from constant discharge (according to Logan's method, Theis' method and the Cooper-Jacob approximation) and step-drawdown (according to Birsoy-Summers method) pumping tests; and
- address the applicability of sustainable yield estimations.

The findings as contained in this dissertation are to be collated with groundwater chemistry data and additional aquifer tests at later stages of the WRC project to better understand Basement aquifers *per se*.

1.3. Methodology

The project is divided into three phases: acquisition, analysis and appraisal. The inherent methodologies are summarised below and are discussed in full detail in the literature review.

1.3.1. Acquisition

This phase of the project entailed attending Steering Committee meetings and field trips for the WRC project, as well as private meetings with the consultants who conducted and analysed the majority of the pumping tests during the GRIP project. A number of pumping tests were also analysed while still in the employment of WSM Leshika Consulting during 2005.

Data has essentially been acquired from the following:

- GRIP (Groundwater Resource Information Project) of the DWAF;
- NGDB National Groundwater DataBase of the DWAF;
- Field work based on the data obtained from the abovementioned sources; and
- A complete literature study from existing sources.

The pumping test data formed part of the GRIP project. The tests were conducted by a variety of consultants as listed in the acknowledgements. The H04, H07, H10, H11, H16, H17 and H20 surface catchments were incorporated into the investigation, and were selected as representative of the Basement aquifers in the South African framework as testing sites during a WRC project Steering Committee meeting. This forms part of the following Quaternary catchments: A62E, A62F, A62H, A71E, A72A, A91 B, A91C, A91F, B81G, B82D and B82F (Figure A-1). The dataset comprised a total of 1 124 boreholes with constant discharge data, step-test data, or – in by far the majority of instances – both.

The parameters extracted from the FC-Programme (Van Tonder *et al*, 2001) included the H-number (borehole numbers based on magisterial locality), coordinates (WGS84), depth of static water level prior to the test, transmissivity (from Logan's estimation, Theis' method, Cooper-Jacob's approximation and Birsoy-Summer's method), effective well radius, storativity, sustainable yield and the prominence of fractures from the derivative plots.

1.3.2. Analysis

Analysis of the data entailed pumping test evaluation by means of the FC-Programme. A basic statistical evaluation followed, comprising comparison of results on similar structures and/or lithologies in terms of parameters determined. This was done by private groundwater

consultants and the author during his employment for WSM Leshika Consulting and later at the University of Pretoria. The Flow Characteristic (FC-) Programme was used in all analyses to ensure consistency in the evaluation of the pumping tests.

The derivative and diagnostic plots were interpreted to identify fractures, fracture intersections, barriers and flow conditions to better understand the groundwater system. Sustainable yields were furthermore calculated to give an indication of the long-term prospects for the boreholes within the study area.

A number of boreholes were identified during the project for further longer-period pumping tests to address the influence of pumping test duration on the results obtained. This testing commenced in November 2007.

All available data has been extracted and incorporated into a database. Where applicable, GRIP data has been merged with NGDB data and personal field observations, geophysical data (Council for Geoscience) and structural detail (University of Pretoria). All this data were obtained from the respective parties involved as noted above.

1.3.3. Appraisal

The appraisal represents the discussion of the results with specific reference to the current technologies and methodologies, and the applicability of these in Basement aquifers. More specifically, the need was to address not only groundwater occurrence in Limpopo on a theoretical level, but also on a practical level where it can be implemented. The appraisal therefore aims to address the groundwater in Basement aquifers for future water supply and characterisation purposes.

The final outcomes of the project include a conceptual model and a proposed classification system for Basement aquifers.

2. LITERATURE REVIEW

2.1. Fracture Flow

In order to understand groundwater movement through Basement aquifers, a clear overview of flow through fractured media is required. Fracture flow generally predominates in Basement aquifers, and this in turn is often directly influenced by prevailing neotectonic stress fields. This section therefore aims to elaborate on the available literature regarding fracture flow, the influence of neotectonic stress conditions and Basement aquifers in general.

2.1.1. *The influence of fractures*

In terms of hydrogeology, a rock mass can be regarded as a combination of porous rock matrix and secondary openings. Fractured or secondary aquifers are not – as some porous or primary aquifers – homogenous and isotropic, and flow is structurally controlled. These structures include joints, shear zones, fracture zones and foliations.

According to Bear (1993), a clear distinction should be made between *fractured rock*, being rock mass with negligibly low or no void space (or primary pores), and *fractured porous rock* when the blocks between the fractures are porous. He also defines a *fracture* as part of the void space but, unlike primary pores that have similar dimensions in all directions, has one dimension (the *aperture*) that is considerably smaller than the other two dimensions.

With the exception of unconsolidated materials, practically all subsurface materials are fractured to some extent and these fractures are scale-dependent, varying from micro-cracks to crustal rifting (Bonnet *et al*, 2001). The problem in such fractured terrains is one of data limitation due to the inherent difficulty in mapping all discontinuities, especially as the smaller zones also influences groundwater movement. Data is usually limited in terms of fracture shapes and sizes and this together with scarce information regarding densities and orientations are required to address fractured aquifers. (Neuman, 2005).

Discontinuities such as fractures are not inherently more permeable than the parent rock. Fractures containing material with lower permeability than the host rock can serve as barriers to flow (Van Golf-Racht, 1982 in Neuman, 2005). Adding to this is the notion that fracture flow might be influenced more by fracture intersections where the rock is more weathered than by fracture plane flow. Subsequently, the mere orientation of the major discontinuities is not necessarily representative of the predominant flow direction (Hsieh & Neuman, 1985 in Neuman, 2005).

The rock mass itself can be permeable or impermeable, storing water within the pores and micro-fractures in the matrix. The rock mass can be so impermeable (e.g. granite) that water exchange between the matrix and fracture is minimal, rendering the rock mass practically inert (Van Tonder *et al*, 2001) with the exception of some diffusion.

As implied by the term fracture flow, migration of water in fractured (also called “secondary”) aquifers is generally within these secondary (i.e. not inherently formed during formation of the rock) openings in the rock. These fractures exist within the rock mass and normally have a higher conductivity than the latter, although exceptions exist where such structures serve as barriers.

These fractures form due to deformation and stress conditions, resulting in anisotropy within the aquifer (Boulding & Ginn, 2003). Where fractures are present, the groundwater flow is affected by the fracture density, orientation, aperture connectivity and rock matrix (Witherspoon *et al*, 1987). The permeability of such fractures is often influenced by secondary cementing materials or minerals within fractures, as well as deformation of the rock.

The influence of fractures on groundwater flow generally decreases with depth as found by the following sources:

- Fracture aperture (which is stress-dependent) results in flow, and subsequently should decrease with depth (Gale, 1982).
- Fissure [*sic.* fracture] permeability and density of fractures should decrease with depth (Wright & Burgess, 1992).
- Fracture frequency mostly decreases with depth (Van Schalkwyk & Vermaak, 2000).
- Increasing stress causes fracture apertures to close up, leading to significant decrease in permeability of fractured rock with depth (Barker, 1991).

As discussed by Bäumlé (2003), there are essentially four factors that complicate the application of fluid flow and transport analyses in fractured rock aquifers. These include:

- Vast differences in the hydraulic parameters of single fractures.
- Physical properties of the fractures, including the geometry, position and interconnectivity; this determines the permeability, anisotropy and flow pattern of the aquifer.
- Scale of the area as a prerequisite for estimating and defining geometric and hydraulic parameters.
- Complexity of characterising all these concepts in the field.

Due to fracture networks in rocks, conventional well flow equations will usually be insufficient to determine aquifer properties for fractured aquifers. As stated by Verweiji and Barker (1999 in Van Tonder *et al*, 2001), the hydraulic parameters such as the hydraulic conductivity and storativity for hard-rock aquifers depend on the scale of the investigation due to the heterogeneity of the rocks. On a small scale, fractures may not be responsible for primary flow, whereas on larger scale, fractures in the same aquifer can control the flow.

According to Bear (1993), any porous material domain comprises a solid matrix and void space distributed throughout the whole medium. This gives rise to the Representative Elementary Volume (REV), where any portion of a porous medium will contain both solid and void spaces. The size of the REV should be determined in order for the parameters representing the void space distribution and solid matrix to be statistically meaningful. To address the abovementioned factors becomes difficult, but it basically amounts to the following: the size of the REV must exceed the scale of microscopic heterogeneity, and should be less than the scale of the domain of interest (Bear, 1993). For this reason, parameters such as dispersivity and permeability are not always helpful as they represent small-scale solid-fluid geometries, and therefore do not comply with the larger-scale requirements that the REV concept is based on (Ingebritsen *et al*, 2006).

Determining the properties of fractured media is difficult for a number of reasons. Firstly, obtaining a reasonably sized representative sample is practically impossible due to the scale effect and heterogeneity, and subsequently it is difficult to determine the REV. Secondly, laboratory simulation or experiments are practically impossible due to the difficulty in sampling fractured rock without disturbing the discontinuities (Jouhanna, 1993).

The effect on porosity n with changing volume and REV is shown in Figure 2-1. Note that, for very small values of $U(x)$ (the volume of a sphere centred at a point x in the medium), the ratio U_v/U (volume of voids in sphere U / volume of sphere) can be either zero or one (Figure 2-2). This depends on whether the point is within an opening or the solid matrix. With increasing volume, the ratio fluctuates until – at a certain volume (where $U = U_{min}$) – the ratio becomes fairly constant (Bear, 1993). At this point in time, the porosity remains fairly constant over the extent of the REV. Beyond a certain maximum volume of sample, U_{max} , heterogeneities can once again lead to varying porosity.

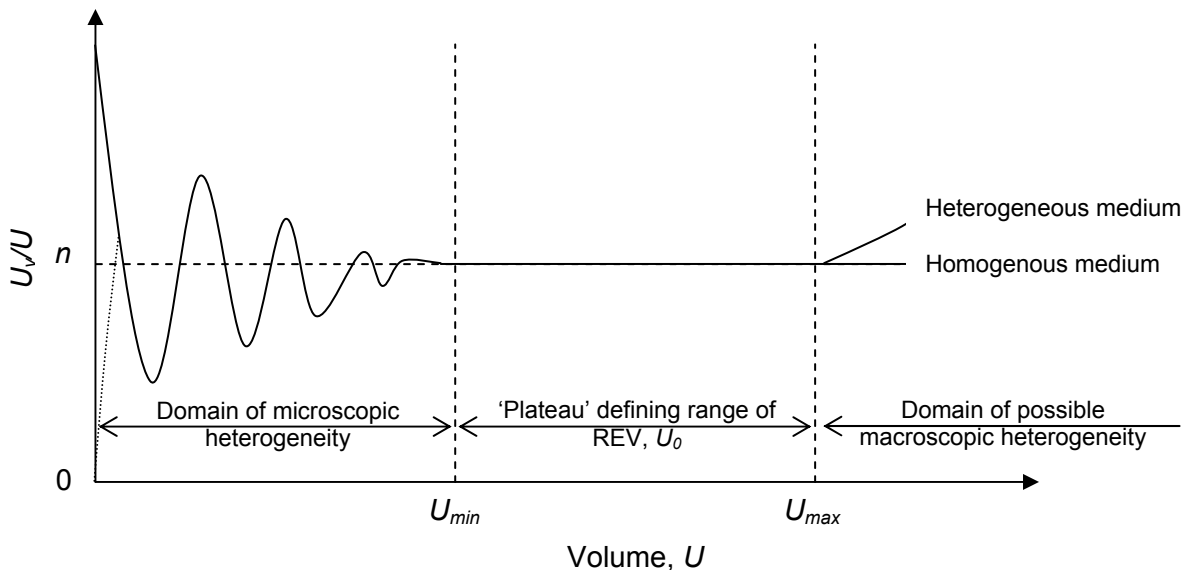


Figure 2-1: Variation in porosity in the vicinity of a point as a function of the averaging volume (after Bear & Bachman, 1990 in Bear, 1993).

Figure 2-2 shows the influence of very small values for $U(x)$.

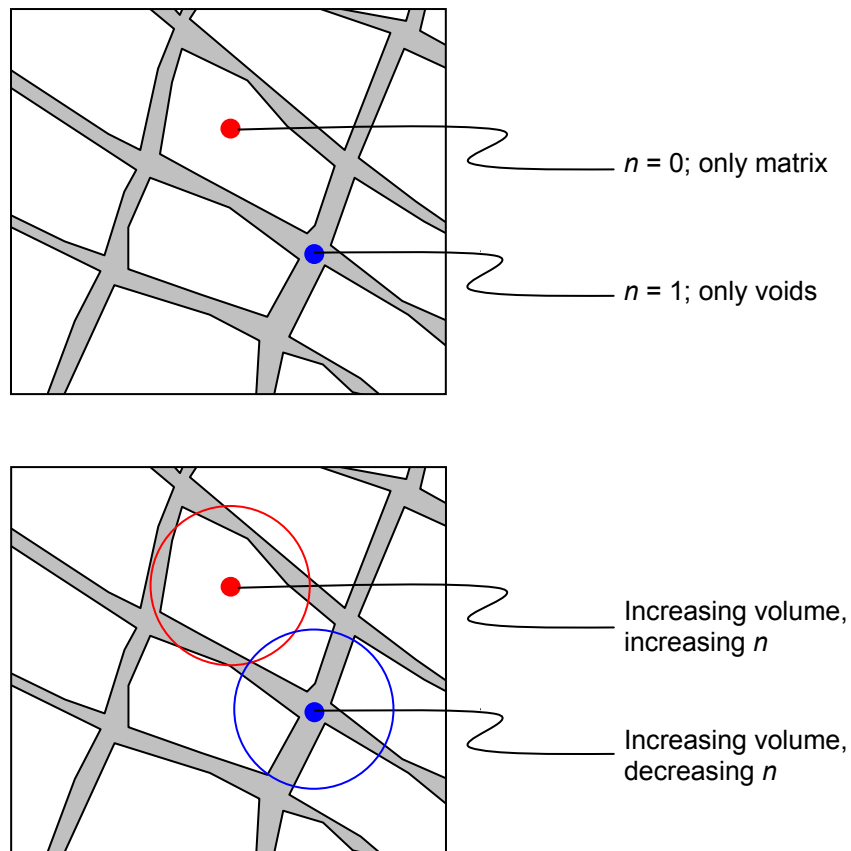


Figure 2-2: Very small volumes can result in a porosity of either zero or one (n = porosity).

2.1.2. Flow through fractures

Barker (1991) elaborates on some processes and factors that affect transport in fractured media. The first of these, fracture morphology, specifically addresses the continuous nature of a fracture system, i.e. whether they serve as significant pathways for flow or not. He continues to define 'fracture zones' as complex systems comprising shear zones, extension fractures, brecciated zones and stress dissolution features, including all filling and alteration products.

Flow within fractures can be turbulent, but often small apertures and subsequently laminar flow prevails. This ensures applicability of some of the well-flow equations, most of which assume porous media (Boulding & Ginn, 2003). Laminar flow of incompressible fluids through smooth, parallel, planar plates (representing the fracture) was described by Witherspoon *et al* (1980). Determination of the hydraulic conductivity of the fracture, K_f , is shown in Equation 1.

$$K_f = \frac{(2b)^2 \rho f g}{12\mu} \quad \text{Equation 1}$$

Where K_f = hydraulic conductivity of fracture [L/T]

b = aperture half-width [L]

ρ = fluid density [L/V]

g = gravity acceleration [L/T²]

μ = viscosity [M/LT]

Other important parameters regarding flow include the Reynolds number, Re , and the friction factor, Ψ . Determination of these two parameters is shown in Equation 2 and Equation 3 (Lomize, 1951; Romm, 1966; Louis, 1969 in Witherspoon *et al*, 1980).

$$Re = \frac{Dv\rho}{\mu} \quad \text{Equation 2}$$

Where Re = Reynolds number

D = hydraulic diameter (= 4b) [L].

v = flow velocity [L/T]

$$\Psi = \frac{D}{(v^2 / 2g)} (\nabla h) \quad \text{Equation 3}$$

Where Ψ = friction factor [-]

h = hydraulic head [L]

Wittke (1990) discusses the influence of roughness (friction) of fracture planes on fracture flow. Because discontinuities are not generally smooth in nature, a hydraulic diameter (Equation 4) of zero rarely exists as flow is no longer laminar. As shown in Figure 2-3, very specific cut-off limits exist in hydraulic diameter to distinguish between so-called irrotational and rotational flow.

$$\bar{D}_h = 4 \frac{A}{P} \rightarrow \frac{k}{\bar{D}_h} = \frac{k}{4\bar{a}_i} \quad \text{Equation 4}$$

Where D_h = hydraulic diameter
 k = absolute wall roughness
 $2a_i$ = mean fissure width

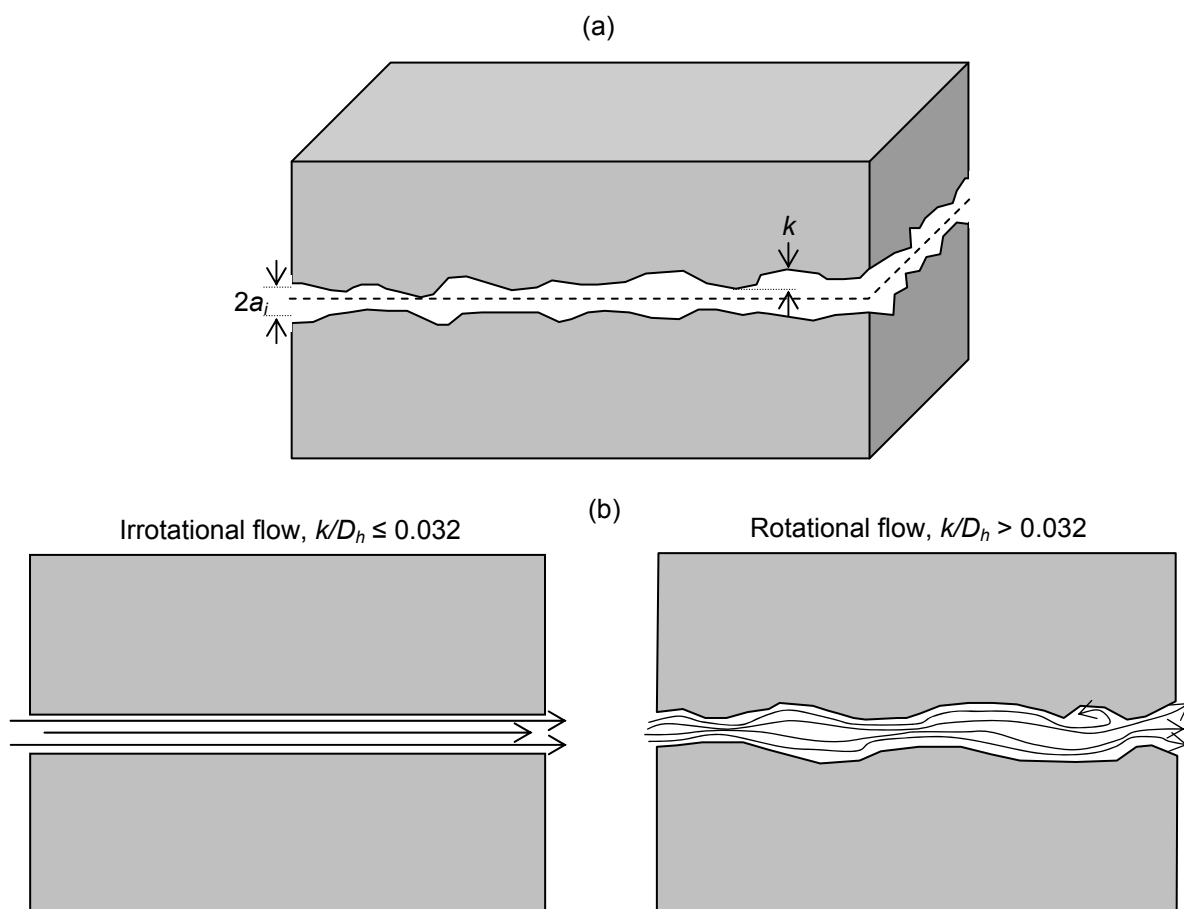


Figure 2-3: Relative roughness variables (a) and types of flow (b) (after Wittke, 1990).

Water movement towards a pumped borehole can be in one of the following ways:

- One-dimensionally along a specific fracture zone with large volumes of isolated hard rock.

- Radial, viz. two-dimensionally via a hard-rock aquifer with a well-connected fracture network, isotropically distributed.
- Spherical, viz. three-dimensional flow into partially penetrating boreholes.

This was defined by Barker's flow dimensions (Barker, 1988 in Black, 1994) as shown in Figure 2-4 and Equation 5 (Walker & Roberts, 2003). The through-flow area A is directly proportional to the distance from the source r raised to the power of flow dimension Df minus one (Black, 1994).

Porous continuum visualisation

Fractured and/or channelled discontinuum visualisation

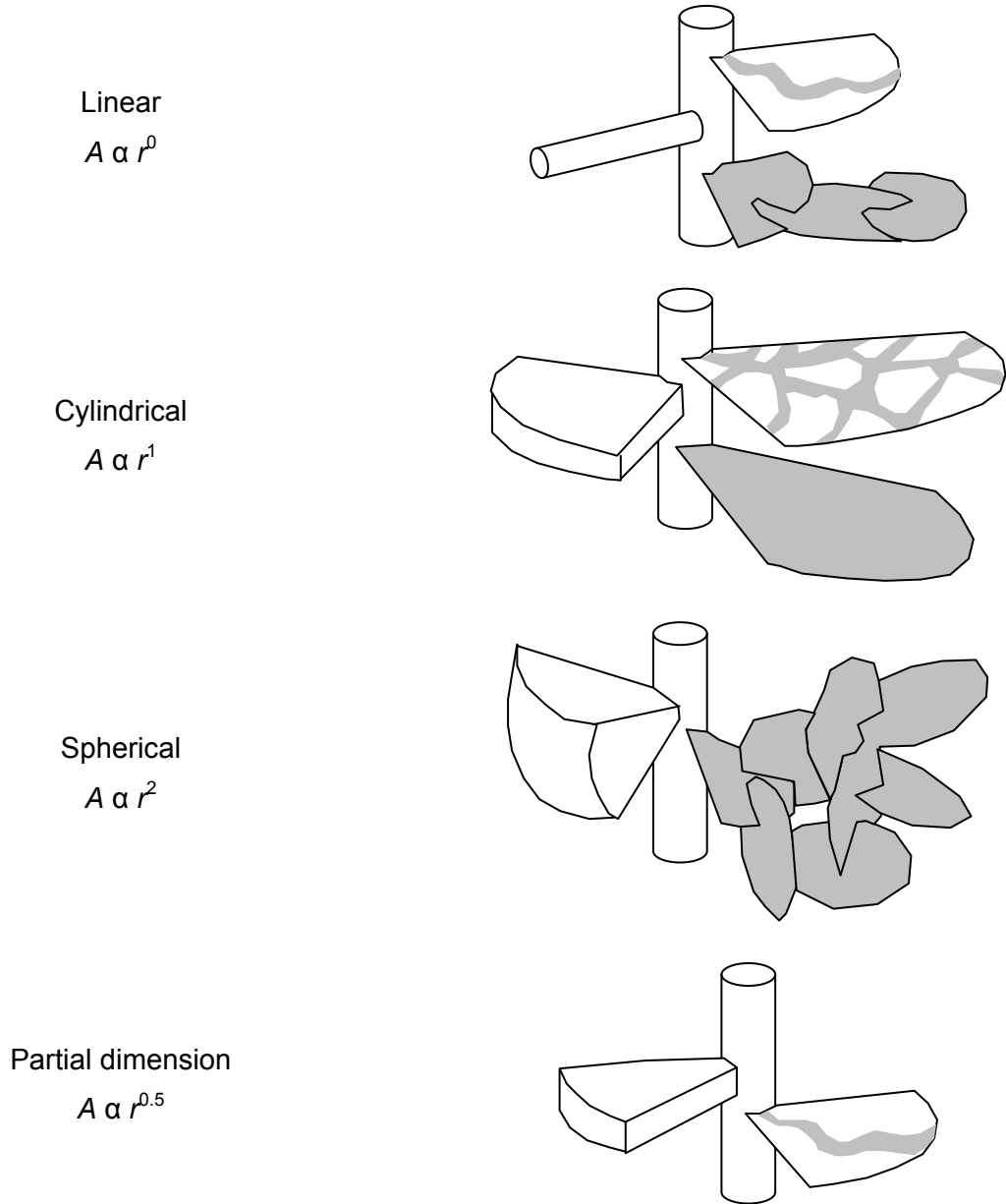


Figure 2-4: Flow dimensions and concept of fracture continuity (Barker, 1988 in Black, 1994).

$$A\alpha r^{(D_f-1)} \quad \text{Equation 5}$$

Where A = through-flow area [L^2]

r = distance from the source [L]

D_f = flow dimension [-]

Addressing the concept of uncertain geometry of rock mass (i.e. porous or fractured dominance and preferred flow directions) requires the use of fractional dimensions (Barker, 1988 in Black, 1994). The generalized radial flow (GRF) model of Barker (1988) can be used in instances where the aquifers are not of simple geometry and have heterogeneous properties. The relationship between the cross-sectional area of flow and the distance from the source is shown in Equation 6 (in Walker & Roberts, 2003).

$$A(r) = \alpha_n r^{D_F-1} \quad \text{Equation 6}$$

$$\alpha_n = b^{3-D_F} \frac{2\pi \frac{D_F}{2}}{\Gamma\left(\frac{D_F}{2}\right)}$$

Where $A(r)$ = cross-sectional area of flow [L^2]

r = radial distance from borehole [L]

b = extent of flow zone [L]

D_F = flow dimension [-]

Γ = gamma function [-]

Based on Equation 6, the GRF governing solution is Equation 7 (Barker, 1988 in Walker & Roberts, 2003).

$$S_s \frac{\partial h}{\partial t} = \frac{K}{r^{D_F-1}} \cdot \frac{\partial}{\partial r} \left(r^{D_F-1} \frac{\partial h}{\partial r} \right) \quad \text{Equation 7}$$

The flow dimension (D_F) is representative of the change in cross-sectional flow due to changing distance from the borehole being tested, as is quantified as a power representing this change plus one. Homogenous, radial systems, for example, have a flow dimension of $D_F = 2$ (Barker, 1988; Walker & Roberts, 2003).

Flow phases furthermore change for fractured porous rock during pumping of a borehole, starting off with linear fracture flow (from fractures open to the borehole), bilinear flow (where fractures are recharged via the pores), linear formation flow (when all fractures have been dewatered and the rock mass determines the water supply to the borehole), and radial flow

(when, after reasonable time, the influence of all structures have been overruled). This is illustrated in Figure 2-5.

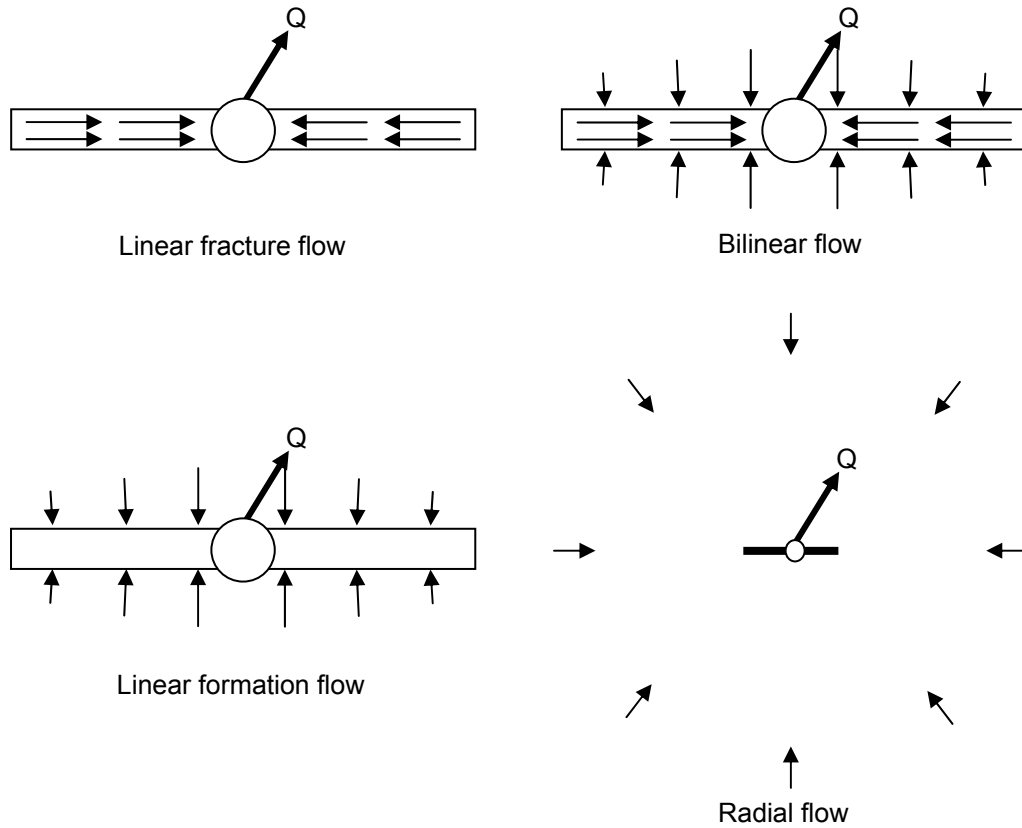


Figure 2-5: Different flow phases with increasing pumping from a borehole, Q.

Radial flow can also be depicted as shown by Li (2007) in Figure 2-6.

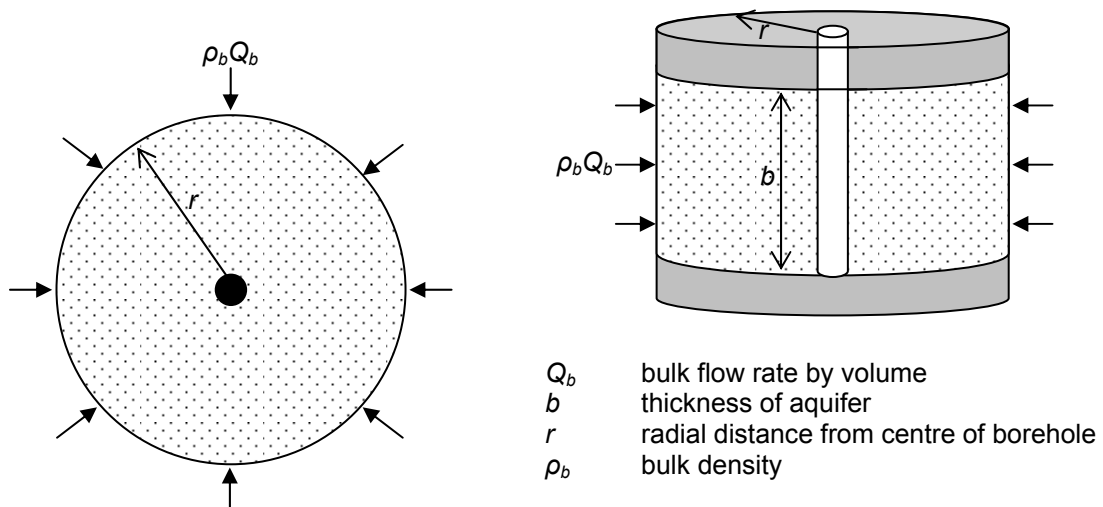
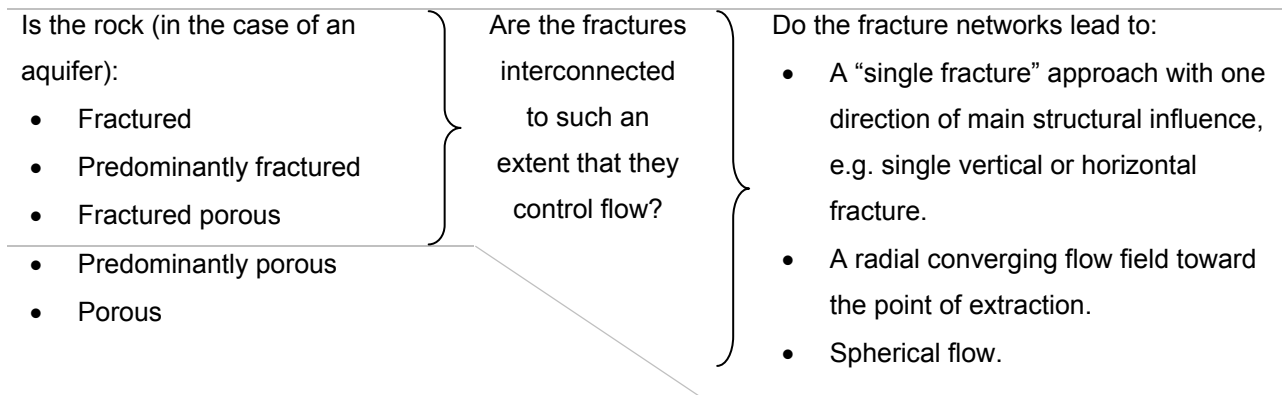


Figure 2-6: Radial flow towards a borehole in a cylindrical confined aquifer (after Li, 2007)

The possible presence of fractures in the aquifer material has a major influence on groundwater flow, and an equally great degree of uncertainty. For all practical purposes, rock with the potential of having fractures can be classified as follows:



Densely interconnected fractures (also called a fracture network continuum) are characterised by larger storage capacities, resulting in considerable yields of boreholes. Determining whether or not a fracture network can be regarded as a continuum is dependent on the representative elementary volume (REV), the fracture connectivity, and the difference in the respective conductivities of the fracture and rock matrices (Van Tonder *et al*, 2001).

Guérin and Billaux (1994) state the importance of realising that a continuum is an approximation, and is dependent on the scale of the investigation and the different properties of the fracture network. This again brings to light the concept of REV below which the continuum approach becomes invalid, and the difficulty in determining the size of the REV.

Long *et al* (1982, in Lebbe and De Breuck, 1997) found after a series of numerical simulations that fractured rock does not inherently behave similar to homogenous porous media, but is rather characterised by lateral anisotropy and has very specific conditions to be met to have a symmetrical permeability tensor, *viz.* dense fractures with fairly constant aperture, the fracture orientation is randomly distributed, and a large tested sample size is required.

Discrepancies exist in the theories applied to fracture flow as the fractures are not generally smooth, parallel and with constant apertures. It is therefore of importance to recognize the effects of channelling within fractured rock, and that flow will not inherently flow in the direction of the fracture alone. As opposed to a “smooth, parallel plate” fracture analogy, fluid flow through fractures may be restricted to distinct channels in the plane of the fracture. This is based on the concept of fluids flowing through pathways of least resistance, *viz.* greater apertures. This channelling is a result of undulating fracture surfaces, closure (partial or

complete) of fractures due to stresses, and minerals precipitating in fractures that lead to partial clogging of the fracture plane (Smith and Schwartz, 1993).

Fracture skin (Moench, 1984 in Barker, 1991), fracture aperture and stress conditions inflicted on the fractures should be regarded as important parameters in determining fracture flow and the effect of channelling. The latter determines flow velocities through determining effective porosities, the amount of sorption and diffusion into the rock matrix, and addresses the sensitivity of flow between intersecting fractures to the density of channels (Barker, 1991).

Adsorption can often be disregarded, but in the instance of multi-phase flow this can serve as a retardation factor. Adding to this is the process of diffusion whereby water can become immobilised, further altering the flow. Dispersion can usually be neglected where transportation is not the major concern, as well as the presence of colloids and multiphase flow (Barker, 1991).

In summary, the major concern when addressing groundwater flow (as opposed to transport) becomes fracture morphology and advection, both being dependent on channelling and/or fractal dimensions.

2.1.3. Basement aquifers

The term 'Basement rock' applies to hard, crystalline or re-crystallised igneous or metamorphic rocks associated with Precambrian age (Arcworth, 1987; Jones, 1985; Wright & Burgess, 1992). These include, according to Key (1992), ancient Archaean cratonic rock (granites, gneisses, greenstones); metamorphic rocks associated with mobile belts (typically deformed and of Proterozoic age); and anorogenic intrusions typically of variable age. The Basement which underlies the study area is of the first and third types, and includes a variety of granites.

These rocks have very low primary porosity and subsequently also very low storage. Groundwater movement is not typically associated with the rock matrix. Secondary features such as fractures, faults, shear zones and weathering zones are responsible for the majority of groundwater movement (Lloyd, 1990). Aquifers in these areas furthermore are typically composite and comprise a fairly constant succession with varying thicknesses. This is shown in Table 2-1 (Dewandel et al, 2003).

Table 2-1: Components of a Basement aquifer system (after Dewandel et al, 2006).

<i>Horizon</i>	<i>Description</i>	<i>Notes</i>
Laterite	Iron or bauxitic crust.	Can be absent.
Saprolite	Clayey material due to <i>in-situ</i> decomposition of bedrock.	Tens of metres thick if not eroded.
Fissured layer	Densely fissured horizontally decreasing with depth.	Few metres thick.
Fresh Basement	Locally permeable due to tectonic fracturing.	Considered 'impermeable' and with low storativity (Maréchal <i>et al</i> , 2004).

Righi and Meunier (1995) subdivide the slope on granitic bedrock into a truncated weathering profile on the hillcrest and pediment, and show iron being leached from higher areas and accumulating as iron oxide on the lower slopes and pediments. This presence of ferricrete is characteristic of South African granites, and is generally representative of a seasonal perched water table. In international context, however, laterite is noted more often. This is the pedogenic material formed from aluminium sesquioxide, and is not commonly found in South Africa. Iron tends to rather mobilise and form ferricrete (Weinert, 1980).

Weathering often controls the rate of recharge and subsequently the ratio between infiltration and runoff over an area. Depending therefore on the depth of weathering, influence of structures and presence of lower permeability pedocretes, infiltration can be lowered leading to less recharge and more surface runoff.

2.1.4. Neotectonics and its influence on fracture flow

According to Sami *et al* (2002) in a study on groundwater exploration in geologically complex and problematic terrain, an understanding of the geodynamics and tectonic history of an area is advantageous in identifying potential targets for hydrogeological exploration. The most obvious targets for hydrogeological exploration are existing structures under tension. This is confirmed by Botha and van Rooy (2001), who found potentially high yielding sites on the Nebo Plateau (also in Limpopo Province) associated with fracture and/or shear zones.

Based on current stress conditions, some structural features and lineaments can be more significant in terms of geohydrology, and such zones of greater potential can be identified with geophysical techniques. In the study of Sami *et al* (2002), Basement aquifers were however not included in the case studies.

2.1.5. Geomorphological history and erosion cycles

Tectonic movements and changes in sea level resulted in a series of erosion cycles due to the new sets of base levels. This caused the stripping-down of the Karoo Supergroup cover, exposing the underlying geological formations. Drainage systems were superimposed on these older formations (Partridge & Maud, 1987). Six such cycles were recognised by King (1975), viz.:

- Gondwana planation, ca. 190 Ma;
- Post-Gondwana cycle, ca. 135 Ma;
- African cycle, ca. 100 Ma;
- Post-African I cycle, ca. 20 Ma;
- Post-African II cycle, ca. 5 Ma; and
- Quaternary cycle, ca. 2 Ma.

These erosion surfaces represent long periods of weathering and erosion, and were also triggered by uplift and sediment accumulation due to changing climate (notably increasing aridity).

2.2. Modelling Aquifers

Various models are being applied to aquifers. Although porous media methods are sometimes used, some of the most common models applied to fractured aquifers include:

- Single fracture model.
- Double porosity model.
- Fractal dimensions.

Smith and Schwartz (1993) distinguished between three different scales of advecting mass transfer through a fracture network:

- Microscopic scale, entailing the spreading on two walls of a fracture.
- Individual fracture planes scale, entailing a two-dimensional configuration through which fluids move.
- Macroscopic scale that includes mixing at fracture intersections, network geometry and variable fluid velocity.

According to the fracture continuum or continuous approach, a model on microscopic level is inadequate, as it cannot integrate variables at different points within one phase. This microscopic problem is therefore converted to a macroscopic problem, based on using the microscopic average values instead of point-specific values. These measurable quantities are

then used in a model depicting the porous medium, and are accepted to occur throughout the whole domain (Bear, 1993).

Jouanna (1993) continues to state that, when the fractures create the porosity, the fractures are assumed to be distributed throughout space. The fractures are then represented by a porous medium with similar properties. However, when fractures have fairly large dimensions with respect to the size of the relevant rock mass, the continuum approach is no longer valid (Jouanna, 1993). In this instance it becomes necessary to regard the fractures *per se* instead of assuming a porous nature. Based on this Jouanna (1993) states that two elementary models are of fundamental importance, *viz.*:

- One closed fracture in a matrix that is impervious and rigid; fluid movement is mostly controlled by inertia and compressibility forces.
- One open fracture in a matrix that is impervious and rigid; fluid movement is mostly controlled by inertia and viscosity.

2.3. Hydraulic Testing

The merit of an aquifer, aquiclude or aquitard as a potential source of water is dependent mainly on its ability to transmit water (transmissivity, T) and its ability to store water (coefficient of storage, S). These parameters aid in addressing the *quantitative* properties of an aquifer or borehole as opposed to the *qualitative* properties which are more easily defined. These parameters are extremely variable and determination should be supported by additional testing and/or suitable information regarding geologic characteristics of the investigated area (Ferris *et al*, 1989). Additional to this, recharge should be considered when evaluating potential groundwater sources.

It should be noted that hydraulic tests comprise aquifer tests (i.e. determining the properties of the aquifer through which groundwater moves) and well tests (i.e. determining the properties of the relevant borehole). According to Jouhanna (1993), most hydraulic tests are well tests, can be conducted in one or more boreholes, and can have different boundary conditions.

Stallman (1976) defines an aquifer test as a “controlled field experiment made to determine the hydraulic properties of water-bearing and associated rocks.” This is based on observations of groundwater flow influenced and controlled by a number of factors such as hydraulic head conditions, pumping rates of wells and changes in recharge rates.

2.3.1. Pumping tests

A variety of methods are available through which the water level is changed in a borehole, and the drawdown and/or recovery of the water level is measured against time and/or space. These methods include bail tests, slug tests and pumping tests. For the purpose of this dissertation, the emphasis will be solely on the latter.

Pumping tests can be subdivided into three phases. The design phase involves planning of the field work to ensure that suitable data is obtained at realistic cost. This includes calculating the pumping rate, estimating the test duration and completing the desk study regarding site geology, groundwater trends and any other information. After this first phase the field observation or data acquisition follows, and finally the data analyses (Stallman, 1976).

As stated by Van Tonder *et al* (2001), the hydraulic behaviour of the borehole, reservoir and reservoir boundaries is required to effectively and efficiently manage the aquifer and well field. By means of the pumping test, these hydraulic properties can be determined for the basic purpose of (Van Tonder *et al*, 2001 and SANS, 2003):

- Understanding the aquifer.
- Determining the hydraulic and physical properties of the aquifer.
- Determining the efficiency and sustainable yield of a certain borehole and, in turn, guarantee effective development of the aquifer.

According to SANS (2003), a pumping test is based on the principle of pumping water from a well (or borehole). The rate of discharge (pumping rate, Q), and drawdown (s) in the well and other piezometers in the vicinity of the well is measured (Figure 2-7). The data is entered into a well-flow equation and consequently the hydraulic parameters of the aquifer are calculated.

SANS (2003) distinguishes between four basic types of pumping tests, *viz.* step-drawdown test or multiple-rate test, constant discharge test, recovery test, and extended step-drawdown test. Step tests assess the performance of a borehole or well, and are often called well tests. As opposed to this, constant discharge tests address the hydraulic properties of the aquifer, and are also referred to as aquifer tests. This is addressed in more detail by Hekel (1994, in Bäümle, 2003)

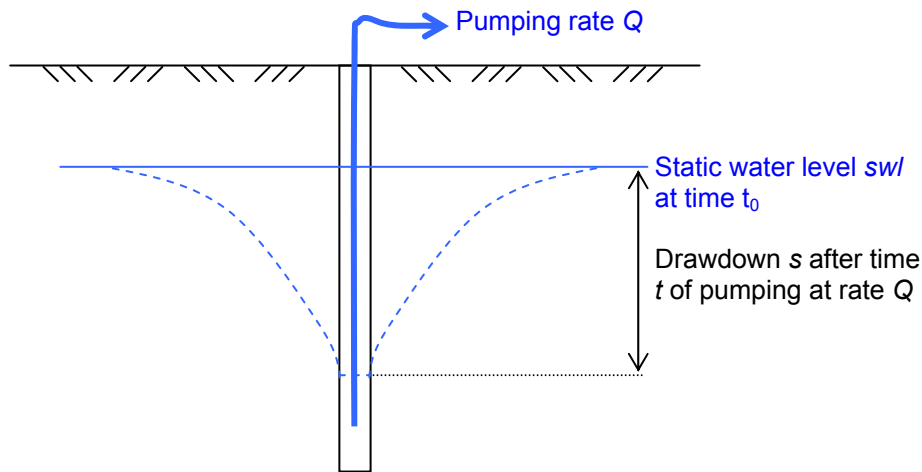


Figure 2-7: Typical pumping test set-up.

2.3.1.1. Step-drawdown test

After determination of the blow yield, this is usually the first test performed on a borehole. The step-drawdown test assesses the performance of the borehole, i.e. the quantity of water that can be pumped, verifies the hydraulic efficiency and determines the discharge rate for the constant discharge test.

The pumping rates have to be kept constant during each step. The following should serve as a guideline on determining the pumping rates (SANS, 2003):

- Step 1: one-third of the expected yield;
- Step 2: two-thirds of the expected yield;
- Step 3: equal to the expected yield; and
- Step 4: one-and-a-half times the expected yield.

2.3.1.2. Constant-discharge test

This test determines the long-term yield of the borehole, the transmissivity and the storage capacity of the aquifer. Longer constant-discharge tests supply more reliable estimates on the long-term yield estimations of aquifers (SANS, 2003). The pumping rate during these tests should vary with less than 5% throughout pumping, and should be based on the results of the step-drawdown test.

2.3.1.3. Recovery test

The pump is switched off after completion of the constant-discharge test and the recovery of the water level is measured. Measurements have to be taken until (SANS, 2003):

- the water level reaches 5% of the total drawdown of the preceding constant-discharge test;

- three successive readings are identical; or
- a time equal to the length of time of the constant-drawdown test has elapsed.

2.3.1.4. Extended step-drawdown test

This test is performed as a combination of step-drawdown and constant discharge tests specifically in boreholes for stock or domestic use that are to be fitted with hand-pumps (SANS, 2003).

2.3.2. Diagnostic and derivative plots

The use of so-called diagnostic plots (the logarithmic derivative of the drawdown as a function of time) was proposed to evaluate pumping test data as it is more sensitive to changes in drawdown than a drawdown-time plot (Bourdet *et al*, 1983, in Renard, 2005). This graphical technique was developed by Chow in 1952 and is applicable when interpreting data with the Theis solution. Chow also found that the logarithmic derivative reaches a constant value at late times in the Theis model, and that the logarithmic derivative's expression is inversely proportional to transmissivity (Renard, 2005). This makes identification of the transmissivity possible at a constant derivative (Chow, 1952).

Kruseman and de Ridder (1989) define diagnostic plots as log-log plots depicting drawdown against time since starting of pumping. This includes the specialized semi-log plots of the same data. These plots aid in identification of the dominant flow regimes. This can be used in conjunction with the derivative plots, aiding in the identification of flow phases and – more specifically – fracture intersections.

The characteristic derivative and diagnostic plots are described in more detail in Table 2-2.

2.3.3. Interpreting pumping test data

In order to interpret pumping test data, a mathematical model is generated that juxtaposes the drawdown in a borehole to the discharge of water in the particular abstraction borehole. A long-term prediction of the borehole's performance can then be deduced based on the determined storativity and transmissivity values. Due to the heterogeneity of fractured rock systems having a major effect on drawdown in the borehole, the conventional methods as developed for homogenous, porous media may not be feasible.

Table 2-2: Information obtained from diagnostic and derivative plots (after Bäumlé, 2003).

Aquifer type	Flow regime	Diagnostic plots		References
		Drawdown	Derivative	
Homogenous, isotropic	Radial symmetric	semi-log : straight	log-log : horizontal line	Theis (1935) Cooper & Jacob (1946)
Double porosity	Radial symmetric	semi-log : two parallel straight-line sections	None noted	Barenblatt <i>et al</i> (1960) Warren & Root (1963) Bourdert & Gringarten (1980) Moench (1984)
Single vertical fracture or dyke	Fracture linear flow	log-log : straight line, slope 0.5	log-log : straight line, slope 0.5	Cinco <i>et al</i> (1978) Cinco & Samaniego (1981) Boonstra & Boehmer (1986) Boehmer & Boonstra (1987)
	Bilinear flow	s vs t^{0.25} : straight log-log : straight line, slope 0.25	log-log : straight line, slope 0.25	
	Formation linear flow	s vs t^{0.5} : straight log-log : straight line, slope 0.5	log-log : straight line, slope 0.5	Gringarten <i>et al</i> (1974) Jenkins & Prentice (1982) Bardenhagen (1999)
	Pseudoradial flow	semi-log : straight	log-log : horizontal line	Theis (1935) Cooper & Jacob (1946)
Single horizontal fracture	Storage type flow	log-log : straight line, slope 1	None noted	Gringarten & Ramey (1974)
	Linear flow	log-log : straight line, slope 0.5	log-log : straight line, slope 0.5	
	Pseudoradial flow	semi-log : straight	log-log : horizontal line	

Due to the unknown geometry of fracture networks in the subsurface, methods of determining aquifer parameters are scarce and often unsound. Sufficient data is not always readily available for numerical flow modelling, and consequently pumping test data is often used as an alternative. The results (transmissivity, hydraulic conductivity and storativity) are however dependent on the scale of the investigation due to the heterogeneity of the aquifers.

Based on continuous research and the collation of field and laboratory data throughout the past, it has been ascertained that Darcy's Law suitably addresses and approximates groundwater movement. Therefore and due to site-specific boundary conditions, prediction of head distribution in an aquifer in space and time becomes plausible (Stallman, 1976). Renard (2005) summarized the history of aquifer tests in a special edition of the Hydrogeology Journal entitled "The Future of Hydrogeology". Advection (flow) according to Darcy's Law is valid where fracture flow is linear-laminar. In instances of turbulent flow (due to, for instance, friction in the fractures), the validity of Darcy's Law decreases (Barker, 1991).

As shown in Equation 8, the volumetric flow rate q in Darcy's Law is a function of hydraulic conductivity k and hydraulic gradient dh/DL .

$$q = -k \left(\frac{dh}{dL} \right) \quad \text{Equation 8}$$

It took almost 80 years after the publication of Darcy's Law (Equation 8) in 1856 before Theis (1935) compiled the analytical solution that is the foundation of most of the current interpretation techniques (Renard, 2005). The Theis method is shown in Equation 9.

$$s = \frac{Q}{4\pi T} [Ei(u) + 2\delta] \quad \text{Equation 9}$$

where

$$u = \frac{Sr_w^2}{4Tt}$$

$$Ei = \int_u^{\infty} \frac{e^{-x}}{x} dx$$

Where Q = discharge rate [L^3/T]

T = transmissivity [L^2/T]

t = time [T]

r_w = drilled radius [L]

S = storage coefficient [-]

δ = well skin factor [-]

Theis (1935) was the first to assess the nonsteady [*sic.* unsteady] response from an aquifer due to constant discharge of a borehole and addressed the abovementioned variables as follows:

- Well discharge is altered by Q at reference time t_0 .
- The well is open to the aquifer throughout the complete thickness of the aquifer, the well radius is insignificant and flow is uniform.
- The aquifer is homogenous and isotropic, constantly water-saturated, extending to infinite radius from the pumped well, and is bounded by impermeable rocks above and below.
- The storage is directly proportional to the hydraulic head.

The problem, however, with the Theis methods is that they are porous medium interpretations. For such media, flow through a unit volume is considered dependent mainly on the radial distance between the source and the observation points (Black, 1994). These assumptions

obviously do not apply to fractured media, where preferential flow directions are present, and where transmissivities vary three-dimensionally.

According to Tam *et al* (2003), pumping tests in fractured rocks usually exhibit drawdown curves comprising three distinct phases. At early pumping times, flow is mostly from storage in fractures according to the Theis equation or Cooper-Jacob approximation (Equation 10). After this a transition period is reached where the drawdown stabilises to an extent due to dewatering of the matrix blocks. When plotting drawdown versus log time, this is often evident by an inflection point. A third phase at late pumping time represents pumping from both pores and fractures.

$$s \approx \left(\frac{2.3Q}{4\pi T} \right) \log \left(\frac{2.25Tt}{Sr_w^2} \right) \quad \text{Equation 10}$$

During the mid-1900's several additions to the Theis technique were developed. These methods incorporate more complex attributes of the aquifer, boundary conditions and the well itself, and include (Renard, 2005):

- Influence of boundaries – Theis (1941).
- Non-linear head losses in the pumped well during step drawdown pumping tests – Jacob (1947).
- Skin concept to examine the performance of a pumped well – Van Everdinger (1953).
- Unsaturated zone and its effect on unconfined aquifers – Boulton (1954).
- Leakages from adjacent aquifers – Hantush and Jacob (1955).
- Partially penetrating wells – Hantush (1964).
- Wells with large diameters – Papadopulos and Cooper (1967).
- Double porosity concept – Warren and Root (1963).
- Wells intersected by single fractures – Gringarten *et al* (1974).

In order to accurately utilise pumping test data, one should be able to correctly identify inner (e.g. well storage and fracture zone extent) and outer (no-flow boundaries and fixed head boundaries) boundary conditions, as well as characteristic flow regimes (Van Tonder *et al*, 2001).

In fractured aquifers, the approach is often to idealise the fracture occurrence into a uniformly-fractured medium or a double porosity medium. Warren and Root (1963) developed an idealised three-dimensional orthogonal fracture system, approximating fracture networks to a

mathematical describable array. In 1960, Barenblatt *et al* developed the double porosity concept, thereby overlapping two media in a single aquifer, namely the matrix blocks and the fractures. This method assumes unsteady state flow for the fractures and radial flow towards the pumped borehole. Boulton and Streltsova (1977), Najurieta (1980) and Moench (1984) followed with transient block-to-fracture flow models, the latter assuming pseudo-steady state flow (Kruseman & de Ridder, 1989).

However, the assumptions for the fractured and double porosity approaches include an assumed confined aquifer of infinite aerial extent, uniform aquifer thickness with full penetration by the borehole, constant pumping rate from an original horizontal piezometric level and unsteady state flow (Kruseman & de Ridder, 1989).

Bäumle (2003) compared aquifer testing procedures with other methods of flow characterisation in different fractured aquifer systems. Based on the results of his work, it was concluded that single well tests are generally unsuitable for transmissivity determination in the event of high well loss, and that the test design should account for observation holes. Furthermore, major shortcomings are evident regarding the high costs of such tests compared with the lack of uniformity in such aquifers. The importance of diagnostic plots is however accentuated as a key feature in determining analysis methods and aquifer type.

If hydraulic stress is applied via either controlling the flow or the head, water movement from or to the borehole controls the head distribution in the aquifer. This head distribution is variable not only in three-dimensional space, but also as a function of time. Based on this, four variables should be known to assess head distribution in the vicinity of a borehole (Stallman, 1976):

- The type and magnitude of flow that is being applied to the well.
- The radius of the borehole, the depths at which the borehole is open to the aquifer, and the hydraulic parameters in the borehole.
- The three-dimensional variance in hydraulic conductivity in the area under influence from the well.
- The storage properties of the whole aquifer.

A variety of conceptual models relating to fractured aquifer systems exist, the most important probably being boreholes in homogenous aquifers, double-porosity systems, and aquifers with a single horizontal or a single vertical fracture.

2.3.3.1. *Homogenous and isotropic aquifers*

Aquifers of this type include porous rock and rock intersected by a dense, closely-spaced fracture network behaving like a porous aquifer. Theis formulated the mathematical approach in

1935, followed by Cooper and Jacob in 1946 and Agarwal *et al* in 1970. Based on this approach, the drawdown s at a radial distance r from a pumped well can be determined with Equation 9 (Theis, 1935).

2.3.3.2. Double porosity

Barenblatt *et al* (1960) developed the concept of a double-porosity system in 1960, entailing an aquifer comprising of fractures (high permeability, low / secondary porosity, low storage capacity) and porous matrix blocks (low permeability, high / primary porosity, high storage capacity). The fracture network is considered to be dense, homogenous and continuous, and is accepted as the sole pathway of water to the well. The matrix blocks are the source providing water to these fractures.

This approach therefore considers a twofold solution. If plotting s versus $\log(t)$, the shape of the graph represents one straight line indicating fracture flow into the well, and a second straight line representing the combined influence of fractures and the rock matrix.

2.3.3.3. Single vertical fracture flow

Cinco and Samaniego (1981, in Bäumlé, 2003) based the single vertical fracture concept on the assumption that a dyke or a network of vertical fractures can be represented by one single vertical aperture that fully penetrates the confined aquifer. Apart from this vertical fracture with aperture a_f and length $2L_f$, the remainder of the aquifer is assumed to be homogenous. Flow towards a well is unsteady state and occurs as linear flow, bilinear flow, formation linear flow or pseudo-radial flow with time.

Cinco and Samaniego (1981) continued to define mathematical equations for **fracture linear and bilinear flow** to determine the drawdown s within the fracture at a distance x from the pumped well (Equation 11).

$$s(x, t) = \frac{Q}{T_f a_f} \sqrt{\frac{T_f t}{S_f}} \left\{ \frac{e^{-b}}{\sqrt{\pi}} - b \times \operatorname{erfc}(b) \right\}, b = \frac{x}{\sqrt{4 \frac{T_f}{S_f} t}} \quad \text{Equation 11}$$

$$\text{with } b = \frac{y}{\sqrt{4 \frac{T_m t}{S_m}}} = \sqrt{\frac{S_m y^2}{4 T_m t}}$$

Where T_f = transmissivity of the single fracture [L^2/T]

a_f = fracture aperture [L]

S_f = fracture storage coefficient [-]

An approximation of the complementary error function is shown by Equation 12 (Cinco and Samaniego, 1981, in Bäumlé, 2003).

$$erfc(x) = \frac{2}{\sqrt{\pi}} \int_x^{\infty} \exp(-t^2) dt = 1 - \frac{2}{\sqrt{\pi}} \int_0^x \exp(-t^2) dt \quad \text{Equation 12}$$

The drawdown in a pumped well is shown by Equation 13 (Cinco and Samaniego, 1981, in Bäumlé, 2003).

$$s|_{x=0} = \frac{Q}{a_f} \sqrt{\frac{t}{\pi T_f S_f}} \quad \text{Equation 13}$$

Based on these equations, the drawdown – whether in the fracture or the well – is directly proportional to the pumping rate and period of pumping, and indirectly proportional to the transmissivity and storage of the single fracture.

Boonstra & Boehmer (1986) and Boehmer & Boonstra (1987) elaborated these equations in developing approaches to determine drawdown in a fracture/dyke and a well. These approaches considered the vertical dyke to be of infinite extent and finite conductivity.

For **formation linear flow** (Gringarten *et al*, 1974 in Bäumlé, 2003) worked on the unsteady-state linear flow from a rock formation into a fully penetrating well in a high permeability, vertical fracture zone. The fracture was assumed to have zero thickness with negligible storage and very high or infinite conductivity. Two solutions were developed, *viz.* the infinite conductivity (Equation 14) and uniform flux solutions (Equation 15).

$$s(y,t) = \frac{Q}{4\pi T_m} \frac{\sqrt{\pi}}{2} \int_0^{\tau} \exp\left(-\frac{(y/L_f)^2}{4\nu}\right) \left[erfc\left(\frac{0.134}{\sqrt{\nu}}\right) + erfc\left(\frac{0.866}{\sqrt{\nu}}\right) \right] \frac{d\nu}{\sqrt{\nu}} \quad \text{Equation 14}$$

$$s(y,t) = \frac{Q}{4\pi T_m} \frac{\sqrt{\pi}}{2} \int_0^{\tau} \exp\left(-\frac{(y/L_f)^2}{4\nu}\right) \left[erfc\left(\frac{1-x/L_f}{\sqrt{\nu}}\right) + erfc\left(\frac{1+x/L_f}{\sqrt{\nu}}\right) \right] \frac{d\nu}{\sqrt{\nu}} \quad \text{Equation 15}$$

2.3.3.4. Equilibrium approximations

Thiem (1906) developed the Thiem equilibrium equation (Equation 16) to aid in providing initial estimates of aquifer transmissivities where limited drawdown data is available. This equation

forms the basis of other equilibrium approximations as discussed in this section (Missteart, 2001).

$$T = \left(\frac{2.3Q}{2\pi s} \right) \log \frac{r_e}{r_w} \quad \text{Equation 16}$$

Where T = transmissivity [L^2/T]
 Q = well discharge rate [L^3/T]
 s = maximum well drawdown [L]
 r_e = radius of well influence [L]
 r_w = well radius [L]

However, as it is difficult to determine accurate well influence radii and, more specifically, the ratio r_e/r_w without several observation wells, a number of simplifications for this equation have been derived (Missteart, 2001). Applying to confined-aquifer conditions, the Logan approximation (Logan, 1964) has been developed. This is also the method applied to the constant discharge data in the FC-Programme, and assumes a typical value of 3.32 for r_e/r_w ; i.e., the method estimates the influence of the borehole. Due to the logarithmic scale of this ratio, the equation is not very sensitive to changes in the value, and subsequently the transmissivity will vary slightly with changes in this value (Equation 17).

$$T = 1.22 \frac{Q}{s} \quad \text{Equation 17}$$

2.3.3.5. Variable-discharge tests

Birsoy and Summers (1980) determined an analytical solution to describe the drawdown in a confined aquifer where pumping is changed step-wise or intermittently. Their approach is based on the Cooper-Jacob approximation of the Theis equation, and the drawdown at time t during the n th pumping period where pumping is intermittently or stepped is given as (Equation 18):

$$s_n = \frac{2.30Q_n}{4\pi KD} \log \left\{ \left(\frac{2.25KD}{r^2 S} \right) \beta_{t(n)}(t - t_n) \right\} \quad \text{Equation 18}$$

$\beta_{t(n)}(t-t_n)$ for the above equation changes depending on whether pumping is intermittently (i.e. interrupted, Equation 19) or step-wise (i.e. not interrupted, Equation 20).

$$\begin{aligned}
 \beta_{t(n)}(t - t_n) &= \prod_{i=1}^{n-1} \left(\frac{t - t_i}{t - t'_i} \right)^{Q_i / Q_n} && \text{Equation 19} \\
 &= \left(\frac{t - t_{1i}}{t - t'_{1i}} \right)^{Q_1 / Q_n} \times \left(\frac{t - t_2}{t - t'_2} \right)^{Q_2 / Q_n} \times \dots \times \left(\frac{t - t_n}{t - t'_n} \right)^{Q_{n-1} / Q_n}
 \end{aligned}$$

$$\begin{aligned}
 \beta_{t(n)}(t - t_n) &= \prod_{i=1}^n (t - t_i)^{\Delta Q_i / Q_n} && \text{Equation 20} \\
 &= (t - t_1)^{\Delta Q_1 / Q_n} \times (t - t_2)^{\Delta Q_2 / Q_n} \times \dots \times (t - t_n)^{\Delta Q_n / Q_n}
 \end{aligned}$$

2.3.4. Problems pertaining to pumping tests

A number of factors, many of which are avoidable, influence pumping test data. This becomes a tremendous problem due to the fact that pumping tests are often the only insight into the subsurface, and verification of the results is problematic. These factors can for all practical purposes be divided into three classes, viz. avoidable flaws, inherent flaws and interpretative flaws. This is summarized in Figure 2-8.

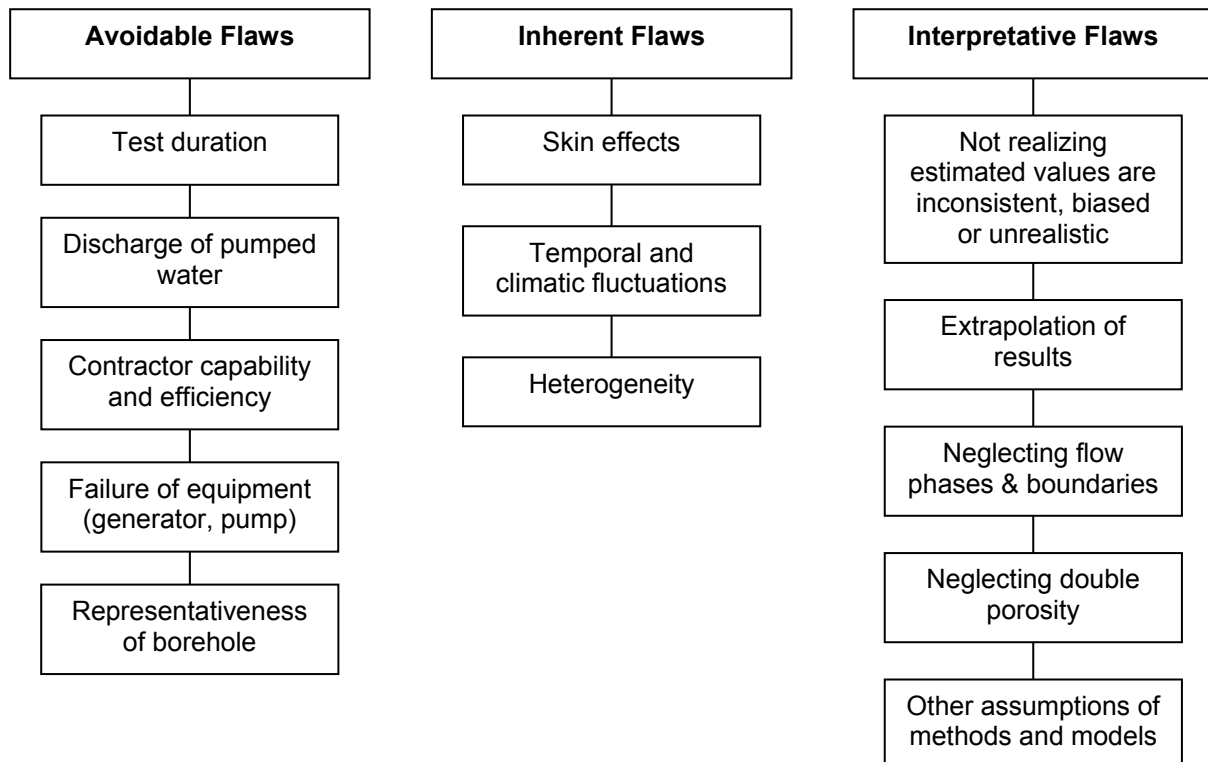


Figure 2-8: Some factors influencing pumping test data.

Well and reservoir effects comprise all the skin effects, including well-bore storage (water stored in the borehole that is being pumped before the aquifer is stressed), well-bore skin (low storage

area between borehole and aquifer), partial penetration skin (less infiltration area due to imperforated borehole screening) and fracture skin (change in permeability of fractures due to clogging). This is shown in Figure 2-9.

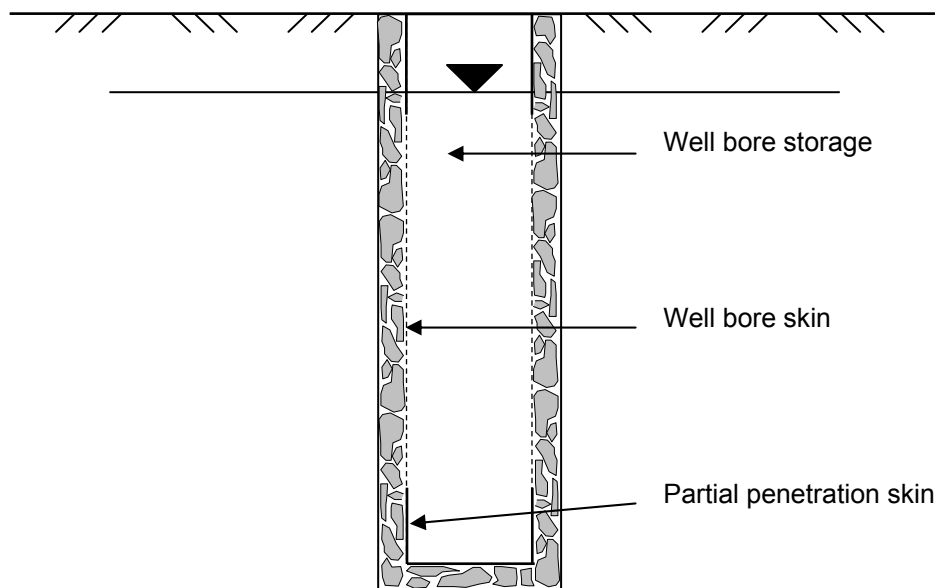


Figure 2-9: Skin effects influencing early pumping test data.

It is evident that the connection between the borehole and the aquifer is not always perfect, and that a number of factors can influence fluid migration during a pumping test. It is for this reason that pumping test duration (in terms of time) is so important. It ensures that all these so-called skin effects are overruled before estimating borehole and/or aquifer parameters based on irrelevant data.

Other influences on data include boundaries (barriers and recharge zones), as well as variations and fluctuations during the test (i.e. proximate boreholes being pumped, climate, tides).

It should also be known that the various methods have different assumptions. It almost never applies that all assumptions are valid for a specific scenario when fractured aquifers are involved, and subsequently one has to consider the potential inaccuracies inherent to the method applied. Some typical assumptions pertaining to various methods include (Kruseman & De Ridder, 1989):

- Confined aquifer.
- Infinite aerial extent.
- Homogenous, isotropic aquifer with uniform thickness.
- Horizontal piezometric surface.
- Constant discharge (pump) rate.

- Fully penetrating well.
- Water removed from storage is immediately discharged (for unsteady-state).
- Well diameter and storage negligibly small (for unsteady-state).

2.4. Sustainable Yield

Sustainable yield can be defined as that rate at which water can be pumped from a borehole so as not to deplete the water source (Kendy, 2003). Another source defines sustainable yield as the long-term rate at which water can be withdrawn from a borehole without resulting effects such as exhaustion of the reservoir, excessive pumping costs, or deterioration in the water quality (Caro & Eagleson, 1981). Considering the definition of a sustainable pumping rate, it is therefore only relevant to the particular borehole being tested, and does not include abstraction from other boreholes in the proximity of the tested borehole.

However, other groundwater users do exist within the same catchment, and subsequently the abstraction from these boreholes influence the groundwater availability in the tested borehole by decreasing the amount of water available. The predefined concept of a “sustainable yield” therefore can be considered a best-case scenario as it overestimates safe pumping rates based on the assumption that no other groundwater users are present in the proximity of the tested borehole.

In order to more accurately define the sustainability of abstraction from a particular borehole, one has to consider the catchment as a whole. A certain amount of groundwater is available per catchment and a sustainable yield per catchment is a much more plausible approach. Based on this, a safe extractable volume of water can be determined. This however poses another problem: how can groundwater allocation be controlled to prevent depletion or overexploitation of the groundwater reserve? As not all knowledge regarding groundwater abstraction is always available, the true abstraction from the catchment is always an underestimate.

Calculation of the sustainable yield is shown in Equation 21 - Equation 23, and is based on the constant discharge test data. Drawdown s at given time t_{long} and pumping rate Q is required, all being dependent on transmissivity T and storativity S . The maximum drawdown available is $s_{available}$ which is required to determine the sustainable yield $Q_{sustainable}$ (Van Tonder *et al*, 1998).

$$\frac{s(t = t_{long})}{Q} = const_{well}(T, S) \quad \text{Equation 21}$$

$$s'_{available} = s_{available} - 2\sigma_s \quad \text{Equation 22}$$

$$Q_{sustainable} = Q_{pumpingtest} \frac{s_{available}(t = t_{long}) - 2\sigma_s(t = t_{long})}{s_{extrapolation_pumpingtest}(t = t_{long})} \quad \text{Equation 23}$$

Kendy (2003) states that groundwater information alone is not suitable to address groundwater sustainability, but that the whole hydrological cycle has to be considered as a whole. A water budget (and subsequently stabilising of the water table) depends on historical, present and proposed future usage, as well as water added to the groundwater regime via processes such as recharge, and water removed from the water cycle via processes such as evaporation and transpiration. These aboveground consumption rates are in fact the important parameter in determining sustainable pumping rates.

A number of considerations are applicable in addressing sustainable yield. These include a clear understanding of the spatial aspects of the problem (i.e. the scale of reference), development of a conceptual water budget, clear understanding of the system boundaries, understanding the water requirements and needs, realizing that it is a problem of time and space, noting that technology is changing, understanding tradeoffs (i.e. that water is needed, but environment should not be harmed in the process), and realizing that our knowledge is limited (Maimon, 2004).

2.5. Flow Characteristic (FC) Programme

The Institute for Groundwater Studies (IGS) of the University of the Free State (UFS), South Africa was funded by the Water Research Commission (WRC) to develop a method for pumping test analyses in fractured-rock aquifers. This programme collates a number of mathematical and graphical approaches to determine hydrological parameters including transmissivity and storage coefficient. The FC Programme aims to estimate a sustainable yield based on risk. This is done for each borehole and utilises a variety of methods. In a South African context, this is especially important for water supply to rural communities. (Van Tonder et al, 2001).

This programme was used in this study to evaluate all the available pumping test data.

3. CASE STUDY

The area of interest is situated within the Limpopo and Luvuvhu/Letaba Water Management Areas (WMAs 1 and 2). Testing sites have been outlined within these portions and are indicated in (Figure A-1, Appendix A).

3.1. Study Area

The two Water Management Areas (WMAs) of interest are situated in the northern part of South Africa, and are predominantly underlain by Basement rocks, mainly characterised by hard, crystalline, fractured igneous rocks. These were selected as part of the WRC project and are shown in Figure A-1, Appendix A. The topography of the study areas is shown in Figure 3-1.

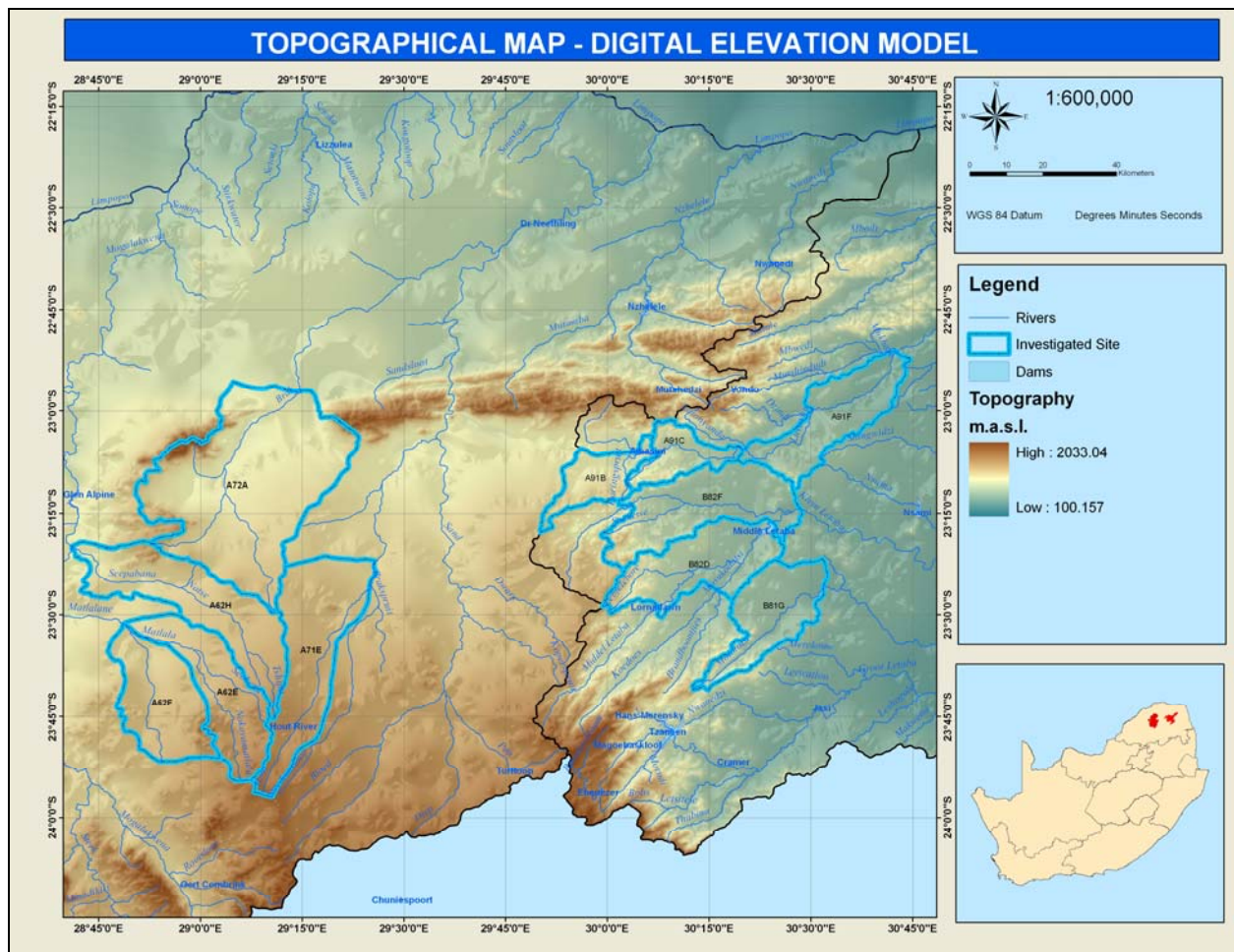


Figure 3-1: Topography of study area.

3.1.1. Limpopo Water Management Area

The Limpopo Water Management Area (WMA1) is found in the northern part of South Africa and is shared between South Africa, Botswana, Zimbabwe and Mozambique. Surface water flows in the Mokolo, Lephhalala, Mogalakwena, Sand and Nzhelele Rivers. Some smaller tributaries are also present. Essentially, water drains through all these rivers towards the Limpopo River in the north. The Limpopo River flows eastwards and eventually mouths in the Indian Ocean in Mozambique. Surface runoff is limited and highly seasonal due to limited rainfall in this WMA. The Waterberg area has better base flow and subsequently more water is available as surface flow (DWAF, 2003a).

The Limpopo WMA is characterised by semi-arid temperatures in the southern portions to more arid towards the north. Rainfall is seasonal with mean annual precipitation ranging between 300 mm and 700 mm per annum (DWAF, 2003a).

Topography (Figure 3-1) is predominantly flat to rolling with the two major topographic features being the Waterberg in the southern portion and the Soutpansberg in the north-eastern portion (DWAF, 2003a). The topography to the north of Polokwane is fairly flat with the exception of the Blouberg and Soutpansberg. The average elevation in the central part of the Limpopo WMA's project area is between 400 and 800 metres above sea level and between 1 200 and 1 600 metres above seal level at Blouberg and Soutpansberg areas (Alberts, 1985).

The Limpopo WMA is subdivided into five key areas based on the respective sizes, locations, homogeneities of properties, locations of water infrastructure such as dams, and their management and economic development (DWAF, 2003a). These are:

- Matlabas/Mokolo sub-area, comprising Matlabas and Mokolo River catchments.
- Lephhalala sub-area, including the Lephhalala River catchment and some smaller streams draining towards the Limpopo River.
- Mogalakwena sub-area, mainly comprising the catchment of the Mogalakwena River.
- Sand sub-area, including the Sand River catchment and some smaller streams.
- The Nzhelele/Nwanedzi sub-area comprising the catchments of the Nzhelele and Nwanedi Rivers.

Irrigation is the by far the greatest consumer of water in the Limpopo WMA. Approximately 75% of the total water requirements in this WMA are being supplied for irrigation (DWAF, 2003a).

Groundwater recharge reaches approximately 702 million m³/a assuming recharge being 2% of the mean annual precipitation. Sewage effluent from Polokwane adds to this recharge (DWAF, 2004a).

Surface water quality is generally acceptable, although high turbidity can be anticipated during increased runoff. Groundwater, on the other hand, is being used throughout the Limpopo WMA for mainly rural water supply. Recharge to the groundwater regime is mostly through infiltration from sandy riverbeds.

Informal settlements and mining activities may affect the groundwater quality in the Mogalakwena area. Overexploitation and fertilizer usage in the Sand River area increases the nitrate levels that may eventually influence the groundwater quality in the vicinity of Vivo and Dendron. No other major water quality problems have been reported and no major water quality concerns are currently evident for the Nzhelele and Nwanedi areas (DWAF, 2004b).

3.1.2. Luvuvhu-Letaba Water Management Area

The Luvuvhu-Letaba Water Management Area is situated in the north-eastern corner of South Africa. This catchment is bounded by Zimbabwe in the north and Mozambique in the east. Luvuvhu-Letaba also falls within the Limpopo River Basin shared by South Africa, Botswana, Zimbabwe and Mozambique.

Surface drainage is generally controlled by the Luvuvhu, Shingwedzi and Letaba (Groot and Klein Letaba) Rivers. Agriculture is the major economic activity within the area. Over-irrigation and deforestation are major concerns and scattered mining developments are found within the southern portions of the WMA.

Luvuvhu-Letaba WMA is characterised by subtropic temperatures becoming semi-arid and arid. Rainfall occurs mainly in summer and varies between less than 300 mm per annum in the Lowveld region to 1 000 mm per annum along the western escarpment (DWAF, 2003b).

The central, north- and south-eastern parts are low lying areas with average elevation of 200 – 400 metres above sea level (Figure 3-1). The western part of the Luvuvhu/Letaba WMA's project area exhibits elevation of 400 – 800 metres above sea level. Near Tzaneen, the elevation increases up to 1 600 m at Magoebaskloof and Duiwelskloof (Du Toit, 2003b).

The Groot Letaba River and Klein Letaba River are the two main perennial rivers in the Luvuvhu/Letaba WMA's project area.

This catchment has also been subdivided into five key areas (DWAF, 2003b):

- Luvuvhu/Mutale sub-area, comprising Luvuvhu and its main tributary, the Mutale River catchments.
- Shingwedzi sub-area, including the Shingwedzi River catchment falling within the boundaries of South Africa.
- Groot Letaba sub-area, comprising the Groot Letaba River catchment until its confluence with the Klein Letaba River.
- Klein Letaba sub-area, including the Klein Letaba River catchment until its confluence with the Groot Letaba River.
- Lower Letaba sub-area, comprising the Letaba River catchment from the Groot Letaba and Klein Letaba confluence to the Olifants River.

Irrigation is by far the biggest consumer of water in the Limpopo WMA, accounting for approximately three-quarters of the water requirements. Due to the low rainfall in portions of this area, surface runoff is limited and highly seasonal (DWAF, 2003b).

Surface water quality is generally good, especially in the mountainous areas where higher rainfall occurs. Surface water tends to be somewhat polluted with bacteria from rural areas and areas with insufficient sanitation. Groundwater is mainly used for rural water supply and stock watering. Overexploitation of groundwater may furthermore pose problems (DWAF, 2003b).

Eutrophication is the main adverse influence on groundwater quality over the whole area due to sewage treatment and rural settlements. Water in the Luvuvhu/Mutale and Letaba/Shingwedzi areas is generally of good quality (DWAF, 2004b).

3.2. Geology of the Study Area

The study area was chosen to represent Basement aquifers in South Africa. The geology is shown in Figure 3-2.

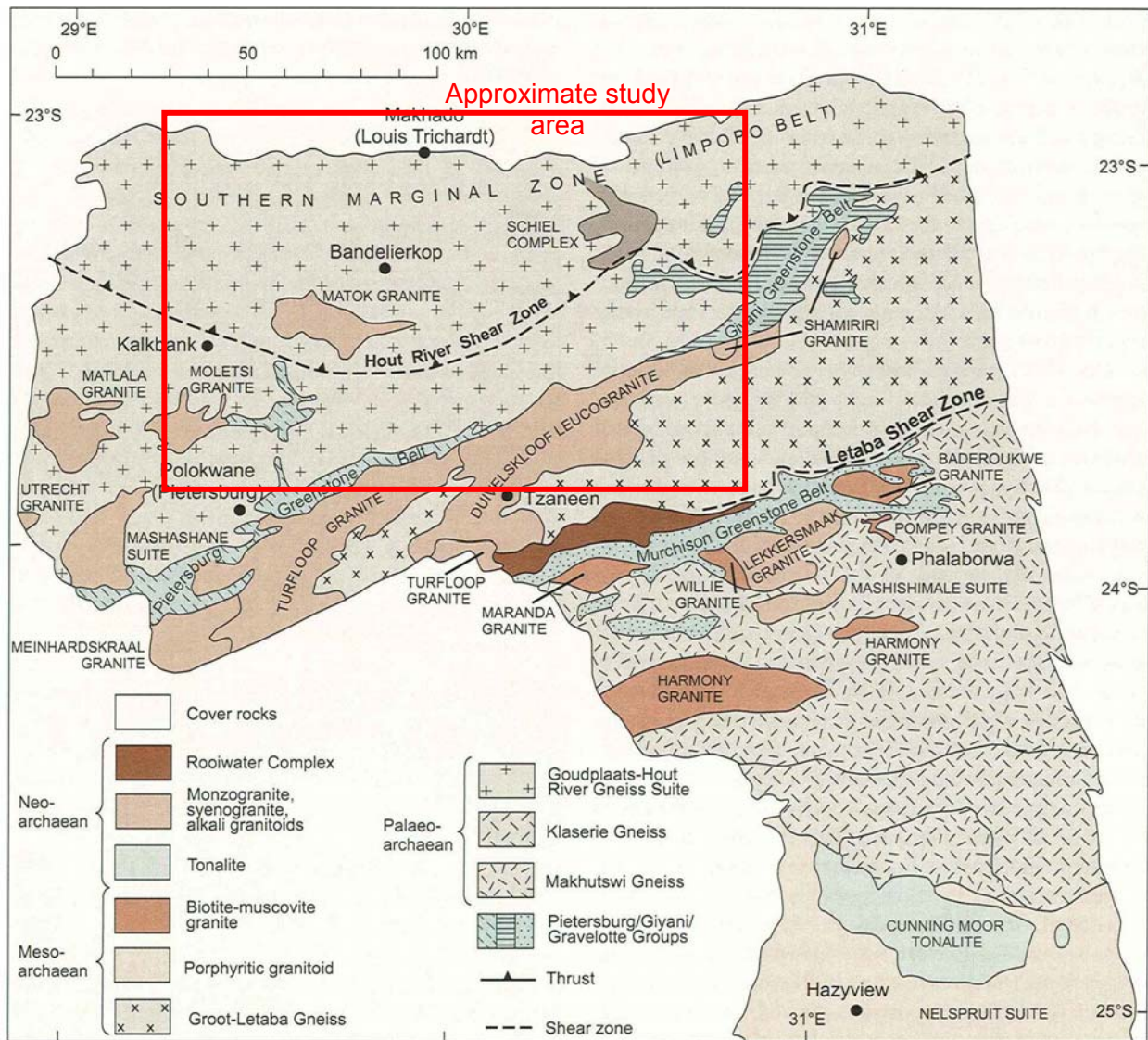


Figure 3-2: Geology of the study area (adapted from Robb *et al*, 2006).

According to Robb *et al* (2006), the north-eastern Kaapvaal craton (north of 25°S) comprise the Goudplaats-Hout River Gneiss Suite of Palaeoarchaean age (3 600 – 3 200 Ma). These gneisses vary greatly, ranging from homogenous to distinctly layered with colour from leucocratic to dark coloured. Various granitoid rocks comprise this suite as is evident from the previous subdivisions into leucocratic migmatitic Hout River gneiss and layered grey Goudplaats gneiss.

Figure 3-3 shows the different igneous rock compositions in terms of quartz, alkali feldspar (orthoclase / potassium feldspar) and plagioclase (sodic and calcic feldspar). The different proportions of these minerals control the classification of granitic rocks and also the nature of weathering, the latter being indicative of expected weathering patterns, secondary clay minerals forming and potential recharge or infiltration capacity.

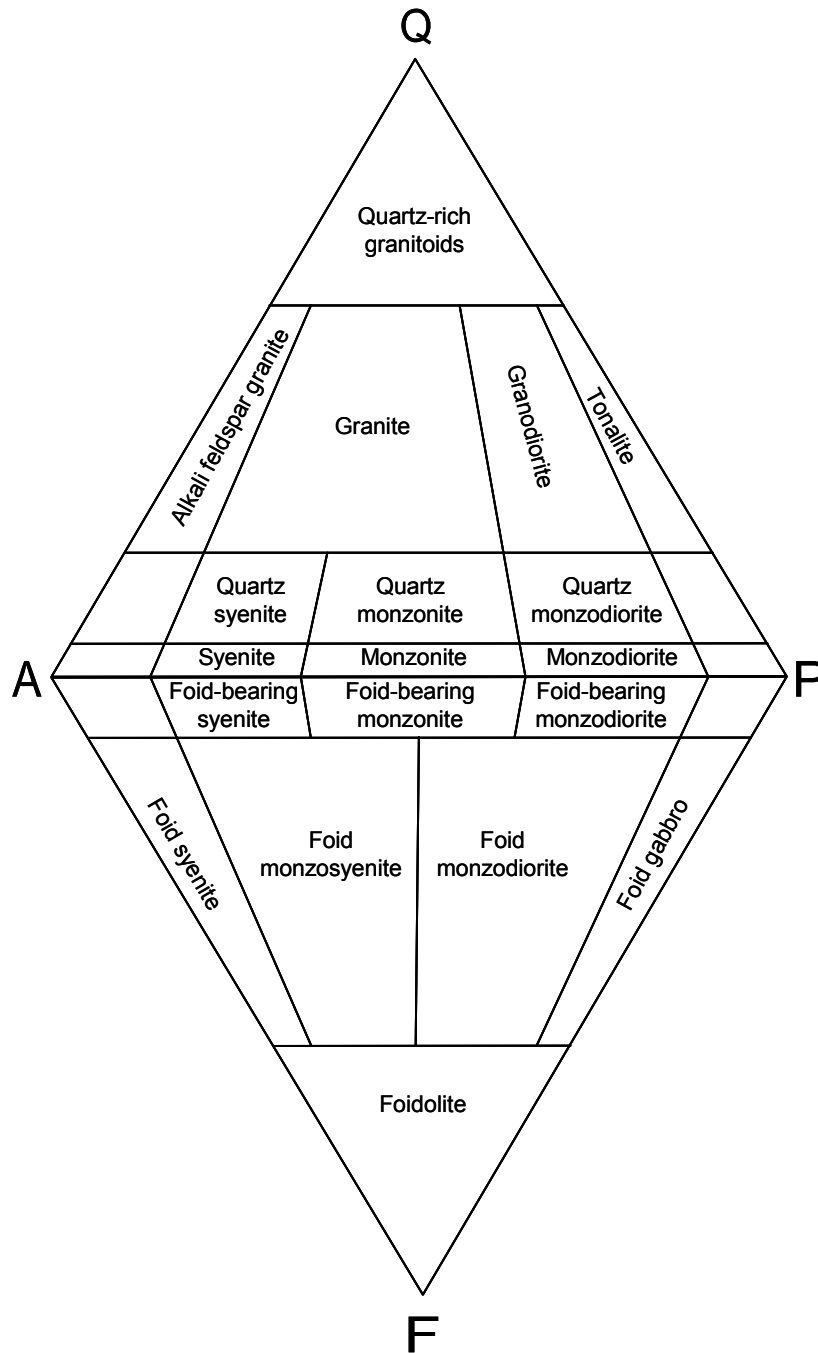


Figure 3-3: Quartz (Q) – Alkali feldspar (A) – Plagioclase (P) – Foid (F) diagram depicting igneous rock composition (after: Blatt & Tracy, 1997).

Near Polokwane, the bedrock is typically homogenous, greyish, medium-grained biotite gneiss with a syenogranitic composition (suggesting prevalence of feldspar to quartz). To the northeast of Polokwane, the gneiss becomes more migmatitic with intruded non-migmatitic gneiss of granodioritic composition (Matlala and Moletsi Granites). Further north, just to the south of the Hout River Shear Zone, the gneiss is coarse-grained, pegmatoidal and leucocratic with minor biotite (Robb *et al*, 2006).

To the north of the Matok Granite near Bandelierkop, bedrock becomes greyish migmatitic gneiss and leucocratic anatectic granite respectively. The gneiss is layered, granodioritic and migmatitic to some extent. The granite is more coarse-grained to pegmatoidal, foliated and monzogranitic to tonalitic in composition (Robb *et al*, 2006).

Towards Giyani, the bedrock is more uniform and characterised by medium-grained leucocratic gneiss with characteristic whitish or pinkish colour and monzogranitic composition. Subordinate darker layered gneiss with monzogranitic to granodioritic composition occurs throughout this area, and often occurs alternating with the leucocratic gneiss in layers with 1 – 10m width. Throughout the Goudplaats area, greyish gneisses with more tonalitic, trondjemitic and granodioritic composition also occur (Robb *et al*, 2006).

Three distinct younger plutons are intruded into the Goudplaats-Hout River Suite to the north and east of Polokwane: the Matlala Granite, Moletsi Granite and Matok Granite. The prior two suites are generally pinkish granitic with biotite as the predominant mafic mineral, whereas the Matok Granite is orthopyroxene-bearing (i.e. charnockitic). The latter granite is also whitish to pinkish in colour, ranging in composition between syenogranite and granodiorite. Three distinct non-igneous outcrops occur in the study area, including the Schiel Complex, Giyani Greenstone Belt and Pietersburg Greenstone Belt (Robb *et al*, 2006). Notably is the orientation of the HRSZ with regard to the Matok Granite, Schiel Complex and Giyani Greenstone Belt as some discrepancies regarding its orientation do exist.

From a structural point of view, this area forms part of the Southern Marginal Zone (SMZ) of the Limpopo Belt. The Hout River Shear Zone (HRSZ) runs west-east through the study area and the Goudplaats-Hout River Gneiss Suite is bounded in the southeast by the Letaba Shear Zone (Robb *et al*, 2006).

The results of the airborne geophysics conducted by the Council for Geoscience are shown in Figure A-2, Appendix A. From this it is evident that the main structural directions vary based on the HRSZ. The areas to the north of the HRSZ is characterised predominantly by ENE-WSW striking structures, whereas the southern portions are mainly deformed by NE-SW striking structures. This can also be a result of the neotectonic influences on the study area, or, as stated by Robb *et al* (2006), the high-grade terrane to the north of the HRSZ and the low-grade terrane to the south.

Kreissig *et al* (2001) dated the shearing event of the Hout River Shear Zone (HRSZ) – a major E-W striking structural influence of groundwater movement in the Limpopo WMA (WMA1) and

Luvuvhu/Letaba WMA (WMA2) – as approximately 2 690 – 2 643 Ma. This event therefore does not represent neotectonic events or prevailing conditions, but an Archaean event of which the influence is still evident. The HRSZ is shown in context of the Limpopo craton in Figure 3-4.

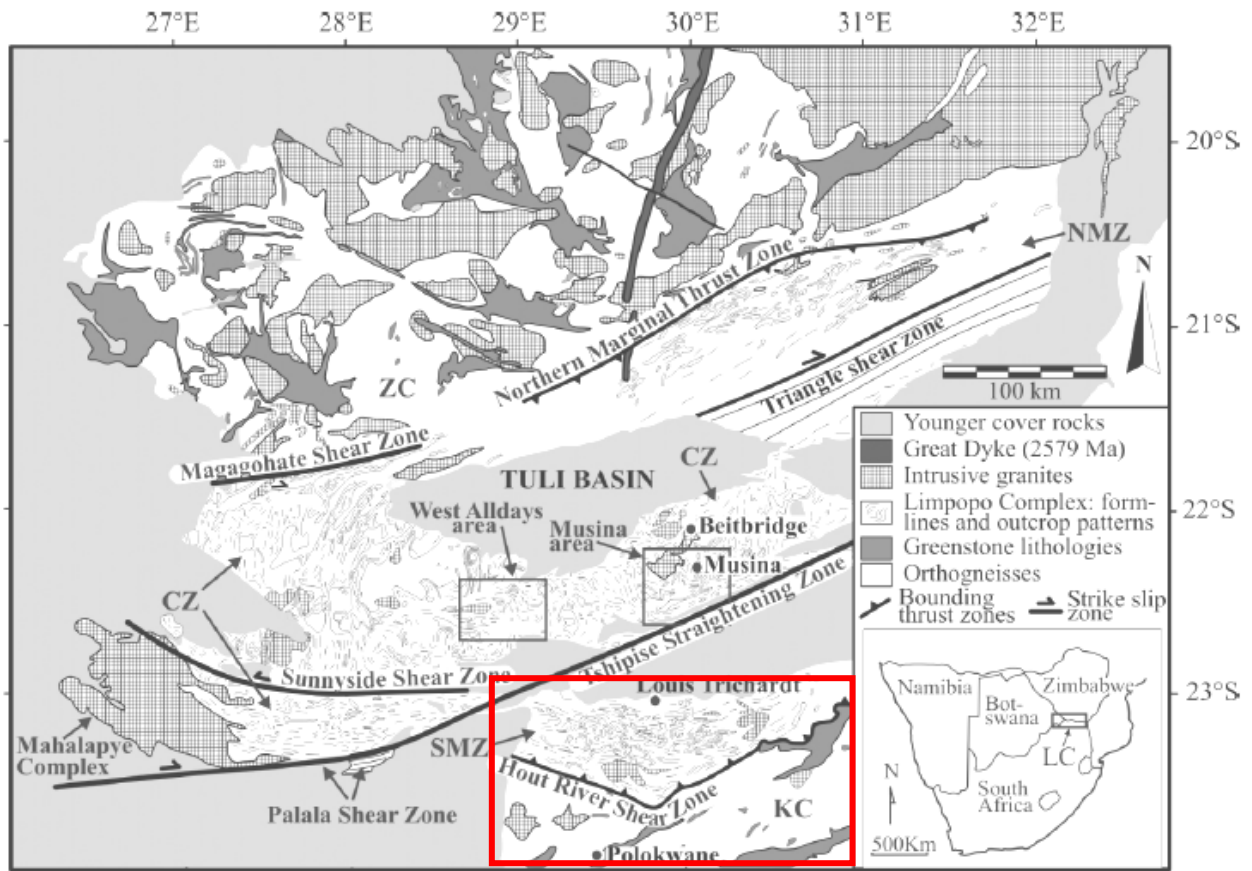


Figure 3-4: Sketch map of the Limpopo Complex showing the Hout River Shear Zone (after Van Reenen *et al*, 1990 and Boshoff, 2004 in Boshoff *et al*, 2006).

The current tectonic stress field in southern Africa is shown in Figure 3-5.

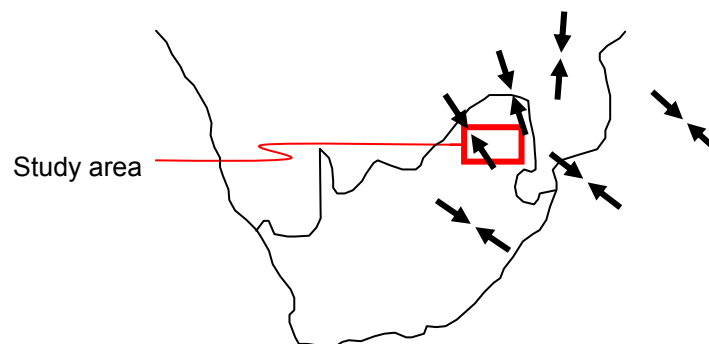


Figure 3-5: Schematic diagram depicting the current compressive stress conditions in Limpopo Province, southern Africa (adapted from Bird *et al*, 2006).

3.3. Terrane Settings (Sub-areas)

Based on the available information, the study areas is subdivided into four settings as shown in Table 3-1. The two variables in the setting determination is the climate (which coincides with the orientation of the HRSZ, and is subsequently labelled north or south; also the catchment area as WMA1 is on average more arid than WMA2) and the structural influences. The precipitation over the study area is shown in Figure A-3, Appendix A.

The areas north of the HRSZ represent Archaean tectonic events outcropping due to erosion of the African erosion surface. This divide is best noted via the distinct change in structural orientations over the HRSZ.

Table 3-1: Definition of the four settings.

<i>Sub-area</i>	<i>WMA</i>	<i>Climate</i>	<i>Prevailing compressive forces</i>	<i>Main structural strike</i>	<i>Inferred "Open structure" strike</i>	<i>Inferred "Closed structure" strike</i>
1N	WMA1 (west)	Very arid (north)	NW-SE	ENE-WSW	NE-SW	NW-SE
1S		Arid (south)	NW-SE	NE-SW	NE-SW	NW-SE
2N	WMA2 (east)	Arid (north)	NNW-SSE	ENE-WSW	ENE-WSW	NNW-SSE
2S		Humid (south)	NNW-SSE	NE-SW	ENE-WSW	NNW-SSE

Each of these settings has very specific influences determining the transmissivities obtained during pumping testing.

3.4. Pumping Tests

A summary of the results of the pumping tests is shown in Table B-1, Appendix B. Table 3-2 shows the boreholes per H-number and the amount of useable data points from each catchment. Although there are many more DWAF boreholes in these areas, the small quantity used is mainly due to:

- Missing coordinates for the boreholes in the GRIP database.
- No pumping tests conducted on boreholes.

A total number of 1 124 boreholes have constant discharge and/or step-test data available with reasonable GPS coordinates. Only these boreholes were subsequently used in the analyses. Different consultants and contractors were used to conduct many of the pumping tests over a

number of years. The data is therefore influenced by long-term climatic fluctuations, seasonal rainfall and changes in groundwater extraction by farmers, communities and mines.

Table 3-2: H-numbers and amount of boreholes used in the investigation.

<i>H-Number</i>	<i>Size of Dataset</i>	<i>No with Constant Tests</i>	<i>No with Step Tests</i>
H-04	310 boreholes	307	291
H-07	238 boreholes	237	228
H-10	87 boreholes	87	87
H-11	44 boreholes	44	44
H-16	166 boreholes	166	165
H-17	122 boreholes	122	122
H-20	157 boreholes	157	157
Total	1 124 boreholes	1 120	1 094

Furthermore, storativity was assumed to be 0.001 for all the tests interpreted with the FC Programme. The methods used in the FC Programme are very insensitive to changes in S, and no observation boreholes were used during the pumping tests. The calculated storativity values are therefore biased and cannot be used further. Due to the insensitivity of the Theis method in the FC Programme (resulting from manual graph fitting), the S-values calculated with this method were not used either.

3.5. Map Compilation

Maps were compiled using ArcView 9.0 © to depict all data and outcomes. A base map was compiled containing the geology, topography and water management areas. Structural data from aeromagnetic investigations was obtained from the Council for Geoscience and was also plotted on the map. The calculated transmissivities (T-values), sustainable yields and static water levels were plotted on this overlay to show the T-value distribution over the study area.

4. ANALYSIS

4.1. Pumping Test Results

Three boreholes are used to show the results of the pumping test interpretation. These boreholes were chosen as representatives of two extreme scenarios (a higher transmissivity borehole reaching steady-state conditions at late times and a low transmissivity borehole influenced by flow barriers at late times) and the intermediate transmissivity scenario. These boreholes are discussed in this section and all other results are summarised in Table B-1, Appendix B.

The boreholes used as examples are:

- High T Scenario: H04-0306.
- Intermediate T Scenario: H10-0084.
- Low T Scenario: H07-0841.

The constant discharge and recovery test data for boreholes H04-0306, H10-0084 and H07-0841 are shown in Table B-2, Table B-3 and Table B-4 (Appendix B). The step-drawdown data for these boreholes are shown in Table B-5, Table B-6 and Table B-7 (Appendix B).

4.1.1. High T Scenario: H04-0306

The static water level (SWL) prior to the pumping test of H04-0306 was measured using an interface meter to be 4.11m below natural ground level. The constant discharge test was done with a pumping rate of 14.1 l/s; the results are shown in Figure 4-1.

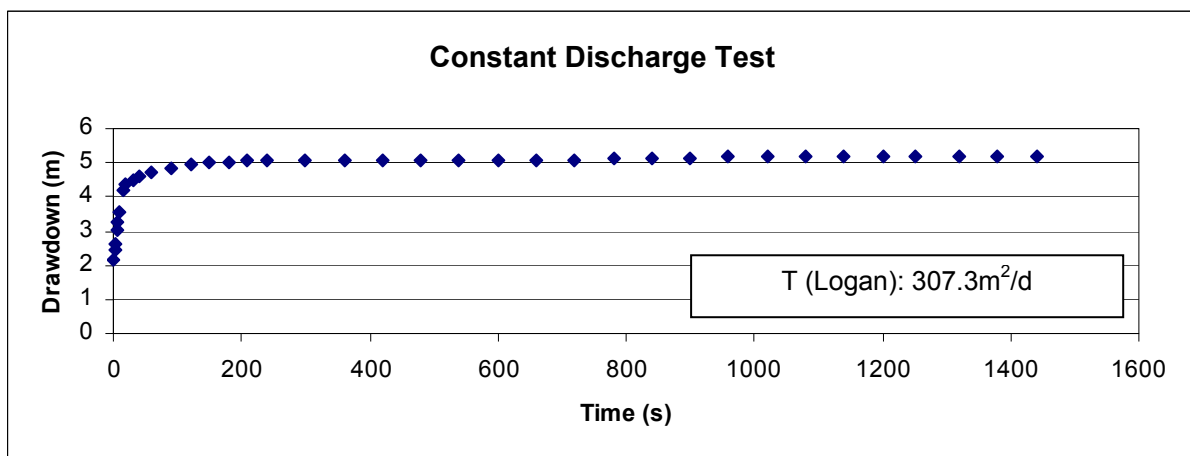


Figure 4-1: Constant discharge test results of borehole H04-0306.

For this borehole, the transmissivity was determined as 307.3 m²/d according to the Logan approximation. Other methods used for the constant discharge test were the Theis method and the Cooper-Jacob approximation. These functions are incorporated in the FC Programmeme where drawdown is plotted against time in minutes on a semi-log plot (Figure 4-2 and Figure 4-3).

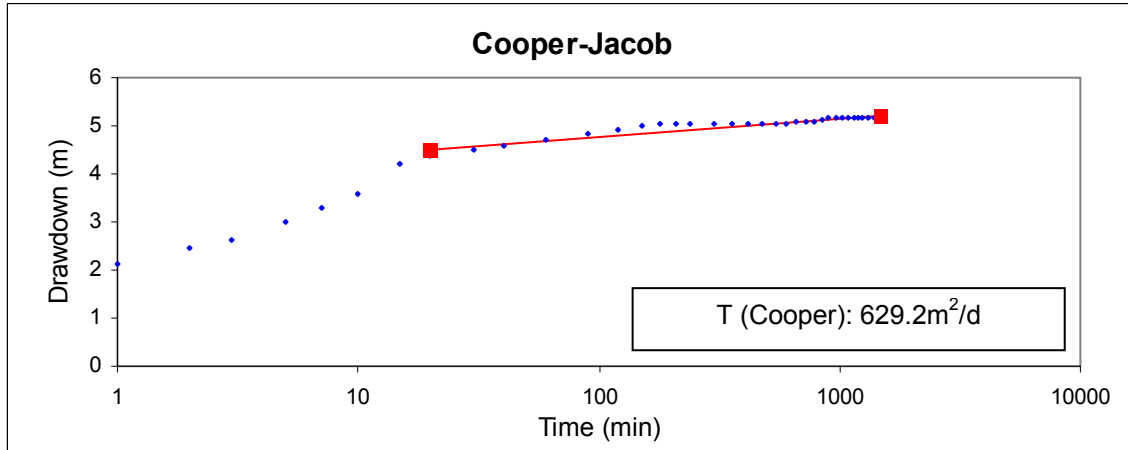


Figure 4-2: Cooper-Jacob fitting for borehole H04-0306.

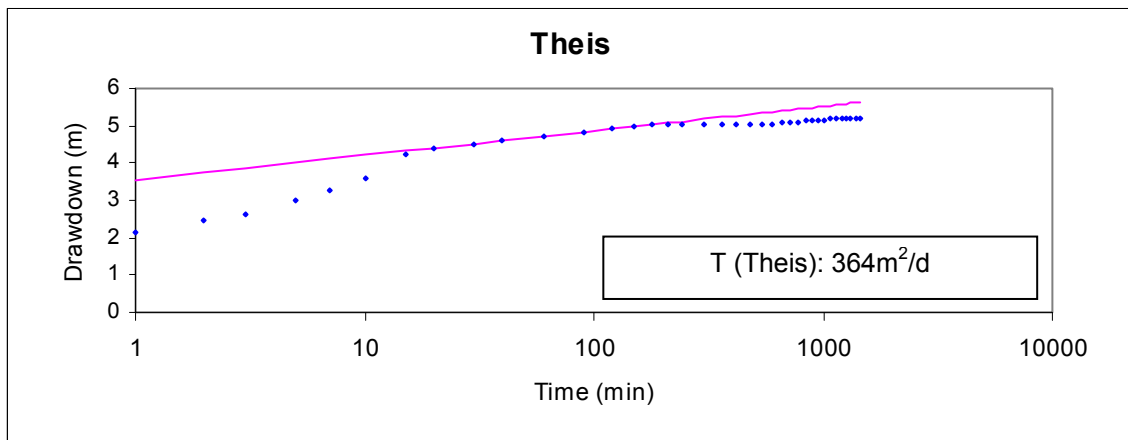


Figure 4-3: Theis fitting for borehole H04-0306.

Based on these latter two methods, transmissivities (T-value) of 629.2 m²/d (Cooper-Jacob) and 364 m²/d (Theis) were calculated respectively. The T-value from the Cooper-Jacob method represents late-time data. In the Theis method, the storativity (S-value) was determined to be ~1x10⁻⁶ by means of graph fitting.

The time-drawdown curve for the step-drawdown test is shown in Figure 4-4.

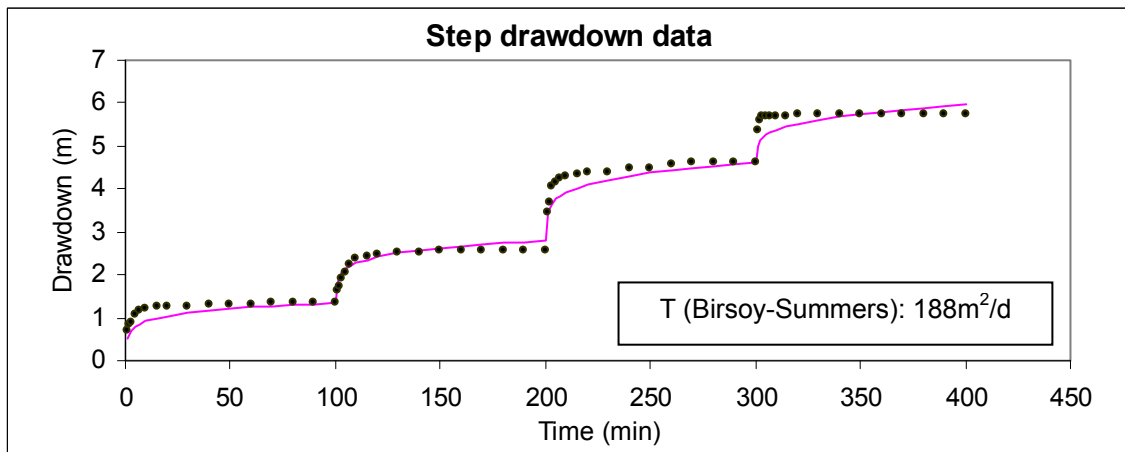


Figure 4-4: Step-drawdown test results of borehole H04-0306.

Based on the step-test data, a T-value of 188.0 m²/d was determined using the the Birsoy-Summers method. An S-value of 0.001 was assumed for the calculation as discussed in Section 3.4.

Borehole H04-0306 (as an example of a High T Scenario borehole) shows high transmissivities ranging between 188.0 m²/d – 629.2 m²/d.

4.1.2. Intermediate T Scenario: H10-0084

The static water level (SWL) prior to the pumping test of H10-0084 was measured using an interface meter to be 47.26m below natural ground level. The constant discharge test was done with a pumping rate of 4.0 l/s; the results are shown in Figure 4-5.

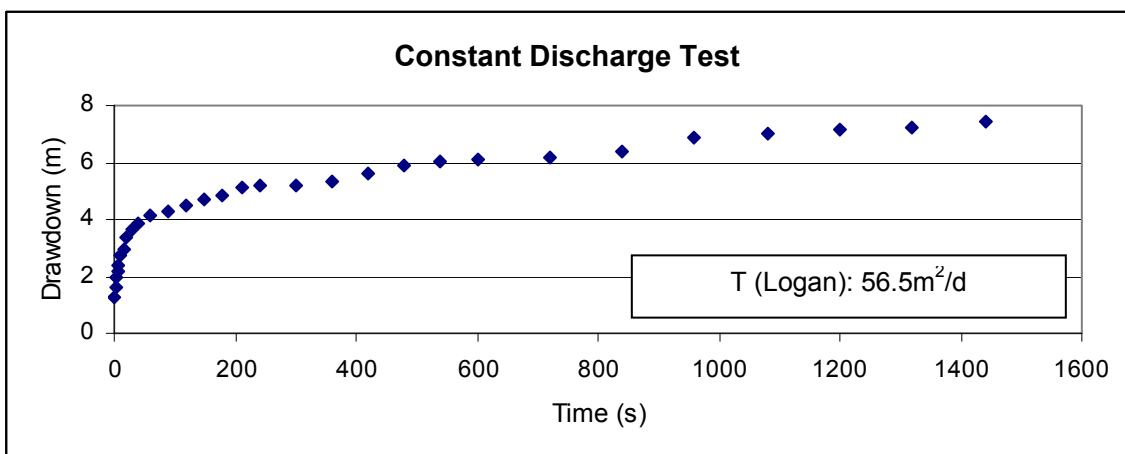


Figure 4-5: Constant discharge test results of borehole H10-0084.

For this borehole, the transmissivity was determined as $56.6 \text{ m}^2/\text{d}$ according to the Logan approximation. Other methods used for the constant discharge test once again were the Theis method and the Cooper-Jacob approximation (Figure 4-6 and Figure 4-7).

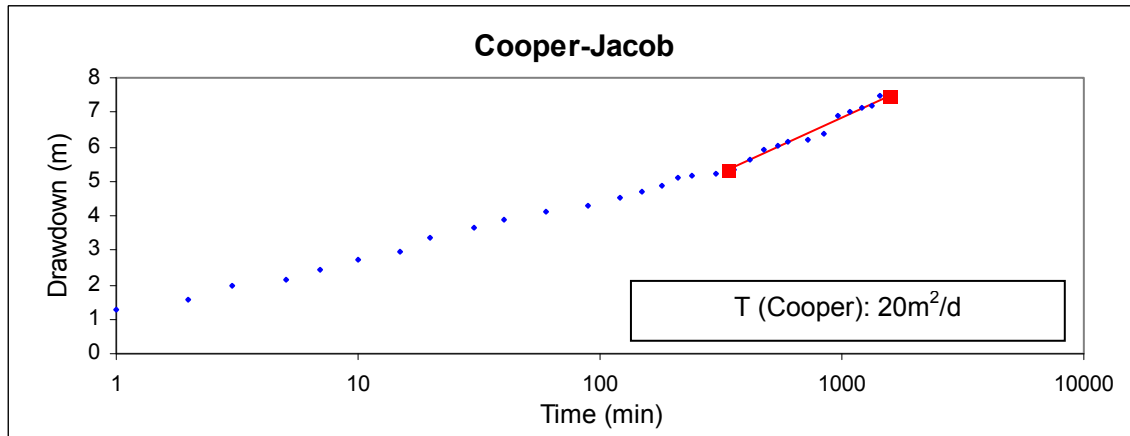


Figure 4-6: Cooper-Jacob fitting for borehole H10-0084.

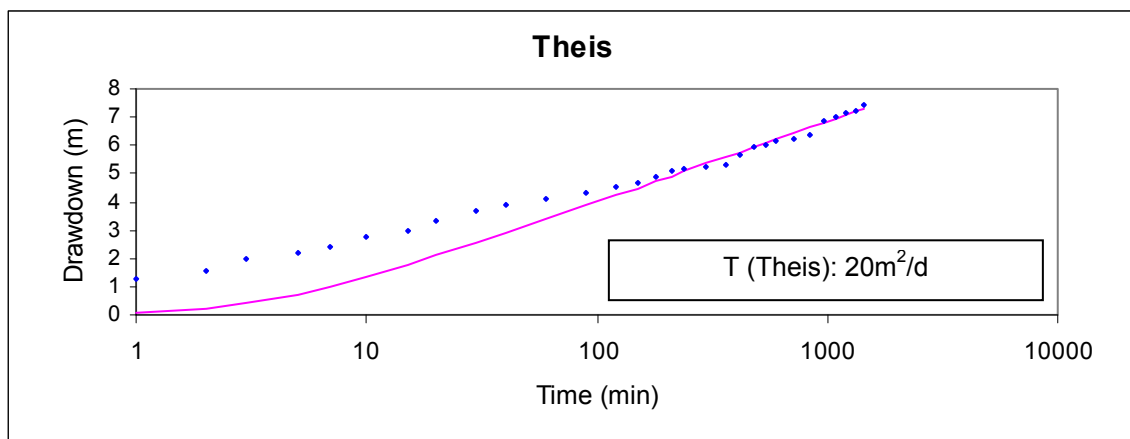


Figure 4-7: Theis fitting for borehole H10-0084.

Based on these latter two methods, transmissivities (T-value) of $20 \text{ m}^2/\text{d}$ (Cooper-Jacob) and $20 \text{ m}^2/\text{d}$ (Theis) were calculated respectively. The T-value from the Cooper-Jacob method once again represents late-time data. In the Theis method, the storativity (S-value) was determined to be $\sim 1.6 \times 10^{-2}$ by means of graph fitting.

The time-drawdown curve for the step-drawdown test is shown in Figure 4-4.

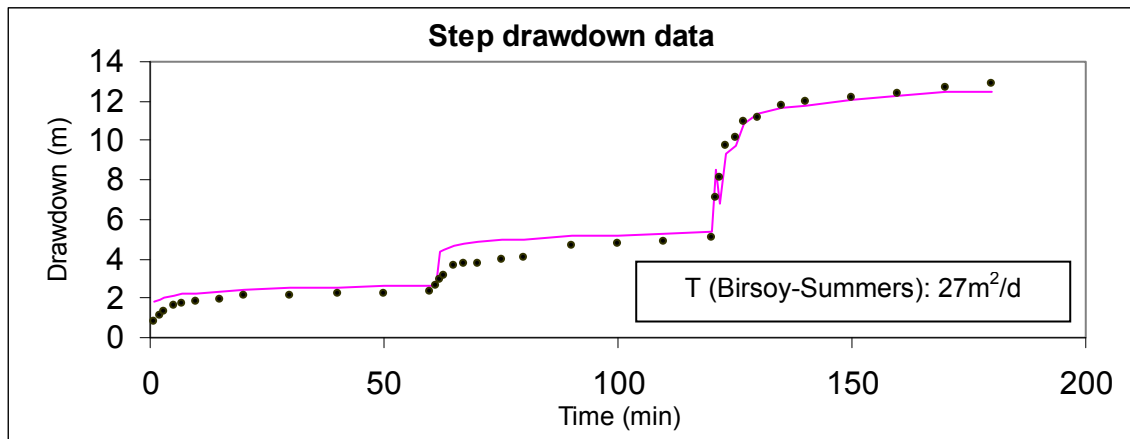


Figure 4-8: Step-drawdown test results of borehole H10-0084.

Based on the step-test data, a T-value of 27 m²/d was determined via the Birsoy-Summers method. An S-value of 0.001 was assumed for the calculation as discussed in Section 3.4.

Borehole H10-0084 (as an example of an Intermediate T Scenario borehole) shows moderate transmissivities ranging between 2.0 m²/d – 56.6 m²/d.

4.1.3. Low T Scenario: H07-0841

The static water level (SWL) prior to the pumping test of H07-0840 was measured using an interface meter to be 8.90m below natural ground level. The constant discharge test was done with a pumping rate of 1.02 l/s; the results are shown in Figure 4-9.

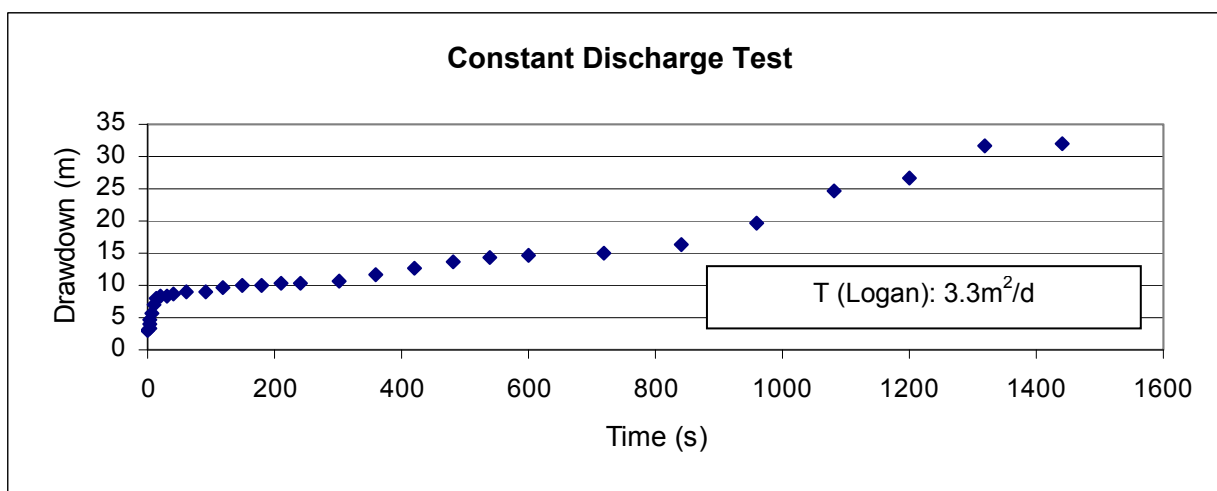


Figure 4-9: Constant discharge test results of borehole H07-0841.

For this borehole, the transmissivity was determined as $3.3 \text{ m}^2/\text{d}$ according to the Logan approximation. Other methods used for the constant discharge test once again were the Theis method and the Cooper-Jacob approximation (Figure 4-10 and Figure 4-11). Note that the Cooper-Jacob fit calculated three T-values based on early, intermediate and late pumping times (Figure 4-10).

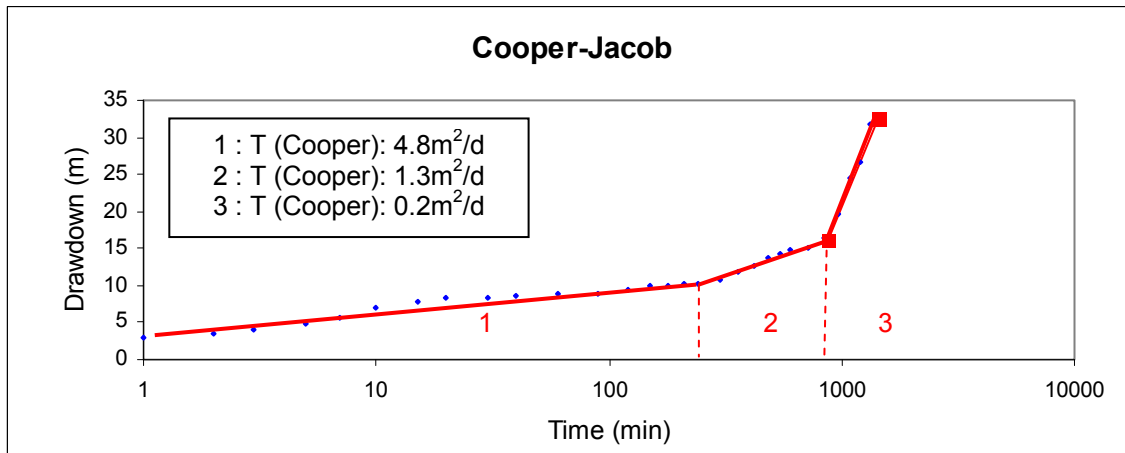


Figure 4-10: Cooper-Jacob fitting for borehole H07-0841.

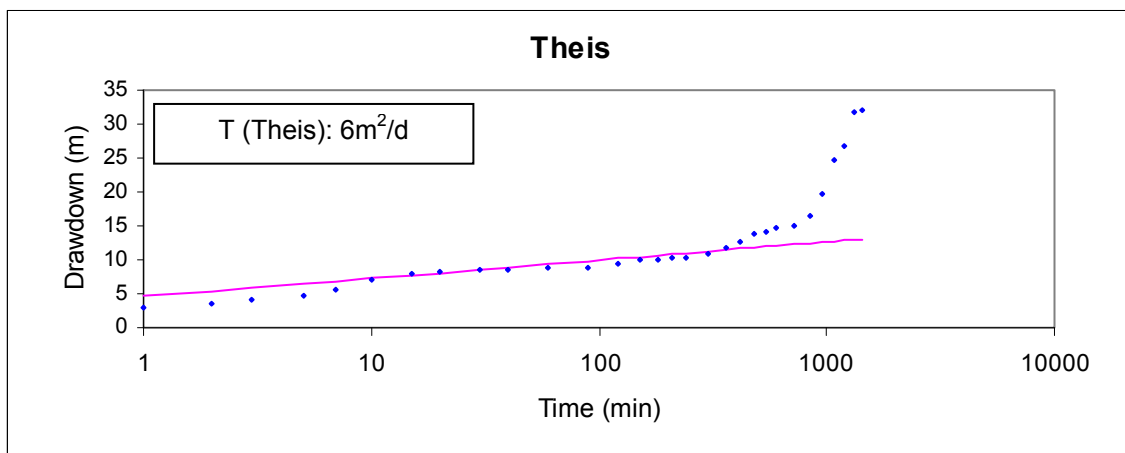


Figure 4-11: Theis fitting for borehole H07-0841.

Based on these latter two methods, transmissivities (T-value) $0.2 - 4.8 \text{ m}^2/\text{d}$ (Cooper-Jacob) and $6 \text{ m}^2/\text{d}$ (Theis) were calculated. In the Theis method, the storativity (S-value) was determined to be $\sim 8.4 \times 10^{-5}$ by means of graph fitting.

The time-drawdown curve for the step-drawdown test is shown in Figure 4-4.

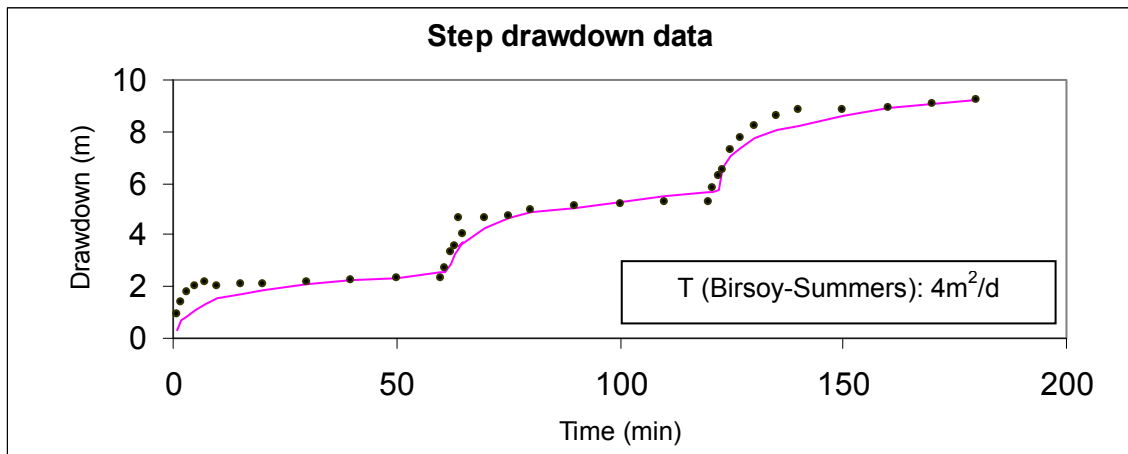


Figure 4-12: Step-drawdown test results of borehole H07-0841.

Based on the step-test data, a T-value of 4 m²/d was determined via the Birsoy-Summers method. An S-value of 0.001 was assumed for the calculation as discussed in Section 3.4.

4.1.4. Derivative and diagnostic plots

The derivative plots are shown in Figure 4-13 – Figure 4-15. Based on the slope of the first derivative (s'), it is evident that fractures influenced the pumping tests in all three scenarios. This is best seen by the decrease in the s' graph at the start of the fracture dewatering, and the increase after fracture dewatering. Also, the second derivative s'' is zero (or negative values where the graph does not plot on the log-log scale), i.e. radial flow dominates in these pumping times.

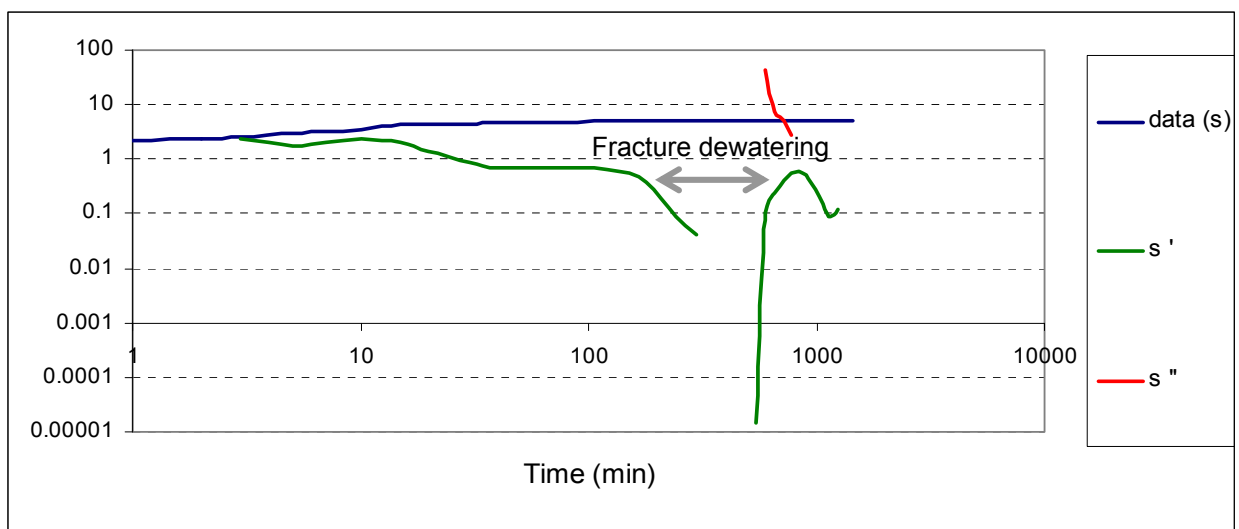


Figure 4-13: High T Scenario: derivative plots for constant discharge test, borehole H04-0306.

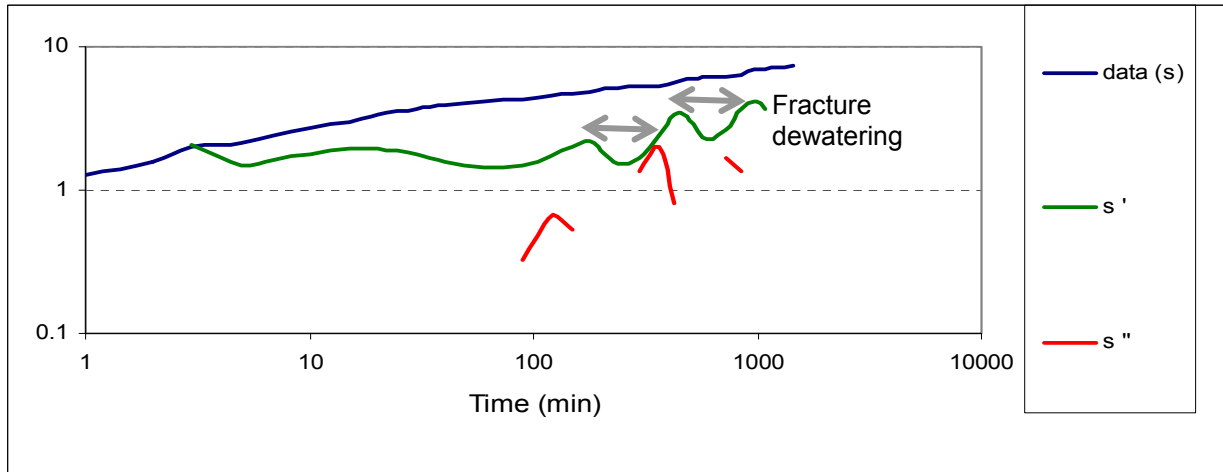


Figure 4-14: Intermediate T Scenario: derivative plots for constant discharge test, borehole H10-0084.

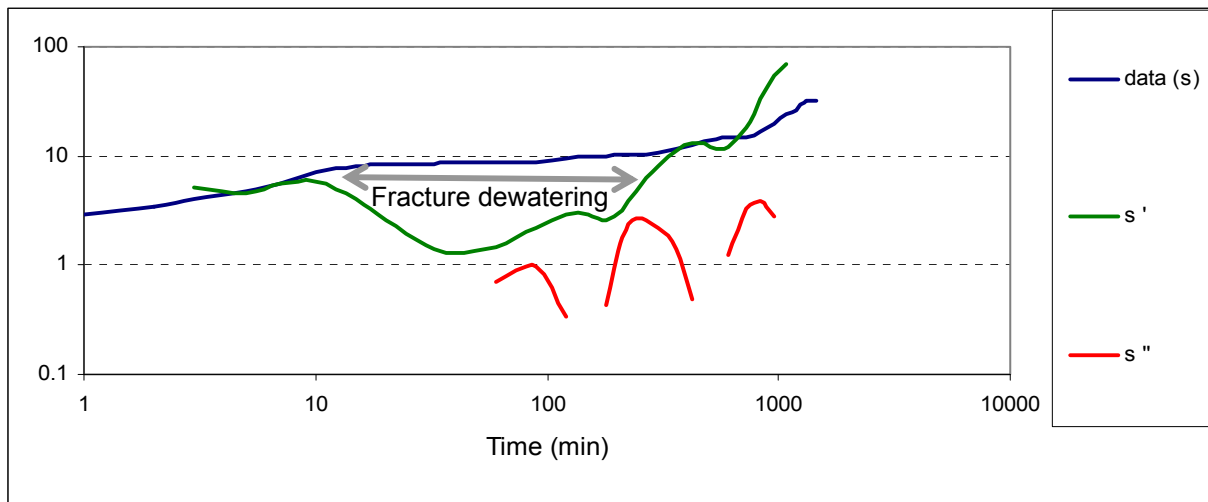


Figure 4-15: Low T Scenario: derivative plots for constant discharge test, borehole H07-0841.

The diagnostic graphs were plotted. Drawdown versus time on a semi-log plot is shown in Figure 4-16 – Figure 4-18. Radial flow predominates at late times for the high T scenario, one no-flow boundary exists for the intermediate T scenario and two no-flow boundaries are shown for the low T scenario.

The log-log plots are shown in Figure 4-19 – Figure 4-21.

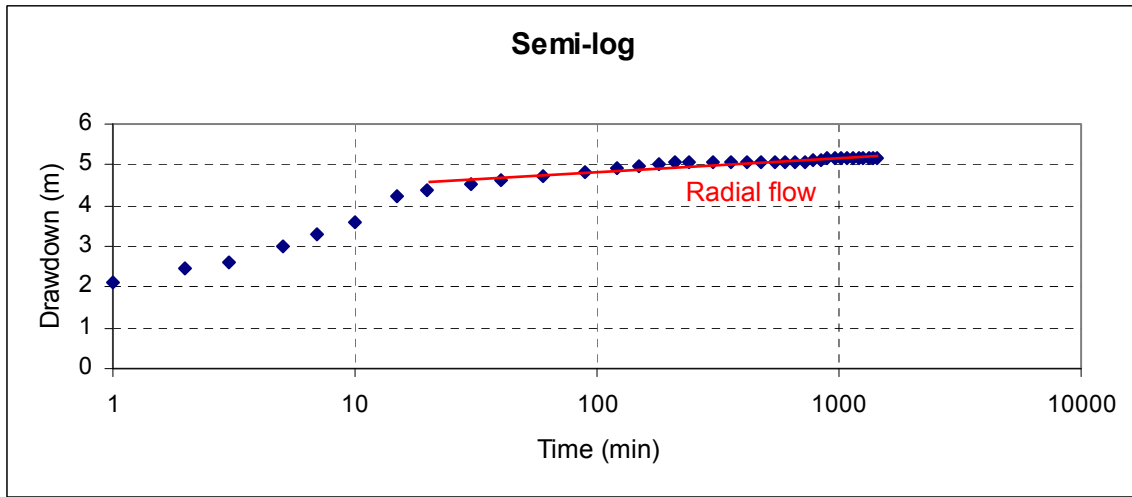


Figure 4-16: High T Scenario: semi-log plot for constant discharge test, borehole H04-0306.

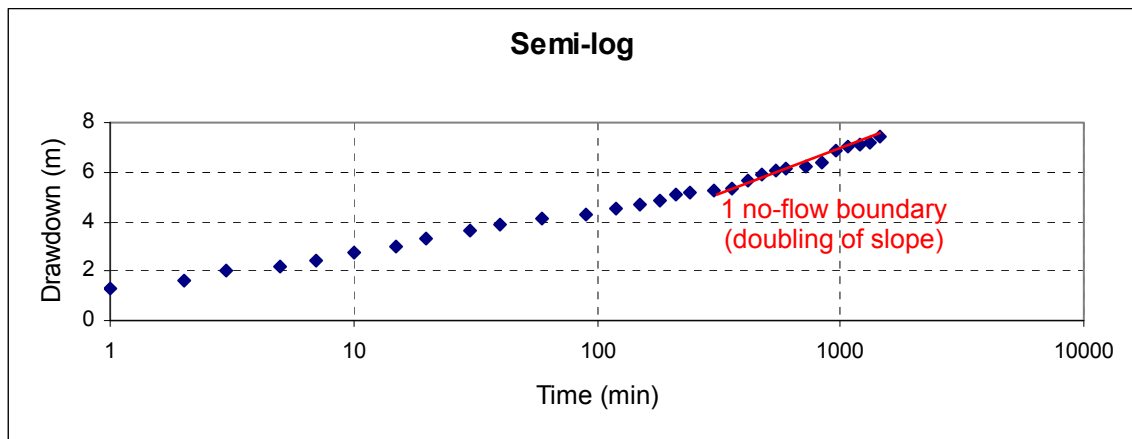


Figure 4-17: Intermediate T Scenario: semi-log plot for constant discharge test, borehole H10-0084.

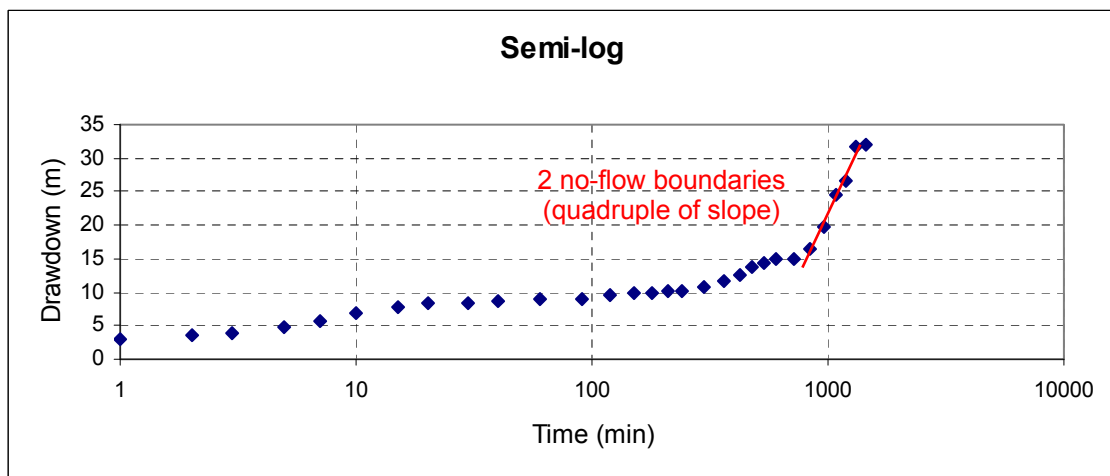


Figure 4-18: Low T Scenario: semi-log plot for constant discharge test, borehole H07-0841.

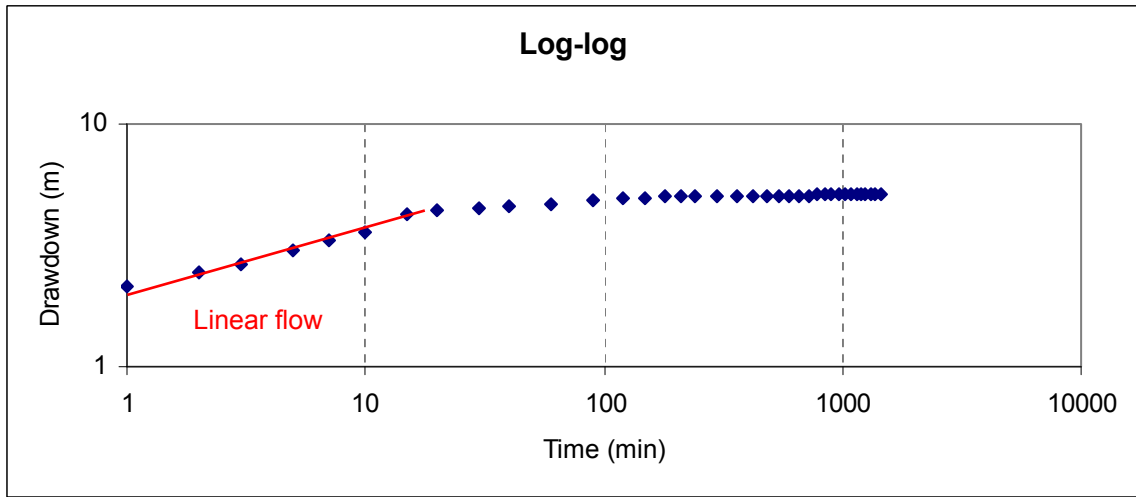


Figure 4-19: High T Scenario: log-log plot for constant discharge test, borehole H04-0306.

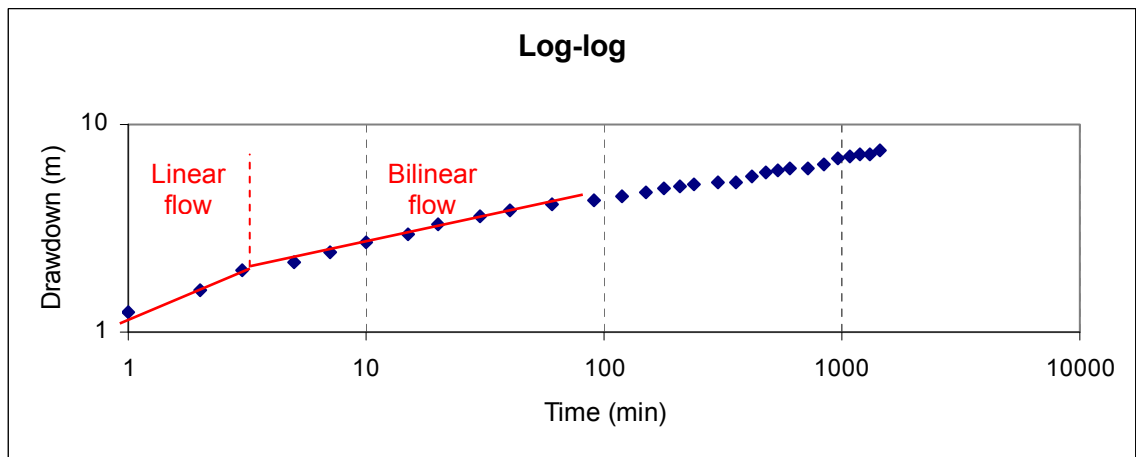


Figure 4-20: Intermediate T Scenario: log-log plot for constant discharge test, borehole H10-0084.

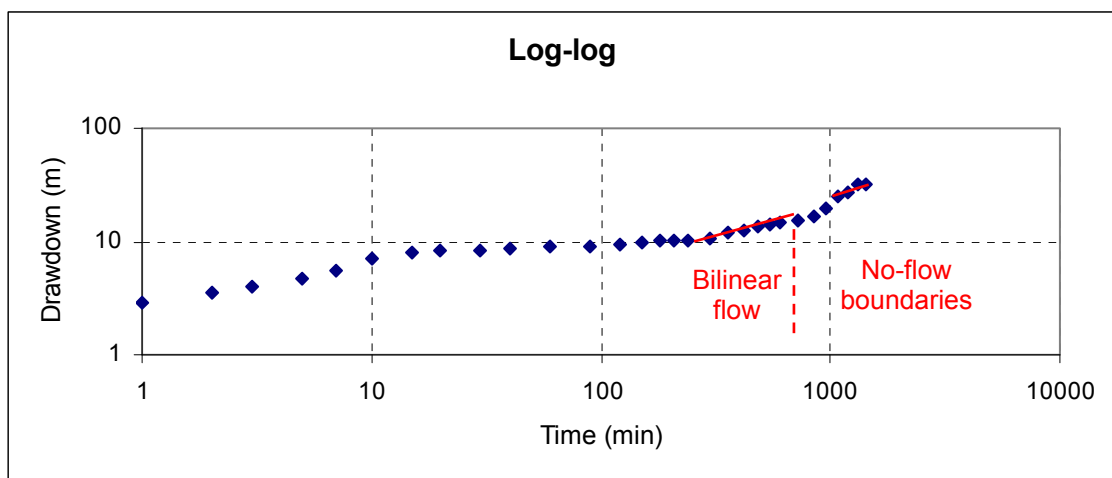


Figure 4-21: Low T Scenario: log-log plot for constant discharge test, borehole H07-0841.

Figure 4-22 – Figure 4-24 show the square root of time plots for the boreholes. Note that the upward shift of the graph origin from (0,0) indicates skin effects at early times for H04-0306. The plots for the intermediate and low T scenarios however commence at the origin, indicating no skin effects at early times, and predominantly linear flow at the beginning of pumping.

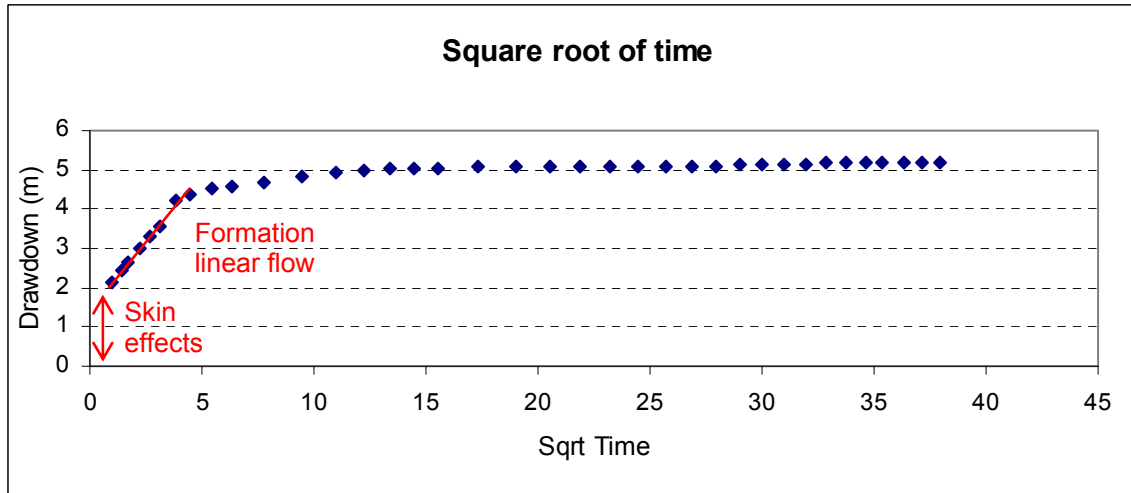


Figure 4-22: High T Scenario: square root of time plot for constant discharge test, borehole H04-0306.

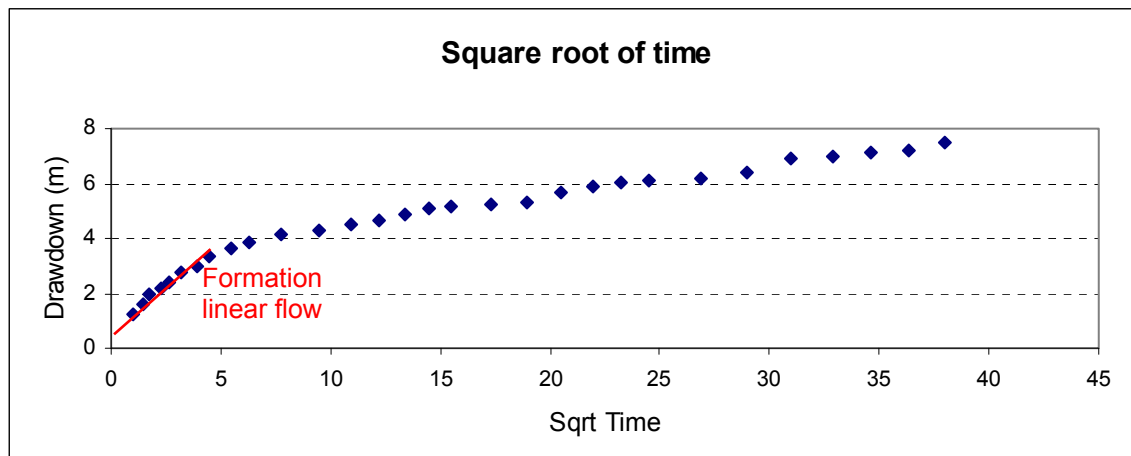


Figure 4-23: Intermediate T Scenario: square root of time plot for constant discharge test, borehole H10-0084.

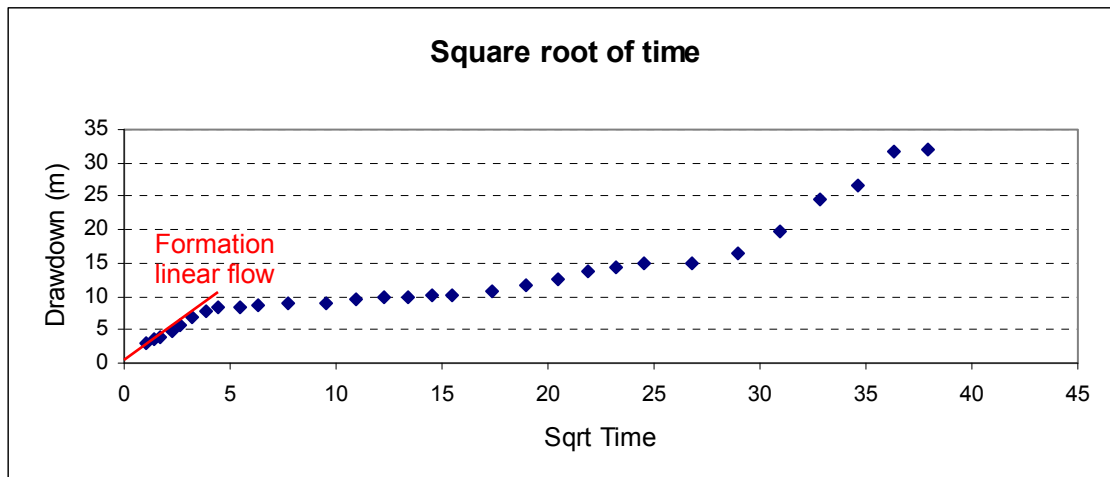


Figure 4-24: Low T Scenario: square root of time plot for constant discharge test, borehole H07-0841.

Based on the pumping test analyses and the diagnostic and derivative plots, the typical results can be summarised as shown in Table 4-1. These high T and low T scenarios together with the intermediate T scenario apply to the whole studied area.

Table 4-1: Comparison of pumping test outcomes.

	<i>High T Scenario</i>	<i>Intermediate T</i>	<i>Low T Scenario</i>
<i>Borehole:</i>	<i>H04-0306</i>	<i>H10-0084</i>	<i>H17-0841</i>
Transmissivity:	Typically (>100m ² /d)	Intermediate values	Typically < 10 m ² /d
• Logan	• 307.3 m ² /d	• 56.5 m ² /d	• 3.3 m ² /d
• Cooper-Jacob	• 629.2 m ² /d	• 20 m ² /d	• 0.2 – 4.8 m ² /d
• Theis	• 364 m ² /d	• 20 m ² /d	• 6 m ² /d
• Birsoy-Summers	• 188.0 m ² /d	• 27 m ² /d	• 4.0 m ² /d
Skin effects:	At early times	Not typically noted	Not typically noted
Steady-state:	At late times	Not generally reached	Flow barriers or closed reservoir
Radial flow:	Evident towards late times	Evident towards late times	Scattered evidence; uncertain
Test duration:	Standard test duration, 24 hours	Tests ceased in unsteady state conditions	Tests often stopped prematurely (holes possibly pumped dry)
Comments:	<ul style="list-style-type: none"> • Flow through fractures and porous rocks mass • Radial flow at late time 	<ul style="list-style-type: none"> • Flow through fractures and porous rocks mass • Radial flow at late time 	<ul style="list-style-type: none"> • Flow through fractures and porous rocks mass • Barriers at late T

4.2. Results

4.2.1. Discussion of T-values

Based on the Logan approximation, Theis method, Cooper-Jacob approximation and Birsoy-Summers methods, average T-values were determined for all the boreholes in the dataset. The coordinates from the GRIP project were used in plotting of the data.

In general, T-values vary from approximately $0.1 \text{ m}^2/\text{d}$ ($1 \times 10^{-1} \text{ m}^2/\text{d}$) to almost $1\,000 \text{ m}^2/\text{d}$ ($1 \times 10^3 \text{ m}^2/\text{d}$). A notable range of T-values over four orders of magnitude is present and the variation between the values was used to derive a conceptual model based on occurrence of higher- and lower-transmissivity boreholes.

Note should however be taken of the following:

- The Birsoy-Summers and Theis methods implemented in the FC Programme cannot calculate T-values below $1 \text{ m}^2/\text{d}$.
- Where possible, T-values were determined at late pumping time with the Cooper-Jacob and Theis methods to account for long-term pumping rates.

Figure A-4 – Figure A-11 (Appendix A) show the T-value distribution for WMA1 and WMA2 through each of the four methods. Statistically, the T-values obtained from the four methods vary by almost four orders of magnitude with mean value for all the methods between approximately $2.5 \times 10^2 \text{ m}^2/\text{d}$ (for Birsoy-Summers' method) and 4.5×10^2 (for Logan's method) m^2/d (Table 4-2). The high ranges are typical where the pumping tests were ceased in unsteady state conditions.

The static water levels (SWL) prior to pumping and the sustainable yields as calculated in the FC Programme are also included in Table 4-2.

The different transmissivities as determined with the four methods are correlated (r^2) in Table 4-3. The good correlation between the Logan and Birsoy-Summers method is evident, as is the good correlation between the Theis and Cooper-Jacob methods. Despite the good correlation, Logan's approximation yielded significantly higher average values than Birsoy-Summers' method. A good correlation between the other two methods is however expected as the Cooper-Jacob method is an approximation of the Theis method.

Despite the varying values determined, all calculated transmissivities are safely within an order of magnitude. The Logan approximation mostly provides the highest estimate of T, and the Birsoy-Summers method the lowest.

Table 4-2: Statistical summary of results – transmissivity (T), static water level prior to test (swl) and sustainable yield (Sust Q).

	T [m^2/d]				SWL [m]	Sust Q [L/s per 24h]
	Logan	Theis	C-J	B-S		
Mean	42.53	32.57	34.63	25.13	14.36	1.11
Standard Error	1.99	2.73	3.19	1.14	0.32	0.04
Median	19.1	12	11.15	12	11.82	0.6
Mode	4.9	1	0.9	2	5.4	0.3
Standard Deviation	63.86	66.82	78.13	35.91	10.42	1.35
Range	749.3	1110	1198.2	330	68.2	9.99
Minimum	0.6	1	0.2	0	0	0.01
Maximum	749.9	1111	1198.4	330	68.2	10
Count n	1028	599	600	999	1032	1032

* C-J: Cooper-Jacob; B-S: Birsoy-Summers

Table 4-3: Coefficient of determination (r^2) values for comparison of T-value estimates.

T (m^2/d)	WMA 1				WMA 2			
	Logan	Theis	C-J	B-S	Logan	Theis	C-J	B-S
Logan	1	0.40	0.44	0.73	1	0.43	0.42	0.80
Theis	0.40	1	0.87	0.48	0.43	1	1.00	0.26
C-J	0.44	0.87	1	0.51	0.42	1.00	1	0.25
B-S	0.73	0.48	0.51	1	0.80	0.26	0.25	1

* C-J: Cooper-Jacob; B-S: Birsoy-Summers

The Logan approximation assumes confined conditions and near-equilibrium conditions when measuring the maximum drawdown (Misstear, 2001). Based on the results, the Logan approximation seems to overestimate the T-values, and is approximately 1.6 times higher than the average between the Theis, Cooper-Jacob and Birsoy-Summers methods. This method is therefore considered an overestimation of the aquifer parameters, and does not sufficiently describe the borehole.

4.2.2. Discussion of static water levels

Figure A-12 – Figure A-13 (Appendix A) show the static water level distribution summarised in Table 4-2. Water levels in WMA 1 typically vary between 0m to almost 70m below surface; the diversity in water level depths is therefore significant. The deeper water levels are associated mainly with the structures as indicated by the geophysical data (especially structures striking parallel to the neotectonic shortening direction; i.e. open structures), whereas the shallower water levels were encountered predominantly at drainage features (discharge areas) and on geological contacts.

In the instance of WMA 2, the same general rule applies, where shallow water levels occur in or near the discharge areas, and deeper water levels on scattered structures. The water levels are however significantly more variable over the study area.

4.2.3. Discussion of sustainable yields

Figure A-14 – Figure A-15 (Appendix A) show the sustainable yield distribution. WMA 1 shows higher average values than WMA 2 which can be ascribed to the distinct climatic differences between the two areas (refer to precipitation map in Figure A-3, Appendix A).

Contrary to expectation, the sustainable yields tend to correlate inversely to the transmissivities: Higher sustainable yields were determined for lower transmissivity boreholes, and vice versa. This applies to both WMA 1 and WMA 2 with the exception of the drainage features where sustainable yields tend to be elevated.

One should furthermore evaluate sustainable yields with care as it does not address water availability on a catchment scale, and the determination is dependent on short-term pumping test data. To adequately address sustainable yields, it may be required to conduct pumping tests over a period of days or weeks as opposed to hours, and to have adequate monitoring boreholes to describe the cone of depression. Recharge should also be considered in the calculations.

4.2.4. Geological, structural, tectonic and geomorphologic influences

Groundwater in the study area occurs mainly within secondary structures as opposed to primary pores within the rock mass. This is confirmed by the strong evidence of fracture dewatering in the time-drawdown plots of the pumping tests and the derivative plots (Figure 4-13, Figure 4-14, Figure 4-15) indicating strong fracture influence in by far the majority of the boreholes.

The influence of present tectonic stress conditions seem to have varied influence on the distribution of water within these structures, as even those supposed to be closed under present stress conditions store and transmit water. This was proven by overlying the T-values determined during pumping testing on the geophysical lineament data obtained from Council for Geoscience (Figure A-2, Appendix A). It appears that groundwater occurrence the eastern portion of the study area (WMA2) is controlled by structures with the strike generally having little influence. The main focus in this area is considered to be the intersection between structures where openings are expected to be larger.

In the western portion (WMA1), this approach no longer applies. Stronger boreholes were identified on geological contacts with significantly higher yields observed in boreholes within the Hout River Shear Zone. Structures identified from the geophysical data show little to no influence on transmissivities of the boreholes in WMA1.

The general approach (Paragraph 2.1.4) that tectonic shortening can close up water-bearing structures and that elongation open these structures are therefore not applicable to the case study. The present tectonic stress field does not explain the T-value distribution over the area. A possibility is decompression fracturing or sheeting of the rock mass in a horizontal to sub-horizontal direction. Due to the complex geomorphological history of the study area, where a series of subsequent erosion cycles have relieved stresses on the underlying rocks, horizontal fracturing forms due to this decompression.

Stronger boreholes were furthermore identified (more pronounced in the western portion, WMA1) within or near surficial drainage features. This can most probably be ascribed to (a) the possibility that these drainage courses follow subsurface geological structures, (b) increased recharge is associated with surface drainage features, and/or (c) the presence of an alluvial aquifer or thicker weathered zone in these areas.

Table 2-1 depicts the typical succession of geological media in Basement terrane. A lateritic (or ferricrete) horizon overlies the saprolite, fissured layer and fresh Basement. Although these horizons do apply to the South African context, the general slope morphology varies slightly from granitic and/or Basement terrain in other parts of the world. In South Africa, Basement granites tend to weather to concave slopes with ferricrete on the middle and lower portions of the slope.

This is shown schematically in Figure 4-25 and Figure 4-26. Note the change in geomorphology and weathering depths for the western, more arid part of the study area where physical

disintegration predominates (WMA1) and the eastern, more humid part of the study area where chemical decomposition predominates (WMA2). In the more arid areas, weathering is controlled by mechanical processes leading to breakdown in particle size as opposed to the mineralogical altering of minerals to clay minerals in the more humid areas. Subsequently, deeper soil horizons and weathering are evident in the humid areas.

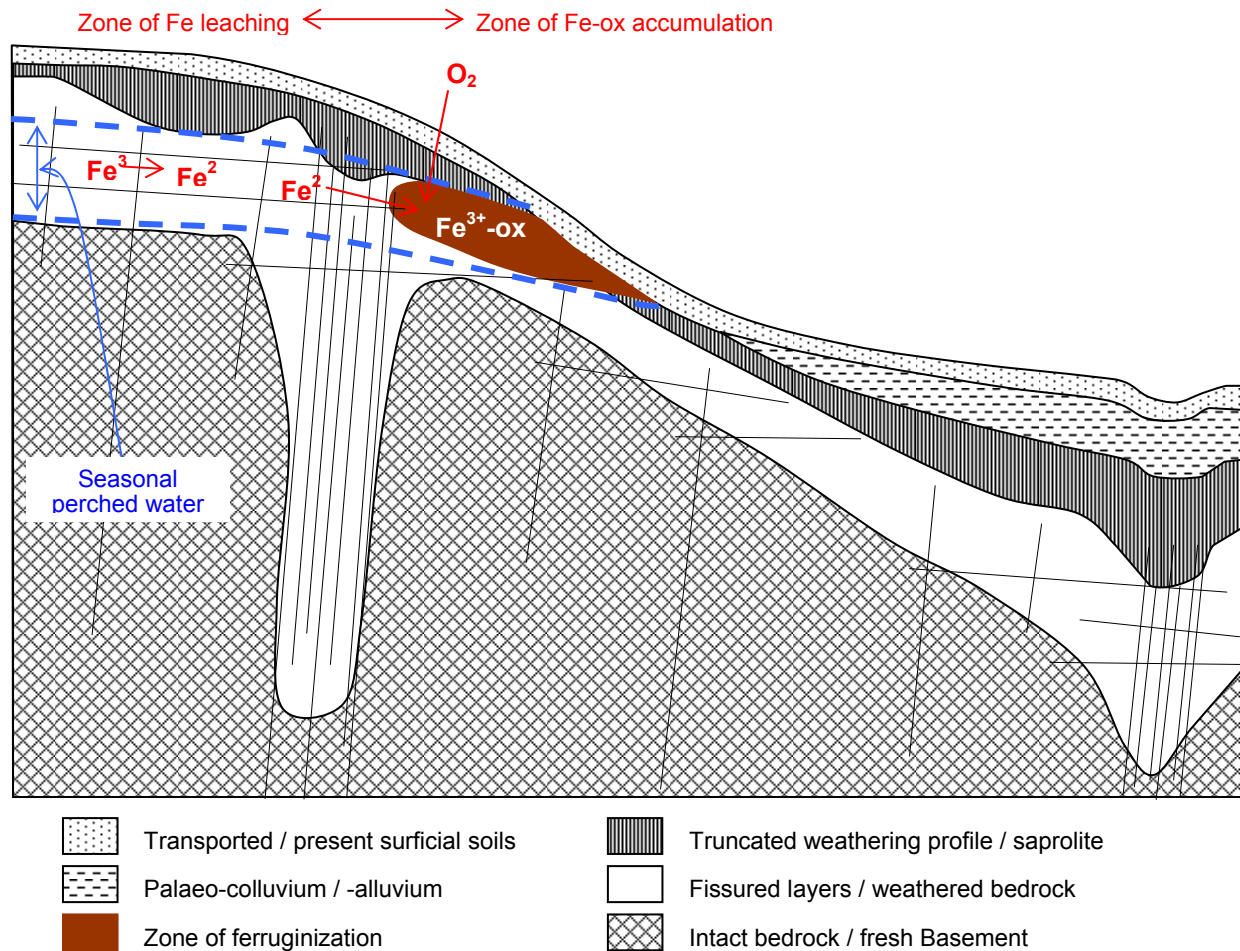


Figure 4-25: Schematic Basement granite profile in high-rainfall areas of decomposition, South Africa.

Rock weathering is dependent on a variety of factors. Chemical reactions between the rock-forming minerals and water however drive the transformation of minerals into clays, and rainfall subsequently determines the rate of weathering and type of soil forming. The rate of this process is increased by temperature (Righi & Meunier, 1993). It is therefore clear that the soils found in the study area where climate varies significantly should also differ.

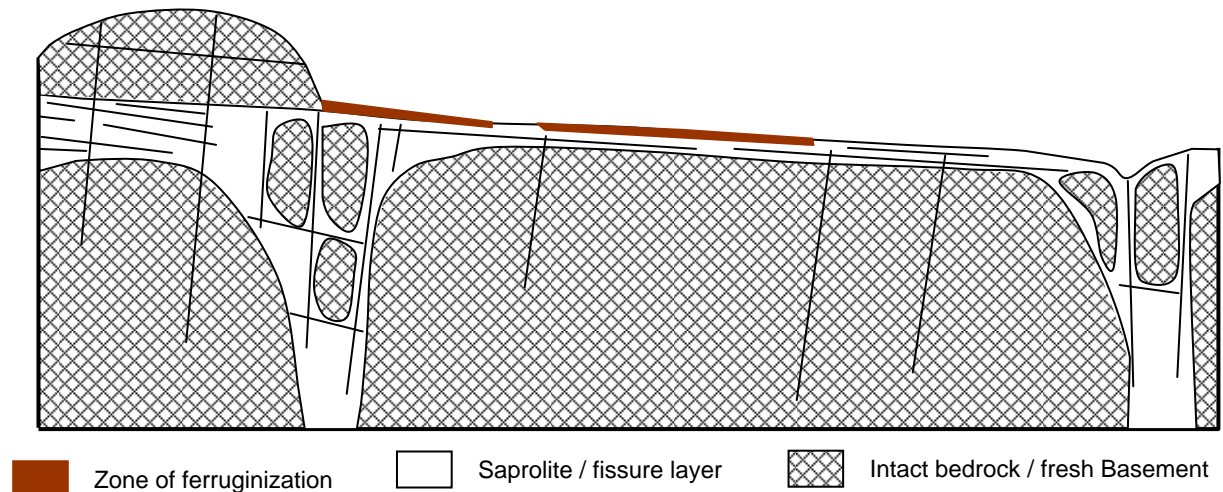


Figure 4-26: Schematic Basement granite profile in low-rainfall areas of disintegration, South Africa.

The main differences between the typical weathering profiles in the arid western and humid eastern portions are the following:

- Soil covering is almost absent in the arid areas, becoming metres to tens of metres of transported and residual soil combined in the humid areas.
- Ferricrete tends to be almost surficial and on the bedrock contact in the arid areas, whereas it predominates on the slopes at depth in the humid areas.
- Corestone formation is prominent in the arid areas.
- Topography and geomorphology appears to be significantly less pronounced in the more arid areas than in the humid areas.
- The weathering products can vary significantly based on the Basement composition. The more quartz-rich granites weathers to a much more sandy material, whereas K-feldspar weathers to non-expansive kaolinite, and plagioclase to a range of more expansive clays that can lower the soil infiltration (and subsequently recharge) capacity. High temperatures and humid conditions furthermore increase the weathering of feldspar and plagioclase to clay minerals.

4.3. Site Characterisation

The classification of the study area is based on three parameters:

- A. Model: what controls groundwater supply to the borehole, namely HRSZ, compressive forces, elongation forces, geological contacts, or decompression sheeting?
- B. Setting: is the borehole situated in an arid or humid environment, and to the north or the south of the HRSZ?

- C. Scenario: is the T-value “high” ($> 100 \text{ m}^2/\text{d}$), “low” ($< 10 \text{ m}^2/\text{d}$) or somewhere in-between?

Based on the interpretation of the results obtained, five distinct models are distinguished based on groundwater occurrence, namely:

- A1. HRSZ – generally higher T-values along the Hout River Shear Zone, applicable to WMA1 and WMA2.
- A2. Closed Structure – parallel to compressive forces; drainage features and structures striking NNW-SSE to NW-SE (parallel to neotectonic shortening) have differing influences on groundwater parameters over the study area.
- A3. Open Structure – perpendicular to compressive forces; drainage features and structures striking NNE-SSW to NE-SW (perpendicular to neotectonic shortening) have differing influences on groundwater parameters over the study area.
- A4. Contacts – geological contacts representing areas with higher or lower T-values over the study area.
- A5. Weathered Aquifer – sheeting / decompression; sub-horizontal jointing due to tectonic equilibration of the African erosion surface as possible groundwater conduits.

The five abovementioned models each applies differently to four very distinct settings as mentioned in Section 3.3 within the study area, namely:

- B1. Arid western WMA 1, north of HRSZ with predominant NE-SW striking structures.
- B2. Arid western WMA 1, south of HRSZ with predominant ENE-WSW striking structures.
- B3. Humid, eastern WMA 2, north of HRSZ with predominant NE-SW striking structures.
- B4. Humid, eastern WMA 2, south of HRSZ with predominant ENE-WSW striking structures.

Within these models and settings one can superimpose the three pumping test scenarios:

- C1. High T Scenario (typically $T > 100 \text{ m}^2/\text{d}$) where steady-state conditions are reached at late times.
- C2. Intermediate T Scenario (typically T between 5 and $100 \text{ m}^2/\text{d}$)
- C2. Low T Scenario (typically $T < 10 \text{ m}^2/\text{d}$) where a sudden increase in drawdown is encountered due to a significant decrease in recharge at late pumping times.

Each of these models will be addressed separately. The classification of the terranes in terms of the models (A1 – A5) is based primarily on the scenarios, i.e. high or low T-values (C1 – C3), which in turn is dependent on the settings (B1 – B4). Static water levels (SWL) prior to the tests and sustainable yields are also incorporated. The different models relevant to groundwater

occurrence (whether favourably or unfavourably) are shown in context to the four different settings in Figure 4-27 and are discussed below in more detail.

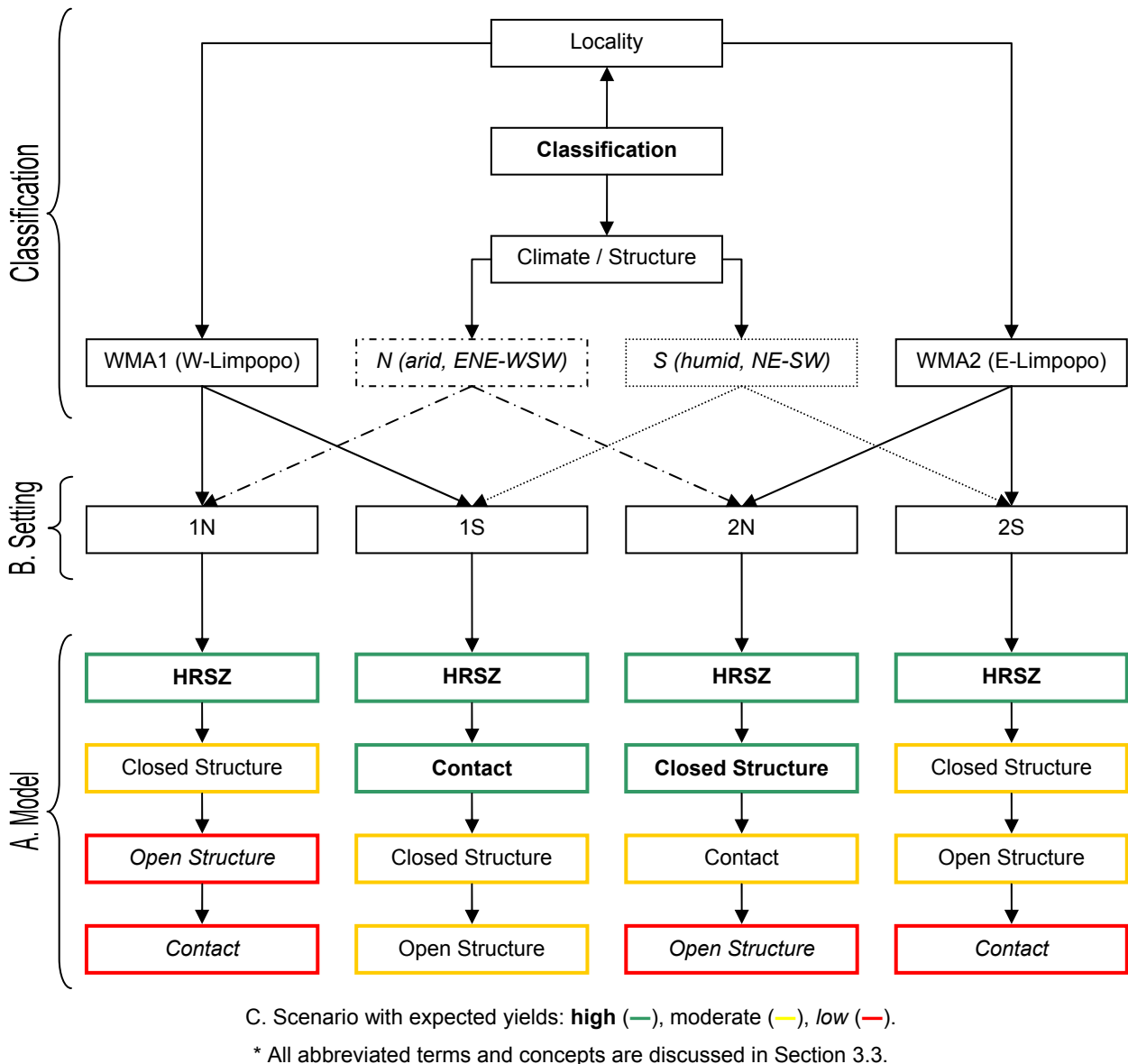


Figure 4-27: Classification of settings and relevance of different models per setting.

4.3.1. Hout River Shear Zone (HRSZ Model)

The HRSZ (Figure 3-4) represents the boundary between the northern (1N and 2N) and southern (1S and 2S) settings. Important differences between the northern and southern settings include:

- The northern portions of WMA1 and WMA2 are respectively more arid than the southern portions. On average WMA1 is more arid than WMA2.

- The structures are predominantly striking ENE-WSW in the northern portions and NE-SW in the southern portions corresponding to inherent neotectonic stresses.

The HRSZ is characterised by brittle deformation of the underlying rocks. For this reason the HRSZ appears to be a favourable structure in groundwater exploration, providing higher-than-average transmissivities and potential sustainable yields than the rest of the study area.

4.3.2. *Open structure parallel to compression (Open Structure Model)*

It is anticipated with prevailing neotectonic stress fields that open structures (with strike perpendicular to compression direction and aperture perpendicular to elongation direction) should be most favourable sites for groundwater supply. Throughout the whole study area, however, only outliers of stronger-than-average boreholes have been identified that potentially correspond to this model. These boreholes are generally poor groundwater sources (typically low T scenario) and the influence of such structures in groundwater occurrence can often be negative.

4.3.3. *Closed structure perpendicular to compression (Closed Structure Model)*

Although an apparent contradiction, some boreholes with high T-values occur on structures striking NW-SE to WNW-ESE. This corresponds to the neotectonic elongation direction, and it should therefore indicate closed structures striking in these directions. These structures have on average higher transmissivities than the supposedly open structures, and particularly in Setting 1N (WMA1, north of HRSZ) they appear to have a fairly strong control on groundwater occurrence.

4.3.4. *Geological Contact Model*

Geological contacts proved to be favourable potential groundwater sources in WMA1 and more specifically setting 1S (WMA1, south of HRSZ). This is the only portion of the study area where Basement rocks are intruded by younger granitic rocks. In the other settings, contacts rather represent inliers or outliers of greenstones, metamorphic rocks and sediments.

These granite-granite contacts represent higher potential for strong boreholes than other contacts in the study area. This can possibly be ascribed to cooling fracturing of the granites during cooling of the intruding magma.

4.3.5. *Weathered Aquifer Model*

Although this model was not investigated in detail during the study, the possibility of decompression jointing due to tectonic release following severe erosion in the recent history of the geological terrain is evident. This can affect groundwater flow, forming shallower weathered aquifers leading to the anomalous occurrences of stronger and weaker boreholes throughout the study area.

5. CONCLUSIONS

The assumption that groundwater follows open structures has dominated groundwater exploration in the past. However, in Basement aquifers in the northern portions of South Africa, these structures seem to have varying influence on groundwater flow, often to such an extent that it represents poorer-than-average potential yields.

The outcomes of the investigation were as follows:

- The Theis and Cooper-Jacob methods for constant discharge pumping test interpretation yielded very similar results. Although the Logan approximation for constant discharge pumping tests and the Birsoy-Summers method for step-drawdown tests yielded varying transmissivities, the results were however still very comparable and within one order of magnitude.
- Five models were identified to classify groundwater occurrence on the site. These are:
 - A1. Hout River Shear Zone.
 - A2. Closed Structure – parallel to compressive forces; drainage features and structures striking NNW-SSE to NW-SE (parallel to neotectonic shortening).
 - A3. Open Structure – perpendicular to compressive forces; drainage features and structures striking NNE-SSW to NE-SW (perpendicular to neotectonic shortening).
 - A4. Contacts – geological contacts representing areas with higher or lower T-values over the study area.
 - A5. Weathered Aquifer – sheeting / decompression; sub-horizontal jointing due to tectonic equilibration of the African erosion surface as possible groundwater conduits.
- These five models are influenced by four distinct settings based on climatic and prevailing tectonic conditions:
 - B1. Arid western WMA 1, north of HRSZ with predominant NE-SW striking structures.
 - B2. Arid western WMA 1, south of HRSZ with predominant ENE-WSW striking structures.
 - B3. Humid, eastern WMA 2, north of HRSZ with predominant NE-SW striking structures.
 - B4. Humid, eastern WMA 2, south of HRSZ with predominant ENE-WSW striking structures.
- The combination of the model and the setting determines the scenario which addresses the potential of high or low yielding boreholes as follows:

- C1. High T Scenario (typically $T > 100 \text{ m}^2/\text{d}$) where steady-state conditions are reached at late times.
- C2. Intermediate T Scenario (typically T between 5 and $100 \text{ m}^2/\text{d}$)
- C2. Low T Scenario (typically $T < 10 \text{ m}^2/\text{d}$) where a sudden increase in drawdown is encountered due to a significant decrease in recharge at late pumping times.

A full summary of the outcomes are supplied in Figure 4-27. Shear zones such as the Hout River Shear Zone is the most prominent water-bearing feature, followed by granite-granite geological contacts where younger plutons intruded into the older Basement. Contacts between Basement and sedimentary or metamorphic rocks however yielded poorer-than-average transmissivities, and therefore represent poor borehole locations.

It is – in conclusion – clear that not only structural geology, but also climate and geomorphology influence groundwater occurrence in Basement terrane. Climate has a direct influence on recharge, and geomorphology can lead to decompression fracturing, creating additional secondary openings not necessarily complying with the neotectonic stress fields.

6. REFERENCES

1. Arcworth, R.I.: 1987. The Development of Crystalline Basement Aquifers in a Tropical Environment. *Quarterly Journal of Engineering Geology* 20. pp. 265 – 272.
2. Bardenhagen, I.: 1999. Skin Localization at Wells Drilled in a Vertical Fault Zone. *Ground Water*. 37(5). pp. 764 – 769.
3. Barenblatt, G. E., Zheltov, I. P. & Kochina, I. N.: 1960. Basic Concepts in the Theory of Seepage of Homogenous Liquids in Fissured Rocks. *J. of Applied Mathematics*. 24(5). pp. 1286 – 1303.
4. Barker, J. A.: 1988. A Generalized Radial-flow Model for Pumping Tests in Fractured Rock. *Water Resour. Res.* 24(10). pp. 1796 – 1804.
5. Barker, J. A.: 1991. Transport in Fractured rock. In: Downing, R. A. & Wilkinson, W. B. (eds). *Applied Groundwater Hydrology*. Clarendon Press. Oxford. pp199 – 216.
6. Bäuml, R.: 2003. Geohydraulic Charactersisation of Fractured Flow Regimes: Regional Studies in Granite (Linday, Black Forest, Germany) and Dolomite (Tsumed Aquifers, Northern Namibia). Ph.D. Dissertation. Universität Karlsruhe. Windhoek, 149 pp.
7. Bear, J. & Bachman, Y.: 1990. Introduction to Modeling of Transport Phenomena in Porous Media. Kluwer Academic Publishers. Dordrecht. 553pp.
8. Bear, J.: 1993. Modeling Flow and Contaminant Transport in Fractured Rocks. From: Bear, J., Tsang, C. and de Marsily, G., *Flow and Contaminant Transport in Fractured Rock*, Academic Press, California, pp. 1 – 35.
9. Bird, P., Ben-Avraham, Z., Schubert, G., Andreoli, M. and Viola, G.: 2006. Patterns of Stress and Strain Rate in Southern Africa. *K. Geophys. Res.* 111(B8). B08402. doi:10.1029/2005JB003882.
10. Birsoy, Y. K. & Summers, W. K.: 1980. Determination of Aquifer Parametes from Step Tests and Intermittent Pumping Data. *Ground Water*. 18. pp. 137 – 146.
11. Black, J. H.: 1994. Hydrogeology of Fractured Rocks – A Question of Uncertainty about Geometry. In: Voss, C. I. & Wilson, W. E. (eds.): 1994. *Applied Hydrogeology*. 2(3). Verlag. Hanover. pp. 56 – 70.
12. Blatt, H. & Tracy, R. J.: 1997. *Petrology: Igneous, Sedimentary, and Metamorphic*. 2nd Edition. W H Freeman & Company.
13. Boehmer, W. K. & Boonstra, J.: 1987. Analysis of Drawdown in the Country Rock of Composite Dike Aquifers. *J. of Hydrology*. 35(1987). Elsevier. Amsterdam. pp. 199 – 214.
14. Bonnet, E., Bour, O. Odling, N. E., Davy, P., Main, I., Cowie, P. and Berkowitz, B.: 2001. Scaling of Fracture Systems in Geologic Media. *Rev. Geophys.* 39(3). pp. 347 – 393.
15. Boonstra, J. & Boehmer, W. K.: 1986. Analysis of Data from Aquifer and Well Tests in Intrusive Dikes. *J. of Hydrology*. 88(1986). Elsevier. Amsterdam. pp. 301 – 317.
16. Boshoff, R., Van Reenen, D. D., Smit, C. A., Perchuk, L. L., Kramers, J. D. and Armstrong, R.: 2006. Geologic History of the Central Zone of the Limpopo Complex: The West Alldays Area. *The Journal of Geology*. 114. pp. 699 – 716.
17. Boshoff, R.: 2004. Formation of Major Fold Types during distinct Geological Events in the Central Zone of the Limpopo Belt, South Africa: new Structural, Metamorphic and Geochronologic Data. MSc theses. Rand Afrikaans University. Johannesburg. 121pp.

18. Botha, F. S. and Van Rooy, J. L.: 2001. Affordable Water Resource Development in the Northern Province, South Africa. *Journal of African Earth Sciences*. 22. pp. 687 – 692.
19. Boulding, J. R. and Ginn, J. S.: 2003. *Practical Handbook of Soil, Vadose Zone, and Ground-Water Contamination: Assessment, Prevention and Remediation*. ISBN 1566706106. Lewis Publishers. 728pp.
20. Boulton, N. S. and Streltsova, T. D.: 1976. The Drawdown near an Abstraction of Large Diameter under Non-steady Conditions in an Unconfined Aquifer. *J. Hydrol.* 30. pp. 29 – 46..
21. Boulton, N. S.: 1954. The Drawdown on the Water Table under Non Steady Conditions near a Pumped Well in an Unconfined Aquifer. *Proc Institution Civil Eng.* 3. pp. 564 – 579.
22. Bourdet, D. & Gringarten, A. C.: 1980. Determination of Fissure Volume and Block Size in Fractured Reservoirs by Type-curve Analysis. Paper SPE 9293 presented at the SPE-AIME 55th Annual Fall Technical Conference and Exhibition. 21 – 24 Sept. Dallas. Referenced in Bäumlé (2003).
23. Bourdet, D., Whittle, T. M., Douglas, A. A. and Pirard, Y. M.: 1983. A New Set of Type Curves simplifies Well Test Analysis. *World Oil*. pp. 95 – 106.
24. Caro, R. & Eagleson, P. S.: 1981. Estimating Aquifer Recharge due to Rainfall. *Journal of Hydrology*, 53, pp. 185 – 211.
25. Chow, V. T.L 1952. On the Determination of Transmissibility and Storage Coefficients from Pumping Test Data. *Trans. Am. Geophys. Union*. 33. pp. 397 – 404.
26. Cinco, L. H. & Samaniego, F. V.: 1981. Transient Pressure Analysis for Fractured Wells. 1749 – 1766.
27. Cinco, L. H., Samaniego, F. V. & Dominguez, N. A.: 1978. Transient Pressure Behaviour for a Well with a Finite Conductivity Vertical Fracture. 253 – 264.
28. Cooper, H. H. & Jacob, C. E. 1946. A Generalized Graphical Model for Evaluating Formation Constants and Summarizing Well Field History. *Am Geophys. Union Trans* 27. pp. 526-534.
29. Dewandel, B., Lachassagne, P., Wyns, R. Maréchal, J. C. and Krishnamurthy, N. S.: 2003. A Generalized 3-D Geological and Hydrogeological Conceptual Model of Granite Aquifers controlled by Single or Multiphase Weathering. *Journal of Hydrology*. 330. pp. 260– 284.
30. Du Toit, W.H., Du Toit, A.J.I. and Jonck, F. (2003). Hydrogeological map series of South Africa, Polokwane 2326 sheet (1:500000).
31. DWAF [Basson, M. S. & Rossouw, J. D.] 2003a. Limpopo Water Management Area: Overview of Water Resources Availability and Utilisation. Department of Water Affairs and Forestry (South Africa) Report Number P WMA 01/000/00/0203. 53pp.
32. DWAF [Basson, M. S. & Rossouw, J. D.] 2003b. Luvuvhu and Letaba Water Management Area: Overview of Water Resources Availability and Utilisation. Department of Water Affairs and Forestry (South Africa) Report Number P WMA 02/000/00/0203. 54pp.
33. DWAF [Department of Water Affairs and Forestry]. 2004a. Internal Strategic Perspective: Limpopo Water Management Area: Prepared by Goba Moahloli Keeve Steyn (Pty) Ltd, in association with Tlou & Matji (Pty) Ltd and Golder Associates (Pty) Ltd. on behalf of the Directorate: National Water Resource Planning. Department of Water Affairs and Forestry (South Africa) Report Number P WMA 01/000/00/0304. 161pp.

34. DWAF [Department of Water Affairs and Forestry]. 2004b. Internal Strategic Perspective: Luvuvhu/Letaba Water Management Area: Prepared by Goba Moahloli Keeve Steyn (Pty) Ltd in association with Tlou and Matji, Golder Associates Africa and BKS on behalf of the Directorate: National Water Resource Planning. Department of Water Affairs and Forestry (South Africa) Report Number P WMA 02/000/00/0304. 191pp.
35. Ferris, D. B., Knowles, R. H., Brown, R. H. and Stallman, R. W.: 1989. Theory of Aquifer Tests. Water-supply Paper 1536-E. 3rd Ed. USGS [United States Geological Survey]. Washington. 113pp.
36. Gale, J.E.: 1982, Assessing the Permeability Characteristics of Fractured Rock, GSA Special Paper 189, Geological Society of America, Boulder, CO, pp. 163-181.
37. Gringarten, A. C. & Ramey, J. R.: 1974. Unsteady State Pressure Distributions created by a Well with a Single Horizontal Fracture, Partial Penetration or Restricted Entry. Society of Petroleum Engineers J. Aug(1974). pp. 413 – 426.
38. Gringarten, A. C., Ramey, J. R., Raghavan, H. J. & Raghavan, R.: 1974. Unsteady State Pressure Distributions created by a Well with a Single Infinite-conductivity Vertical Fracture. Society of Petroleum Engineers J. Aug(1974). pp. 374 – 360.
39. Guérin, F. P. M. & Billaux, D. M.: 1994. On the Relationship between Connectivity and the Continuum Approximation in Fracture-flow and Transport Modelling. In: Voss, C. I. & Wilson, W. E. (eds.): 1994. Applied Hydrogeology. 2(3). Verlag. Hanover. pp. 56 – 70.
40. Hantush, M. S. and Jacob, C. E.: 1955. Nonsteady Radial Flow in an Infinite Leaky Aquifer. Trans. Am. Geophys. Union. 36. pp. 95 – 100.
41. Hantush, M. S.: 1964. Hydraulics of Wells. In: Chow, V. T. (ed). Advances in Hydroscience. Vol. 1. Academic Press. New York and London. pp. 281 – 432.
42. Hekel, I.: 1994. Hydrogeologische Erkundung toniger Festgesteine am Beispiel des Opalinustons (Unteres Aalenium). In: Tübinger Geowissenschaftliche Arbeiten (TGA), Reihe C No. 18, 1994; 170 pp.; Tübingen.
43. Hsieh, P. A. & Neuman, S. P.: 1985. Field Determination of the Three-dimensional Hydraulic Conductivity Tensor of Anisotropic Media: 1. Theory. Water Resour Res 21(11). pp. 1655-1665.
44. Ingebritsen, S. E. Sanford, W. E. and Neuzil, C. E.: 2006. Groundwater in Geologic Processes. 2nd Ed. Cambridge University Press. Cambridge.
45. Jacob, C. E.: 1947. Drawdown Test to Determine Effective Radius of Artesian Well. Am. Soc. Civil. Eng. Trans 112. pp. 1047 – 1064.
46. Jenkins, D. & Prentice, J.: 1982. Theory for Aquifer Test Analysis in Fractured Rocks under Linear (nonradial) Flow Conditions. Ground Water, 20(1). pp. 12 – 21.
47. Jones, M.J.: 1985. The Weathering Zone Aquifers of the Basement Complex Areas of Africa. Quarterly Journal Of Engineering Geology 18. pp. 35 – 46.
48. Jouanna, P.: 1993. A Summary of Field Test Methods in Fractured Rocks. From: Bear, J., Tsang, C. and de Marsily, G., Flow and Contaminant Transport in Fractured Rock, Academic Press, California, pp. 1 – 35.
49. Kendy, E.: 2003. The False Promise of Sustainable Pumping Rates. Vol 41, No 1. Ground Water. Jan-Feb 2003. pp 2 – 4.

50. Key R.M.: 1992. An Introduction to the Crystalline Basement of Africa. In: Wright, E.P. and Burgess, W.G. (eds.). Hydrogeology of Crystalline Basement Aquifers in Africa. Geological Society Special Publication No 66. Geological Society. London.
51. King, L. C.: 1975. Geomorphology: A Basic Study for Civil Engineers. Proceedings of the Sixth Regional Conference for Africa on Soil Mechanics and Foundation Engineering. Durban. Vol 2. pp. 259 – 263.
52. Kreissig, K., Holzer, L., Frei, R., Villa, I. M., Kramers, J. D., Kröner, A., Smit, C. A. and Van Reenen, D. D.: Geochronology of the Hout River Shear Zone and the Metamorphism in the Southern Marginal Zone of the Limpopo Belt, Southern Africa. Precambrian Research. 109. pp. 145 – 173.
53. Kruseman, G. P. and De Ridder, N. A.: 1989. Analysis and Evaluation of Pumping Test Data. 2nd ed. International Institute for Land Reclamation and Improvement. Wageningen, The Netherlands. ISBN 9070754207.
54. Lebbe, L. and De Breuck, W.: 1997. Analysis of a Pumping Test in an Anisotropic Aquifer by Use of an Inverse Numerical Model. Hydrogeology Journal. Vol 5 No 3. pp. 44 – 59.
55. Li, J.: 2007,. Analysis of Radial Movement of a Confined Aquifer due to Well Pumping and Injection. Hydrogeology Journal. 15. pp. 445 – 448.
56. Logan, J. 1964. Estimating Transmissivity from Routine Production Tests of Water Wells. Ground Water 2:35-37.
57. Lomize, G. M.: 1951. Flow in Fractured Rocks (in Russian). Gosenergoizdat. Moscow. 127 pp.
58. Long, L., Van Camp, M., Van Burm, P., De Ceukelaire, M, Wattiez, R. and De Breuck, W.: 1988. The Groundwater in the Paleozoic Complex and in the Landenian in West- and East-Flanders. Water (41). pp. 104 – 108. (In Dutch)
59. Louis, C. A.: 1969. A Study of Groundwater Flow in Jointed Rock and its Influence on the Stability of Rock Masses. Rock. Mech. Res. Rep. 10. 90pp.
60. Maimon, M.: 2004. Defining and Managing Sustainable Yield. Ground Water. 42(6). pp.809 – 814.
61. Maréchal, J. C., Dewandel, B. and Subrahmanyam, K.: 2004. Contribution of Hydraulic Tests at Different Scales to Characterize Fracture Network Properties in the Weathered-fissured Layer of a Hard-rock Aquifer. Water Resources Research. 40. W11508.
62. Misstear, B. D. R. 2001. Editors' Message: The Value of Simple Equilibrium Approximations for Analysing Pumping Test Data. Hydrogeology journal. 9. pp. 125 – 126.
63. Moench, A. F.: 1984. Double-porosity Models for a Fissured Groundwater Reservoir with Fracture Skin. Water Resources Research. 20(7). pp. 831 – 846.
64. Najurietta, H. L.: 1980. A Theory for Pressure Transient Analysis in Naturally Fractured Reservoirs. J. of Petrol. Techn. July 1980. pp. 1241 – 1250.
65. Neuman S. P.:2005. Trends, Prospects and Challenges in Quantifying Flow and Transport through Fractured Rocks. Hydrogeol J 13. pp. 124 – 147.
66. Papadopoulos, I. S. and Cooper, H. H. J.: 1967. Drawdown in a Well of Large Diameter. Water Resour. Res. 3. pp. 241 – 244.
67. Partridge, T. C. and Maud, R. R.: 1987. Geomorphological Evolution of Southern Africa since the Mesozoic. South African Journal of Geology. Vol 90 No 2. June 1987. pp. 179 – 208.

68. Renard, P.: 2005. The Future of Hydraulic Tests. *Hydrogeology Journal*. Vol 13, No 1, March 2005. Springer Verlag. Berlin, pp. 259 – 261.
69. Righi, D. and Meunier, A.: 1993. Origin of Clays by Rock Weathering and Soil Formation. In: Velde, B. (ed). *Origin and Mineralogy of Clays: Clays and the Environment*. Springer. Germany.
70. Robb, L. J., Brandl, G., Anhaeusser, C. R. and Poujol, M.: 2006. Archaean Granitoid Intrusions. In: Johnson, M. R., Anhaeusser, C. R. and Thomas, R. J. (eds.). *The Geology of South Africa*. Geological Society of South Africa, Johannesburg / Council for Geoscience, Pretoria. pp.57 – 93.
71. Romm, E. S.: 1966. *Flow Characteristics of Fractured Rocks* (in Russian). Nedra. Moscow. 283pp.
72. Sami, K., Neumann, I., Gqiba, D., De Kock, G. and Grantham, G.: 2002. Status Groundwater Exploration in Geologically Complex and Problematic Terrain – Guidelines. WRC Report No 966/1/02. Pretoria.
73. SANS [South African National Standards]. 2003. Development, Maintenance and Management of Groundwater Resources Part 4: Test-pumping of Water Boreholes. SANS 10299-4:2003. ISBN 0-626-14912-6. South Africa.
74. Smith, L. and Schwartz, F. W.: 1993. Solute Transport Through Fracture Networks. From: Bear, J., Tsang, C. and de Marsily, G., *Flow and Contaminant Transport in Fractured Rock*, Academic Press, California, pp. 129 – 167.
75. Stallman, R. W. 1976. Techniques of Water-Resources Investigations of the United States Geological Survey: Chapter B1: Aquifer-test Design, Observation and Data Analysis. United States Geological Survey (USGS). Washington. 31pp.
76. Tam, V. T., De Smedt, F., Batellaan, O. & Dassargues, A. 2003. Interpretation and Analysis of Aquifer Tests in Fractured-Karstified Carbonate Limestone. In: Krásný, Hrkal & Bruthans (eds). *Groundwater in Fractured Rocks*. Prague. pp. 299-300.
77. Theis, C. V.: 1935. The Relation between the Lowering of the Piezometric Surface and the Rate and Duration of Discharge of a Well using Ground-water Wtorage. *Am. Geophys. Union Trans.*, v. 14, pt. 2, p. 519-524.
78. Theis, C. V.: 1941. The Effect of a Well on the Flow of a Nearby Stream. *Trans. Am. Geophys. Union*. 22. pp. 734 – 738.
79. Thiem, G.: 1906. *Hydrologische Methoden*. Gebbhardt, Leipzig.
80. Van Everdinger, A. F.: 1953. The Skin Effect and its Influence on the Productive Capacity of a Well. *Petrol Trans. AIME* 198. pp. 171 – 176.
81. Van Golf-Racht, T. D.: 1982. *Fundamentals of Fractured Reservoir Engineering*. Dev Petrol Sci 12. Elsevier. Amsterdam. 720pp.
82. Van Reenen, D. D., Roering, C., Brandl, G, Smit, C. A. and Barton, J. M. Jr.: 1990. The Granulite-facies Rocks of the Limpopo Belt, Southern Africa. In Vielzeuf, D. and Vidal, P. (eds.) *Granulites and Crustal Evolution*. NATO ASI Ser. C 311. Dordrecht. Kluwer. pp. 257 – 289.
83. Van Schalkwyk, A. & Vermaak, J. J. G.: 2000. The Relationship between the Geotechnical and Hydrogeological Properties of Residual Soils and Rocks in the Vadose Zone, WRC Report No. 701/1/11, Water Research Commission.

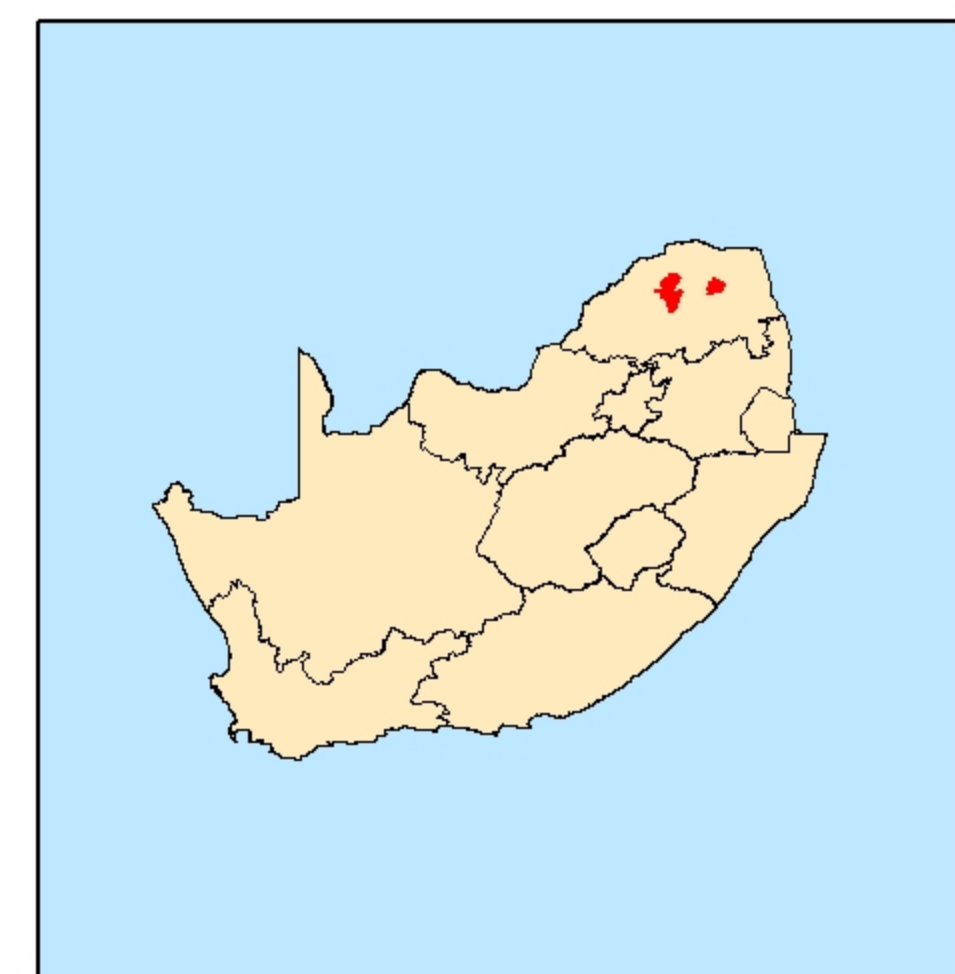
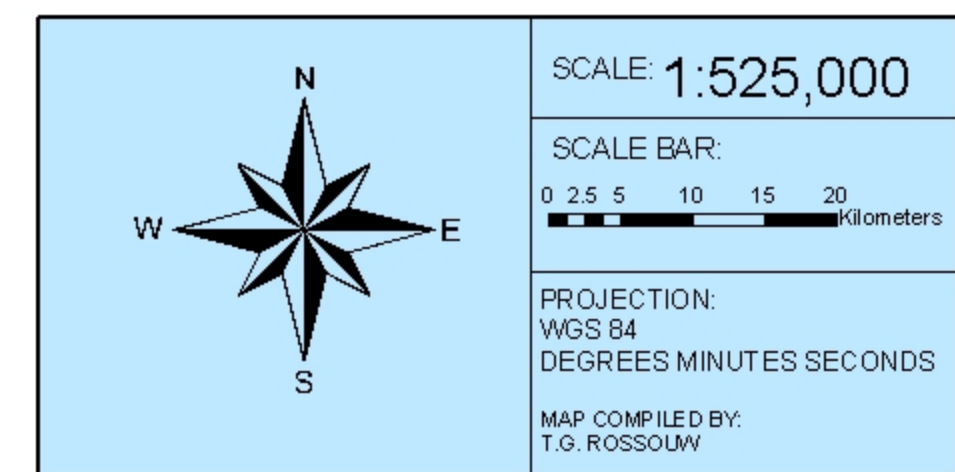
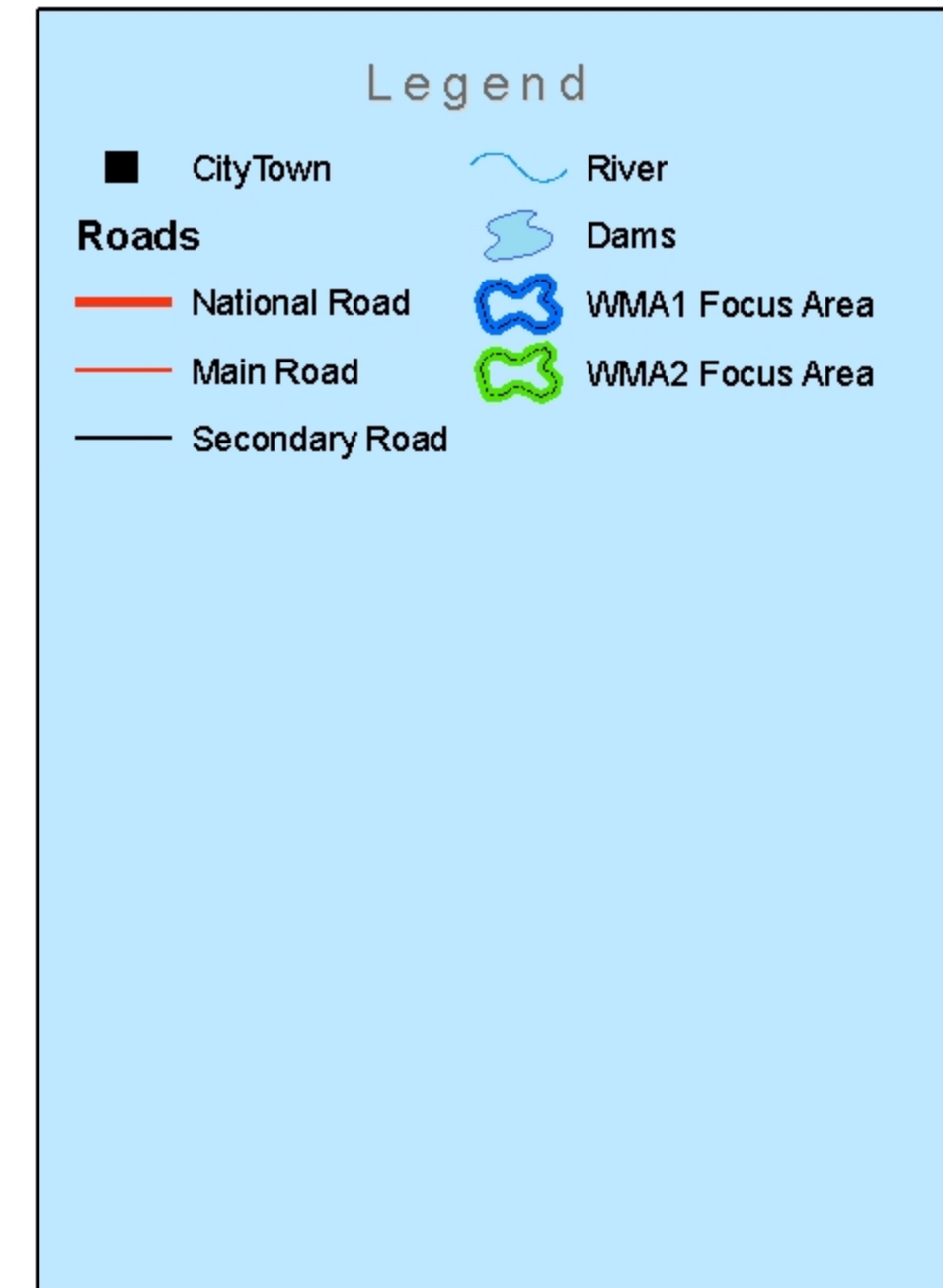
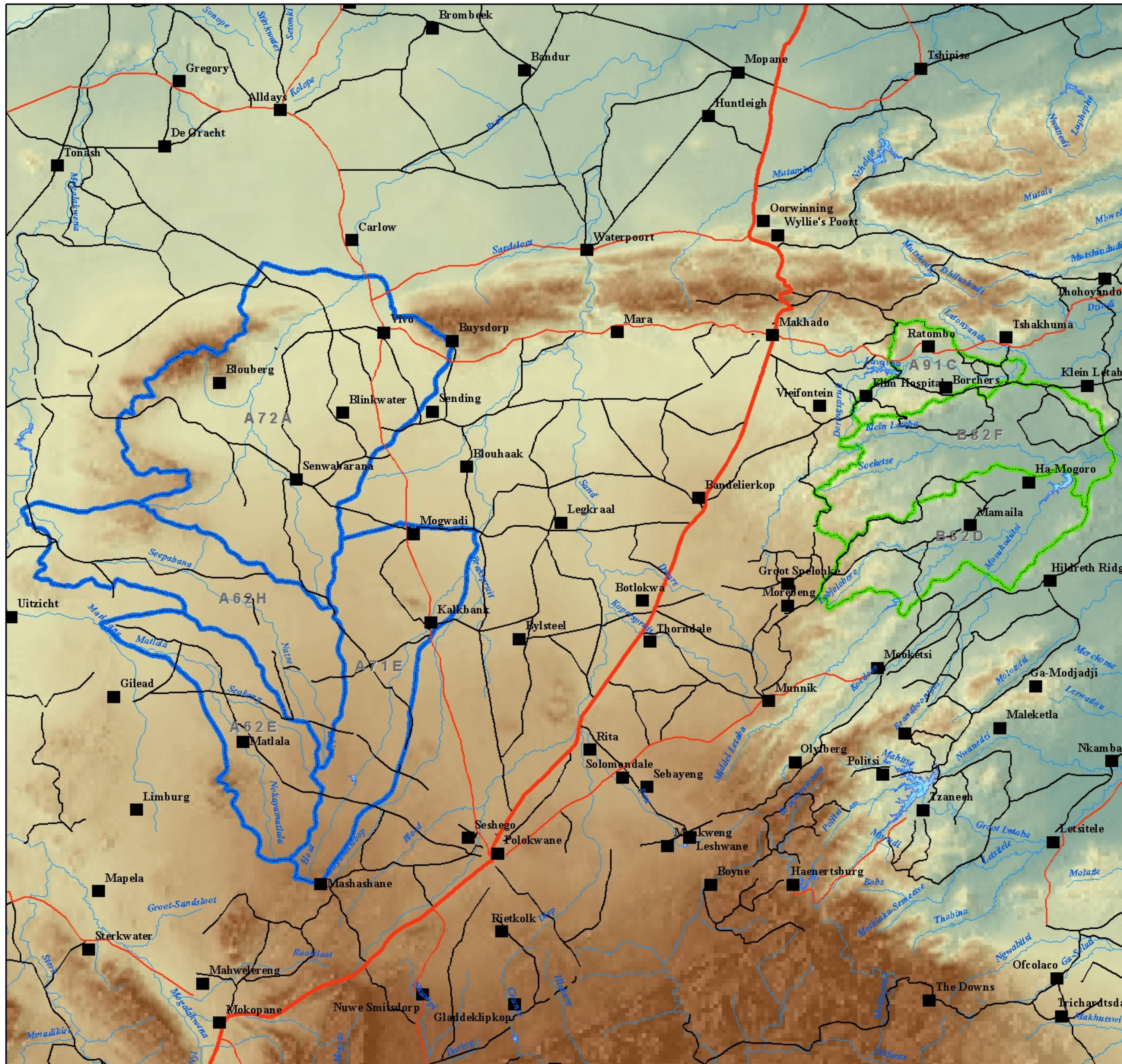
84. Van Tonder, G., Bardenhager, I., Riemann, K., Van Bosch, J., Dzanga, P. & Xu, Y.: 2001. Manual on Pumping Test Analysis in Fractured-Rock Aquifers. Institute for Groundwater Studies, University of the Free State. Bloemfontein.
85. Walker, D. D. & Roberts, R. M.: 2003. Flow Dimensions Corresponding to Hydrogeologic Conditions. *Water Resour. Res.* 39(12). pp. 7.1 – 7.8.
86. Warren, J. E. and Root, P. J.: 1963. The Behaviour of Naturally Fractured Reservoirs. *Soc. Petrol. Eng. J.* 3. pp. 245 – 255.
87. Weinert, H. H.: 1980. *The Natural Road Construction Materials of Southern Africa.* Human & Rousseau. Cape Town.
88. Witherspoon, P. A., Long, J. C. S., Majer, E. L. & Myer, L. R.: 1987, A New Seismic Hydraulic Approach to Modeling Flow in Fractured Rocks, In: *Proceedings of NWWA/IGWMC Conference on Solving Ground-Water Problems with Models (Denver, CO), National Water Well Association, Dublin, OH, pp. 793-826.*
89. Witherspoon, P. A., Wang, J. S. Y., Iwai, K. and Gale, J. E.: 1980. Validity of Cubic Law for Fluid Flow in a Deformable Rock Fracture. *Water Resources Research.* 16/6. pp. 1016 – 1024.
90. Wittke, W.: 1990. *Rock Mechanics: Theory and Applications with Case Histories.* Translated by Richard Sykes. Springer-Verlag. Berlin.
91. Wright, E.P. and Burgess, W.G. (eds.): 1992. *The Hydrogeology of Crystalline Basement Aquifers in Africa.* Geological Society Special Publication No 66. Geological Society. London.

7. APPENDICES

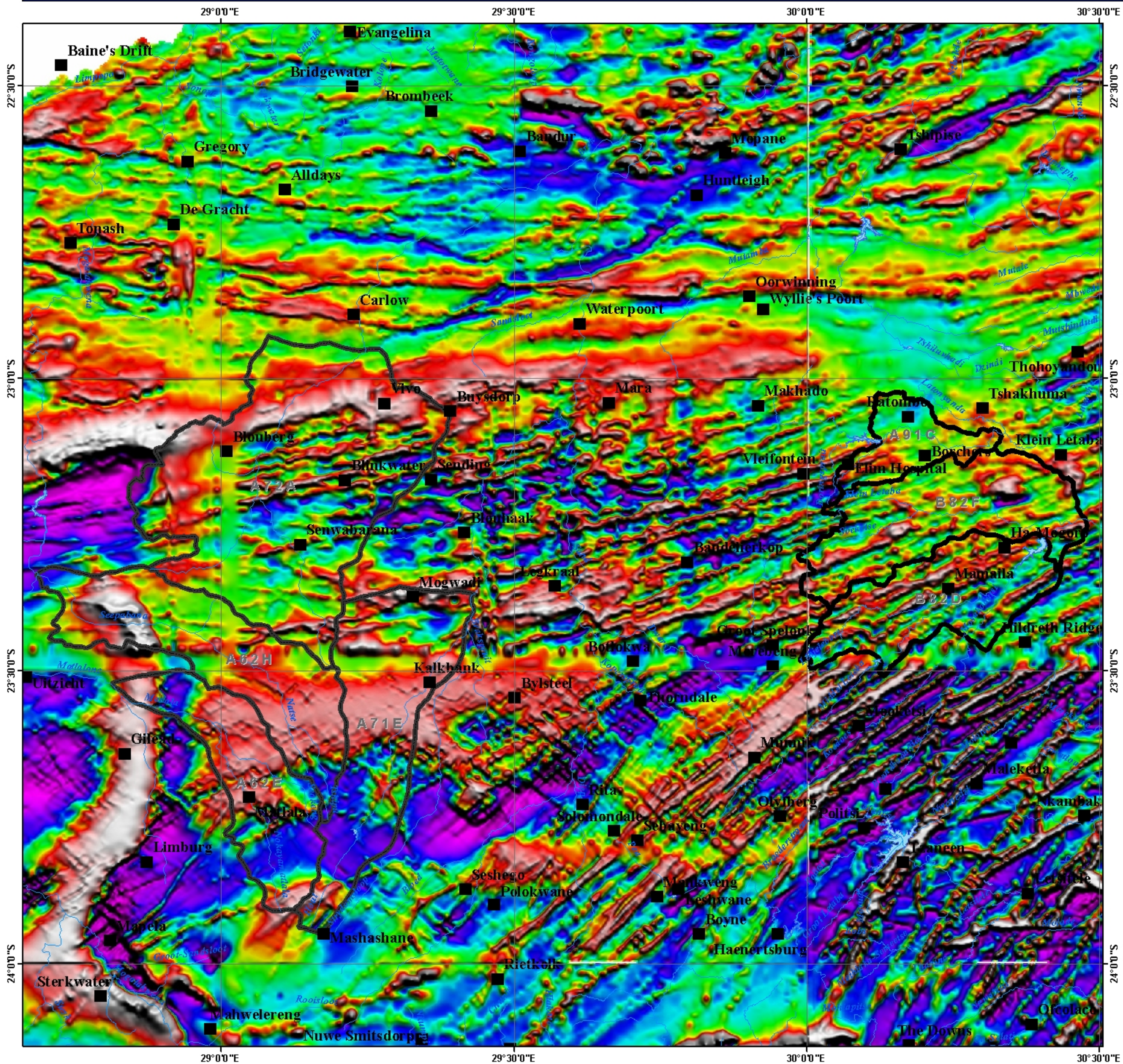
APPENDIX A: FIGURES

- Figure A-1: Site Locality and Quaternary Catchments.**
- Figure A-2: Geophysical Data (CGS).**
- Figure A-3: Precipitation of the Study Area.**
- Figure A-4: T-values for WMA 1 (Logan method).**
- Figure A-5: T-values for WMA 2 (Logan method).**
- Figure A-6: T-values for WMA 1 (Cooper-Jacob method).**
- Figure A-7: T-values for WMA 2 (Cooper-Jacob method).**
- Figure A-8: T-values for WMA 1 (Theis method).**
- Figure A-9: T-values for WMA 2 (Theis method).**
- Figure A-10: T-values for WMA 1 (Birsoy-Summers method).**
- Figure A-11: T-values for WMA 2 (Birsoy-Summers method).**
- Figure A-12: Water Levels prior to Pumping Tests for WMA 1.**
- Figure A-13: Water Levels prior to Pumping Tests for WMA 2.**
- Figure A-14: Sustainable Yields determined for WMA 1.**
- Figure A-15: Sustainable Yields determined for WMA 2.**

Locality Map and Quaternary Catchments



Geophysical Map



Legend

- CityTown
- ~ River
- ☞ Dams
- ⬭ Focus Area

SCALE: 1:525,000

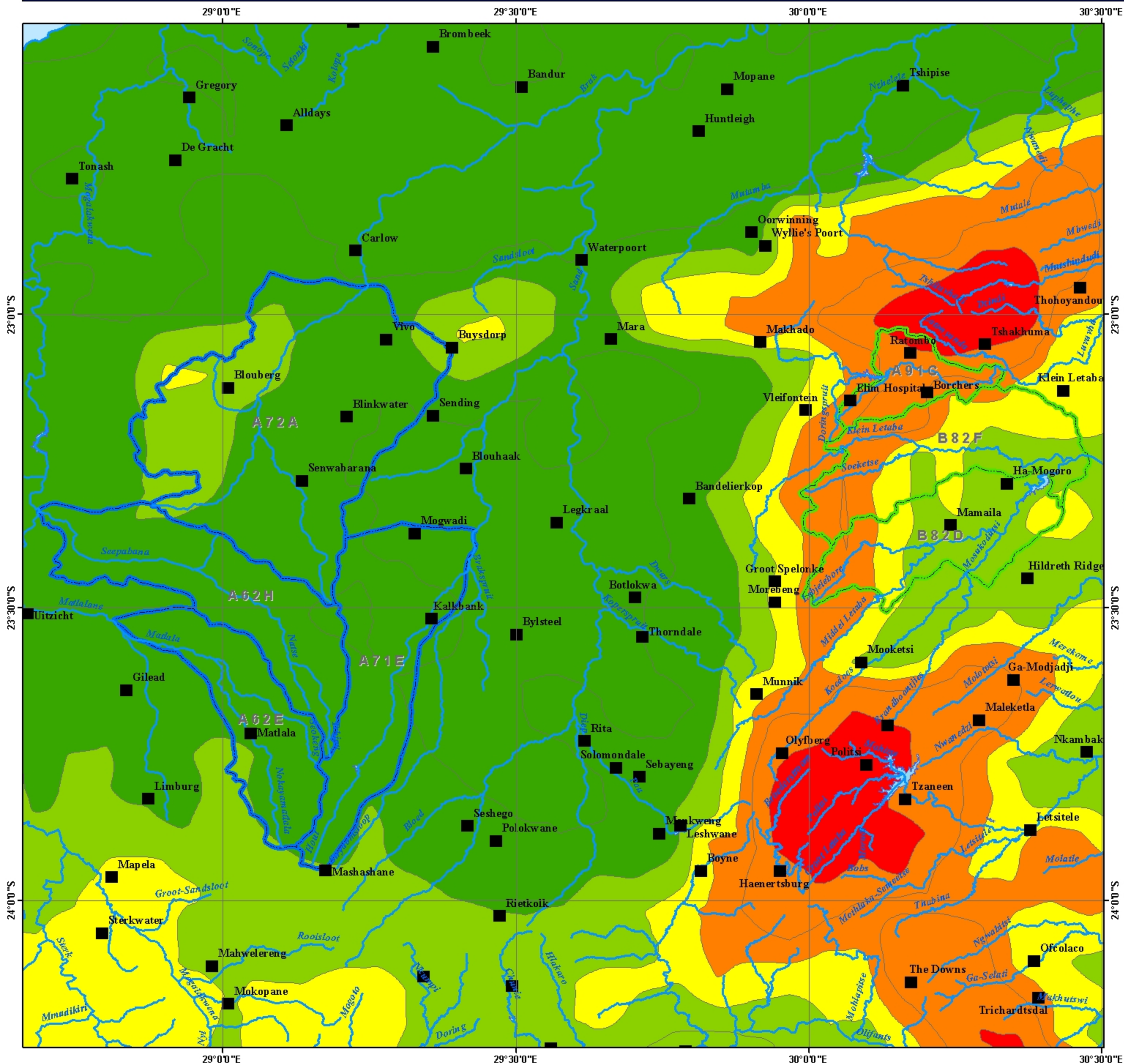
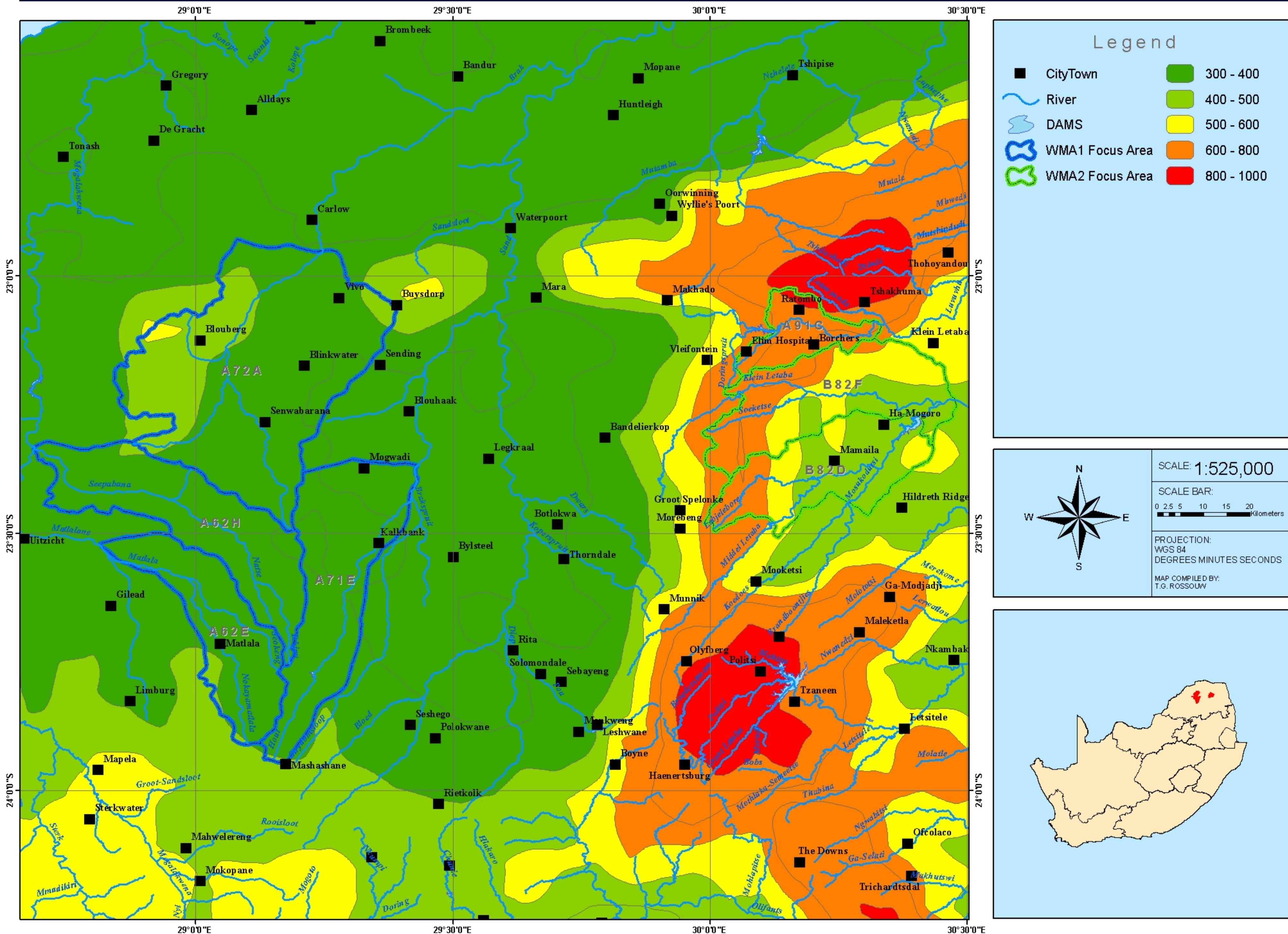
SCALE BAR:

0 2.5 5 10 15 20 Kilometers

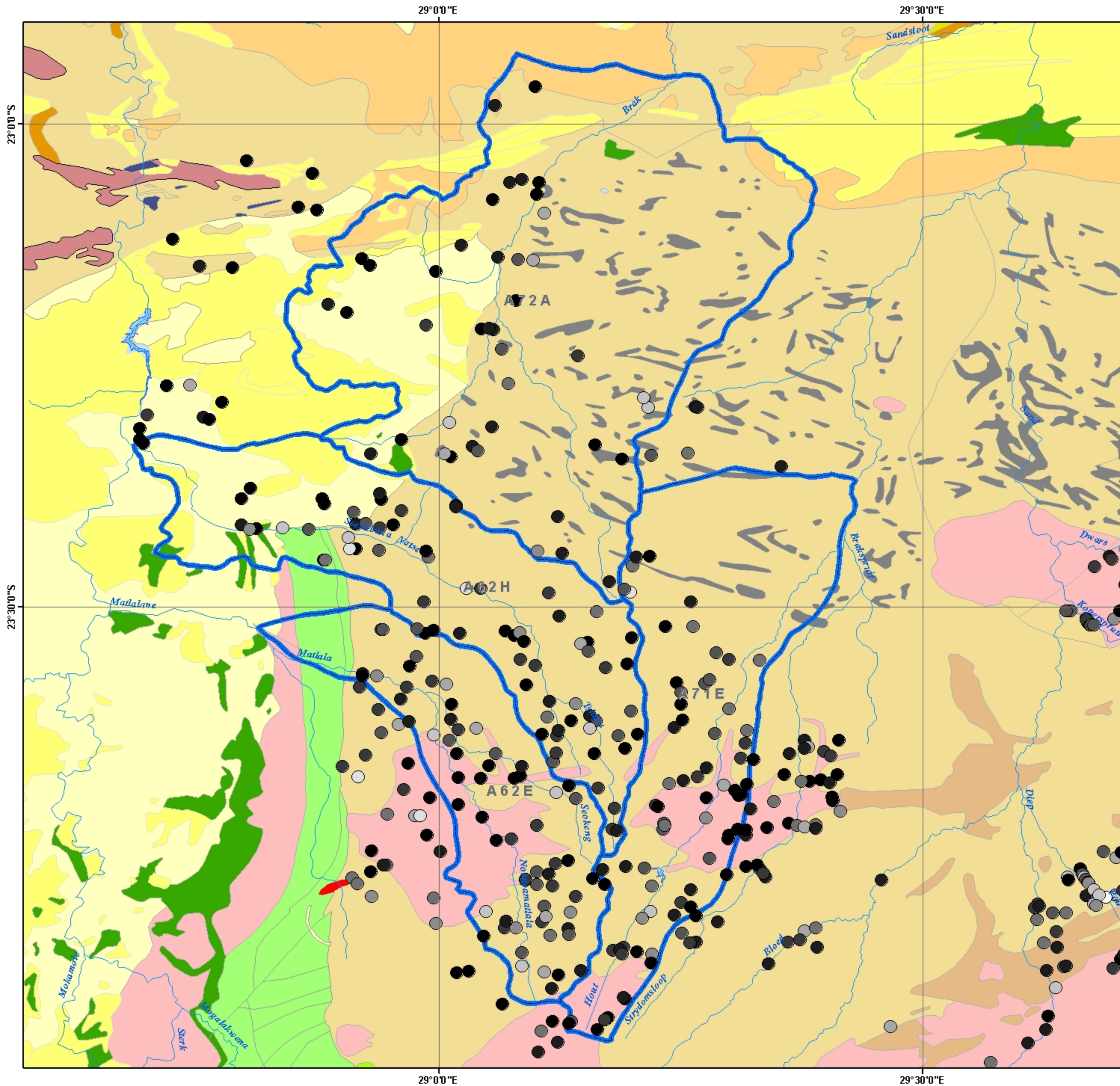
PROJECTION:
WGS 84
DEGREES MINUTES SECONDS
MAP COMPILED BY:
T.G. ROSSOUW
SOURCE:
COUNCIL FOR GEOSCIENCE



Mean annual Precipitation (mm)



Transmissivity of WMA1 - Logan's method



Legend

- River
- DAMS
- WMA1 Focus Area
- WMA2 Focus Area
- DOLERITE
- SEDIMENTARY
- ARENITE
- MUDSTONE
- SHALE
- QUARTZITE
- MARBLE
- DOLOMITE
- BASALT
- LAVA
- CLINOPYROXENITE
- GABBRO
- NORITE
- RHYOLITE
- DIORITE
- SYENITE
- ANORTHOSITE
- GRANITE
- AMFIBOLITE, MAFIC GRANULITE, METAPELITE
- GNEISS

Borehole Data

Logan

- 0.00 - 11.60
- 11.61 - 26.20
- 26.21 - 45.00
- 45.01 - 67.00
- 67.01 - 92.60
- 92.61 - 131.00
- 131.01 - 177.70
- 177.71 - 257.50
- 257.51 - 447.20
- 447.21 - 749.90

SCALE: 1:325,000

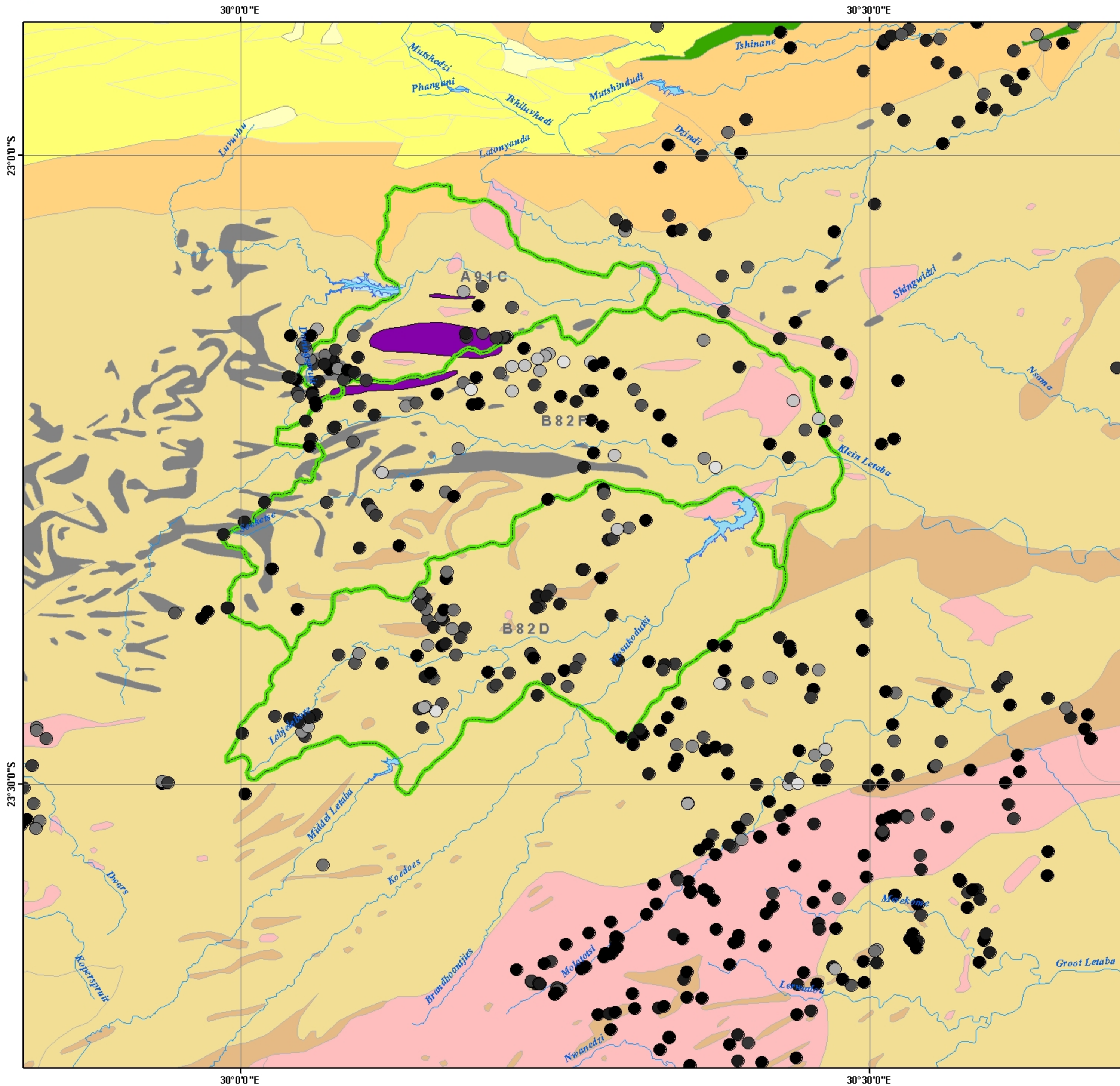
SCALE BAR:
0 1.5 3 6 9 12 Kilometers

PROJECTION:
WGS 84
DEGREES MINUTES SECONDS

MAP COMPILED BY:
T.G. ROSSOUW



Transmissivity of WMA2 - Logan's method



Legend

- River
- DAMS
- WMA2 Focus Area

Borehole Data

Logan

- 0.00 - 11.60
- 11.61 - 26.20
- 26.21 - 45.00
- 45.01 - 67.00
- 67.01 - 92.80
- 92.81 - 131.00
- 131.01 - 177.70
- 177.71 - 257.50
- 257.51 - 447.20
- 447.21 - 749.90

- DOLERITE
- SEDIMENTARY
- ARENITE
- MUDSTONE
- SHALE
- QUARTZITE
- MARBLE
- DOLOMITE
- BASALT
- LAVA
- CLINOPYROXENITE
- GABBRO
- NORITE
- RHYOLITE
- DIORITE
- SYENITE
- ANORTHOSITE
- GRANITE
- AMFIBOLITE, MAFIC GRANULITE, METAPELITE
- GNEISS

SCALE: 1:250,000

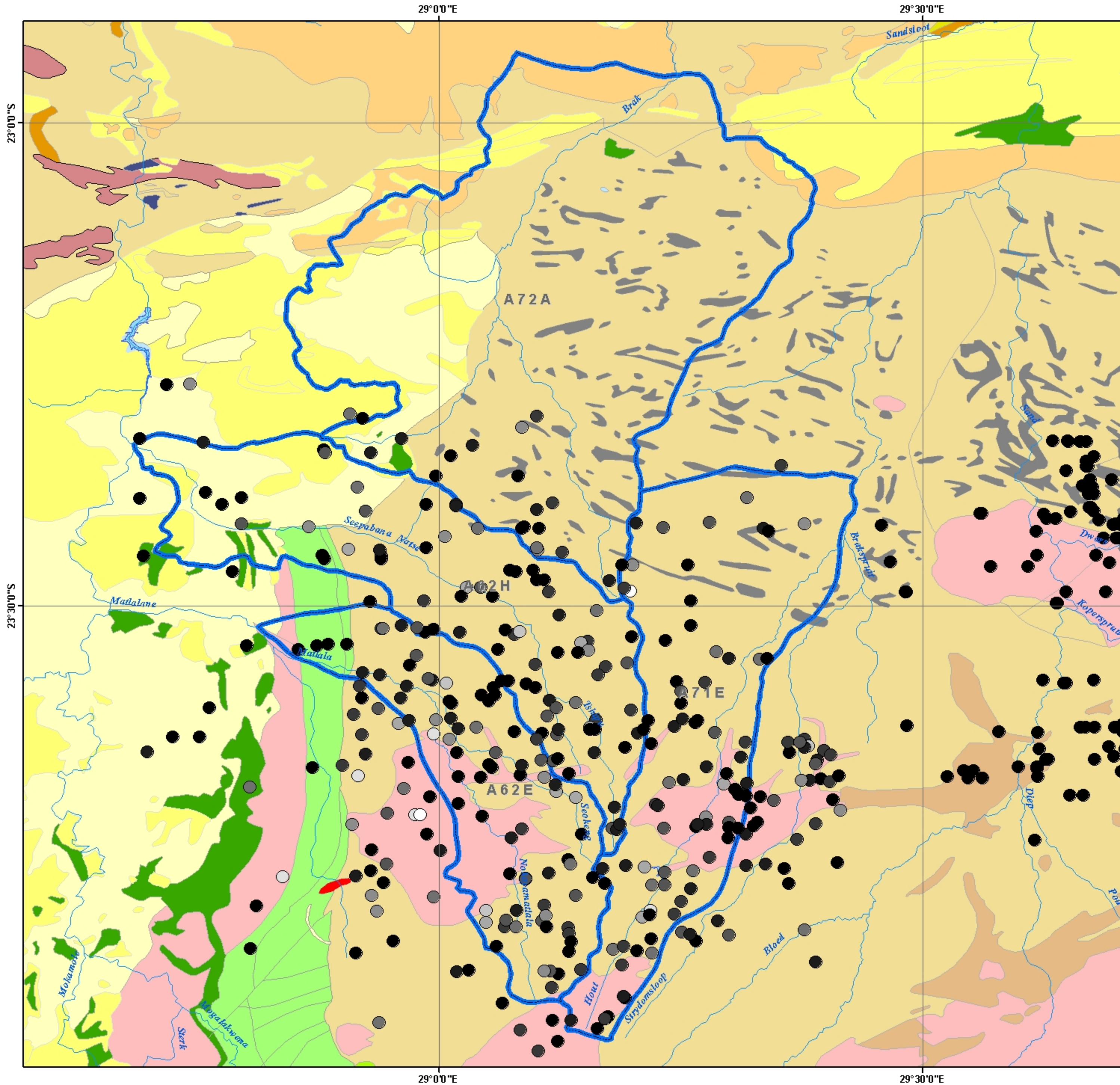
SCALE BAR:
0 1.252.5 5 7.5 10 Kilometers

PROJECTION:
WGS 84
DEGREES MINUTES SECONDS

MAP COMPILED BY:
T.G. ROSSOUW



Transmissivity of WMA1 - Cooper-Jacob



Legend

- River
- DAMS
- WMA1 Focus Area
- WMA2 Focus Area
- DOLERITE
- SEDIMENTARY
- ARENITE
- MUDSTONE
- SHALE
- QUARTZITE
- MARBLE
- DOLOMITE
- BASALT
- LAVA
- CLINOPYROXENITE
- GABBRO
- NORITE
- RHYOLITE
- DIORITE
- SYENITE
- ANDRTHOSITE
- GRANITE
- AMFIBOLITE, MAFIC GRANULITE, METAPELITE
- GNEISS

Borehole Data

C-J

- 0.000 - 7.000
- 7.001 - 20.700
- 20.701 - 39.300
- 39.301 - 65.400
- 65.401 - 95.700
- 95.701 - 141.100
- 141.101 - 200.400
- 200.401 - 263.600
- 263.601 - 430.700
- 430.701 - 1198.400

SCALE: 1:325,000

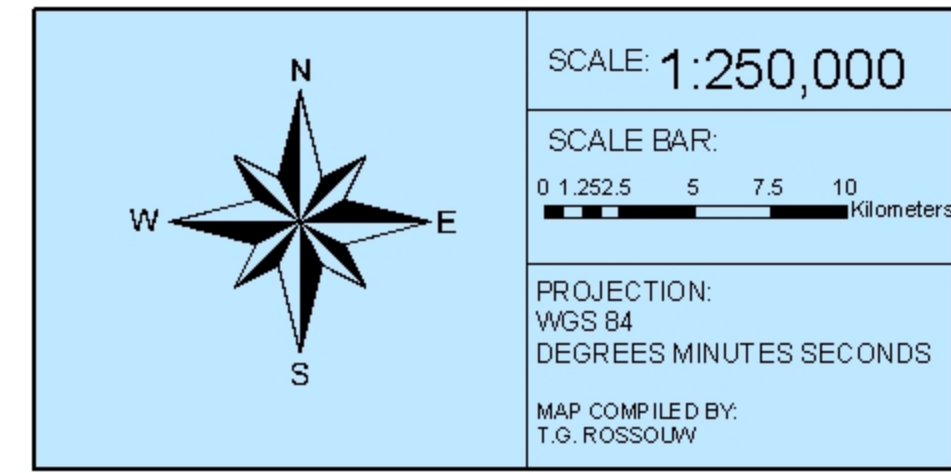
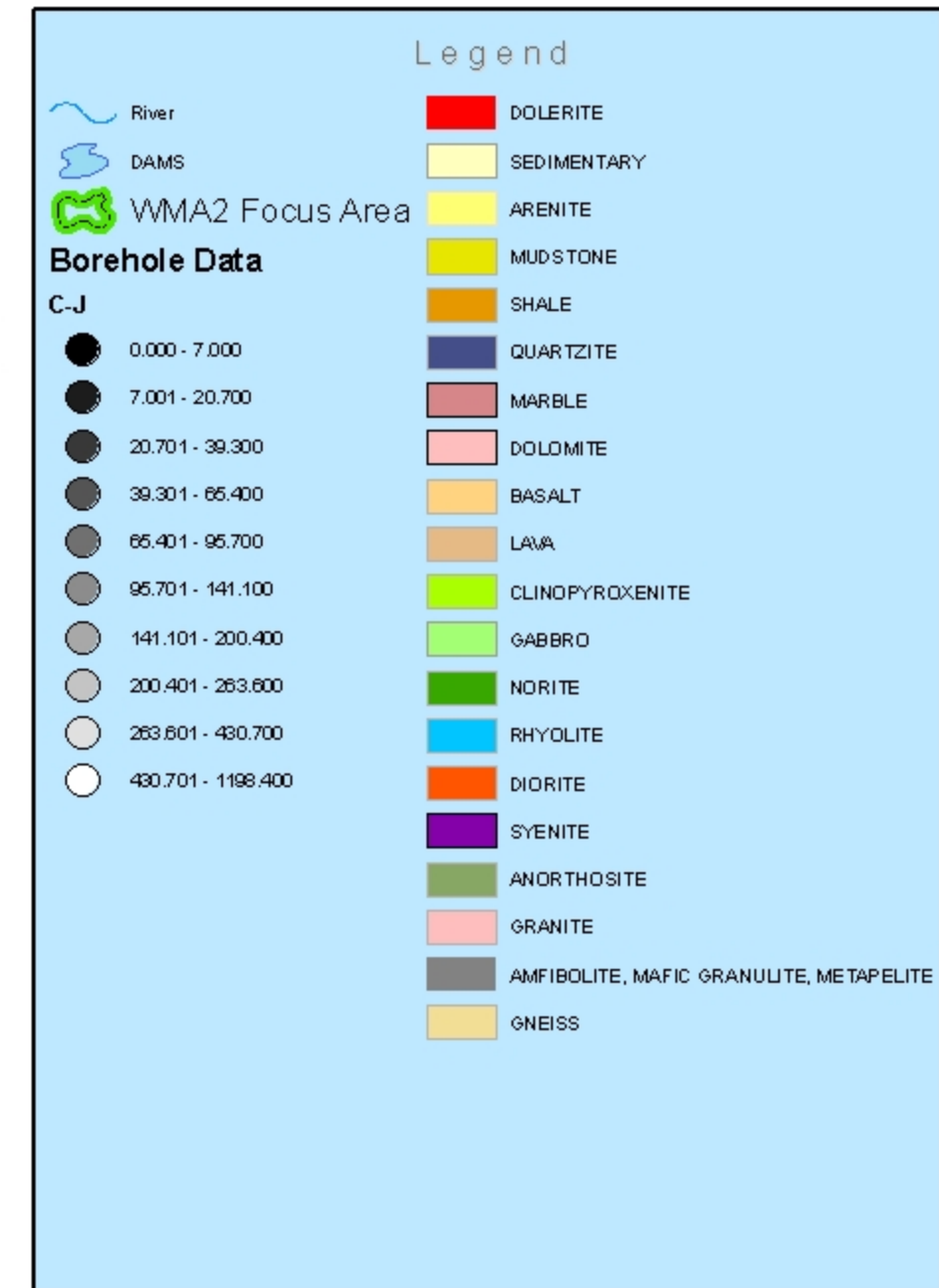
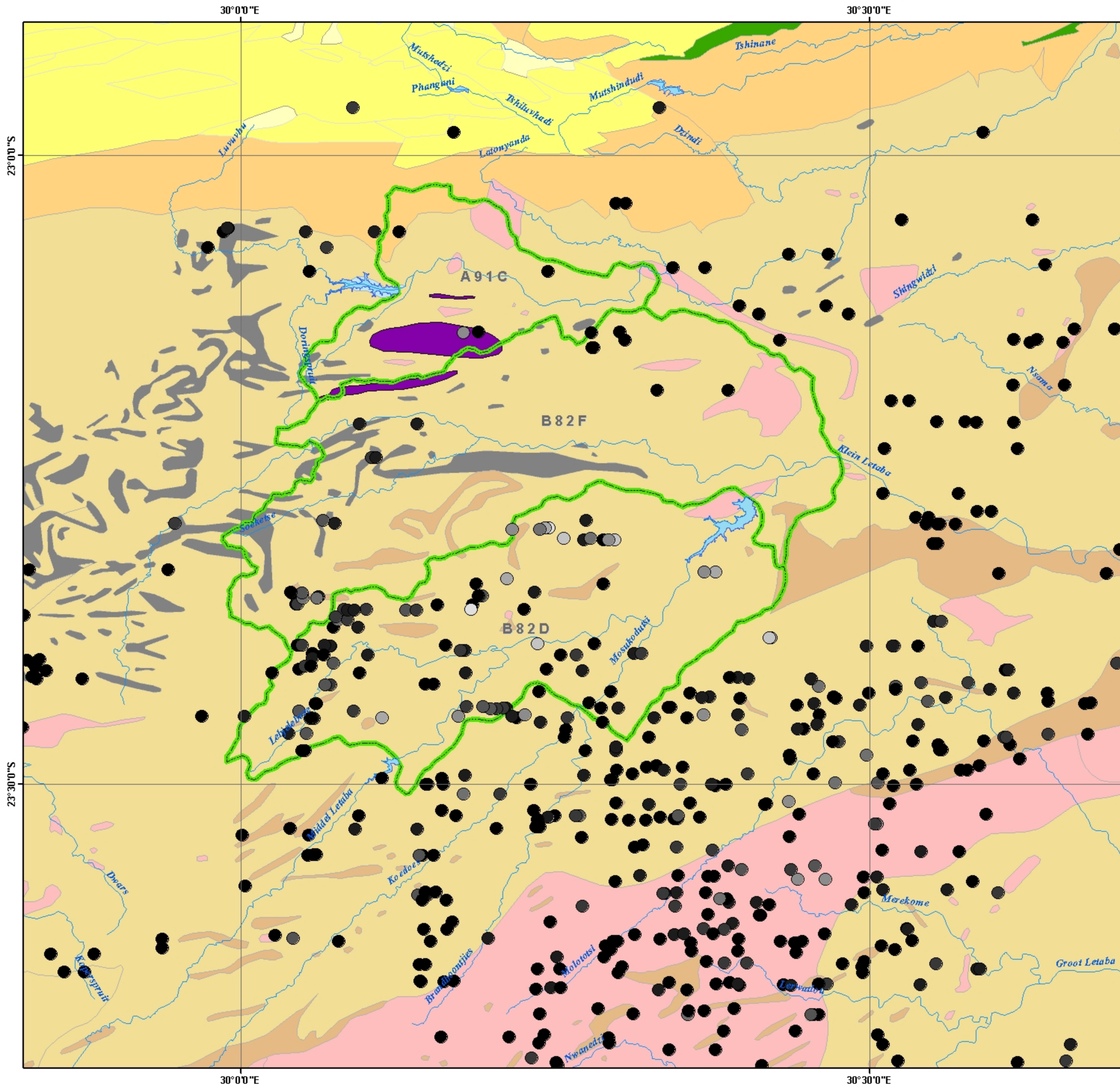
SCALE BAR:
0 1.5 3 6 9 12 Kilometers

PROJECTION:
WGS 84
DEGREES MINUTES SECONDS

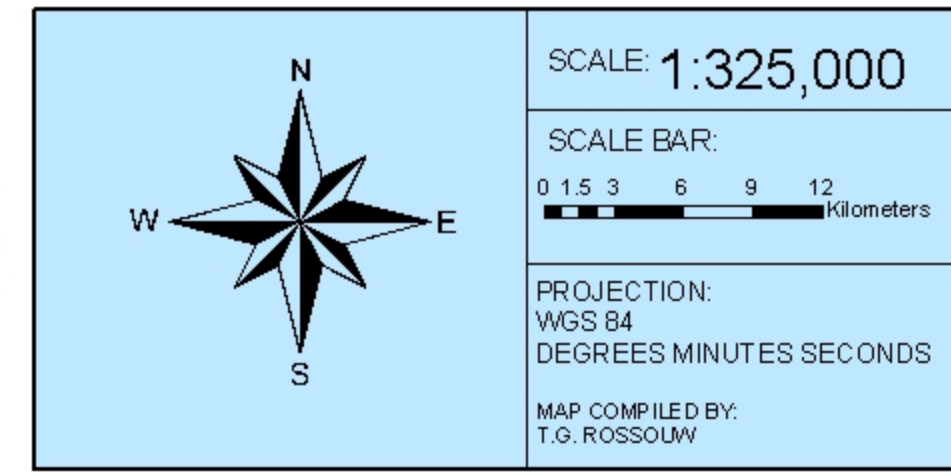
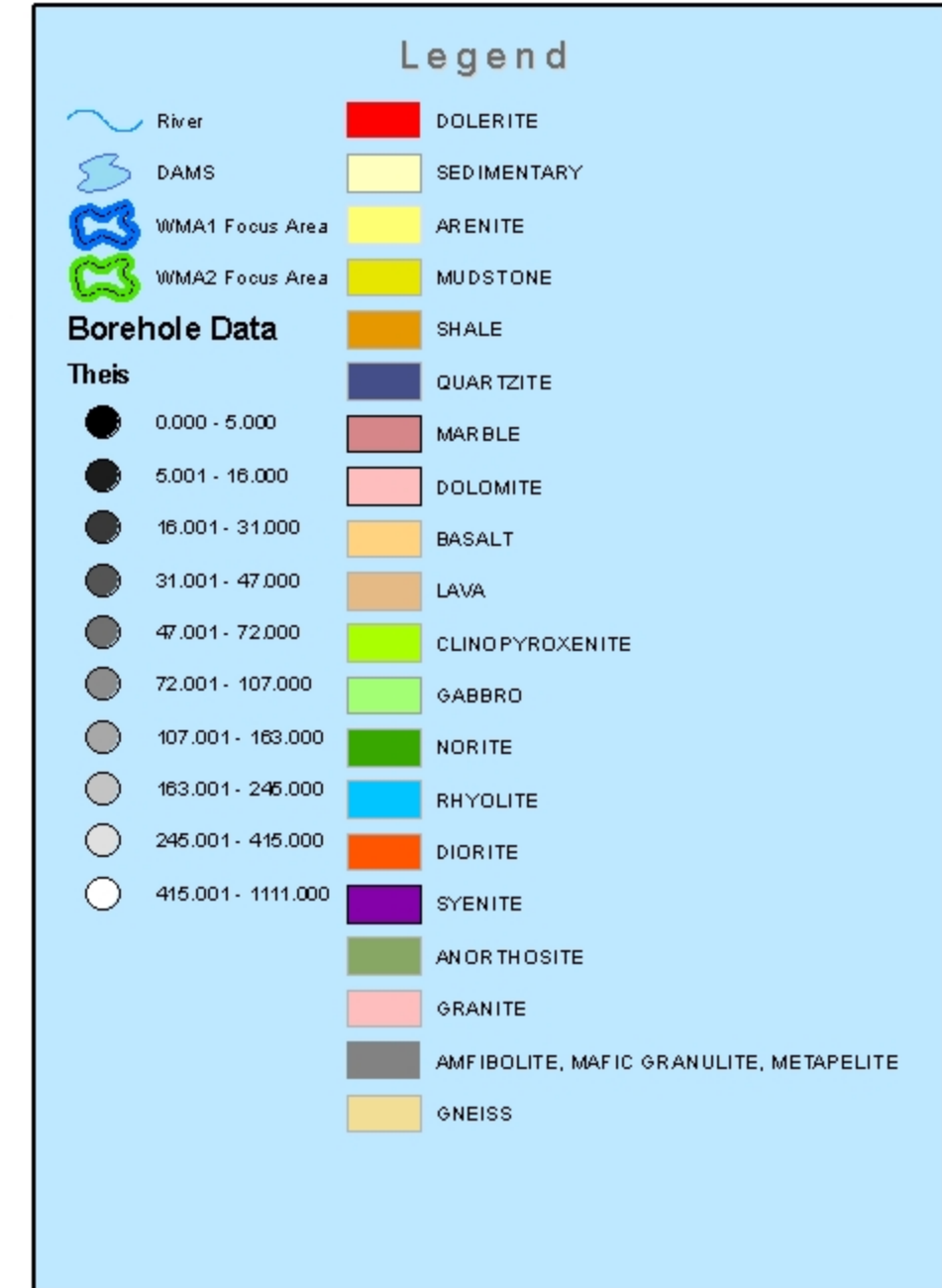
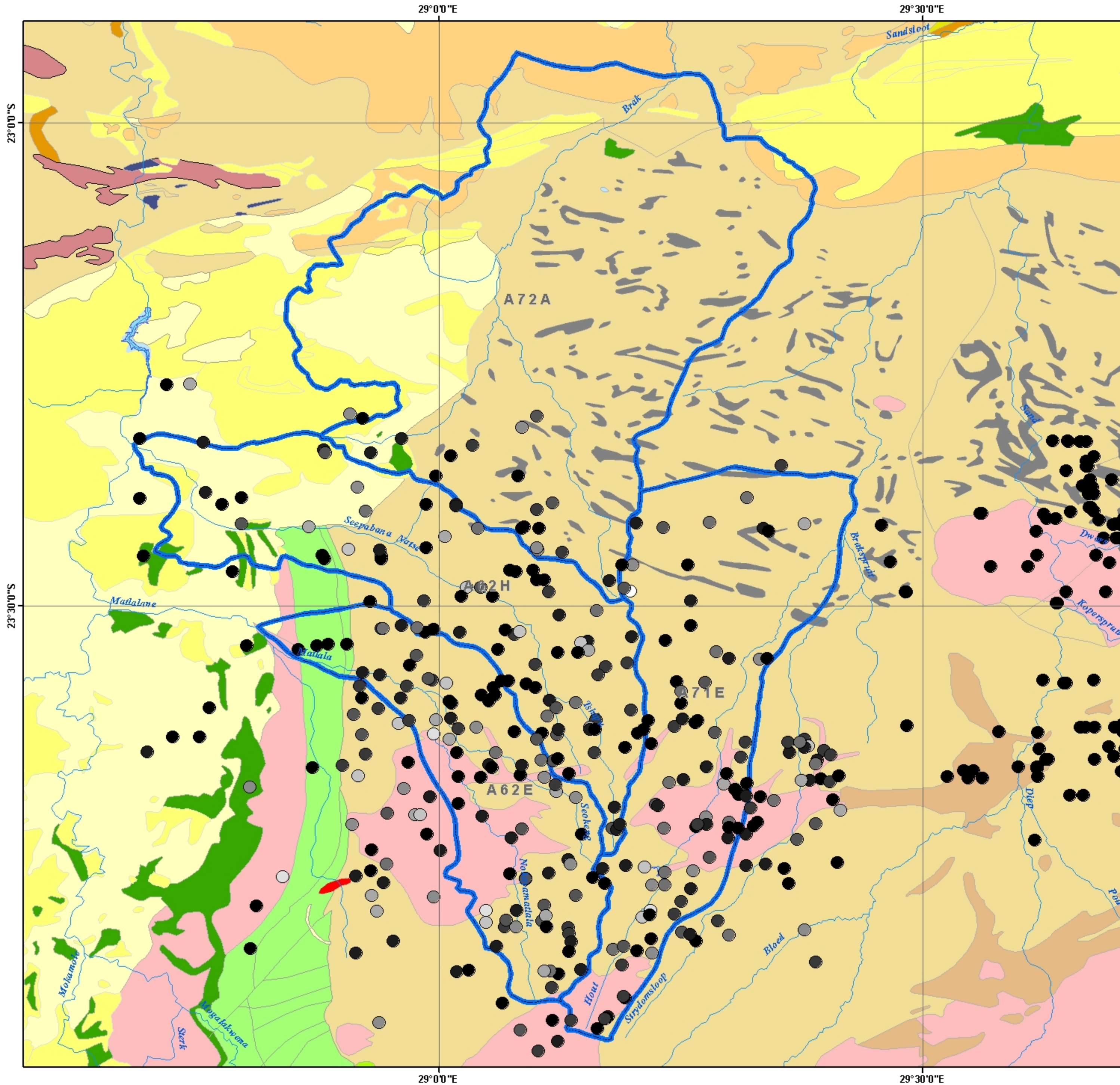
MAP COMPILED BY:
T.G. ROSSOUW



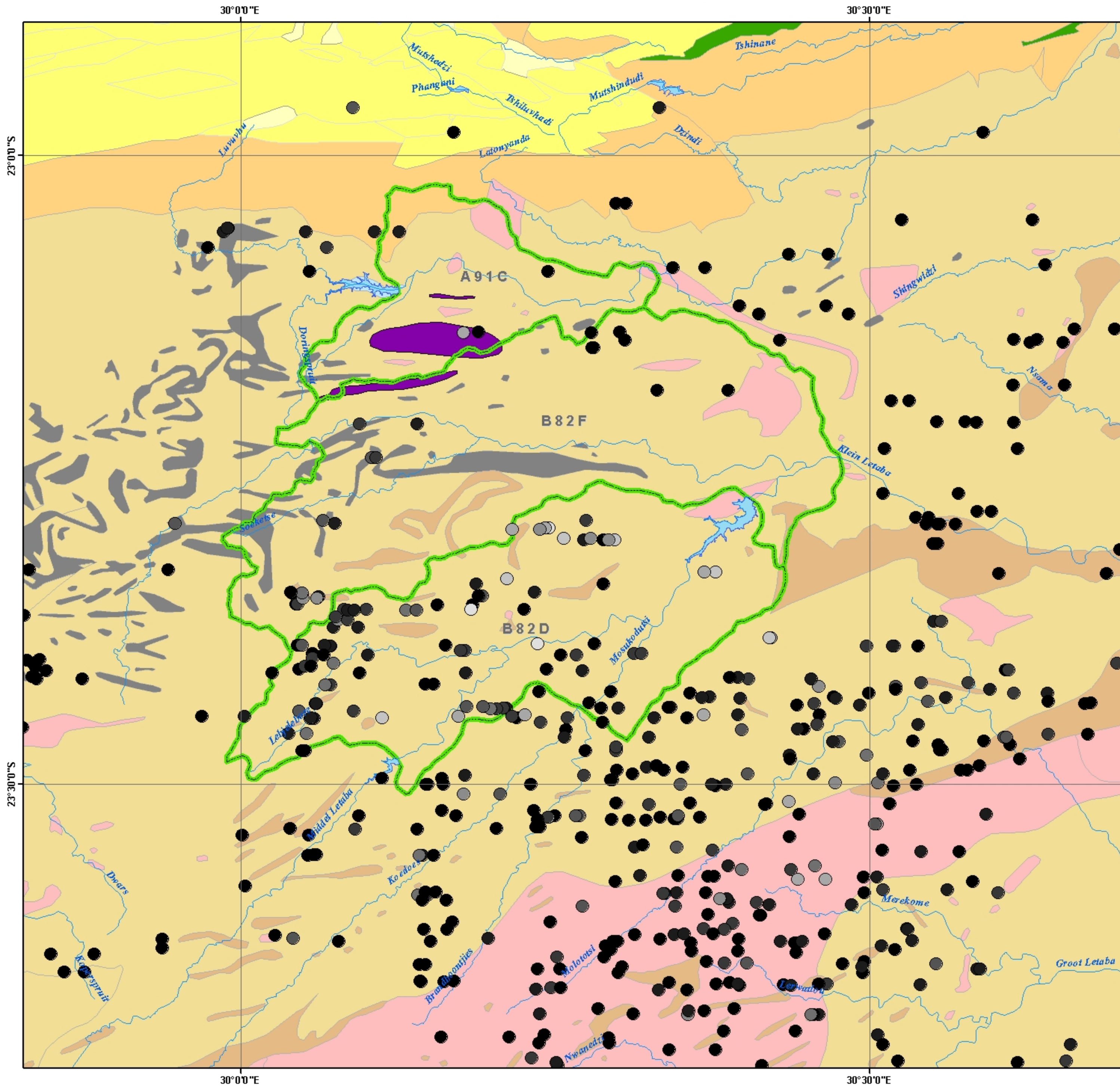
Transmissivity of WMA2 - Cooper-Jacob



Transmissivity of WMA1 - Theis



Transmissivity of WMA2 - Theis



Legend

- River
- DAMS
- WMA2 Focus Area

Borehole Data

Theis

- 0.000 - 5.000
- 5.001 - 16.000
- 16.001 - 31.000
- 31.001 - 47.000
- 47.001 - 72.000
- 72.001 - 107.000
- 107.001 - 163.000
- 163.001 - 245.000
- 245.001 - 415.000
- 415.001 - 1111.000

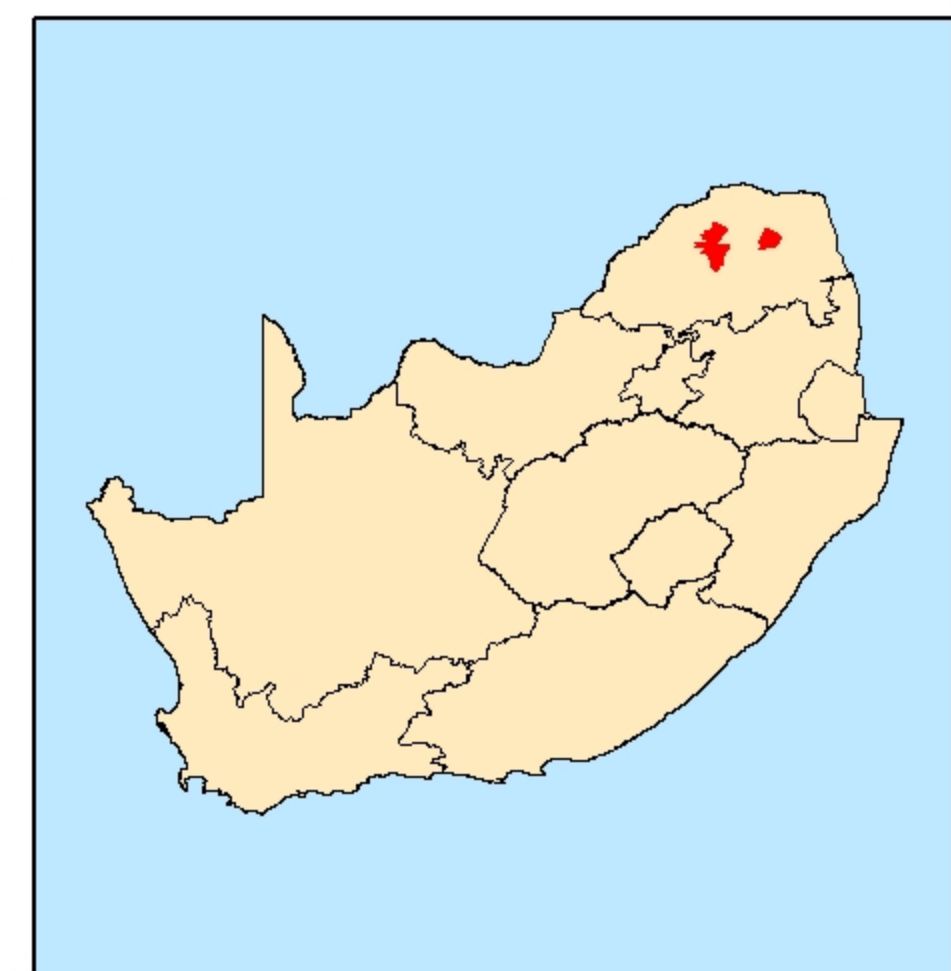
- DOLERITE
- SEDIMENTARY
- ARENITE
- MUDSTONE
- SHALE
- QUARTZITE
- MARBLE
- DOLOMITE
- BASALT
- LAVA
- CLINOPYROXENITE
- GABBRO
- NORITE
- RHYOLITE
- DIORITE
- SYENITE
- ANORTHOSITE
- GRANITE
- AMFIBOLITE, MAFIC GRANULITE, METAPELITE
- GNEISS

SCALE: 1:250,000

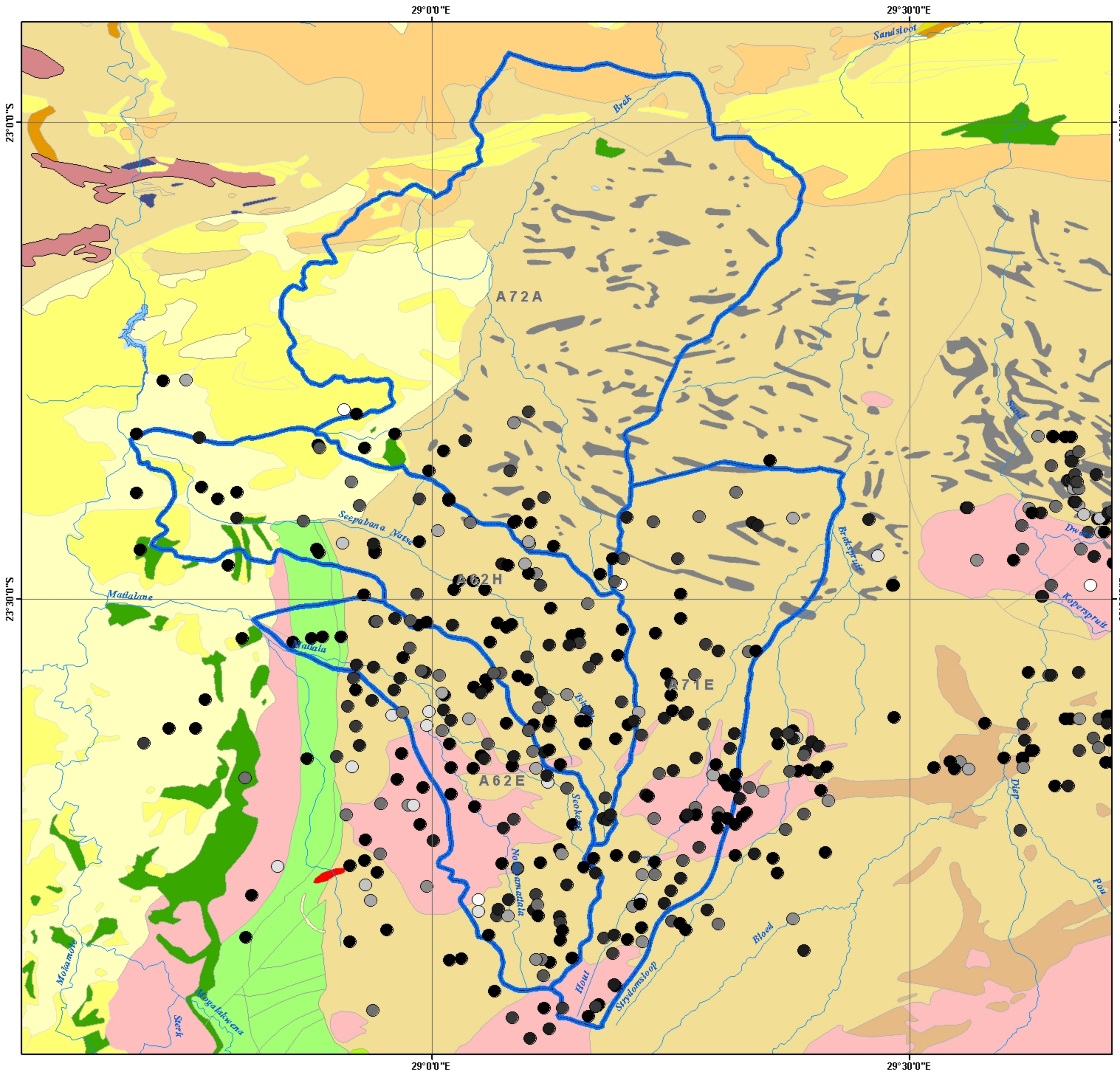
SCALE BAR:
0 1.252.5 5 7.5 10 Kilometers

PROJECTION:
WGS 84
DEGREES MINUTES SECONDS

MAP COMPILED BY:
T.G. ROSSOUW



Transmissivity of WMA1 - Birsoy-Summers



Legend

- River
- DAMS
- WMA1 Focus Area
- WMA2 Focus Area
- DOLERITE
- SEDIMENTARY
- ARENITE
- MUDSTONE
- SHALE
- QUARTZITE
- MARBLE
- DOLOMITE
- BASALT
- LAVA
- CLINOPYROXENITE
- GABBRO
- NORITE
- RHYOLITE
- DIORITE
- SYENITE
- ANORTHOSITE
- GRANITE
- AMFIBOLITE, MAFIC GRANULITE, METAPELITE
- GNEISS

Borehole Data

B-S

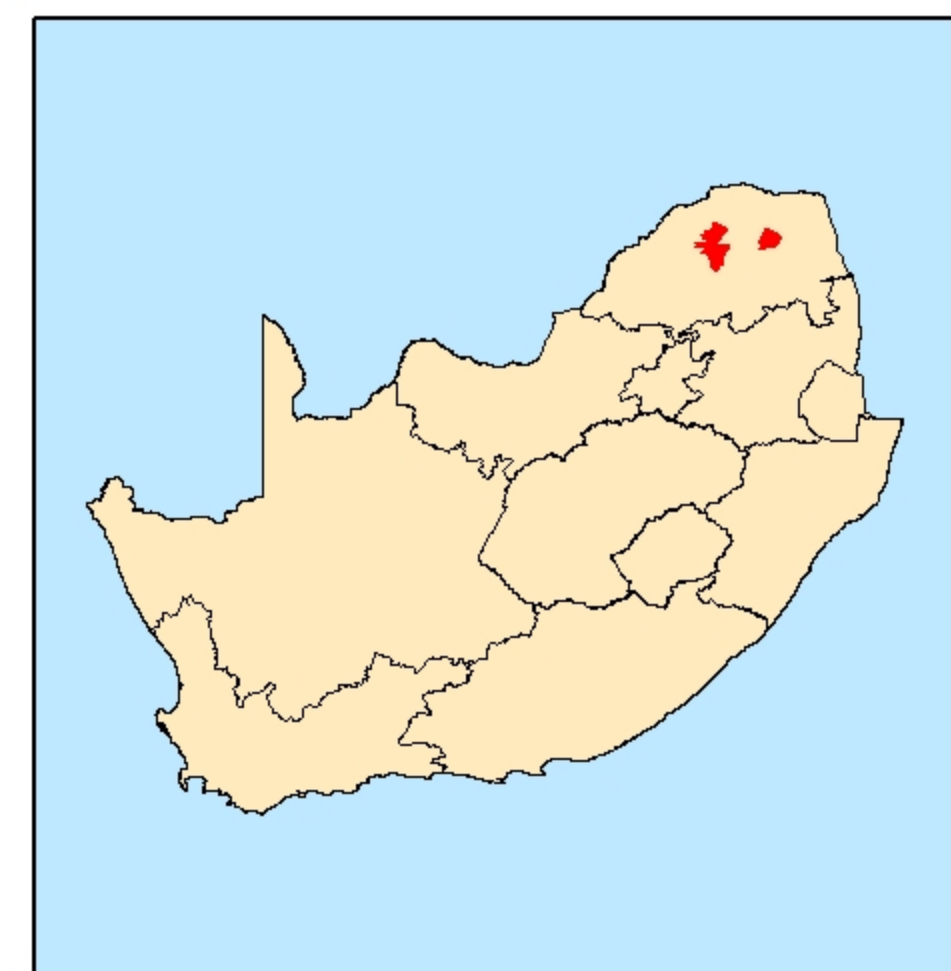
- 0.000 - 9.000
- 9.001 - 20.000
- 20.001 - 32.000
- 32.001 - 46.000
- 46.001 - 63.000
- 63.001 - 82.000
- 82.001 - 104.000
- 104.001 - 134.000
- 134.001 - 200.000
- 200.001 - 330.000

SCALE: 1:325,000

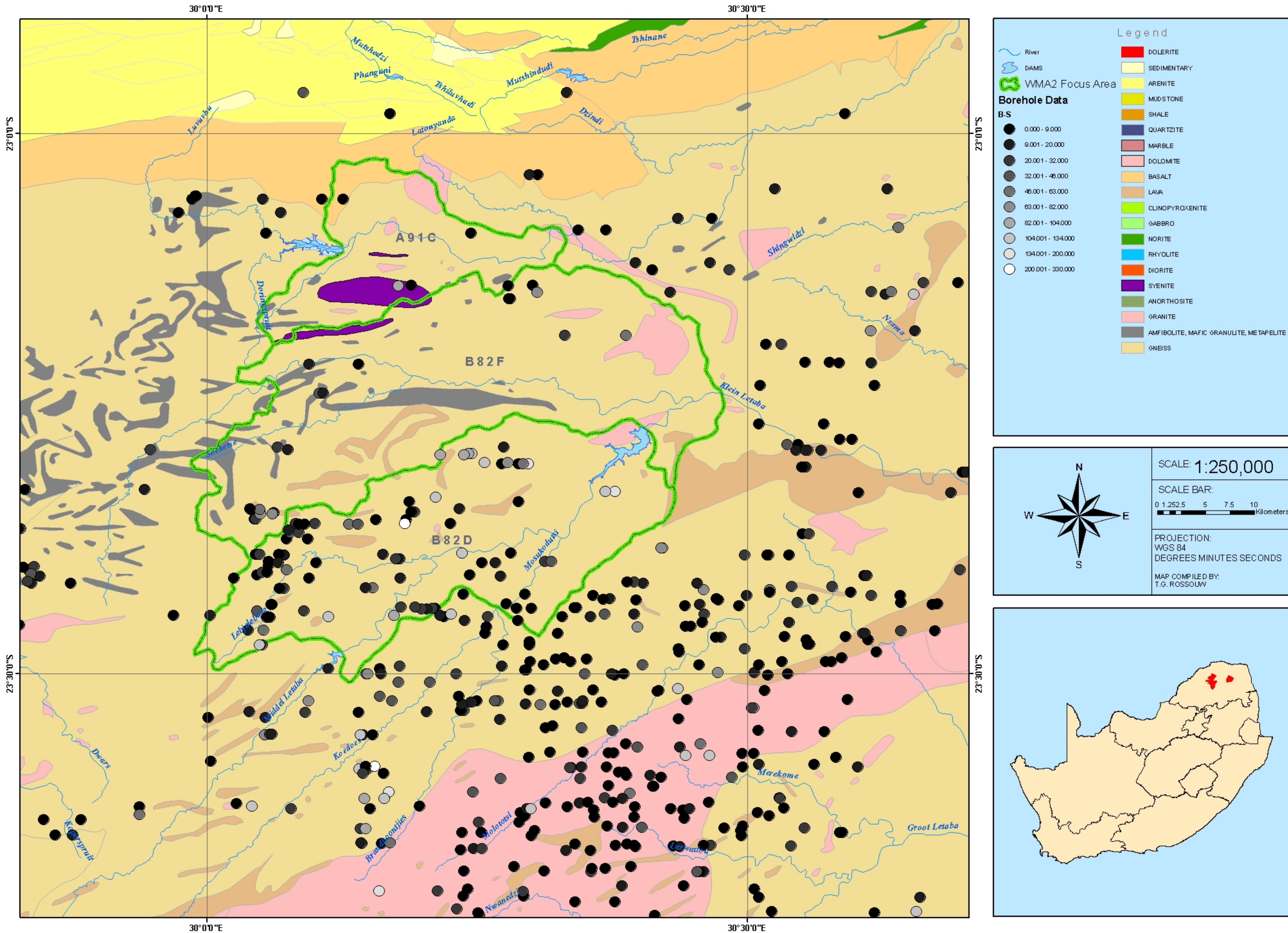
SCALE BAR:
0 1.5 3 6 9 12 Kilometers

PROJECTION:
WGS 84
DEGREES MINUTES SECONDS

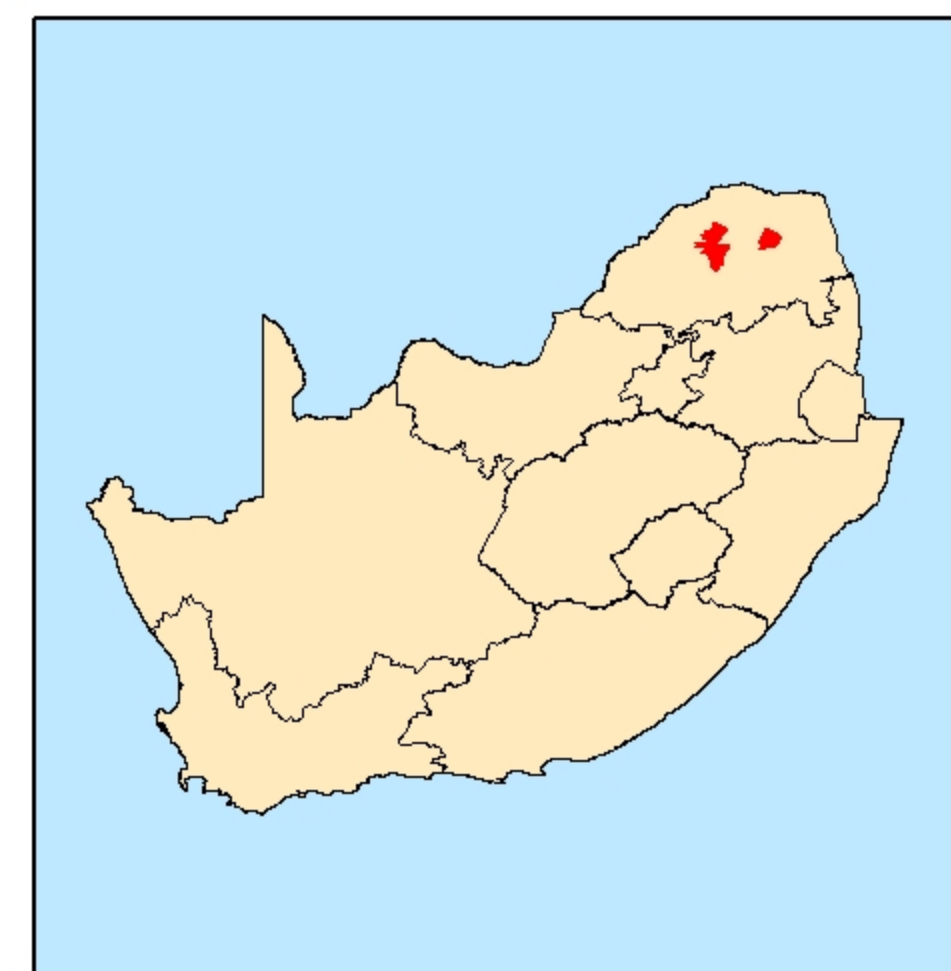
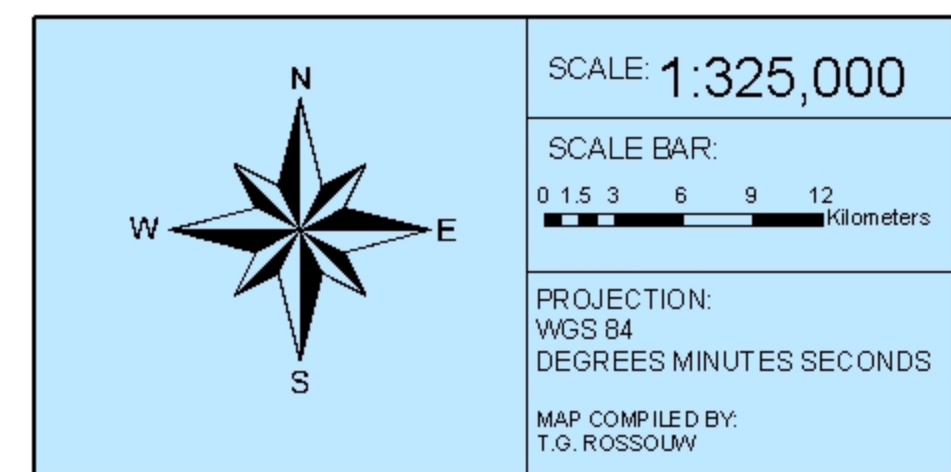
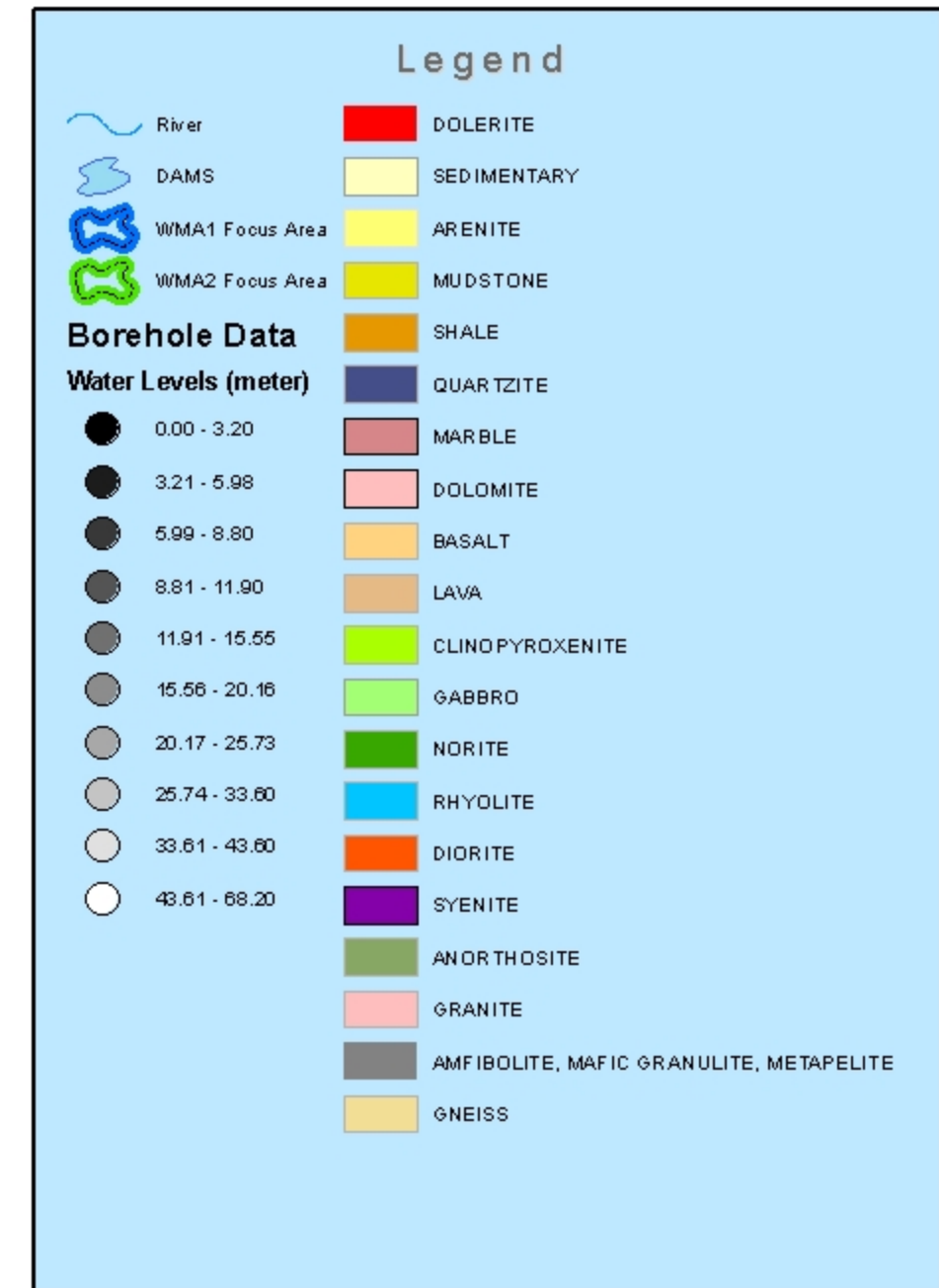
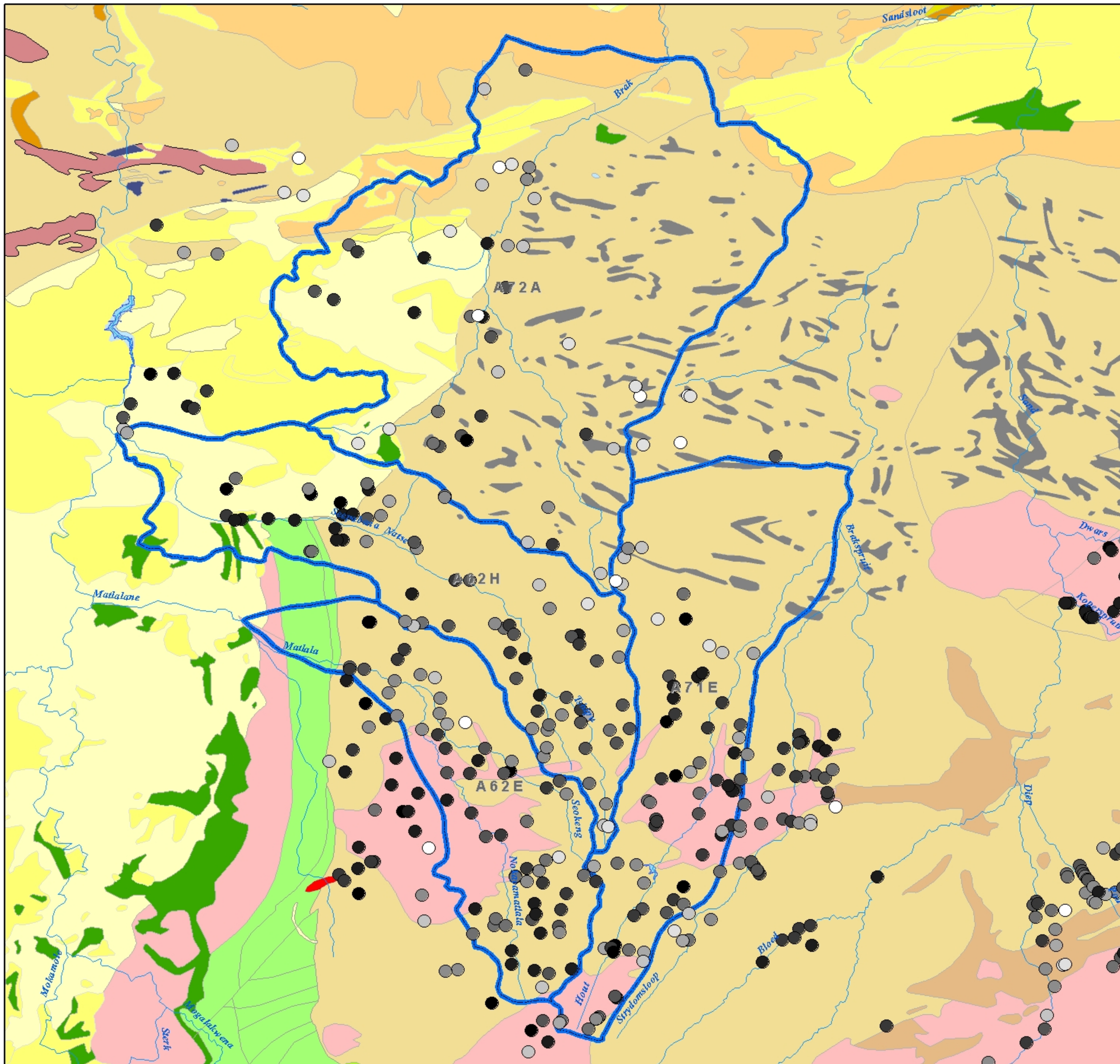
MAP COMPILED BY:
T.G. ROSSOUW



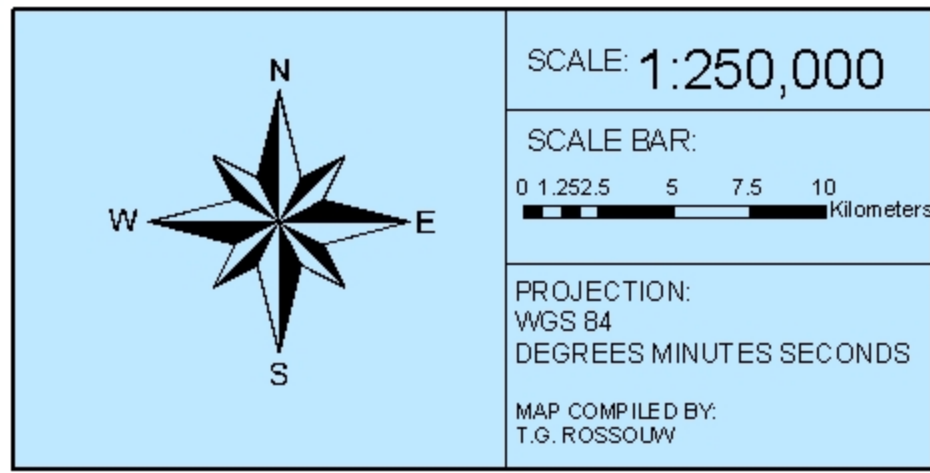
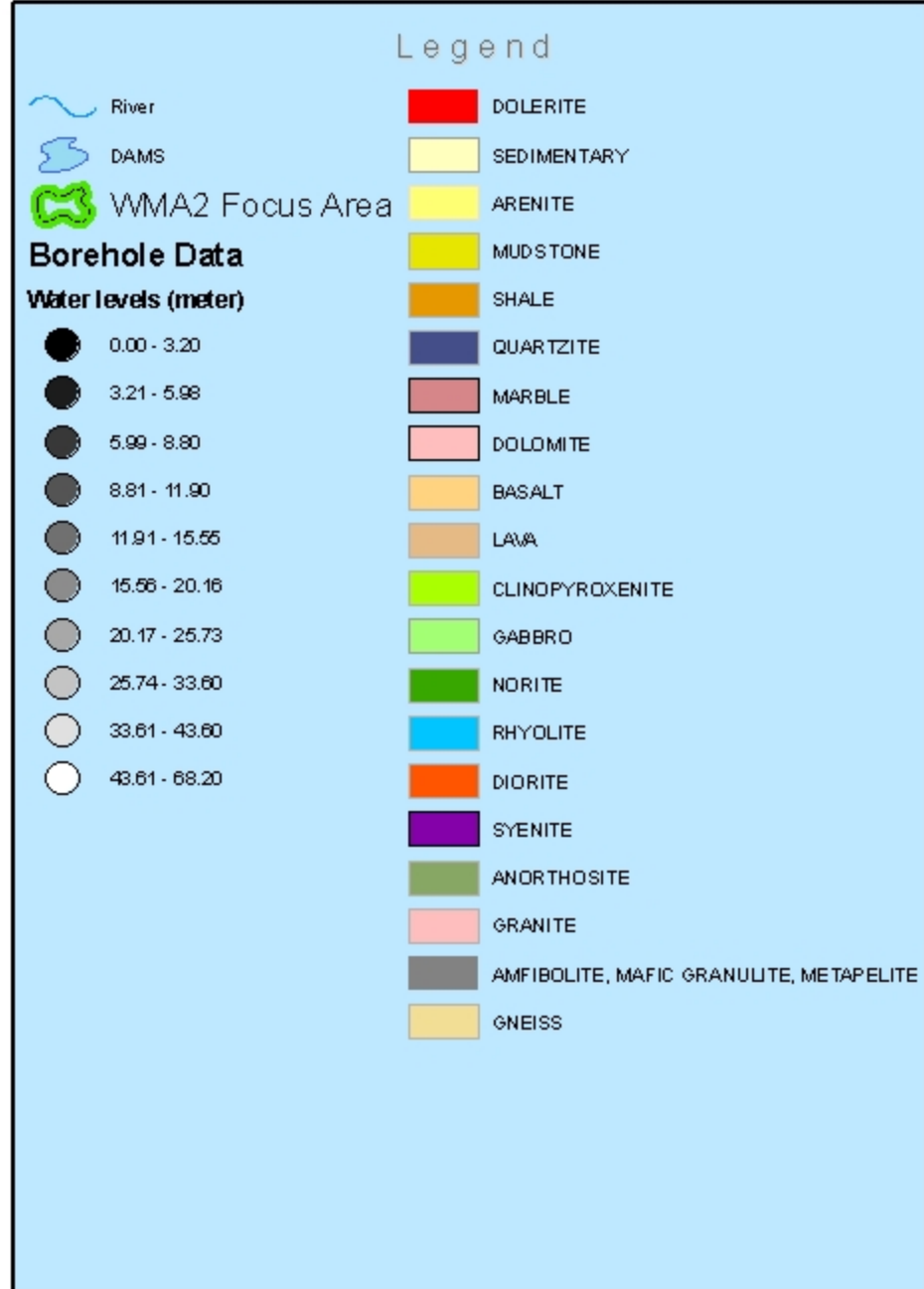
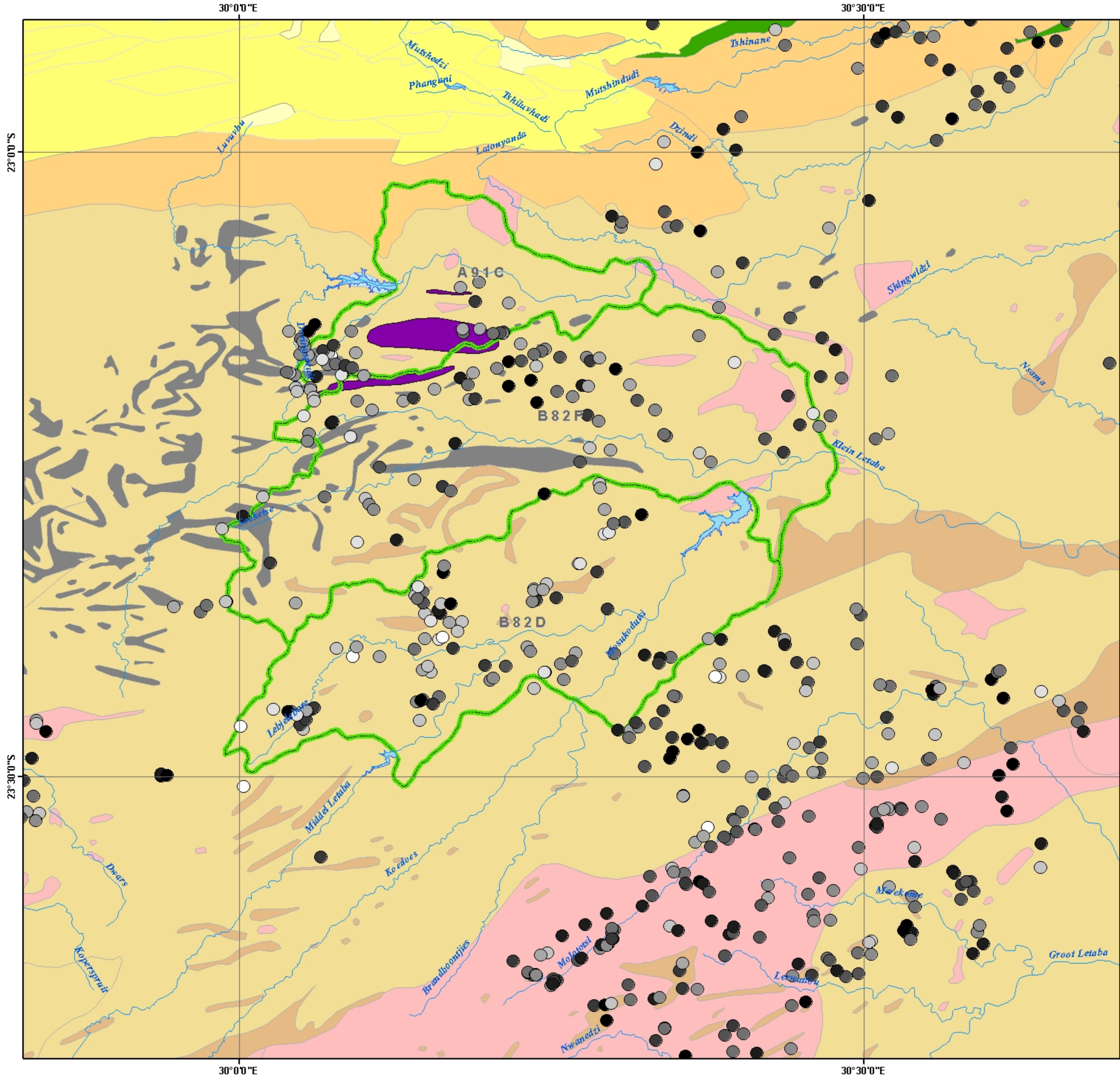
Transmissivity of WMA2 - Birsoy-Summers



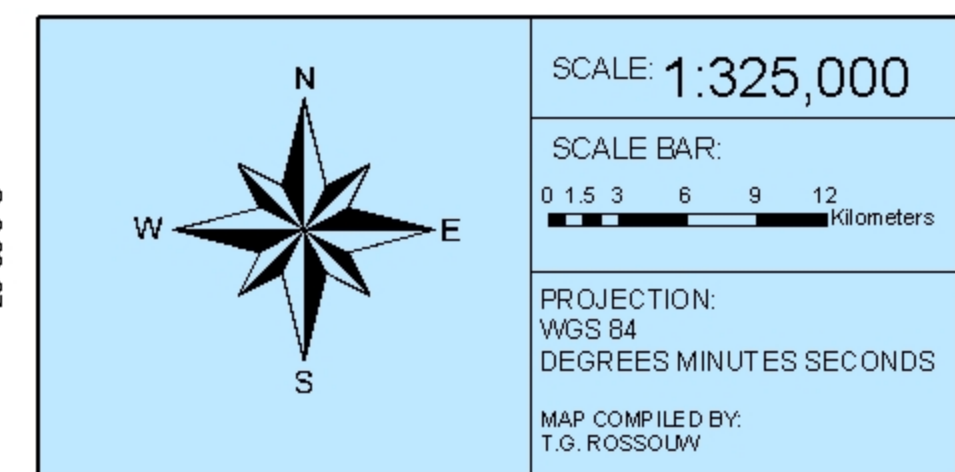
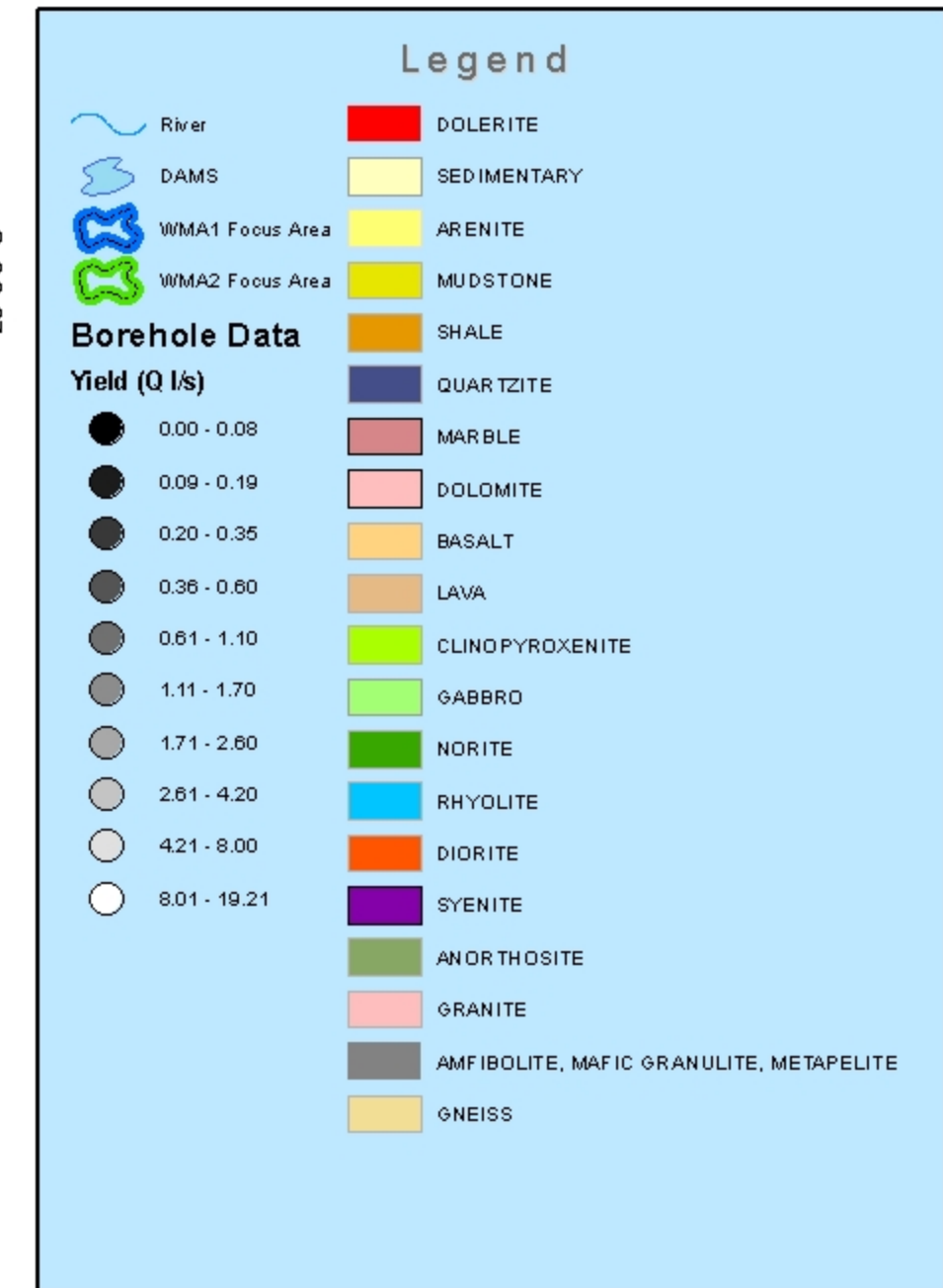
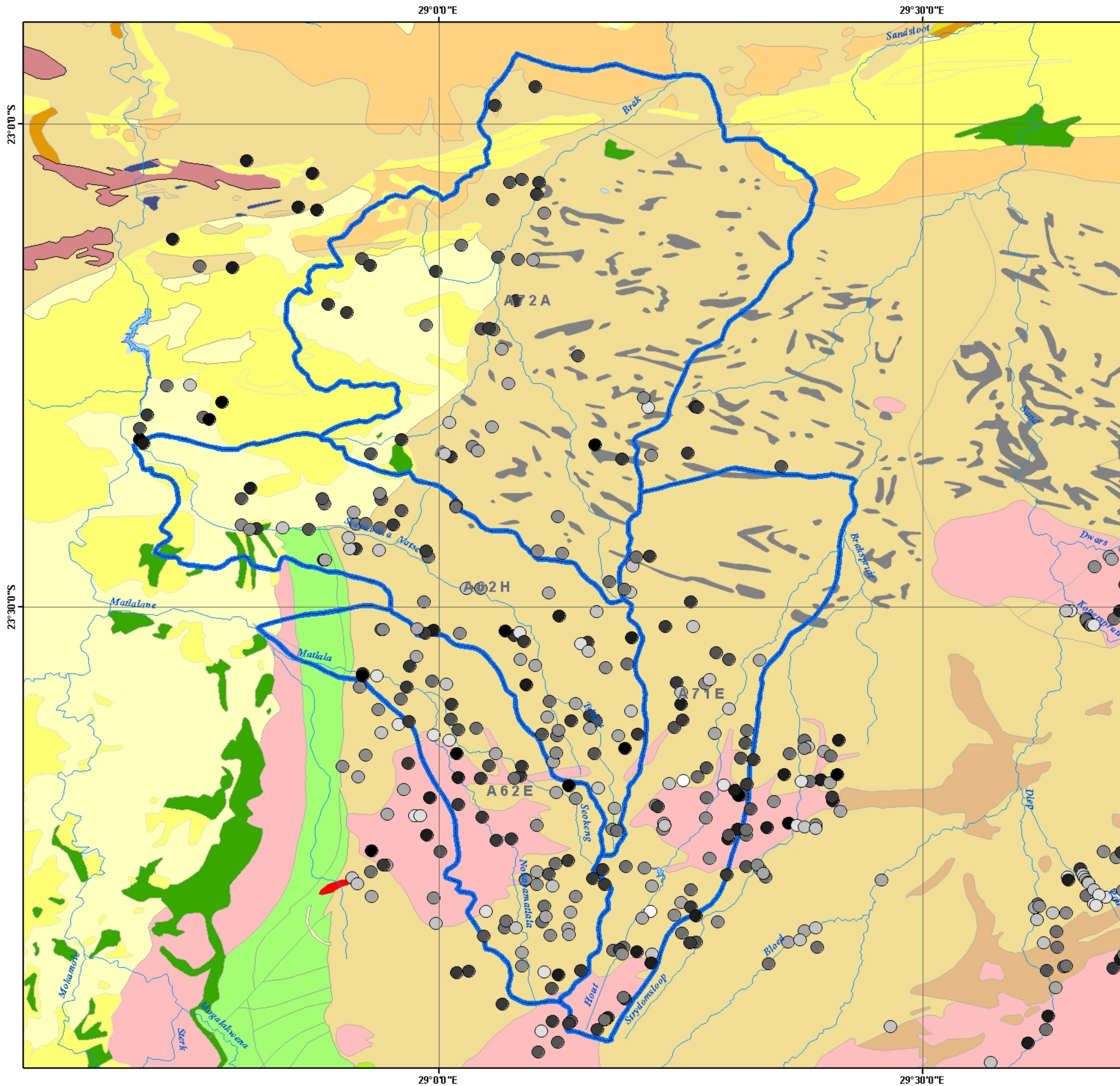
Water Levels of WMA1



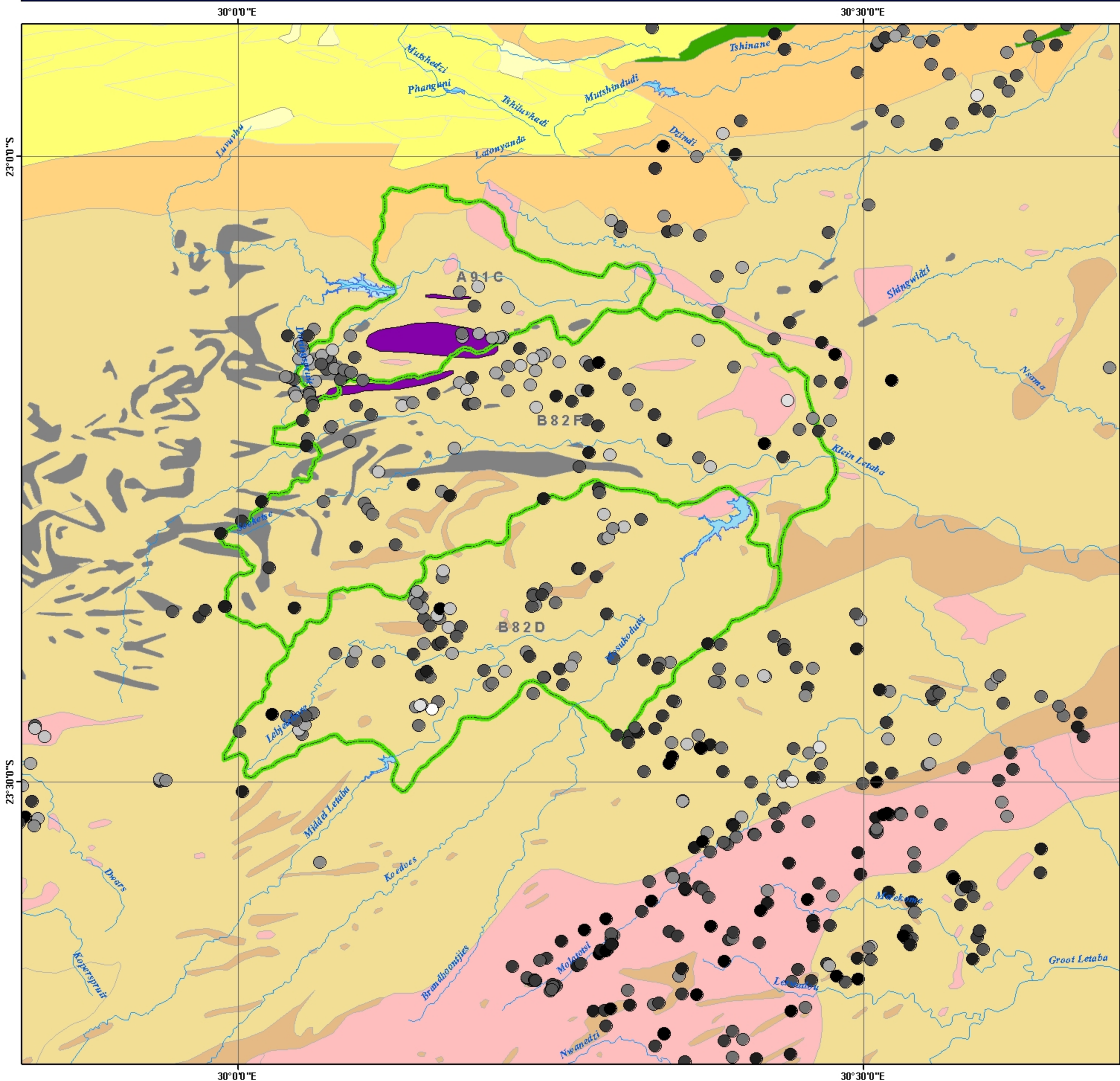
Water levels of WMA2



Sustainable Yields of WMA1



Sustainable Yields of WMA2



Legend

- River
- DAMS
- WMA2 Focus Area

Borehole Data

Yield (Q l/s)

- 0.00 - 0.08
- 0.09 - 0.19
- 0.20 - 0.35
- 0.36 - 0.60
- 0.61 - 1.10
- 1.11 - 1.70
- 1.71 - 2.60
- 2.61 - 4.20
- 4.21 - 8.00
- 8.01 - 19.21

- DOLERITE
- SEDIMENTARY
- ARENITE
- MUDSTONE
- SHALE
- QUARTZITE
- MARBLE
- DOLOMITE
- BASALT
- LAVA
- CLINOPYROXENITE
- GABBRO
- NORITE
- RHYOLITE
- DIORITE
- SYENITE
- ANORTHOSITE
- GRANITE
- AMFIBOLITE, MAFIC GRANULITE, METAPELITE
- GNEISS

SCALE: 1:250,000

SCALE BAR:
0 1.252.5 5 7.5 10 Kilometers

PROJECTION:
WGS 84
DEGREES MINUTES SECONDS

MAP COMPILED BY:
T.G. ROSSOUW



APPENDIX B: DATA

Table B-1:	Results of Pumping Test Interpretation
Table B-2:	Constant discharge data for high T scenario: borehole H04-0306
Table B-3:	Constant discharge data for intermediate T scenario: borehole H10-0084
Table B-4:	Constant discharge data for low T scenario: borehole H17-0841
Table B-5:	Step-drawdown data for high T scenario: borehole H04-0306
Table B-6:	Step-drawdown data for intermediate T scenario: borehole H10-0084
Table B-7:	Step-drawdown data for low T scenario: borehole H17-0841

Table B-1: Results of Pumping Test Interpretation

H-No	swl (m)	T (m ² /d)				Re (step)	S (step)	Sust Q (l/s per 24h)	Long	Lat
		Logan	Theis	C-J	B-S					
H04-0001	11.55	98.80	77.00	137.50	51.00	3.00	0.001	1.60	29.27556	-23.71824
H04-0006	10.50	6.50	3.00	8.10	3.00	1.60	0.001	0.35	29.31873	-23.68327
H04-0007	4.34	33.80	20.00	17.40	18.00	1.20	0.001	0.60	29.31264	-23.65625
H04-0009	4.40	26.30	20.00	28.70	18.00	0.80	0.001	2.10	29.39812	-23.64896
H04-0013	7.97	12.00	20.00	39.20	4.00	2.10	0.001	0.70	29.37823	-23.63775
H04-0015	31.81	72.70	44.00	37.60	39.00	6.20	0.001	1.40	29.38955	-23.72457
H04-0016	6.81	5.40	3.00	3.20	3.00	6.40	0.001	0.15	29.40726	-23.70039
H04-0019	12.50	21.10	17.00	2.60	11.00	10.00	0.001	0.60	29.32260	-23.70834
H04-0022	27.72	92.50	69.00	65.40	65.00	0.70	0.001	1.40	29.34613	-23.70088
H04-0024	3.51	11.60	6.00	5.70	5.00	3.00	0.001	0.15	29.29933	-23.73933
H04-0043	16.16	22.10	20.00	12.20	10.00	3.30	0.001	1.20	29.28809	-23.82516
H04-0044	18.36	24.00	23.00	23.70			0.001	1.00	29.81819	-23.27378
H04-0049	6.59	52.80	43.00	29.50	29.00	1.80	0.001	1.30	29.27999	-23.75936
H04-0053	10.48	16.60	31.00	29.40	5.00	2.70	0.001	0.50	29.35422	-23.35422
H04-0055	21.48	11.80	15.00	15.10	7.00	1.40	0.001	0.80	29.31741	-23.73599
H04-0057	15.80	10.00	11.00	15.60	5.00	1.00	0.001	0.40	29.31749	-23.76840
H04-0061	11.62	3.80	3.00	4.10	2.00	0.60	0.001	0.20	29.24608	-23.57760
H04-0062	6.32	69.50	55.00	94.10	40.00	3.60	0.001	3.00	29.23785	-23.68210
H04-0065	11.43	2.20	1.00	1.10	1.00	0.90	0.001	0.03	29.19208	-23.64585
H04-0066	11.40	4.20	4.00	8.70	2.00	0.30	0.001	0.25	29.20555	-23.63135
H04-0069	22.52	47.00	26.00	24.50	24.00	1.40	0.001	0.50	29.16255	-23.61696
H04-0084	17.56	36.70	37.00	60.80	17.00	1.50	0.001	1.00	29.12221	-23.63314
H04-0093	15.00	6.50	23.00	36.20	3.00	1.00	0.001	0.25	29.07797	-23.52922
H04-0094	17.60	3.80	3.00	1.90	2.00	0.40	0.001	0.04	29.06889	-23.52422
H04-0096	9.65	27.70	33.00	51.80			0.001	1.20	29.04299	-23.48049
H04-0098	29.45	104.60	91.00	115.30	80.00	3.20	0.001	1.60	29.10197	-23.44182
H04-0104	8.54	16.20	17.00	24.80	4.00	2.40	0.001	1.30	29.12706	-23.44394
H04-0105A	29.50	292.50	1111.0	1198.4	250.00	0.10	0.001	3.00	29.19783	-23.48453
H04-0106	32.40	14.40	11.00	8.60	9.00	4.20	0.001	1.00	29.17604	-23.47312
H04-0114	13.00	14.30	8.00	6.90	5.00	3.20	0.001	0.25	29.26058	-23.49448
H04-0116	23.28	8.00	7.00	6.50	4.00	0.80	0.001	0.10	29.19956	-23.53181
H04-0120	34.95	79.50	60.00	95.40	48.00	3.00	0.001	3.00	29.16334	-23.50439
H04-0121	17.91	14.90	9.00	11.50	8.00	1.20	0.001	0.15	29.12395	-23.50876
H04-0122	4.80	5.50	16.00	24.30	3.00	0.40	0.001	0.20	29.15368	-23.53578
H04-0125	15.72	4.66	31.00	54.30	7.00	0.60	0.001	0.70	29.19503	-23.55870
H04-0129	2.63	23.80	20.00	12.60	12.00	1.10	0.001	0.50	29.24375	-23.62414
H04-0141	35.30	50.20	50.00	66.20	23.00	2.60	0.001	0.40	29.28690	-23.54666
H04-0159	29.62	26.70	16.00	14.20	14.00	1.20	0.001	0.40	29.29970	-23.55403
H04-0179	22.73	82.30	100.00	81.60	50.00	2.40	0.001	2.00	29.33140	-23.55505
H04-0183	9.80	4.40	5.00	5.60	2.00	0.70	0.001	0.15	29.09052	-23.57992
H04-0192	17.90	49.50	80.00	162.10	34.00	0.30	0.001	1.70	29.14145	-23.69745
H04-0197	13.97	5.80	4.00	3.20			0.001	0.30	29.15895	-23.78049
H04-0198	25.07	19.70	12.00	9.60			0.001	0.30	29.16915	-23.77131
H04-0201	7.90	17.00	25.00	33.70	15.00	0.20	0.001	1.50	29.13368	-23.83216
H04-0201A	9.93	25.20	25.00	24.50	15.00	0.60	0.001	2.00	29.13368	-23.83216
H04-0202	18.62	49.00	29.00	27.50	28.00	5.20	0.001	1.80	29.13424	-23.83823
H04-0203	8.15	41.50	36.00	41.40	17.00	4.20	0.001	1.50	29.14146	-23.79923
H04-0205	17.00	72.60	80.00	82.30	82.00	1.40	0.001	2.00	29.21998	-23.78794
H04-0206	17.07	51.80	172.00	190.40	19.00	6.10	0.001	1.50	29.21233	-23.76952
H04-0212	14.55	11.70	5.00	6.30	6.00	7.00	0.001	0.40	29.26560	-23.84632
H04-0219	42.50	57.60	47.00	45.10	45.00	1.60	0.001	1.00	29.25110	-23.83724
H04-0222	2.78	10.60	5.00	5.00	4.00	3.90	0.001	0.60	28.79579	-23.38755
H04-0225	10.01	7.00	5.00	5.00	5.00	0.20	0.001	0.30	29.01184	-23.34445
H04-0227	10.01	24.80	18.00	17.70	17.00	0.80	0.001	1.40	29.03467	-23.33375
H04-0236	21.73	21.70	26.00	33.90	10.00	1.80	0.001	1.00	29.01716	-23.39488
H04-0239	3.87	30.50	31.00	28.30	23.00	0.40	0.001	1.50	28.98458	-23.49436
H04-0241	13.86	3.20	2.00	1.50	2.00	0.50	0.001	0.15	28.99396	-23.52350
H04-0243	26.65	4.90	2.00	1.10	2.00	1.30	0.001	0.20	28.98573	-23.52705
H04-0252	2.44	41.00	28.00	28.30	28.00	0.50	0.001	0.70	28.94013	-23.52292



H-No	swl (m)	T (m ² /d)				Re (step)	S (step)	Sust Q (l/s per 24h)	Long	Lat
		Logan	Theis	C-J	B-S					
H04-0257	8.09	5.80	4.00	3.30	3.00	2.00	0.001	0.25	28.96978	-23.56056
H04-0261	6.07	51.60	45.00	44.70	45.00	0.40	0.001	2.40	28.97623	-23.55108
H04-0264	18.56	27.70	20.00	18.50	19.00	0.20	0.001	0.80	28.99266	-23.57621
H04-0268	19.63	7.60	4.00	4.00	4.00	2.20	0.001	0.20	29.01309	-23.60026
H04-0274	7.91	28.80	23.00	18.70	20.00	0.90	0.001	1.20	28.92355	-23.65278
H04-0276	4.95	296.30	240.00	430.70	172.00	1.80	0.001	2.00	28.91591	-23.67518
H04-0280	1.58	33.30	31.00	54.00	12.00	4.30	0.001	1.20	28.93689	-23.60588
H04-0287	5.65	5.50	3.00	2.90	3.00	1.20	0.001	0.35	28.96831	-23.66155
H04-0297	13.20	77.40	46.00	45.50	47.00	2.20	0.001	1.90	28.94658	-23.71385
H04-0305	2.41	148.50	163.00	392.60	70.00	6.50	0.001	5.00	28.97521	-23.71544
H04-0306	4.11	307.30	240.00	760.80	188.00	4.40	0.001	5.00	28.98011	-23.71547
H04-0307	3.60	1.40	1.00	0.60	1.00	1.70	0.001	0.05	28.92995	-23.75175
H04-0308	3.66	9.80	4.00	4.90	5.00	1.90	0.001	0.70	28.92938	-23.77321
H04-0312	1.89	234.90	101.00	107.90	100.00	7.30	0.001	4.00	28.93014	-23.79907
H04-0313	2.94	104.60	140.00	120.40	120.00	0.10	0.001	2.50	28.93018	-23.79908
H04-0328	3.37	1.40	1.00	0.50	1.00	0.30	0.001	0.10	28.98737	-23.73535
H04-0329	46.10	23.40	16.00	13.20	16.00	6.00	0.001	0.50	29.00090	-23.75305
H04-0333	16.20	83.50	75.00	80.00	64.00	0.60	0.001	1.50	28.99395	-23.80086
H04-0346	13.07	23.50	16.00	16.80	17.00	0.90	0.001	0.25	28.92076	-23.56868
H04-0348	24.56	37.70	23.00	19.80	19.00	2.40	0.001	0.60	29.01955	-23.62655
H04-0352	11.03	6.40	4.00	2.40	3.00	1.80	0.001	0.16	29.01956	-23.67635
H04-0353	7.50	6.40	4.00	3.10	3.00	1.30	0.001	0.20	29.04278	-23.67692
H04-0356	8.72	29.70	16.00	13.80	14.00	1.50	0.001	0.20	29.07490	-23.73949
H04-0360	2.36	4.90	3.00	2.50	3.00	0.40	0.001	0.30	29.08392	-23.67438
H04-0361	17.00	23.60	16.00	13.00	13.00	1.00	0.001	0.25	29.08574	-23.66477
H04-0365	8.89	63.50	52.00	48.50	39.00	2.60	0.001	2.00	29.05823	-23.65126
H04-0368	3.27	67.00	36.00	29.20	29.00	3.90	0.001	0.80	29.10895	-23.80916
H04-0372	12.45	44.70	25.00	28.10	22.00	1.70	0.001	0.83	29.06768	-23.83184
H04-0373	12.94	119.80	94.00	95.70	95.00	0.60	0.001	3.00	29.07939	-23.83128
H04-0375	13.75	25.70	37.00	45.70	19.00	0.20	0.001	1.00	29.06916	-23.82432
H04-0380	17.08	4.90	3.00	2.60	3.00	0.40	0.001	0.25	29.03106	-23.87640
H04-0382	19.87	7.80	9.00	7.90	4.00	0.70	0.001	0.30	29.01816	-23.87779
H04-0385	2.00	10.90	3.00	3.00	5.00	5.80	0.001	0.30	29.06548	-23.91081
H04-0396	30.81	15.10	29.00	28.90	46.00	10.00	0.001	0.50	29.11658	-23.89433
H04-0399	9.21	3.60	2.00	1.60	2.00	1.00	0.001	0.15	29.12367	-23.88008
H04-0402	4.58	18.30	15.00	21.60	7.00	3.10	0.001	0.30	29.14683	-23.87607
H04-0407	21.50	35.50	62.00	80.10	28.00	0.20	0.001	1.00	29.18017	-23.85510
H04-0408	3.70	2.30	2.00	2.60	1.00	1.90	0.001	0.20	29.19207	-23.90487
H04-0410	12.55	9.50	6.00	6.00	6.00	0.60	0.001	0.25	29.17425	-23.92472
H04-0411	16.24	8.10	5.00	6.10	4.00	0.20	0.001	0.25	29.17320	-23.92611
H04-0413	12.47	7.00	4.00	5.30	4.00	0.70	0.001	0.25	29.16338	-23.93667
H04-0424	10.00	4.60	3.00	2.50	3.00	1.40	0.001	0.20	29.11761	-23.92798
H04-0428	27.40	19.00	23.00	22.90	11.00	1.00	0.001	0.60	29.10254	-23.95964
H04-0429	12.80	50.40	29.00	19.50	28.00	6.60	0.001	0.60	29.13693	-23.92830
H04-0433	4.20	15.00	6.00	5.30	13.00	0.40	0.001	0.50	29.12281	-23.94983
H04-0456	18.27	9.40	4.00	2.10	5.00	8.00	0.001	0.50	29.10666	-23.63102
H04-0458	6.50	136.30	97.00	90.70	73.00	6.20	0.001	2.00	29.37816	-23.83493
H04-0469	4.10	173.50	169.00	166.70	167.00	0.10	0.001	5.00	28.95788	-23.62140
H04-0474	45.46	162.90	100.00	88.00	88.00	3.00	0.001	0.70	29.03817	-23.62502
H04-0478	10.60	31.30	33.00	44.30	18.00	3.70	0.001	1.00	29.10669	-23.82534
H04-0487	9.20	19.00	18.00	17.20	17.00	0.30	0.001	0.80	29.19105	-23.90361
H04-0498	13.07	73.30	56.00	79.00	52.00	1.20	0.001	3.00	29.08961	-23.78170
H04-0505	9.75	134.90	168.00	153.90			0.001	6.00	29.14654	-23.53737
H04-0507	28.47	41.20	29.00	34.60	24.00	3.10	0.001	2.50	29.11375	-23.48533
H04-0511	21.60	32.40	28.00	33.60	18.00	0.20	0.001	0.50	29.31695	-23.64015
H04-0516	10.00	38.70	25.00	21.80	16.00	3.40	0.001	1.70	29.17224	-23.56252
H04-0520	16.21	20.50	12.00	13.80	13.00	0.10	0.001	0.70	28.95998	-23.59486
H04-0534	6.96	10.40	7.00	6.00	6.00	0.70	0.001	0.30	29.04482	-23.71730
H04-0552	6.36	311.80	228.00	190.70			0.001	3.00	29.02822	-23.48019
H04-0557	4.72	177.70	131.00	125.90	91.00	6.70	0.001	3.40	28.74188	-23.26974
H04-0561	26.23	32.50	23.00	35.30	21.00	0.80	0.001	1.30	28.90019	-23.66441



H-No	swl (m)	T (m ² /d)				Re (step)	S (step)	Sust Q (l/s per 24h)	Long	Lat
		Logan	Theis	C-J	B-S					
H04-0568	3.97	10.20	7.00	5.50	5.00	1.40	0.001	0.40	29.05146	-23.66343
H04-0573	15.80	38.80	24.00	22.20	22.00	3.00	0.001	1.00	29.17123	-23.92699
H04-0577	5.55	14.60	9.00	9.60	10.00	0.30	0.001	0.90	29.11438	-23.59709
H04-0580	39.16	6.30	12.00	13.40	4.00	0.60	0.001	0.30	28.96137	-23.32640
H04-0593	8.34	45.60	40.00	53.70	30.00	2.10	0.001	2.50	29.28525	-23.63025
H04-0599	14.33	29.10	40.00	38.40	16.00	0.90	0.001	1.20	29.22394	-23.70460
H04-0601	14.60	15.30	9.00	11.30	5.00	4.10	0.001	1.00	29.19316	-23.76827
H04-0606	26.01	144.60	245.00	250.90	60.00	14.20	0.001	4.00	29.00782	-23.57956
H04-0644	19.82	64.90	50.00	42.40	42.00	2.40	0.001	2.00	28.97749	-23.52182
H04-0652	3.38	57.90	39.00	35.00	35.00	1.80	0.001	1.70	29.27476	-23.57841
H04-0655	6.79	11.40	13.00	12.20	6.00	0.50	0.001	0.35	29.25165	-23.61649
H04-0658	10.16	100.20	65.00	69.90	70.00	1.00	0.001	2.00	29.14127	-23.59969
H04-0660	9.72	6.70	20.00	13.10	4.00	0.30	0.001	0.50	29.16067	-23.65125
H04-0665	2.72	47.30	67.00	92.50	43.00	0.10	0.001	1.20	28.94167	-23.52274
H04-0672	8.45	25.50	46.00	43.90	16.00	5.40	0.001	1.50	28.79535	-23.41465
H04-0679	18.62	28.90	12.00	9.00	21.00	0.40	0.001	2.00	29.18170	-23.70803
H04-0682	9.96	214.50	120.00	164.30	112.00	5.90	0.001	2.00	29.15617	-23.62525
H04-0684	9.05	57.80	30.00	28.80	24.00	9.20	0.001	4.00	29.19885	-23.60725
H04-0723	8.50	4.90	20.00	20.00	20.00	3.00	0.001	0.40	29.31334	-23.69363
H04-0724	3.63	5.60			3.00	5.80	0.001	0.07	29.31002	-23.69469
H04-0727	5.98	28.10	29.00	38.50	16.00	0.90	0.001	1.00	29.40475	-23.65330
H04-0729	5.67	138.70	200.00	256.40	107.00	0.70	0.001	4.00	29.38164	-23.64466
H04-0732	8.99	4.70	4.00	4.80	2.00	0.40	0.001	0.10	29.39529	-23.67824
H04-0733	13.95	11.20	10.00	8.00	8.00	0.90	0.001	0.90	29.38337	-23.68037
H04-0735	6.89	77.80	130.00	118.60	46.00	1.80	0.001	6.00	29.37511	-23.68005
H04-0739	59.97	117.70	128.00	137.50	70.00	2.80	0.001	2.00	29.41514	-23.71054
H04-0741	9.98	21.30	27.00	25.70	18.00	0.30	0.001	2.60	29.40463	-23.68191
H04-0754	8.28	2.40	2.00	2.60	1.00	1.40	0.001	0.10	29.30947	-23.72917
H04-0779	7.61	76.30	55.00	47.80	47.00	3.00	0.001	2.00	29.11211	-23.61380
H04-0782	8.10	17.10	10.00	11.00	10.00	3.10	0.001	1.50	29.37833	-23.64611
H04-0783	7.41	12.20	7.00	3.70	4.00	4.10	0.001	0.70	29.36258	-23.65142
H04-0787	36.29	13.10	10.00	16.10	9.00	0.40	0.001	0.50	28.92946	-23.34087
H04-0792	19.90	11.80	16.00	17.10	7.00	0.60	0.001	1.00	29.01760	-23.39642
H04-0801	7.50	5.90	3.00	2.70	20.00	3.00	0.001	0.20	29.17174	-23.78650
H04-0817	1.93	6.40	4.00	3.30	3.00	3.00	0.001	0.80	28.71837	-23.27063
H04-0819	28.50	0.60	1.00	0.30			0.001	0.03	28.69062	-23.32647
H04-0822	10.37	22.60	14.00	13.80	14.00	0.70	0.001	1.50	29.02147	-23.52651
H04-0825	5.35	37.70	26.00	24.00	24.00	2.60	0.001	2.30	29.09946	-23.56007
H04-0828	12.03	16.50	9.00	8.90	9.00	3.30	0.001	1.70	29.12316	-23.62708
H04-0835	17.80	46.70	40.00	41.50	20.00	4.00	0.001	2.00	29.11828	-23.65984
H04-0842	26.00	39.00	39.00	41.40	20.00	4.10	0.001	1.20	29.17936	-23.72962
H04-0843	38.17	13.70	9.00	10.60	10.00	0.50	0.001	1.00	29.18405	-23.73088
H04-0847	6.65	184.90	156.00	159.10	160.00	0.50	0.001	2.00	29.12156	-23.69159
H04-0848	1.00	17.60	10.00	9.70	10.00	0.60	0.001	19.21	29.25231	-23.67947
H04-0852	13.31	20.20	11.00	11.40	12.00	2.30	0.001	0.60	29.27631	-23.66639
H04-0853	13.86	8.50	10.00	9.20	4.00	0.90	0.001	0.30	29.22619	-23.70625
H04-0858	2.66	20.10	15.00	15.00	11.00	1.60	0.001	0.70	29.26060	-23.79237
H04-0859	6.11	27.10	21.00	21.60	20.00	2.20	0.001	2.50	29.25053	-23.80548
H04-0864	5.11	3.20	2.00	1.40	1.00	1.90	0.001	0.15	29.30629	-23.68931
H04-0865	38.23	9.20	6.00	3.40	6.00	3.60	0.001	0.20	29.13374	-23.76186
H04-0869	13.75	39.20	42.00	42.30	42.00	0.20	0.001	1.40	29.08956	-23.78185
H04-0870	19.80	12.10	10.00	10.70	6.00	1.40	0.001	0.50	29.11365	-23.77606
H04-0871	16.19	18.70	10.00	9.70	10.00	0.70	0.001	0.50	29.01212	-23.61542
H04-0885	4.36	4.60	3.00	2.50	3.00	1.80	0.001	0.30	28.91811	-23.58251
H04-0887	16.70	30.20	18.00	16.40	16.00	0.80	0.001	0.30	28.96652	-23.58263
H04-0889	19.50	11.70	19.00	18.70	60.00	0.20	0.001	0.20	28.96871	-23.61791
H04-0895	4.15	3.80	6.00	5.80	1.00	0.60	0.001	0.10	28.99079	-23.69695
H04-0897	3.39	31.20	81.00	89.70			0.001	2.00	28.96344	-23.68881
H04-0900	8.28	2.50	1.00	1.10	1.00	1.10	0.001	0.07	29.01837	-23.65120
H04-0903	7.15	63.30	110.00	110.70	62.00	0.10	0.001	5.00	29.01042	-23.63773
H04-0905	8.20	155.90	140.00	165.40	96.00	2.00	0.001	7.00	29.29437	-23.68368



H-No	swl (m)	T (m ² /d)				Re (step)	S (step)	Sust Q (l/s per 24h)	Long	Lat
		Logan	Theis	C-J	B-S					
H04-0915	3.84	4.20	2.00	2.00	2.00	1.30	0.001	0.20	29.02016	-23.70412
H04-0924	8.28	102.40	200.00	222.20			0.001	6.00	29.08358	-23.52599
H04-0937	1.80	42.40	32.00	30.40	20.00	1.70	0.001	0.85	29.19101	-23.85198
H04-0938	4.40	141.90	127.00	127.10	61.00	0.10	0.001	2.50	29.11049	-23.81967
H04-0939	45.60	65.90	39.00	34.50	34.00	5.70	0.001	0.70	29.19155	-23.48098
H04-0943	27.60	80.70	107.00	105.20	39.00	1.60	0.001	3.00	29.20019	-23.45738
H04-0946	6.75	50.60	120.00	114.60	30.00	1.00	0.001	2.80	29.15462	-23.54569
H04-0949	17.50	224.90	310.00	301.90	180.00	0.10	0.001	6.00	28.99439	-23.63222
H04-0950	4.03	29.30	20.00	21.60	21.00	0.10	0.001	1.30	28.91784	-23.58280
H04-0958	7.56	49.10	60.00	51.80	51.00	0.10	0.001	2.00	28.94560	-23.76694
H04-0961	11.65	17.00	27.00	26.30	18.00	0.10	0.001	1.50	29.24341	-23.81884
H04-0962	10.50	193.50	273.00	317.00	155.00	0.40	0.001	10.00	29.21838	-23.81442
H04-0963	7.90	112.30	180.00	200.40	77.00	0.40	0.001	2.50	29.21040	-23.82164
H04-0965	14.60	1.90	1.00	0.80	1.00	0.50	0.001	0.10	29.20436	-23.85627
H04-0969	25.28	114.80	76.00	70.90	71.00	8.10	0.001	3.00	29.22034	-23.85853
H04-0972	4.70	1.80	1.00	0.90	1.00	0.50	0.001	0.10	29.25011	-23.60035
H04-0975	5.40	66.10	52.00	44.40	20.00	3.00	0.001	3.00	29.25030	-23.58796
H04-0977	8.18	20.10	11.00	11.50	20.00	11.80	0.001	1.60	29.07996	-23.75398
H04-0988	6.27	395.00	259.00	236.30	235.00	21.00	0.001	9.00	29.04871	-23.81477
H04-0989	3.90	222.40	179.00	176.60	176.00	4.10	0.001	5.00	29.04879	-23.81452
H04-0992	29.64	120.10	121.00	102.90	145.00	7.40	0.001	4.00	28.99662	-23.82708
H04-1003	16.50	10.30	6.00	5.60			0.001	0.20	29.13699	-23.61706
H04-1008	22.50	31.80	14.00	15.10	9.00	5.60	0.001	0.25	29.25979	-23.84693
H04-1014	4.34	77.80	55.00	53.10	53.00	2.10	0.001	1.20	29.11502	-23.83922
H04-1022	4.50	191.10	110.00	104.60	65.00	28.30	0.001	0.60	29.10912	-23.87715
H04-1022A	5.40	173.80	102.00	104.40	104.00	25.00	0.001	7.00	29.10906	-23.87718
H04-1031	9.16	5.90	4.00	3.50	4.00	0.50	0.001	0.70	29.07797	-23.67712
H04-1033	17.90	56.90	38.00	34.70	35.00	6.30	0.001	3.50	28.94017	-23.62963
H04-1048	6.86	13.00	3.00	3.50	4.00	3.10	0.001	0.60	29.07304	-23.78898
H04-1057	19.14	15.00	11.00	10.00	10.00	0.90	0.001	0.80	29.20411	-23.44754
H04-1067	15.25	3.10	1.00	1.50	2.00	0.40	0.001	0.30	29.29752	-23.77702
H04-1076	5.93	17.70	11.00	9.50	9.00	1.10	0.001	1.20	28.91398	-23.41351
H04-1080	9.98				2.00	2.30	0.001	0.10	29.35705	-23.67268
H04-1082	7.15	19.10	12.00	10.10	10.00	3.00	0.001	1.00	29.33765	-23.77866
H04-1086	9.76	49.10			37.00	0.60	0.001	2.00	29.33253	-23.77122
H04-1090	9.22	11.30	4.00	3.60			0.001	1.50	29.32947	-23.76655
H04-1098	13.44		11.00	10.40			0.001	0.90	29.27680	-23.69712
H04-1107	11.26	57.50	54.00	47.40	48.00	2.40	0.001	1.80	29.23225	-23.72342
H04-1108	10.40	72.90	55.00	55.20			0.001	6.00	29.23332	-23.72544
H04-1109	8.45	62.40	44.00	41.60	42.00	2.40	0.001	1.50	29.23164	-23.72960
H04-1114	11.71	26.40	15.00	14.80	18.00	3.00	0.001	2.50	29.33509	-23.77515
H04-1116	4.10		1.00	0.70			0.001	0.30	28.81096	-23.41818
H04-1117	4.97	123.10	78.00	71.30	60.00	0.90	0.001	1.20	28.80391	-23.41952
H04-1119	12.33	5.90	3.00	3.00	3.00	0.20	0.001	0.30	29.26040	-23.80990
H04-1121	13.88	38.50	27.00	24.00	24.00	8.10	0.001	3.00	29.16470	-23.68690
H04-1302	37.11	8.50	5.00	4.40	4.00	1.30	0.001	0.20	29.23399	-23.52008
H04-1306	9.00	95.00	132.00	118.20	96.00	0.10	0.001	5.00	28.93581	-23.57066
H04-1312	11.50	5.60	2.00	2.50	3.00	0.10	0.001	0.20	29.08825	-23.53570
H04-1313	6.32	105.60	78.00	78.40	78.00	0.40	0.001	2.30	29.13600	-23.81565
H04-1317	5.41	216.60	415.00	406.00	155.00	1.60	0.001	4.00	28.83826	-23.41765
H04-1322	6.36	12.30	7.00	6.80	7.00	1.60	0.001	0.30	28.94266	-23.76669
H04-1365	7.51	72.90	90.00	101.10	51.00	0.60	0.001	3.00	28.91027	-23.77955
H04-1366	6.90	67.80	100.00	82.30	55.00	0.30	0.001	3.50	28.91507	-23.78605
H04-1367	5.12	72.20	80.00	89.30	90.00	0.10	0.001	5.00	29.10117	-23.72597
H04-1379	13.43	28.80	20.00	20.40	14.00	1.10	0.001	1.30	29.10117	-23.72597
H04-1381	13.77	1.60	1.00	0.80	1.00	0.10	0.001	0.10	28.80467	-23.37650
H04-1391	4.28	11.00	6.00	5.60	6.00	1.30	0.001	0.25	28.91396	-23.43953
H04-1392	22.60	26.90	16.00	14.70	16.00	1.70	0.001	0.50	28.96069	-23.40015
H04-1423	8.02	19.10	12.00	11.50	11.00	0.10	0.001	0.25	29.18732	-23.85409
H04-1425	1.88	32.00	23.00	22.00	22.00	1.10	0.001	1.60	29.18888	-23.85870
H04-1426	1.30	79.60	95.00	88.60	45.00	1.00	0.001	3.00	29.26273	-23.51973



H-No	swl (m)	T (m ² /d)				Re (step)	S (step)	Sust Q (l/s per 24h)	Long	Lat
		Logan	Theis	C-J	B-S					
H04-1435	6.88	81.50	52.00	48.00	48.00	1.90	0.001	4.00	29.23325	-23.72548
H04-1438	4.33	197.50	100.00	100.90	80.00	9.50	0.001	1.30	29.08574	-23.87080
H04-1442	8.07	55.00	34.00	31.90	32.00	0.80	0.001	2.00	29.10091	-23.77393
H04-1443	7.34	37.00	33.00	30.30	30.00	0.20	0.001	3.00	29.11712	-23.78806
H04-1445	11.27	3.30	2.00	1.70	2.00	4.10	0.001	0.40	28.68994	-23.31468
H04-1447	3.80	22.80	14.00	12.50	13.00	2.40	0.001	0.70	28.75609	-23.30341
H04-1448	0.00	8.50	6.00	6.60	4.00	2.10	0.001	0.90	28.75816	-23.31367
H04-1449	2.47	5.80	4.00	2.70	3.00	1.60	0.001	0.70	28.88135	-23.39337
H04-1450	3.58	2.70	1.00	1.30	1.00	2.30	0.001	0.40	28.93994	-23.38808
H04-1454	23.80	3.10	2.00	1.50	2.00	0.60	0.001	0.10	28.69408	-23.33056
H04-1461	13.89	19.10	11.00	11.30	11.00	2.00	0.001	1.40	28.93880	-23.38234
H04-1463	14.00	11.40	7.00	6.40	6.00	1.80	0.001	0.25	28.88056	-23.45075
H04-1464	14.20	77.30	47.00	44.20	44.00	6.50	0.001	2.30	28.88242	-23.45097
H04-1465	19.45	90.30	35.00	44.90	45.00	7.40	0.001	0.80	28.98922	-23.44811
H04-1466A	11.63	7.30	3.00	2.90	4.00	0.60	0.001	0.35	28.98628	-23.44144
H04-1467	3.15	63.50	72.00	85.00	50.00	0.50	0.001	2.50	29.03985	-23.33819
H04-1469	13.38	133.10	120.00	125.70	84.00	2.40	0.001	4.00	29.00611	-23.34099
H04-1470	5.60	50.90	53.00	48.60	48.00	0.40	0.001	3.00	29.27985	-23.57462
H04-1472	3.62	312.30	74.00	76.20	243.00	34.40	0.001	3.50	28.90774	-23.43951
H04-1474	3.52	51.50	115.00	127.90	40.00	28.00	0.001	0.60	28.86527	-23.41928
H04-1475	3.67	189.20	180.00	172.50	111.00	6.80	0.001	3.40	28.90602	-23.42815
H04-1478	5.12	58.60	50.00	54.30	35.00	0.40	0.001	0.70	28.92360	-23.41317
H04-1481	8.66	38.50	10.00	9.60	22.00	9.60	0.001	0.30	28.69775	-23.30056
H04-1486	9.63	37.80	15.00	18.30	13.00	6.20	0.001	0.90	28.93894	-23.41764
H04-1487	15.70	46.90	76.00	75.50	47.00	10.40	0.001	3.00	28.93776	-23.44095
H04-1489	2.33	59.40	35.00	32.10	32.00	3.60	0.001	1.80	28.91137	-23.40135
H04-1504	17.20	40.60	45.00	47.50	35.00	0.40	0.001	1.50	29.12128	-23.65021
H04-1515	8.10	1.10	1.00	0.50			0.001	0.03	28.92102	-23.57057
H04-1517	24.85	2.60	3.00	3.10			0.001	0.20	29.13433	-23.93061
H04-1518	6.05	12.40	6.00	6.10	6.00	0.80	0.001	0.30	29.15582	-23.61196
H04-1519	5.29	71.00	52.00	49.50	50.00	1.00	0.001	2.00	29.29989	-23.60481
H04-1525	6.90	1.40	1.00	0.40			0.001	0.06	28.76212	-23.30540
H04-1536	14.06	2.40	1.00	0.80	1.00	1.60	0.001	0.04	29.41178	-23.67291
H04-1541	10.69	80.40	68.00	70.90	54.00	0.40	0.001	0.80	29.31838	-23.62728
H04-1542	10.71	1.50	1.00	0.70	1.00	0.20	0.001	0.06	29.36146	-23.72317
H04-1545	6.68	78.80	57.00	53.00	53.00	0.70	0.001	4.00	29.29994	-23.60486
H04-1550	9.62	62.30	40.00	34.60	24.00	4.00	0.001	2.00	28.92042	-23.48419
H04-1575	13.77	27.90	22.00	20.70	20.00	1.20	0.001	1.00	29.12065	-23.76506
H04-1591	15.80	7.60	4.00	4.20	4.00	0.60	0.001	0.50	28.87939	-23.38735
H04-1601	19.10	61.70	40.00	35.60	35.00	2.30	0.001	1.60	29.10122	-23.78675
H04-1604	14.29	9.90	6.00	5.80	6.00	1.40	0.001	0.60	29.04628	-23.84043
H04-1633	13.60	56.60	34.00	33.90	28.00	3.00	0.001	2.00	29.18545	-23.63306
H04-1635	9.39	1.10	1.00	0.20			0.001	0.01	29.13436	-23.68451
H04-1644	28.60	4.40	3.00	2.30	2.00	2.20	0.001	0.20	29.21807	-23.44715
H04-1647	4.06	4.00	2.00	2.00	2.00	0.60	0.001	0.15	29.41366	-23.63774
H04-1650	26.84	2.60	1.00	1.10	1.00	0.80	0.001	0.10	29.12255	23.47405
H04-1658	9.96	2.30	1.00	0.90	1.00	1.90	0.001	0.10	29.14776	23.55075
H04-1663	5.54	48.50	34.00	33.40	27.00	3.00	0.001	2.40	29.08594	-23.85714
H04-1667	27.10	3.40	1.00	1.10	1.00	1.80	0.001	0.10	29.26598	-23.81939
H04-1679	24.60	27.20	21.00	19.50	15.00	1.90	0.001	1.00	29.26760	-23.67499
H04-1689	17.31	6.60	4.00	4.10	4.00	0.40	0.001	0.35	29.32522	-23.65755
H04-1697	20.86	5.00	2.00	2.20	3.00	1.30	0.001	0.60	29.29956	-23.73585
H04-1699	12.20	11.50	7.00	6.50	6.00	1.30	0.001	0.80	29.31756	-23.73049
H04-1700	15.24	3.80	2.00	1.80	2.00	0.10	0.001	0.12	29.33898	-23.72788
H04-1702	6.36	73.90	40.00	39.30	39.00	5.80	0.001	6.00	29.37034	-23.72599
H04-1708	18.37	173.30	116.00	110.90	90.00	6.80	0.001	4.00	29.37825	-23.72724
H04-1715	31.80	22.50	18.00	16.00	16.00	2.60	0.001	3.00	29.38952	-23.72900
H04-1719	6.40	7.20	4.00	3.80			0.001	0.25	29.40674	-23.69603
H04-1725	6.75	35.00	32.00	32.20	27.00	2.00	0.001	2.00	29.08381	-23.55422
H04-1776	10.89	8.00	7.00	6.40	4.00	0.40	0.001	0.20	29.05899	-23.74119
H04-1805	18.43	8.80	6.00	5.70	5.00	1.40	0.001	0.30	28.95270	-23.41468



H-No	swl (m)	T (m ² /d)				Re (step)	S (step)	Sust Q (l/s per 24h)	Long	Lat
		Logan	Theis	C-J	B-S					
H04-1808	30.48	3.00	1.00	1.40	1.00	2.60	0.001	0.10	29.21954	-23.86818
H04-1810	2.65	2.20	1.00	0.90	1.00	1.20	0.001	0.10	29.11086	-23.98634
H04-1871	2.62	73.00	60.00	55.90	56.00	0.80	0.001	5.00	29.10600	-23.93861
H04-1911	5.90	20.30	11.00	11.00	11.00	2.20	0.001	1.00	29.39128	-23.85168
H04-1916	6.39	27.50	29.00	28.70	18.00	2.30	0.001	2.50	29.36098	-23.84630
H04-1917	7.00	43.20	60.00	55.10	32.00	0.80	0.001	3.00	29.37322	-23.84365
H04-1924	8.31	87.10	60.00	62.30	36.00	5.10	0.001	3.50	29.38928	-23.83175
H07-0006	13.62	14.30	7.00	7.00	8.00	10.80	0.001	0.45	30.23481	-23.65903
H07-0009	32.50	26.90	20.00	18.00	18.00	3.00	0.001	0.30	30.24653	-23.64086
H07-0011	8.61	15.90	3.00	2.30	24.00	3.00	0.001	0.32	30.25417	-23.66317
H07-0012	11.30	42.90	20.00	20.50	26.00	1.60	0.001	0.20	30.25156	-23.66214
H07-0014	18.90	1.90	1.00	0.90	3.00	4.80	0.001	0.05	30.28897	-23.63733
H07-0015	30.20	21.90	9.00	9.90	16.00	2.30	0.001	0.22	30.34486	-23.61958
H07-0022	13.66	7.00	2.00	3.20	3.00	1.70	0.001	0.10	30.31339	-23.67853
H07-0023	8.10	3.40	1.00	1.30	3.00	5.00	0.001	0.15	30.28394	-23.68303
H07-0025	4.16	4.40	2.00	1.80	2.00	2.10	0.001	0.30	30.39264	-23.62642
H07-0036	14.22	20.10	7.00	6.30	12.00	1.20	0.001	0.18	30.45964	-23.61067
H07-0037	14.50	2.50	1.00	0.70			0.001	0.02	30.45581	-23.59389
H07-0044	13.24	1.40	1.00	0.70	1.00	1.30	0.001	0.10	30.44069	-23.56508
H07-0047	18.44	5.40	3.00	5.00	5.00	7.20	0.001	0.10	30.35778	-23.58603
H07-0063	14.42	11.30	11.00	9.90	19.00	5.00	0.001	0.50	30.39111	-23.55000
H07-0063A	14.20	62.00	19.00	18.20	50.00	1.30	0.001	0.40	30.39106	-23.55000
H07-0066	11.11	13.20	9.00	9.30	6.00	1.00	0.001	0.50	30.38806	-23.54842
H07-0079	25.02	26.20	18.00	17.50	18.00	0.50	0.001	0.40	30.41059	-23.50031
H07-0082	14.50	9.80	8.00	7.50	9.00	0.10	0.001	0.30	30.38803	-23.49169
H07-0083	13.62	100.80	63.00	56.10	62.00	5.10	0.001	1.30	30.45672	-23.47661
H07-0085	1.80	21.80	25.00	23.20	13.00	1.00	0.001	1.20	30.60228	-23.42217
H07-0089	25.62	9.60	4.00	4.70	3.00	1.60	0.001	0.30	30.37000	-23.47292
H07-0095A	8.40	82.70	33.00	35.20	39.00	15.90	0.001	1.30	30.34661	-23.46825
H07-0098	25.20	16.90	7.00	6.50	6.00	2.20	0.001	0.30	30.31347	-23.46283
H07-0102	19.60	4.60	3.00	2.90	2.00	1.50	0.001	0.13	30.31972	-23.46033
H07-0103	19.75	86.30	37.00	34.40	34.00	4.20	0.001	2.00	30.34994	-23.43578
H07-0110	4.50	8.70	7.00	6.60	6.00	1.00	0.001	0.45	30.38600	-23.38972
H07-0117	20.70	54.40	34.00	32.00	34.00	1.10	0.001	1.30	30.40311	-23.41933
H07-0118	10.40	8.00	6.00	5.20	5.00	1.90	0.001	0.30	30.45538	-23.42417
H07-0127	22.60	4.50	6.00	5.90	4.00	0.10	0.001	0.40	30.43628	-23.38997
H07-0137	10.75	44.40	72.00	69.10	30.00	0.30	0.001	3.00	30.49786	-23.37011
H07-0139	26.33	123.50	86.00	77.50	71.00	5.50	0.001	1.50	30.45978	-23.40897
H07-0142	14.40	73.80	41.00	41.10	56.00	1.80	0.001	1.30	30.52125	-23.42728
H07-0148	4.32	8.10	4.00	4.00	4.00	4.10	0.001	0.30	30.55617	-23.43372
H07-0149	13.50	8.20	5.00	4.20	3.00	1.10	0.001	0.30	30.55817	-23.42772
H07-0153	2.05	6.20	3.00	3.20	3.00	1.10	0.001	0.40	30.55489	-23.43014
H07-0156	2.17	9.80	4.00	5.00	5.00	1.30	0.001	0.40	30.61219	-23.43706
H07-0158	13.90	42.90	40.00	35.80	28.00	1.70	0.001	2.50	30.60739	-23.41600
H07-0159	14.20	33.60	38.00	37.50	14.00	2.20	0.001	1.00	30.60906	-23.41519
H07-0162	36.29	26.00	28.00	28.20	28.00	0.10	0.001	1.10	30.64253	-23.43167
H07-0163	10.15	5.60	3.00	2.90	5.00	5.30	0.001	0.24	30.67394	-23.44447
H07-0164	13.22	4.40	2.00	2.20	2.00	1.20	0.001	0.10	30.67178	-23.45589
H07-0169	14.20	23.60	20.00	20.60	14.00	2.00	0.001	0.60	30.45597	-23.53150
H07-0175	28.90	6.10	20.00	18.60	24.00	4.20	0.001	0.15	30.49803	-23.57356
H07-0177	18.37	0.70	1.00	0.40	1.00	0.10	0.001	0.10	30.53892	-23.59600
H07-0180	13.50	35.70	26.00	25.70	27.00	8.90	0.001	1.10	30.54119	-23.60428
H07-0182	8.40	38.60	29.00	28.30	27.00	0.40	0.001	1.50	30.57892	-23.58633
H07-0185	5.45	18.20	9.00	8.80	9.00	1.90	0.001	0.40	30.59603	-23.63386
H07-0191	20.75	4.90	2.00	2.70	3.00	1.80	0.001	0.30	30.52089	-23.52603
H07-0200	24.00	49.10	41.00	39.80	41.00	0.20	0.001	2.00	30.51956	-23.46556
H07-0202	7.90	11.20	9.00	8.40	7.00	0.40	0.001	0.35	30.51872	-23.45228
H07-0203	12.80	7.90	10.00	10.00	6.00	0.10	0.001	0.45	30.55169	-23.48611
H07-0204	29.80	29.60	28.00	26.40	31.00	0.60	0.001	2.00	30.55711	-23.46606
H07-0211	3.17	4.90	2.00	2.50	3.00	2.00	0.001	0.30	30.60861	-23.49894
H07-0213	3.71	20.10	20.00	18.80	18.00	4.40	0.001	1.30	30.61100	-23.51589



H-No	swl (m)	T (m ² /d)				Re (step)	S (step)	Sust Q (l/s per 24h)	Long	Lat
		Logan	Theis	C-J	B-S					
H07-0218	1.84	27.60	17.00	16.10	24.00	1.50	0.001	1.20	30.61500	-23.52733
H07-0225	27.04	7.80	6.00	4.80	5.00	2.00	0.001	0.20	30.64206	-23.57292
H07-0228	5.25	7.10	4.00	3.90	4.00	0.50	0.001	0.10	30.64239	-23.55350
H07-0231	17.70	51.10	42.00	41.80	22.00	3.00	0.001	1.00	30.54661	-23.52408
H07-0233	19.63	12.00	5.00	4.20	12.00	7.40	0.001	0.60	30.49983	-23.50119
H07-0241	1.37	7.20	4.00	4.00	4.00	0.80	0.001	0.20	30.35741	-23.72391
H07-0247	16.96	16.20	11.00	11.30	12.00	0.50	0.001	0.70	30.37267	-23.73242
H07-0254	10.02	1.90	2.00	1.40	2.00	0.70	0.001	0.15	30.47194	-23.73642
H07-0257	6.37	12.50	8.00	7.70	7.00	0.30	0.001	0.50	30.49222	-23.75022
H07-0276	13.32	0.70	1.00	0.20			0.001	0.03	30.44222	-23.68358
H07-0279	0.09	15.60	12.00	11.40	10.00	0.10	0.001	1.00	30.45386	-23.68011
H07-0286	12.69	31.30	19.00	18.40	19.00	1.40	0.001	1.00	30.40408	-23.70600
H07-0288	7.62	23.20	8.00	7.90	24.00	1.30	0.001	0.50	30.39567	-23.69928
H07-0293	9.80	11.40	4.00	3.00	6.00	0.70	0.001	0.30	30.38917	-23.70711
H07-0299	3.28	10.90	6.00	6.00	6.00	1.60	0.001	0.40	30.39755	-23.73033
H07-0313	17.34	9.50	6.00	5.70	5.00	0.40	0.001	0.20	30.47342	-23.61467
H07-0315	17.50	18.30	5.00	5.50	25.00	0.30	0.001	0.12	30.46019	-23.61525
H07-0320	13.00	20.10	12.00	11.70	12.00	1.50	0.001	1.00	30.39547	-23.71997
H07-0340	5.06	4.50	2.00	2.00	2.00	1.50	0.001	0.20	30.44777	-23.65000
H07-0343	15.64	18.30	11.00	9.90	9.00	0.70	0.001	0.60	30.44336	-23.65922
H07-0352	34.15	175.10	89.00	78.00	77.00	6.30	0.001	3.50	30.50592	-23.63133
H07-0354	26.60	75.40	40.00	30.20	25.00	3.80	0.001	0.90	30.50456	-23.63267
H07-0359	18.96	15.40	8.00	8.60	8.00	1.40	0.001	0.50	30.50622	-23.64231
H07-0361	12.72	2.70	1.00	1.00	2.00	0.80	0.001	0.10	30.49531	-23.64133
H07-0371	10.43	53.90	15.00	15.90	39.00	5.00	0.001	0.50	30.48606	-23.66036
H07-0383	8.06	4.30	6.00	5.60	3.00	0.10	0.001	0.50	30.42025	-23.51394
H07-0384	5.18	3.20	2.00	2.00	3.00	4.30	0.001	0.10	30.41267	-23.54164
H07-0386	14.20	7.10	4.00	3.80	5.00	1.90	0.001	0.50	30.41306	-23.54214
H07-0387	32.24	19.50	9.00	8.00	11.00	4.10	0.001	0.30	30.34675	-23.57316
H07-0390	10.92	1.70	1.00	1.00	1.00	0.50	0.001	0.05	30.49619	-23.65797
H07-0395	19.70	8.10	3.00	3.40	8.00	0.10	0.001	0.10	30.44175	-23.71788
H07-0404	6.70	4.90	2.00	2.20	2.00	0.80	0.001	0.20	30.33372	-23.71114
H07-0408	20.20	8.30	4.00	4.30	4.00	1.20	0.001	0.15	30.36519	-23.55247
H07-0411	20.12	8.30	4.00	3.60	6.00	3.00	0.001	0.20	30.59097	-23.62442
H07-0414	1.62	2.90	1.00	1.10	1.00	1.70	0.001	0.30	30.53467	-23.61933
H07-0416	5.48	19.00	13.00	12.10	15.00	0.90	0.001	0.50	30.53906	-23.62478
H07-0417	8.20	10.70	20.00	19.90	6.00	4.60	0.001	0.20	30.45858	-23.65917
H07-0422	3.67	4.60	2.00	2.00	7.00	1.10	0.001	0.20	30.35133	-23.62317
H07-0432	4.20	7.60	6.00	6.30	6.00	3.00	0.001	0.28	30.32294	-23.60336
H07-0443	17.20	65.10	40.00	38.00	20.00	3.00	0.001	1.50	30.47561	-23.59119
H07-0445	13.05	14.90	6.00	6.20	8.00	3.00	0.001	0.35	30.47083	-23.64494
H07-0446	11.70	140.70	85.00	82.30	75.00	3.00	0.001	1.90	30.47258	-23.64706
H07-0448	31.60	27.90	63.00	64.60	11.00	3.00	0.001	2.00	30.50703	-23.48897
H07-0451	11.60	6.20	3.00	2.80	3.00	1.40	0.001	0.30	30.41680	-23.62839
H07-0454	10.83	24.00	17.00	16.50	18.00	0.30	0.001	0.50	30.32488	-23.49144
H07-0455	1.93	2.10	1.00	0.60	38.00	0.50	0.001	0.05	30.34506	-23.48486
H07-0456	2.76	4.60		2.50	20.00	3.00	0.001		30.34736	-23.48000
H07-0458	14.70	6.20	4.00	4.50	5.00	2.00	0.001	0.32	30.34786	-23.43517
H07-0464	6.67	15.30	9.00	8.80			0.001	0.40	30.31778	-23.45686
H07-0465	4.14	24.70	14.00	13.40	14.00	0.70	0.001	0.50	30.54144	-23.56794
H07-0467	5.65	8.90	3.00	4.40	4.00	3.40	0.001	0.30	30.57156	-23.57589
H07-0471	17.40	12.50	6.00	6.10	6.00	2.20	0.001	0.35	30.59319	-23.61881
H07-0474	32.70	9.50	4.00	4.30	5.00	2.80	0.001	0.40	30.44414	-23.47306
H07-0477	11.05	1.90	1.00	0.90	1.00	2.60	0.001	0.12	30.37781	-23.47014
H07-0483	23.70	1.30	1.00	0.40			0.001	0.02	30.51914	-23.52515
H07-0491	5.62	1.60	1.00	0.80	1.00	0.80	0.001	0.10	30.41433	-23.72150
H07-0498	7.82	52.10	14.00	14.70	30.00	3.20	0.001	0.60	30.25236	-23.66397
H07-0513	29.40	6.00	10.00	10.40	5.00	0.10	0.001	0.60	30.58081	-23.48850
H07-0522	9.50	9.70	6.00	5.60	6.00	3.70	0.001	0.50	30.46481	-23.49650
H07-0526	6.50	4.70	3.00	2.90	3.00	0.70	0.001	0.20	30.33947	-23.44697
H07-0530	18.34	5.40	2.00	1.70	4.00	0.70	0.001	0.13	30.51339	-23.42603



H-No	swl (m)	T (m ² /d)				Re (step)	S (step)	Sust Q (l/s per 24h)	Long	Lat
		Logan	Theis	C-J	B-S					
H07-0539	5.64	17.20	11.00	10.20	12.00	0.80	0.001	0.60	30.42897	-23.38361
H07-0542	20.50	5.80	3.00	3.20	3.00	0.40	0.001	0.20	30.35558	-23.51514
H07-0545	20.20	170.50	100.00	95.60	29.00	5.40	0.001	1.80	30.35539	-23.51525
H07-0548	32.70	41.40	60.00	56.80	36.00	0.10	0.001	1.40	30.45392	-23.43094
H07-0560	14.08	8.70	6.00	5.30	5.00	0.40	0.001	0.40	30.35617	-23.57758
H07-0561	0.83	4.80	3.00	3.30	3.00	0.30	0.001	0.20	30.36883	-23.58397
H07-0562	20.30	4.00	3.00	3.60	4.00	10.20	0.001	0.50	30.23750	-23.65875
H07-0563	2.56	11.90	5.00	4.70	6.00	2.40	0.001	0.30	30.29286	-23.68297
H07-0567	25.20	1.70	1.00	1.70	5.00	3.00	0.001	0.40	30.24150	-23.64314
H07-0568	24.23	5.60	6.00	5.30	6.00	3.00	0.001	0.26	30.50703	-23.48897
H07-0569	10.10	2.30	1.00	0.70			0.001	0.03	30.51100	-23.49980
H07-0575	10.99	16.60	13.00	12.60	12.00	4.30	0.001	0.70	30.66031	-23.44697
H07-0580	23.80	2.00	1.00	0.90	2.00	3.00	0.001	0.19	30.42374	-23.59711
H07-0582	17.90	35.40	18.00	18.50	28.00	3.00	0.001	1.50	30.42344	-23.58697
H07-0586	3.15	50.90	24.00	22.40	26.00	3.00	0.001	1.20	30.36791	-23.46275
H07-0600	10.90	12.30	6.00	6.10	6.00	2.90	0.001	0.30	30.52969	-23.52494
H07-0601	11.24	48.10	14.00	14.70	28.00	8.00	0.001	0.70	30.53061	-23.52600
H07-0605	21.50	10.50	21.00	21.60	10.00	4.60	0.001	0.70	30.38461	-23.40953
H07-0617	29.00	70.60	30.00	29.80	119.00	3.00	0.001	0.80	30.65650	-23.43919
H07-0643	42.78	13.30	4.00	4.00	7.00	3.50	0.001	0.35	30.52264	-23.49283
H07-0646	12.13	2.40	1.00	1.20	1.00	1.50	0.001	0.10	30.49500	-23.39364
H07-0654	12.90	6.80	5.00	5.40	7.00	3.00	0.001	1.00	30.30005	-23.62266
H07-0659	9.20	3.30	2.00	1.90	2.00	2.40	0.001	0.20	30.43186	-23.53572
H07-0668	28.60	26.70	11.00	10.00	32.00	3.00	0.001	0.90	30.54039	-23.55636
H07-0674	21.20	1.90	1.00	0.90	1.00	0.30	0.001	0.15	30.52028	-23.58833
H07-0683	3.96	1.40	1.00	0.30	1.00	3.40	0.001	0.08	30.29444	-23.60936
H07-0698	10.50	2.30	1.00	0.90	1.00	1.80	0.001	0.10	30.39539	-23.53394
H07-0699	7.81	6.30	4.00	4.50	5.00	2.10	0.001	0.35	30.35835	-23.73380
H07-0713	37.30	34.70	24.00	23.70	18.00	3.00	0.001	0.90	30.38467	-23.42003
H07-0724	12.17	57.80	35.00	34.90	35.00	5.70	0.001	2.40	30.40281	-23.52794
H07-0728	4.88	1.00	1.00	0.30			0.001	0.03	30.37053	-23.47325
H07-0735	13.14	2.20	1.00	1.00	1.00	1.20	0.001	0.10	30.49594	-23.55686
H07-0745	13.30	3.20	1.00	1.40	1.00	1.00	0.001	0.10	30.39647	-23.53497
H07-0747	11.70	18.30	16.00	15.10	15.00	0.40	0.001	0.40	30.43786	-23.49544
H07-0748	11.72	200.40	135.00	130.00	98.00	8.20	0.001	6.00	30.43586	-23.49983
H07-0749	10.07	192.00	110.00	108.10	111.00	6.30	0.001	7.00	30.43614	-23.50022
H07-0750	26.60	7.60	3.00	3.30	7.00	3.00	0.001	0.40	30.43639	-23.52058
H07-0754	11.90	9.00	4.00	4.20	10.00	2.80	0.001	0.15	30.27117	-23.64700
H07-0757	4.60	3.70	2.00	1.40	4.00	3.00	0.001	0.40	30.37178	-23.58558
H07-0760	11.15	3.70	2.00	2.00	2.00	1.10	0.001	0.50	30.37672	-23.59214
H07-0761	8.92	0.60	1.00	0.40	1.00	0.50	0.001	0.06	30.38908	-23.64325
H07-0766	3.77	1.10	1.00	0.40			0.001	0.02	30.34064	-23.70128
H07-0780	20.56	2.70	1.00	0.60	6.00	3.00	0.001	0.10	30.23103	-23.65708
H07-0781	13.20	43.70	30.00	29.30	28.00	0.90	0.001	0.60	30.23144	-23.65666
H07-0791	12.78	1.40	1.00	0.70	1.00	3.00	0.001	0.03	30.34103	-23.70156
H07-0797	10.14	6.10	3.00	4.10	4.00	3.60	0.001	0.50	30.37744	-23.55605
H07-0799	45.30	43.80	28.00	27.00	27.00	1.30	0.001	1.20	30.37547	-23.54039
H07-0802	15.20	3.80	2.00	2.00	2.00	1.50	0.001	0.15	30.51036	-23.52886
H07-0810	6.82	10.30	7.00	6.50	6.00	0.80	0.001	0.50	30.53406	-23.62494
H07-0819	11.08	3.20	2.00	1.50	2.00	7.20	0.001	0.20	30.46447	-23.58067
H07-0822	20.67	3.10	2.00	1.50	2.00	0.30	0.001	0.15	30.37569	-23.38917
H07-0827	10.80	12.20	6.00	6.00	6.00	5.30	0.001	0.60	30.42944	-23.52497
H07-0831	8.50	18.50	7.00	6.90	12.00	3.00	0.001	0.60	30.44672	-23.40814
H07-0835	3.68	1.10	1.00	0.50	1.00	0.90	0.001	0.06	30.37819	-23.61519
H07-0838	9.50	9.70	10.00	9.40	7.00	0.10	0.001	0.70	30.39539	-23.62489
H07-0839	4.34	4.30	2.00	2.00	6.00	3.00	0.001	0.30	30.39625	-23.62022
H07-0841	8.90	3.30	1.00	0.20	4.00	1.80	0.001	0.30	30.33356	-23.45694
H07-0843	20.60				1.00	0.70	0.001	0.08	30.37161	-23.54772
H07-0845	6.75	15.40	8.00	7.00	9.00	0.40	0.001	0.70	30.38681	-23.47261
H07-0861	54.20	183.30	82.00	88.80			0.001	0.90	30.38122	-23.41947
H07-0865	5.55	6.70	4.00	4.10	4.00	0.30	0.001	0.20	30.30342	-23.46278



H-No	swl (m)	T (m ² /d)				Re (step)	S (step)	Sust Q (l/s per 24h)	Long	Lat
		Logan	Theis	C-J	B-S					
H07-0868	17.86	5.60	6.00	6.40	2.00	1.50	0.001	0.40	30.49450	-23.36531
H07-0875	7.60	14.30	9.00	8.70	8.00	1.30	0.001	0.50	30.58611	-23.58369
H07-0876	9.57	16.10	9.00	8.20	8.00	1.90	0.001	0.60	30.58831	-23.59181
H07-0877	9.92	9.10	5.00	4.80	4.00	2.30	0.001	0.20	30.57839	-23.59836
H07-0890	4.96	1.00	2.00	1.80	2.00	0.20	0.001	0.01	30.57267	-23.57736
H07-0892	4.61	10.80	6.00	5.50	6.00	0.90	0.001	0.40	30.50983	-23.53939
H07-0894	4.84	2.20	1.00	1.00	2.00	2.70	0.001	0.10	30.29033	-23.63478
H07-0896	7.57	6.20	6.00	6.30	5.00	0.40	0.001	0.25	30.51081	-23.54056
H07-0897	10.03	1.90	1.00	0.80	1.00	0.50	0.001	0.90	30.31150	-23.66667
H07-0899	10.80	1.40	1.00	0.80	1.00	0.40	0.001	0.02	30.33072	-23.59525
H07-0944	3.60	7.10	2.00	2.60	6.00	4.10	0.001	0.13	30.58756	-23.64189
H07-0951	5.40	4.50	2.00	2.30	3.00	0.20	0.001	0.20	30.43703	-23.39428
H07-0959	1.76	5.80	4.00	3.20	4.00	1.50	0.001	0.20	30.61981	-23.48997
H07-0964	4.57	7.30	5.00	4.60	5.00	5.60	0.001	0.30	30.67619	-23.46403
H07-0974	3.75	1.10	1.00	0.40	1.00	0.10	0.001	0.04	30.27700	-23.61817
H07-0976	4.20	1.30	1.00	0.50	1.00	0.20	0.001	0.10	30.25883	-23.62719
H07-0977	11.10	99.70	40.00	44.20	74.00	3.00	0.001	2.00	30.39819	-23.54436
H07-0977A	9.30	103.20	61.00	64.20	36.00	3.00	0.001	1.10	30.39822	-23.54425
H07-0981	12.30	29.90	29.00	29.20	12.00	3.00	0.001	0.60	30.43789	-23.49542
H07-0983	15.10	303.80	127.00	122.80	134.00	2.70	0.001	5.00	30.44328	-23.49958
H07-0984	7.90	193.50	147.00	141.10	132.00	3.00	0.001	5.50	30.46497	-23.47197
H07-0986	8.40	13.40	8.00	9.00	8.00	0.60	0.001	1.20	30.35267	-23.65533
H07-0988	4.10	8.50	2.00	2.10	6.00	3.00	0.001	0.20	30.27394	-23.64528
H07-0991	10.10	19.40	17.00	12.90	8.00	3.00	0.001	0.44	30.29833	-23.62480
H07-0991A	10.10	22.00	30.00	30.90	12.00	3.00	0.001	0.40	30.29831	-23.62480
H07-0992	13.30	6.90	17.00	16.10	3.00	2.20	0.001	0.50	30.29855	-23.62166
H07-0994	17.80	41.10	40.00	49.80	19.00	3.00	0.001	1.50	30.34792	-23.57647
H07-0997	22.00	6.80	4.00	3.60	5.00	3.00	0.001	0.60	30.24989	-23.66750
H07-0998	9.01	2.80	1.00	1.50	2.00	2.30	0.001	0.25	30.61828	-23.47700
H07-1000	5.40	6.60	6.00	6.70	3.00	1.60	0.001	0.40	30.25081	-23.66617
H07-1012	7.75	3.70	3.00	2.40	2.00	0.70	0.001	0.25	30.35475	-23.66978
H07-1013	3.74	25.60	15.00	14.60	17.00	3.00	0.001	0.90	30.33239	-23.67769
H07-1019	18.00	6.40	5.00	7.50	3.00	3.00	0.001	0.33	30.33636	-23.67647
H07-1020	3.40	2.00	1.00	0.80	2.00	0.70	0.001	0.20	30.29936	-23.62950
H07-1024	3.73	16.00	11.00	12.20	9.00	3.00	0.001	0.40	30.29580	-23.63394
H07-1028	18.16	3.60	1.00	0.50	5.00	3.00	0.001	0.06	30.29414	-23.63533
H07-1034	22.00	5.80	2.00	1.50	10.00	3.00	0.001	0.15	30.35517	-23.64950
H07-1036	10.10	7.90	7.00	7.80	4.00	3.00	0.001	0.40	30.32892	-23.57964
H07-1039	15.80	17.60	5.00	5.00	8.00	8.10	0.001	0.20	30.23703	-23.65833
H07-1049	2.40	4.40	1.00	2.90	4.00	1.40	0.001	0.20	30.29431	-23.69544
H07-1061	9.80	233.50	237.00	263.60	157.00	3.00	0.001	8.00	30.42158	-23.41558
H07-1068	4.95	126.70	184.00	210.20	71.00	3.00	0.001	3.00	30.42033	-23.41494
H07-1074	7.21	1.60	1.00	0.70	1.00	1.20	0.001	0.10	30.29878	-23.63003
H07-1075	7.66	5.60	2.00	2.00	2.00	2.90	0.001	0.13	30.35744	-23.58502
H07-1076	10.20	1.80	1.00	0.60	1.00	2.20	0.001	0.08	30.41819	-23.60291
H07-1078	22.61	3.10	2.00	1.50	2.00	0.20	0.001	0.07	30.51653	-23.52594
H07-1079	21.83	22.40	13.00	11.40	12.00	1.40	0.001	0.50	30.56089	-23.42933
H07-1082	15.80	5.50	8.00	7.60	7.00	3.90	0.001	0.06	30.36669	-23.67033
H07-1084	26.06	1.20	1.00	0.50	1.00	0.50	0.001	0.04	30.29792	-23.68153
H07-1097	9.55	1.80	1.00	1.10	1.00	0.40	0.001	0.15	30.58253	-23.58383
H07-1099	12.05	13.30	8.00	8.00	8.00	1.10	0.001	0.60	30.56197	-23.53392
H07-1109	5.87	35.10	20.00	19.40	19.00	2.70	0.001	1.00	30.51064	-23.53739
H07-1147	16.78	46.90	28.00	26.40	26.00	3.00	0.001	0.70	30.46633	-23.48533
H07-1148	23.93	4.20	2.00	2.20	2.00	2.50	0.001	0.15	30.45992	-23.49631
H07-1177	14.20	5.50	2.00	1.60			0.001	0.20	30.31225	-23.46838
H07-1204	16.60	12.20	7.00	6.90	7.00	8.30	0.001	0.30	30.23761	-23.65867
H07-1235	3.75	3.00	3.00	2.40	3.00	0.20	0.001	0.04	30.47880	-23.65531
H07-1237	12.80	59.90	35.00	31.50	31.00	4.10	0.001	2.00	30.55328	-23.48525
H07-1238	0.62	1.90	1.00	0.80	1.00	0.60	0.001	0.05	30.53242	-23.62319
H07-1249	13.80	1.00	1.00	0.60	2.00	1.90	0.001	0.10	30.53747	-23.63039
H07-1250	4.38	20.90	12.00	11.40	11.00	3.40	0.001	0.50	30.37463	-23.74194



H-No	swl (m)	T (m ² /d)				Re (step)	S (step)	Sust Q (l/s per 24h)	Long	Lat
		Logan	Theis	C-J	B-S					
H07-1257	6.85	6.10	4.00	3.50			0.001	0.30	30.21911	-23.64736
H10-0001	18.80	58.40	30.00	31.80	31.00	8.40	0.001	0.60	30.26000	-23.42236
H10-0002	12.30	32.30	23.00	21.40	22.00	2.10	0.001	1.60	30.34567	-23.40439
H10-0004	37.65	89.50	42.00	36.90	37.00	5.10	0.001	0.10	30.27158	-23.32900
H10-0005	5.70	18.10	8.00	10.00	10.00	2.50	0.001	0.70	30.33742	-23.40475
H10-0006	8.80	38.20	30.00	28.30	28.00	0.10	0.001	0.30	30.33611	-23.40900
H10-0007	4.00	9.40	7.00	6.60	6.00	0.40	0.001	0.30	30.32444	-23.40219
H10-0010	17.00	9.70	6.00	5.40	5.00	1.20	0.001	0.30	30.25731	-23.40953
H10-0011	20.40	47.40	42.00	42.50	42.00	0.10	0.001	1.20	30.26928	-23.40056
H10-0012	9.70	43.10	35.00	35.60	35.00	0.50	0.001	2.30	30.26608	-23.40739
H10-0013	39.20	134.40	346.00	356.00	61.00	2.00	0.001	0.70	30.24506	-23.41600
H10-0014	37.24	33.40	19.00	18.60	18.00	3.10	0.001	0.50	30.24464	-23.41606
H10-0015	38.60	48.70	17.00	17.80	35.00	8.30	0.001	0.60	30.27156	-23.32911
H10-0016	35.20	20.20	12.00	10.50	10.00	1.40	0.001	0.60	30.27144	-23.32950
H10-0018	12.70	11.90	11.00	10.50	9.00	0.10	0.001	0.40	30.30033	-23.40153
H10-0021	6.80	4.80	2.00	2.30	2.00	0.90	0.001	0.20	30.28642	-23.33564
H10-0022	37.30	17.60	17.00	15.10	15.00	0.10	0.001	0.20	30.27292	-23.32944
H10-0024	25.46	42.80	11.00	10.10	21.00	3.00	0.001	0.40	30.17844	-23.37539
H10-0024A	26.06	34.00	22.00	7.80	12.00	10.30	0.001	0.50	30.17844	-23.37544
H10-0028	27.98	36.10	20.00	21.30	21.00	4.10	0.001	0.40	30.17486	-23.38342
H10-0076	6.74	8.80	9.00	12.80	4.00	2.40	0.001	0.40	30.19661	-23.41058
H10-0083	16.50	160.60	47.00	41.10	107.00	13.90	0.001	2.00	30.04142	-23.44739
H10-0084	47.26	56.50	22.00	20.00	27.00	0.10	0.001	1.00	30.09108	-23.40344
H10-0088	13.65	9.30	5.00	10.20	5.00	3.00	0.001	0.20	30.14022	-23.39794
H10-0100	27.73	43.00	6.00	6.00	13.00	9.50	0.001	0.80	30.14419	-23.45478
H10-0142	31.50	187.20	62.00	63.10	114.00	7.20	0.001	2.50	30.14214	-23.34937
H10-0143	31.50	187.20	63.00	61.10	112.00	6.20	0.001	2.00	30.14081	-23.35508
H10-0151	26.75	51.00	21.00	19.30	23.00	6.00	0.001	0.40	30.14875	-23.36925
H10-0154	21.90	121.80			145.00	0.10	0.001	2.80	30.16833	-23.37644
H10-0158	27.40	66.00			36.00	2.80	0.001	0.90	30.24597	-23.34539
H10-0165	8.01	33.40			28.00	0.10	0.001	1.40	30.23764	-23.35836
H10-0166	18.30	15.50			9.00	0.80	0.001	0.50	30.23472	-23.35950
H10-0167	30.60	31.10			15.00	12.60	0.001	0.70	30.23628	-23.34936
H10-0181	15.97	52.20			47.00	0.20	0.001	1.40	30.20092	-23.42253
H10-0191	29.00	57.30			54.00	19.50	0.001	1.10	30.15344	-23.41608
H10-0198	22.50	15.00			11.00	0.80	0.001	0.30	30.14667	-23.41433
H10-0205	8.70	13.00			16.00	1.40	0.001	0.25	30.29497	-23.36581
H10-0209	33.00	12.90			10.00	0.50	0.001	0.70	30.23581	-23.42908
H10-0213	29.30	36.80			25.00	0.70	0.001	1.00	30.05097	-23.46167
H10-0214	6.76	131.00			105.00	1.30	0.001	3.50	30.04839	-23.45836
H10-0215	6.85	149.80			80.00	19.70	0.001	2.30	30.05361	-23.45433
H10-0341	43.30	16.50			9.00	1.00	0.001	0.50	30.15336	-23.37503
H10-0400	19.10	27.30			14.00	5.90	0.001	0.90	30.20300	-23.42089
H10-0421	1.67	21.20			15.00	0.10	0.001	0.80	30.03906	-23.44792
H10-0423	23.91	23.60			11.00	1.60	0.001	1.00	30.11233	-23.40358
H10-0424	37.20	4.40			2.00	2.10	0.001	0.20	30.15986	-23.39000
H10-0429	5.80	25.60			15.00	0.50	0.001	0.70	30.16131	-23.36917
H10-0431	10.30	84.10			44.00	14.20	0.001	2.40	30.14750	-23.36086
H10-0436	23.50	102.50			73.00	1.90	0.001	1.30	30.14836	-23.38911
H10-0442	23.00	35.70			22.00	7.00	0.001	1.20	30.23056	-23.39594
H10-0446	19.20	2.40			7.00	2.20	0.001	0.20	30.23283	-23.39933
H10-0461	13.10	50.40			42.00	1.00	0.001	1.00	30.15975	-23.43550
H10-0472	22.10	19.20			9.00	2.10	0.001	0.50	30.23589	-23.35069
H10-0519	6.87	13.80			7.00	1.10	0.001	0.70	30.25389	-23.35664
H10-0548	7.70	276.10			330.00	0.10	0.001	10.00	30.15508	-23.44186
H10-0550	12.20	13.30			8.00	0.40	0.001	0.40	30.14689	-23.35214
H10-0554	0.40	9.60			5.00	1.20	0.001	0.90	30.16369	-23.33656
H10-0578	18.09	47.70			29.00	1.90	0.001	2.00	30.14444	-23.43939
H10-0579	20.04	32.00			24.00	0.50	0.001	1.60	30.14217	-23.43978
H10-0580	18.40	159.80			86.00	8.70	0.001	1.70	30.14681	-23.43786
H10-0593	9.33	43.00			31.00	2.00	0.001	2.50	30.21328	-23.41108



H-No	swl (m)	T (m ² /d)				Re (step)	S (step)	Sust Q (l/s per 24h)	Long	Lat
		Logan	Theis	C-J	B-S					
H10-0598	5.40	91.60			148.00	0.10	0.001	4.00	30.15922	-23.36656
H10-0600	30.84	9.60			3.00	3.00	0.001	0.03	30.16169	-23.36150
H10-0609	36.30	86.40			63.00	2.10	0.001	2.10	30.14314	-23.34772
H10-0611	2.60	88.30			62.00	0.20	0.001	3.70	30.16964	-23.36156
H10-0612	13.50	32.50			20.00	1.00	0.001	1.00	30.14275	-23.35742
H10-0613	33.60	36.80			26.00	6.30	0.001	2.50	30.29269	-23.30528
H10-0614	35.30	24.10			21.00	0.10	0.001	0.70	30.29283	-23.30558
H10-0616	3.35	61.80			30.00	2.00	0.001	1.80	30.05825	-23.44572
H10-0617	7.04	18.60			18.00	0.10	0.001	0.80	30.06011	-23.44472
H10-0618	22.60	15.30			11.00	1.50	0.001	0.40	30.05414	-23.44681
H10-0624	50.30	14.40			7.00	3.90	0.001	0.50	30.00106	-23.45939
H10-0628	2.76	5.70			3.00	0.90	0.001	0.50	30.32214	-23.29003
H10-0629	11.90	84.40			56.00	1.30	0.001	2.80	30.30869	-23.29581
H10-0633	37.30	26.80			20.00	0.30	0.001	2.00	30.29594	-23.30397
H10-0634	15.50	228.10			120.00	8.90	0.001	1.50	30.29953	-23.29697
H10-0635	68.20	5.00			3.00	0.70	0.001	0.16	30.00331	-23.50758
H10-0636	24.20	10.40			6.00	0.60	0.001	0.13	30.04511	-23.36061
H10-0638	57.70	22.00			10.00	10.20	0.001	0.20	30.16294	-23.38839
H10-0641	6.60	54.40			39.00	0.10	0.001	2.00	30.17142	-23.39686
H10-0645	23.62	126.90			70.00	3.50	0.001	2.50	30.09408	-23.39603
H10-0651	25.14	13.30			6.00	2.40	0.001	0.20	30.24289	-23.35014
H10-0656	36.56	16.20			7.00	3.40	0.001	0.60	30.04622	-23.45069
H10-0657	2.19	156.00			99.00	2.40	0.001	6.50	30.14558	-23.43903
H10-0713	18.71	77.60			109.00	0.10	0.001	3.50	30.16372	-23.33133
H10-0748	33.13	2.40			1.00	2.40	0.001	0.15	30.15114	-23.41136
H10-0753	29.92	27.20			32.00	0.30	0.001	1.00	30.07786	-23.39733
H10-0754	43.55	31.40			6.00	1.80	0.001	0.06	30.02722	-23.44564
H11-0790	47.03	22.80			11.00	0.10	0.001	0.35	29.26473	-23.29258
H11-0801	45.66	82.70			31.00	11.90	0.001	0.20	29.25760	-23.34039
H11-0817	26.17	11.20			5.00	1.30	0.001	0.30	29.18948	-23.34682
H11-0832	17.10	18.10			14.00	1.00	0.001	1.50	29.12244	-23.40608
H11-0904	40.26	37.00			20.00	1.20	0.001	0.50	29.14384	-23.24019
H11-0917	27.48	134.90			71.00	4.90	0.001	1.30	29.10900	-23.09202
H11-0925	15.78	7.40			5.00	1.50	0.001	0.22	29.10106	-23.07291
H11-0928	17.95	6.80			3.00	0.30	0.001	0.20	29.10334	-23.06030
H11-0930	42.26	13.90			8.00	2.00	0.001	0.50	29.08577	-23.05760
H11-0932	44.89	23.30			11.00	3.00	0.001	0.40	29.07307	-23.06016
H11-0954	26.72	142.60			91.00	2.80	0.001	1.80	29.09686	-23.14051
H11-0955	25.14	59.90			32.00	3.50	0.001	1.00	29.08155	-23.13996
H11-1010	5.54	5.30			2.00	7.10	0.001	0.20	28.99631	-23.15250
H11-1047	5.60	15.90			7.00	2.50	0.001	1.00	29.05621	-23.21304
H11-1062	14.02	4.20			2.00	2.80	0.001	0.30	29.09928	-22.96156
H11-1076	26.38	13.70			8.00	0.50	0.001	0.30	29.05778	-22.98092
H11-1087	12.58	10.20			7.00	1.30	0.001	0.50	29.04382	-23.21195
H11-1090	47.03	23.60			12.00	0.10	0.001	0.35	29.05147	-23.21131
H11-1159	13.27	215.60			95.00	10.70	0.001	3.50	29.01082	-23.30872
H11-1166	26.68	88.50			41.00	1.40	0.001	1.80	29.07171	-23.26831
H11-1183	9.13	66.60			35.00	2.00	0.001	2.00	29.06458	-23.23270
H11-1233	11.45	14.50			7.00	1.60	0.001	0.35	28.88509	-23.18670
H11-1235	8.80	6.20			4.00	1.10	0.001	0.25	28.90469	-23.19458
H11-1295	7.20	5.30			3.00	0.50	0.001	0.16	28.72433	-23.11936
H11-1297	24.54	18.40			9.00	16.00	0.001	0.80	28.75242	-23.14677
H11-1311	31.31	2.50			1.00	2.70	0.001	0.17	28.80083	-23.03792
H11-1321	42.08	4.60			2.00	0.90	0.001	0.11	28.87378	-23.08911
H11-1326	53.64	1.80			1.00	0.40	0.001	0.15	28.86903	-23.05100
H11-1338	6.04	25.40			15.00	1.70	0.001	2.00	29.05482	-23.31303
H11-1342A	12.97	10.30			6.00	0.50	0.001	0.40	28.91984	-23.13917
H11-1350	41.48	60.50			22.00	4.50	0.001	1.60	29.21975	-23.34256
H11-1368	4.37	32.80			26.00	0.10	0.001	1.00	28.98697	-23.20831
H11-1381	7.64	2.00			1.00	1.30	0.001	0.08	28.77544	-23.28789
H11-1396	33.07	6.70			4.00	1.70	0.001	0.50	29.05559	-23.07803



H-No	swl (m)	T (m ² /d)				Re (step)	S (step)	Sust Q (l/s per 24h)	Long	Lat
		Logan	Theis	C-J	B-S					
H11-1424	38.69	13.20			8.00	0.70	0.001	0.70	29.02308	-23.12571
H11-1536	10.11	9.70			5.00	1.60	0.001	0.20	29.07964	-23.18248
H11-1578	18.20	10.60			5.00	1.60	0.001	0.15	28.78642	-23.14845
H11-1594	43.60	20.90			11.00	0.60	0.001	0.30	29.26739	-23.29314
H11-1698	47.55	187.30			86.00	7.00	0.001	5.00	29.21606	-23.29320
H11-1699	41.95	210.40			20.00	3.00	0.001	1.60	29.21152	-23.28305
H11-1793	8.60	4.70			2.00	0.40	0.001	0.07	29.16174	-23.33199
H11-1843	4.48	20.60			8.00	2.50	0.001	0.50	29.06058	-23.13770
H11-1942	37.84	1.50			1.00	1.90	0.001	0.15	28.85406	-23.08622
H11-2005	7.60	7.20			4.00	2.40	0.001	0.30	28.92833	-23.14597
H16-0001	29.90	5.40			3.00	2.30	0.001	0.10	29.78462	-23.95609
H16-0002	9.14	107.00			82.00	0.40	0.001	0.70	29.79296	-23.98944
H16-0003	6.21	122.10			79.00	1.20	0.001	3.00	29.79520	-23.98670
H16-0005	5.21	25.60			17.00	0.20	0.001	0.70	29.79834	-23.97940
H16-0006	11.03	33.80			20.00	3.00	0.001	0.70	29.79206	-23.99327
H16-0008	5.58	104.60			69.00	1.60	0.001	2.00	29.79898	-24.00668
H16-0009	15.15	7.20			4.00	4.60	0.001	0.30	29.80691	-23.99711
H16-0011	11.82	27.10			17.00	0.10	0.001	0.50	29.81344	-24.01968
H16-0015	16.47	61.30			41.00	0.40	0.001	1.50	29.69266	-24.03231
H16-0016	15.77	49.60			39.00	0.10	0.001	0.80	29.69908	-24.05197
H16-0017	10.09				1.00	1.30	0.001	0.10	29.66347	-24.02506
H16-0018	20.84	9.10			5.00	3.30	0.001	0.25	29.66850	-24.03286
H16-0022	22.57	70.60			68.00	0.20	0.001	1.00	29.67822	-24.04503
H16-0025	11.55	4.70			2.00	2.00	0.001	0.13	29.71225	-24.08133
H16-0027	17.06	9.50			6.00	9.80	0.001	0.40	29.70789	-24.09547
H16-0029	9.67	36.30			17.00	5.20	0.001	1.00	29.67772	-24.10036
H16-0031	58.17	7.00			4.00	1.40	0.001	0.10	29.62458	-24.07765
H16-0032	31.22	2.20			1.00	1.10	0.001	0.10	29.61894	-24.08310
H16-0033	12.84	0.80			1.00	1.00	0.001	0.04	29.76017	-23.87099
H16-0034	6.24	113.70			60.00	10.20	0.001	1.90	29.76021	-23.88178
H16-0038	14.57	4.50			2.00	2.00	0.001	0.15	29.78012	-23.82660
H16-0044	10.70	4.40			2.00	1.20	0.001	0.12	29.61869	-24.09789
H16-0046	24.84	3.10			3.00	2.20	0.001	0.25	29.59914	-24.08442
H16-0054	18.50	80.30			70.00	5.20	0.001	3.50	29.55258	-24.12681
H16-0057	5.70	4.90			2.00	2.00	0.001	0.30	29.54314	-24.15461
H16-0068	8.25	1.90			1.00	1.10	0.001	0.12	29.54775	-24.18400
H16-0070	2.97	209.80			86.00	16.60	0.001	1.90	29.56228	-24.13108
H16-0074	14.10	4.50			2.00	2.90	0.001	0.20	29.52547	-24.18617
H16-0076	9.19	109.80			64.00	1.50	0.001	1.00	29.61941	-23.80704
H16-0077	30.48	8.90			4.00	6.00	0.001	0.30	29.57931	-24.11742
H16-0078	24.53	111.50			92.00	0.40	0.001	1.80	29.76554	-23.69625
H16-0084	2.93	11.20			7.00	7.10	0.001	0.70	29.79991	-23.82322
H16-0089	7.00	8.10			3.00	2.40	0.001	0.30	29.82073	-23.78113
H16-0090	3.13	2.00			1.00	1.10	0.001	0.05	29.84834	-23.79525
H16-0092	26.91	4.90			4.00	0.10	0.001	0.20	29.88338	-23.82799
H16-0098	12.60	28.70			6.00	10.80	0.001	0.30	29.85961	-23.85256
H16-0108	33.25	20.00			10.00	16.90	0.001	0.80	29.87552	-23.90904
H16-0110	34.17	60.50			34.00	4.30	0.001	1.00	29.64662	-23.87156
H16-0111	34.17	25.30			13.00	2.20	0.001	0.90	29.64852	-23.87090
H16-0112	28.09	2.80			2.00	5.00	0.001	0.12	29.62983	-23.92250
H16-0114	9.35	13.80			7.00	2.10	0.001	1.00	29.62753	-23.93697
H16-0118	18.74	5.90			3.00	1.20	0.001	0.15	29.65278	-24.99028
H16-0120	24.65	33.30			17.00	2.00	0.001	0.50	29.66625	-24.00108
H16-0122	9.10	9.20			4.00	0.70	0.001	0.15	29.70500	-23.86392
H16-0123	12.04	26.80			16.00	2.50	0.001	0.35	29.69756	-23.87314
H16-0125	16.35	192.50			132.00	10.00	0.001	6.00	29.69985	-23.79747
H16-0126	6.89	116.90			80.00	1.00	0.001	3.50	29.72956	-23.79618
H16-0127	11.40	28.50			15.00	1.20	0.001	1.70	29.70743	-23.79270
H16-0128	9.69	128.20			48.00	7.40	0.001	2.10	29.74422	-23.79618
H16-0129	12.27	19.50			20.00	3.00	0.001	0.35	29.75825	-23.80132
H16-0130	7.18	12.60			8.00	0.30	0.001	0.40	29.75145	-23.80065



H-No	swl (m)	T (m ² /d)				Re (step)	S (step)	Sust Q (l/s per 24h)	Long	Lat
		Logan	Theis	C-J	B-S					
H16-0131	1.34	14.90			11.00	0.40	0.001	1.00	29.77253	-23.79059
H16-0132	4.18	180.00			200.00	0.10	0.001	1.00	29.75505	-23.79619
H16-0133	23.53	33.40			20.00	1.00	0.001	1.00	29.73667	-23.77329
H16-0134	15.59	61.00			45.00	0.60	0.001	0.90	29.73458	-23.77573
H16-0135	24.17	54.60			32.00	6.80	0.001	1.70	29.68746	-23.75258
H16-0136	6.35	166.30			112.00	7.50	0.001	1.30	29.70089	-23.75906
H16-0137	9.42	4.90			3.00	0.90	0.001	0.35	29.70563	-23.75326
H16-0138	29.69	6.90			5.00	0.10	0.001	0.10	29.71319	-23.75341
H16-0143	20.28	5.50			3.00	0.50	0.001	0.10	29.76566	-23.78072
H16-0145	2.28	30.90			32.00	0.20	0.001	2.50	29.79193	-23.78012
H16-0150	14.46	58.70			28.00	4.40	0.001	0.70	29.78857	-23.73769
H16-0152	5.75	39.10			42.00	0.10	0.001	2.50	29.79066	-23.72518
H16-0154	17.12	9.90			4.00	7.40	0.001	0.25	29.78149	-23.72638
H16-0160	29.65	54.00			27.00	0.10	0.001	1.30	29.78672	-23.69993
H16-0162	16.51	139.50			88.00	10.10	0.001	1.20	29.81445	-23.72035
H16-0164	7.62	61.50			46.00	0.50	0.001	2.00	29.81639	-23.72798
H16-0167	25.01	613.20			240.00	19.30	0.001	5.00	29.68985	-23.80003
H16-0170	49.14	72.40			38.00	2.00	0.001	1.60	29.64907	-23.81575
H16-0172	17.40	43.40			21.00	3.20	0.001	0.90	29.63879	-23.83518
H16-0174	24.76	21.40			13.00	1.10	0.001	0.90	29.63955	-23.85143
H16-0179	9.00	42.50			30.00	0.60	0.001	0.50	29.78837	-23.73639
H16-0180	13.28	117.10			90.00	1.30	0.001	2.50	29.79826	-23.75881
H16-0185	13.05	37.00			31.00	10.60	0.001	1.50	29.67828	-23.45833
H16-0188	16.87	23.20			14.00	1.20	0.001	0.50	29.74894	-23.50781
H16-0192	16.87	12.30			6.00	2.90	0.001	0.20	29.73501	-23.50059
H16-0194	5.30	103.60			54.00	7.60	0.001	0.90	29.69797	-23.51198
H16-0201	18.89	4.60			2.00	4.90	0.001	0.20	29.48308	-24.18114
H16-0202	15.99	4.70			3.00	2.70	0.001	0.12	29.48278	-24.18311
H16-0203	8.17	7.10			4.00	1.70	0.001	0.30	29.48361	-24.18075
H16-0205	0.48	9.30			4.00	3.00	0.001	0.35	29.93744	-23.49925
H16-0206	5.48	96.00			48.00	6.70	0.001	2.50	29.93747	-23.49736
H16-0210	9.34	37.20			26.00	0.40	0.001	0.90	29.61924	-23.80717
H16-0213	11.62	41.40			32.00	1.80	0.001	2.00	29.61664	-23.81049
H16-0221	21.73	193.20			50.00	10.20	0.001	0.90	29.72890	-23.47768
H16-0226	6.75	12.00			7.00	1.10	0.001	0.60	29.71008	-23.47622
H16-0230	6.11	25.60			18.00	0.50	0.001	1.30	29.62117	-23.80941
H16-0250	12.50	70.10			38.00	4.40	0.001	2.50	29.61752	-24.08496
H16-0287	10.50	749.90			153.00	72.00	0.001	3.50	29.76915	-23.48125
H16-0288	23.00	45.00			30.00	1.70	0.001	2.00	29.77452	-23.47932
H16-0312	12.30	66.70			26.00	10.00	0.001	0.25	29.83478	-23.51564
H16-0315	15.08	64.80			67.00	0.10	0.001	4.00	29.63512	-23.81603
H16-0324	32.69	48.50			25.00	7.40	0.001	1.80	29.73569	-23.82550
H16-0342		35.80			19.00	37.00	0.001	1.20	29.94192	-23.49910
H16-0345	8.64	72.00			69.00	0.10	0.001	3.00	29.62559	-23.84708
H16-0348	34.14	1.20			1.00	1.80	0.001	0.03	29.77813	-23.81535
H16-0349	19.27	200.80			20.00	3.00	0.001	2.50	29.63798	-23.89325
H16-0350	15.68	16.30			8.00	0.80	0.001	0.40	29.62833	-23.87605
H16-0358	5.30	61.80			58.00	1.00	0.001	8.00	29.65358	-23.50390
H16-0371	22.41	74.80			20.00	3.00	0.001	0.50	29.83758	-23.45453
H16-0373	3.11	57.90			20.00	3.00	0.001	3.00	29.84525	-23.46344
H16-0374	3.49	14.80			10.00	0.70	0.001	0.70	29.70817	-23.85961
H16-0383	6.79	35.20			20.00	3.00	0.001	1.80	29.81763	-23.45035
H16-0386	26.34	73.30			31.00	1.60	0.001	2.30	29.83959	-23.52896
H16-0387	17.40	67.30			38.00	4.90	0.001	1.40	29.83690	-23.53511
H16-0389	2.60	29.80			23.00	0.10	0.001	1.30	29.71256	-23.85597
H16-0393	27.66	65.10			20.00	3.00	0.001	1.00	29.81667	-23.46578
H16-0397	1.16	20.20			15.00	0.20	0.001	0.55	29.76546	-23.71003
H16-0405	4.50	25.80			20.00	3.00	0.001	2.00	29.45764	-23.78207
H16-0412	19.23	1.50			1.00	3.00	0.001	0.05	29.87381	-23.88692
H16-0416	17.40	7.00			4.00	0.70	0.001	0.30	29.83165	-23.77789
H16-0426	11.96	238.90			72.00	14.00	0.001	7.00	29.65036	-23.77883



H-No	swl (m)	T (m ² /d)				Re (step)	S (step)	Sust Q (l/s per 24h)	Long	Lat
		Logan	Theis	C-J	B-S					
H16-0428	13.67	2.40			1.00	1.70	0.001	0.10	29.65109	-23.78218
H16-0430	17.40	15.10			9.00	2.00	0.001	1.00	29.66997	-23.79801
H16-0432	20.41	189.90			95.00	5.90	0.001	6.00	29.67723	-23.80719
H16-0443	22.47	7.80			3.00	1.00	0.001	0.05	29.82978	-23.52786
H16-0464	7.62	336.60			170.00	24.20	0.001	5.50	29.80333	-23.47494
H16-0467	11.82	5.80			6.00	4.90	0.001	0.25	29.75129	-23.48175
H16-0471	11.62	279.50			200.00	0.60	0.001	8.00	29.79848	-23.75895
H16-0474	10.08	5.90			3.00	1.30	0.001	0.20	29.66362	-23.77025
H16-0481	10.01	52.40			38.00	1.00	0.001	3.50	29.66601	-23.77576
H16-0485	10.90	208.60			20.00	3.00	0.001	7.50	29.66741	-23.77896
H16-0486	14.76	51.60			32.00	0.80	0.001	2.00	29.66901	-23.78098
H16-0487	15.37	19.50			12.00	7.30	0.001	2.00	29.67152	-23.78442
H16-0488	10.90	112.80			83.00	11.90	0.001	4.20	29.67212	-23.78520
H16-0490	15.80	206.60			60.00	12.90	0.001	4.00	29.67755	-23.79219
H16-0492	4.25	183.60			123.00	2.60	0.001	6.00	29.68256	-23.79779
H16-0496	16.28	95.00			57.00	4.30	0.001	5.00	29.67954	-23.80824
H16-0510	13.58	74.30			37.00	5.40	0.001	4.00	29.61873	-23.82286
H16-0518	3.04	36.20			19.00	1.60	0.001	0.60	29.56014	-24.16508
H16-0519	1.26	19.90			12.00	2.40	0.001	0.35	29.56114	-24.16461
H16-0532	27.10	46.70			20.00	3.20	0.001	1.00	29.67242	-24.04242
H16-0533	26.78	19.30			10.00	1.40	0.001	0.40	29.67397	-24.04258
H16-0537	7.70	3.60			2.00	1.00	0.001	0.12	29.82603	-23.79833
H16-0545	2.30	20.70			12.00	8.50	0.001	2.30	29.69394	-23.44700
H16-0550	5.44	83.00			42.00	2.40	0.001	5.00	29.66929	-23.51097
H16-0551	5.43	63.10			40.00	12.50	0.001	7.00	29.67074	-23.51273
H16-0553	5.06	60.60			24.00	6.30	0.001	3.00	29.67144	-23.51577
H16-0554	5.74	26.50			15.00	0.80	0.001	1.00	29.66978	-23.51305
H16-0555	4.75	33.10			17.00	2.40	0.001	1.90	29.69611	-23.45044
H16-0561	4.01	63.00			32.00	2.20	0.001	1.10	29.67355	-23.51837
H16-0563	4.10	86.60			38.00	14.00	0.001	2.50	29.67465	-23.51845
H16-0566	7.50	72.00			30.00	12.00	0.001	3.50	29.67578	-23.51774
H16-0567	5.15	65.00			44.00	1.80	0.001	6.00	29.67748	-23.51812
H16-0578	3.30	38.40			23.00	9.20	0.001	1.70	29.74797	-23.47098
H16-0580	5.40	184.50			113.00	2.70	0.001	10.00	29.74323	-23.47359
H16-0581	8.50	104.20			50.00	1.60	0.001	1.00	29.75208	-23.46984
H16-0591	4.65	58.70			34.00	3.10	0.001	4.00	29.64843	-23.50373
H16-0597	2.52	4.90			2.00	1.00	0.001	0.15	29.79228	-23.82939
H16-0601	1.26	3.60			4.00	2.30	0.001	0.10	29.79428	-23.82756
H16-0605	0.73	0.90			0.00	3.00	0.001	0.05	29.79693	-23.82559
H16-0639	4.72	25.80			11.00	2.20	0.001	0.70	29.34113	-23.86910
H16-0710	15.32	0.80			1.00	1.70	0.001	0.02	29.82017	-23.79713
H16-0715	28.94	77.60			20.00	3.00	0.001	3.00	29.83711	-23.45692
H16-0722	10.00	295.40			20.00	3.00	0.001	5.00	29.80578	-23.47522
H16-0730	5.62	40.60			26.00	1.40	0.001	2.00	29.83356	-23.48506
H16-0768	6.43	39.50			23.00	2.10	0.001	2.50	29.82747	-23.50280
H16-0769	11.63	4.00			2.00	0.50	0.001	0.20	29.82475	-23.53261
H16-0783	16.00	2.80			2.00	2.80	0.001	0.10	29.73635	-23.51970
H16-0825	5.15	4.50			2.00	0.90	0.001	0.15	29.70444	-23.50333
H16-0967	4.25	2.10			1.00	0.60	0.001	0.15	29.71339	-24.02900
H16-1023	7.65	3.15			20.00	1.50	0.001	2.00	29.77239	-23.85197
H16-1031	6.82	14.10			6.00	0.50	0.001	0.15	29.60914	-23.95086
H16-1034	16.75	73.80			65.00	0.70	0.001	3.50	29.57092	-23.97061
H16-1087	5.40	87.80			33.00	8.90	0.001	0.80	29.72108	-23.43125
H16-1223	6.18	167.80			164.00	0.90	0.001	4.00	29.46689	-23.93340
H17-0004	51.62	15.60	8.00	7.00	7.00	2.20	0.001	0.40	30.07333	-23.16242
H17-0006	23.10	15.80	13.00	14.50	9.00	0.60	0.001	0.40	30.09330	-23.16029
H17-0007	29.80	21.40	27.00	25.30	25.00	0.20	0.001	0.80	30.07111	-23.16020
H17-0010	7.50	67.50	50.00	52.50			0.001	2.50	30.06722	-23.15861
H17-0012	19.50	29.20	13.00	14.20			0.001	2.00	30.05800	-23.16589
H17-0013	25.47	70.20	110.00	117.00	80.00	0.10	0.001	3.00	30.05526	-23.16177
H17-0015	9.50	36.60	25.00	24.00	24.00	0.70	0.001	1.20	30.69700	-23.16866



H-No	swl (m)	T (m ² /d)				Re (step)	S (step)	Sust Q (l/s per 24h)	Long	Lat
		Logan	Theis	C-J	B-S					
H17-0016	5.00	63.50	60.00	56.80	55.00	1.20	0.001	2.00	30.07380	-23.21662
H17-0017	18.85	10.60	6.00	5.50	5.00	2.60	0.001	0.40	30.07037	-23.16965
H17-0018	20.72	30.60	11.00	12.10	17.00	25.00	0.001	0.30	30.07108	-22.17002
H17-0020	11.94	100.50	89.00	69.40	40.00	4.00	0.001	1.50	30.07717	-23.16892
H17-0021	7.70	55.00	31.00	30.40	24.00	4.90	0.001	1.80	30.08497	-23.17376
H17-0022	42.32	39.40	27.00	24.10	22.00	3.90	0.001	0.40	30.08202	-23.17821
H17-0023	25.73	40.20	27.00	23.70	22.00	3.40	0.001	1.00	30.09947	-23.17876
H17-0027	43.21	15.80	8.00	7.80	6.00	8.90	0.001	0.55	30.06652	-23.16574
H17-0028B	10.11	53.90	32.00	30.50	30.00	11.00	0.001	1.00	30.04834	-23.16333
H17-0039	18.00	9.10	5.00	4.50	5.00	2.10	0.001	0.50	30.05717	-23.18814
H17-0040	21.40	18.90	17.00	15.00	6.00	2.70	0.001	1.00	30.05701	-23.19000
H17-0042	26.40	11.00	6.00	5.70	4.00	2.10	0.001	0.40	30.05953	-23.19578
H17-0043	28.60	10.70	8.00	6.90	5.00	1.70	0.001	0.40	30.06012	-23.19872
H17-0044	4.07	24.10	12.00	11.00	11.00	3.00	0.001	2.00	30.06173	-23.17929
H17-0045	17.38	6.90	3.00	3.40	3.00	2.50	0.001	0.40	30.04429	-23.17797
H17-0047	17.54	7.50	3.00	4.00	4.00	0.40	0.001	0.50	30.04396	-22.17986
H17-0049	28.21	41.80	29.00	28.10	28.00	2.10	0.001	1.70	30.04487	-23.18851
H17-0050	28.30	50.30	44.00	39.80	39.00	0.20	0.001	2.50	30.04622	-23.19126
H17-0054	16.40	54.80	27.00	26.30	27.00	19.00	0.001	1.20	30.08964	-23.14307
H17-0059	1.23	148.50	90.00	93.40	70.00	4.80	0.001	1.30	30.06062	-23.13780
H17-0064	15.55	104.30	80.00	78.40	80.00	0.90	0.001	4.00	30.04900	-23.14893
H17-0065	13.70	6.30	4.00	3.50	3.00	9.00	0.001	0.60	30.21174	-23.14358
H17-0069	9.89	269.80	170.00	157.00	119.00	9.20	0.001	5.20	30.21173	-23.14354
H17-0070	17.87	14.70	12.00	12.40	7.00	4.20	0.001	1.00	30.21122	-23.14481
H17-0071	11.48	42.90	28.00	25.10	25.00	1.30	0.001	2.50	30.20836	-23.14430
H17-0072	13.59	32.00	31.00	31.70	19.00	0.90	0.001	2.50	30.20314	-23.14505
H17-0073B	21.32	55.30	60.00	58.10	24.00	3.90	0.001	2.00	30.19845	-23.14409
H17-0074	22.77	50.90	40.00	41.70	29.00	0.90	0.001	1.90	30.19256	-23.14128
H17-0076	14.00	38.20	36.00	32.30	32.00	0.60	0.001	1.80	30.17961	-23.14397
H17-0077	21.00	20.70	12.00	9.90	10.00	11.90	0.001	0.90	30.17886	-23.14140
H17-0078	3.99	7.50	5.00	4.10	4.00	3.10	0.001	0.90	30.73930	-23.15516
H17-0079	6.00	38.10	30.00	26.00	19.00	5.20	0.001	3.00	30.07554	-23.15413
H17-0081	8.74	7.70	9.00	9.30	4.00	0.90	0.001	0.90	30.08491	-23.17019
H17-0082	10.53	14.30	8.00	7.50	7.00	1.90	0.001	1.10	30.09034	-23.17234
H17-0083	30.32	29.20	20.00	18.00	14.00	0.10	0.001	0.90	30.04041	-23.17629
H17-0084	17.83	104.30	60.00	57.70	48.00	9.00	0.001	2.20	30.04841	-23.16130
H17-0091	22.05	101.90	50.00	46.90	54.00	5.00	0.001	3.00	30.13106	-23.19919
H17-0092	6.29	52.30	37.00	36.40	33.00	0.80	0.001	1.20	30.13952	-23.19657
H17-0097	22.94	8.80	4.00	4.50	5.00	0.70	0.001	0.40	30.15634	-23.18964
H17-0099	21.72	6.90	2.00	2.20	2.00	2.60	0.001	0.22	30.18430	-23.19794
H17-0111	22.50	221.10	220.00	219.00	160.00	0.30	0.001	4.00	30.29718	-23.23795
H17-0112	11.02	14.60	8.00	8.00	8.00	0.90	0.001	0.60	30.27305	-23.24775
H17-0113	28.13	9.10	5.00	4.90	3.00	2.50	0.001	0.20	30.28851	-23.26472
H17-0117	22.70	56.10	97.00	99.30	54.00	0.40	0.001	3.50	30.29280	-23.28580
H17-0120	3.88	107.40	120.00	118.20	96.00	0.20	0.001	2.40	30.17283	-23.23313
H17-0140	22.65	59.50	20.00	19.10	19.00	3.00	0.001	2.20	30.21578	-23.12059
H17-0142	9.34	183.60	128.00	114.40	114.00	7.80	0.001	3.00	30.22561	-23.16657
H17-0146	15.70	106.50	108.00	113.20	37.00	7.40	0.001	2.50	30.36789	-23.14663
H17-0150	9.47	217.50	205.00	199.90	122.00	2.80	0.001	3.00	30.11230	-23.25190
H17-0152	17.71	12.80	7.00	6.60	7.00	1.80	0.001	0.80	30.05577	-23.22532
H17-0155	13.00	22.30	16.00	15.10	15.00	1.70	0.001	1.70	30.03805	-23.17582
H17-0156	16.60	82.40	60.00	52.00	52.00	4.10	0.001	4.00	30.05188	-23.15535
H17-0159	4.20	30.60	17.00	16.80	19.00	2.70	0.001	2.00	30.27498	-23.18669
H17-0163	8.56	75.30	42.00	42.90	24.00	4.80	0.001	1.40	30.06506	-23.56411
H17-0169	20.10	142.10	320.00	338.70	114.00	2.00	0.001	2.00	30.24498	-23.15728
H17-0171	13.60	133.70	160.00	164.40	90.00	2.50	0.001	1.80	30.24170	-23.15916
H17-0172	9.13	363.50	230.00	252.60	113.00	8.00	0.001	2.00	30.25713	-23.16410
H17-0174	16.76	225.70	100.00	89.80	79.00	9.40	0.001	2.10	30.27811	-23.16395
H17-0175	26.45	148.80	100.00	90.90	98.00	0.60	0.001	2.50	30.23803	-23.17114
H17-0177	1.19	194.00	109.00	107.40	102.00	15.00	0.001	1.30	30.21568	-23.18722
H17-0178	16.78	51.20	40.00	36.60	37.00	1.80	0.001	2.50	30.20632	-23.17252



H-No	swl (m)	T (m ² /d)				Re (step)	S (step)	Sust Q (l/s per 24h)	Long	Lat
		Logan	Theis	C-J	B-S					
H17-0179	4.35	92.60	80.00	89.40	34.00	5.00	0.001	2.50	30.17734	-23.18037
H17-0180	13.08	447.20	300.00	299.60	217.00	6.80	0.001	3.00	30.18324	-23.18561
H17-0184	24.35	7.50	5.00	4.30	4.00	2.10	0.001	0.30	30.22523	-23.15289
H17-0185	15.00	237.90	260.00	261.90	115.00	8.00	0.001	3.50	30.23593	-23.16145
H17-0186	8.72	8.70	4.00	4.50	3.00	1.80	0.001	0.30	30.28128	-23.16709
H17-0187	17.21	21.40	26.00	23.90	14.00	0.20	0.001	0.35	30.26670	-23.19559
H17-0189	13.32	1.90	1.00	0.90	1.00	1.00	0.001	0.14	30.25456	-23.19104
H17-0192	20.21	50.00	21.00	20.20	26.00	0.40	0.001	1.00	30.31281	-23.18576
H17-0193	9.82	60.10	25.00	25.90	38.00	5.30	0.001	1.40	30.31875	-23.19827
H17-0212	16.02	53.30	40.00	42.70	27.00	2.30	0.001	4.00	30.19223	-23.10373
H17-0218	6.27	6.70	4.00	3.70	4.00	0.30	0.001	0.50	30.18880	-23.11937
H17-0240	1.83	40.80	17.00	17.40	17.00	3.90	0.001	3.00	30.23857	-23.19985
H17-0243	17.43	5.10	3.00	2.90	3.00	4.00	0.001	0.35	30.28764	-23.21490
H17-0252	12.60	10.90	7.00	6.40	6.00	0.30	0.001	0.30	30.34205	-23.22686
H17-0253	13.60	4.80	3.00	2.70	2.00	1.90	0.001	0.20	30.34009	-23.22582
H17-0255	19.47	291.00	190.00	174.10	174.00	3.00	0.001	4.00	30.37735	-23.24753
H17-0258	28.47	129.90	130.00	115.80	114.00	2.00	0.001	0.80	30.36856	-23.24065
H17-0286	43.60	19.80	4.00	4.20	7.00	3.90	0.001	0.20	30.09441	-23.31201
H17-0299	7.38	8.90	4.00	4.40	5.00	0.20	0.001	0.30	30.02478	-23.32839
H17-0306	30.27	16.60	9.00	8.00	8.00	1.70	0.001	0.70	30.10115	-23.27678
H17-0310A	13.64	12.90	5.00	3.90	10.00	8.30	0.001	0.10	30.06611	-23.33506
H17-0320	4.90	19.10	10.00	10.70	10.00	1.50	0.001	0.30	30.00273	-23.29088
H17-0340	12.40	5.00	3.00	2.50	2.00	1.80	0.001	0.20	29.96904	-23.36803
H17-0353	22.80	47.30	34.00	28.50	25.00	3.60	0.001	0.60	29.94714	-23.36397
H17-0363	3.80	20.10	10.00	9.40	11.00	1.20	0.001	1.00	30.07463	-23.21565
H17-0364	21.00	0.70	1.00	0.20			0.001	0.03	30.28847	-23.16453
H17-0366	21.40	10.30	6.00	5.40	6.00	0.10	0.001	0.25	30.18733	-23.17637
H17-0383	21.67	4.80	3.00	2.70	3.00	1.00	0.001	0.30	30.03964	-23.14303
H17-0387	0.82	28.20	16.00	15.90	16.00	3.00	0.001	1.80	30.23343	-23.18248
H17-0393	16.59	40.50	25.00	24.70	22.00	2.60	0.001	1.00	30.05114	-23.15136
H17-0394	0.00	6.60	4.00	3.20	2.00	3.30	0.001	0.25	30.05583	-23.14292
H17-0401	19.30	72.80	38.00	35.60	35.00	22.90	0.001	0.80	30.10416	-23.28171
H17-0403	18.00	38.40	22.00	20.70	20.00	5.90	0.001	0.90	30.10777	-23.28555
H17-0407	16.31	4.10	1.00	0.90			0.001	0.10	30.05429	-23.23119
H17-0415	2.50	3.70	2.00	1.70	2.00	1.50	0.001	0.10	30.24439	-23.27319
H17-0435	11.96	2.70	1.00	1.20	1.00	2.90	0.001	0.20	29.97361	-23.36256
H17-0438	13.80	28.90	23.00	24.30	16.00	7.90	0.001	0.90	30.06844	-23.27584
H17-0440	3.57	8.90	6.00	5.30	5.00	0.60	0.001	0.40	30.12605	-23.31008
H17-0451	30.43	13.90	6.00	6.00	6.00	2.90	0.001	0.10	29.98588	-23.30128
H17-0497	27.23	29.40	20.00	19.20	16.00	3.20	0.001	1.00	29.98977	-23.35958
H17-0499	32.94	15.00	10.00	8.60	8.00	1.10	0.001	0.13	29.98906	-23.35982
H17-0534	40.63	24.80	12.00	10.80	11.00	1.90	0.001	0.30	30.05160	-23.21070
H17-0564	25.47	15.60	8.00	8.60	8.00	0.30	0.001	0.50	30.10613	-23.20611
H17-0695	24.02	172.90	109.00	100.30	100.00	3.00	0.001	1.60	30.17707	-23.10780
H17-0704	7.49	5.10	4.00	3.20	3.00	1.10	0.001	0.40	30.27862	-23.21037
H17-0732	0.01	2.80	2.00	1.40	2.00	0.30	0.001	0.40	30.30167	-23.17362
H17-0774	8.62	10.60	5.00	4.90	5.00	2.00	0.001	0.70	30.18903	-23.19694
H17-0775	23.42	5.80	3.00	2.20	2.00	1.70	0.001	0.12	30.27972	-23.18733
H17-0776	27.74	4.30	2.00	1.50			0.001	0.10	30.28058	-23.23639
H17-0777	17.50	32.80	17.00	15.90	17.00	2.30	0.001	0.60	30.09431	-23.19917
H17-0778	23.82	10.70	8.00	8.30	7.00	14.00	0.001	0.10	30.14000	-23.26189
H17-0779	16.86	10.90	11.00	10.40	10.00	0.20	0.001	0.20	30.33294	-23.20628
H17-0781	38.21	55.20	38.00	37.50	37.00	2.20	0.001	0.70	30.08917	-23.22778
H17-0786	13.95	4.70	3.00	2.80	2.00	5.20	0.001	0.15	30.16959	-23.27110
H20-0001	8.40	3.80			2.00	1.30	0.001	0.15	30.59095	-22.86046
H20-0004	17.40	27.70			14.00	5.00	0.001	0.35	30.61525	-22.86188
H20-0005	3.88	8.50			4.00	1.90	0.001	0.15	30.58536	-22.86226
H20-0009	4.42	6.30			3.00	1.00	0.001	0.20	30.55406	-22.85510
H20-0010	6.45	12.70			7.00	1.40	0.001	0.50	30.57648	-22.82238
H20-0014	11.03	29.60			14.00	1.40	0.001	0.40	30.55460	-22.83105
H20-0015	9.02	9.10			5.00	0.80	0.001	0.40	30.55074	-22.83082



H-No	swl (m)	T (m ² /d)				Re (step)	S (step)	Sust Q (l/s per 24h)	Long	Lat
		Logan	Theis	C-J	B-S					
H20-0016	10.35	2.40			1.00	2.10	0.001	0.15	30.57114	-22.83426
H20-0019	6.10	1.60			1.00	0.50	0.001	0.15	30.51114	-22.91117
H20-0020	1.35	8.20			5.00	0.50	0.001	0.30	30.61822	-22.85021
H20-0022	5.70	14.10			7.00	3.90	0.001	0.90	30.51216	-22.90810
H20-0023	6.47	48.60			26.00	1.00	0.001	0.60	30.33113	-22.89681
H20-0024	3.70	86.40			48.00	9.10	0.001	3.50	30.38778	-22.98120
H20-0027	17.62	42.00			29.00	4.20	0.001	0.70	30.53185	-22.89911
H20-0032	1.90	16.30			8.00	1.20	0.001	0.30	30.51756	-22.90419
H20-0037	39.40	17.00			12.00	1.10	0.001	1.00	30.39643	-23.16807
H20-0042	8.39	14.70			10.00	0.60	0.001	0.40	30.46558	-23.17928
H20-0043	9.15	25.10			12.00	1.90	0.001	0.40	30.42883	-23.14554
H20-0045	17.30	110.80			70.00	1.90	0.001	1.00	30.30541	-23.05997
H20-0046	12.15	18.30			6.00	3.90	0.001	0.60	30.30608	-23.05545
H20-0047	4.06	42.60			20.00	2.90	0.001	2.00	30.29839	-23.05079
H20-0048	16.41	9.00			3.00	2.40	0.001	0.20	30.34343	-23.05945
H20-0049	2.09	18.00			9.00	1.40	0.001	1.00	30.36925	-23.06267
H20-0050	8.75	54.10			20.00	3.00	0.001	2.00	30.52596	-22.90315
H20-0051	3.46	18.60			12.00	0.50	0.001	0.30	30.62970	-22.85470
H20-0052	9.12	16.00					0.001	1.00	30.69960	-22.81318
H20-0053	6.82	38.70			13.30	37.00	0.001	0.80	30.70287	-22.80972
H20-0056	7.89						0.001	1.20	30.71797	-22.81442
H20-0057	9.77	26.40			18.00	0.80	0.001	1.20	30.72409	-22.81069
H20-0058	3.20	15.40			9.00	2.00	0.001	0.70	30.71480	-22.79489
H20-0059	4.91	13.10			15.00	3.00	0.001	0.30	30.72549	-22.79567
H20-0063	4.31	8.50			5.00	0.80	0.001	0.17	30.83533	-22.77665
H20-0064	3.35	7.40			3.00	5.00	0.001	0.90	30.85297	-22.76099
H20-0066	6.60	7.50			4.00	1.70	0.001	0.70	30.54723	-22.80759
H20-0073	6.65	56.00			35.00	6.70	0.001	4.00	30.53736	-22.87512
H20-0081	11.07	4.60			2.00	0.10	0.001	0.06	30.46765	-22.85125
H20-0085	53.60	18.60			11.00	0.10	0.001	0.30	30.43622	-22.83131
H20-0086	32.10	7.90			4.00	0.70	0.001	0.40	30.41194	-22.85722
H20-0087	6.40	38.20			21.00	2.10	0.001	2.00	30.48376	-22.84400
H20-0089	3.53	99.00			65.00	5.00	0.001	2.00	30.61463	-22.81158
H20-0093	9.45	21.00			14.00	1.40	0.001	0.60	30.65536	-22.84757
H20-0097	16.04	225.40			115.00	3.00	0.001	1.50	30.65432	-22.86678
H20-0101	4.65	24.60			12.00	1.50	0.001	0.50	30.62830	-22.87698
H20-0105	9.02	19.90			13.00	1.50	0.001	1.50	30.54561	-22.90783
H20-0108	16.77	47.50			29.00	1.80	0.001	0.50	30.55620	-22.90662
H20-0112	11.40	21.80			14.00	2.60	0.001	1.00	30.55456	-22.92558
H20-0116	4.96	21.00			12.00	2.70	0.001	1.00	30.56846	-22.93353
H20-0118	4.44	11.50			7.00	1.70	0.001	0.40	30.58566	-22.89389
H20-0119	5.69	3.50			4.00	0.30	0.001	0.35	30.59746	-22.88758
H20-0121	9.17	6.10			4.00	0.80	0.001	0.10	30.60326	-22.88355
H20-0125	25.13	27.20			16.00	1.70	0.001	0.40	30.68913	-22.86715
H20-0126	14.20	0.60			1.00	1.10	0.001	0.05	30.69556	-22.85892
H20-0131	11.69	46.70			30.00	0.30	0.001	0.50	30.66317	-22.89397
H20-0135	2.45	68.40			52.00	1.30	0.001	1.10	30.64021	-22.91166
H20-0136	14.02	108.20			55.00	0.20	0.001	0.90	30.63376	-22.90318
H20-0139	6.42	33.20			21.00	3.00	0.001	1.40	30.61509	-22.91629
H20-0141	12.76	51.20			24.00	11.10	0.001	0.35	30.92532	-22.60439
H20-0144	8.36	11.80			6.00	1.20	0.001	0.50	30.60969	-22.93980
H20-0146	15.08	12.30			7.00	0.50	0.001	0.70	30.61628	-22.94704
H20-0147	7.43	7.50			4.00	1.30	0.001	0.40	30.62271	-22.93447
H20-0151	7.01	11.10			5.00	3.00	0.001	0.20	30.65416	-22.91004
H20-0155	8.40	51.60			29.00	2.00	0.001	5.00	30.59120	-22.95080
H20-0160	8.44	15.50			8.00	1.10	0.001	0.40	30.60091	-22.96344
H20-0163	15.30	3.30			2.00	0.80	0.001	0.20	30.58929	-22.96123
H20-0167	3.12	18.70			10.00	2.10	0.001	1.00	30.57117	-22.97291
H20-0173	11.44	18.30			9.00	2.50	0.001	0.50	30.95653	-22.55304
H20-0175	3.94	18.20			10.00	4.00	0.001	1.00	30.52773	-22.97151
H20-0182	4.38	14.40			8.00	1.30	0.001	0.70	30.50450	-23.03807



H-No	swl (m)	T (m ² /d)				Re (step)	S (step)	Sust Q (l/s per 24h)	Long	Lat
		Logan	Theis	C-J	B-S					
H20-0189	6.01	37.20			27.00	0.80	0.001	0.40	30.51497	-22.96295
H20-0196	7.10	4.10			2.00	0.40	0.001	0.17	30.46237	-23.10399
H20-0198	20.24	5.30			3.00	6.00	0.001	0.50	30.47227	-23.06051
H20-0210	10.30	35.30			20.00	3.00	0.001	1.50	30.34060	-23.04708
H20-0212	7.50	12.80			6.00	3.10	0.001	0.17	30.46686	-23.14846
H20-0215	5.26	2.10			1.00	1.10	0.001	0.08	30.47746	-23.15761
H20-0216	13.77	4.80			2.00	3.00	0.001	0.20	30.48216	-23.18061
H20-0220	12.40	0.60			1.00	1.30	0.001	0.05	30.52297	-23.17894
H20-0222	21.10	3.70			2.00	1.10	0.001	0.20	30.51968	-23.22533
H20-0225	13.56	3.30			2.00	0.50	0.001	0.13	30.50975	-23.22925
H20-0231	14.80	66.50			30.00	6.00	0.001	1.30	30.47328	-23.21098
H20-0232	16.00	8.30			4.00	1.30	0.001	0.30	30.46425	-23.21888
H20-0234	35.95	186.40			117.00	2.00	0.001	1.60	30.45964	-23.20906
H20-0285	10.60	2.40			1.00	2.30	0.001	0.12	30.77573	-22.79651
H20-0286	3.72	8.00			5.00	0.10	0.001	0.30	30.79636	-22.78781
H20-0290	9.60	6.80			4.00	0.20	0.001	0.30	30.78355	-22.76417
H20-0293	11.87	0.90			1.00	0.70	0.001	0.10	30.74349	-22.82328
H20-0299	18.57	27.00			15.00	0.30	0.001	1.30	30.76962	-22.81718
H20-0300	10.43	2.90					0.001	0.07	30.81794	-22.78039
H20-0302	14.86	3.50			1.00	0.90	0.001	0.14	30.88504	-22.76252
H20-0303	8.94	2.40			1.00	1.40	0.001	0.20	30.87508	-22.75704
H20-0305	3.77	4.90			3.00	0.10	0.001	0.20	30.88501	-22.72636
H20-0306	3.40	4.20			2.00	0.80	0.001	0.20	30.87240	-22.71756
H20-0311	5.40	6.60			3.00	0.20	0.001	0.40	30.84352	-22.70773
H20-0315	7.20	4.40			2.00	1.80	0.001	0.08	30.83242	-22.72531
H20-0321	10.13	3.20			2.00	0.50	0.001	0.30	30.84822	-22.72098
H20-0324	21.54	8.40			4.00	3.00	0.001	0.20	30.57414	-22.85607
H20-0325	13.30	1.50			1.00	2.40	0.001	0.05	30.57494	-22.85829
H20-0326	5.69	52.60			36.00	11.90	0.001	3.00	30.92622	-22.59137
H20-0337	4.45	8.00			6.00	0.30	0.001	0.70	30.90540	-22.59564
H20-0339	7.34	123.70			84.00	3.00	0.001	2.50	30.40296	-23.08797
H20-0412	15.45	26.80			19.00	2.90	0.001	1.00	30.86516	-22.53725
H20-0431	5.09	2.90			2.00	0.70	0.001	2.00	30.50110	-22.80501
H20-0472	1.37	89.70			42.00	1.00	0.001	0.50	30.90670	-22.59489
H20-0474	0.00	45.70			30.00	1.30	0.001	1.80	30.90872	-22.59466
H20-0481	17.41	11.80			7.00	1.10	0.001	0.40	30.82684	-22.65177
H20-0482	9.16	3.80			2.00	1.70	0.001	0.15	30.81113	-22.62674
H20-0486	2.49	115.90			54.00	0.90	0.001	0.80	30.90545	-22.59561
H20-0520	12.13	24.00			11.00	0.60	0.001	0.60	30.40222	-22.97109
H20-0521	7.30	3.60			2.00	1.40	0.001	0.30	30.48903	-22.83158
H20-0522	6.47	8.20			5.00	0.30	0.001	0.08	30.47726	-22.82759
H20-0530	15.00	10.40			6.00	0.80	0.001	0.20	30.43694	-22.91361
H20-0539	10.91	65.50			37.00	2.10	0.001	1.10	30.43389	-22.80464
H20-0540	18.15	19.20			10.00	1.60	0.001	0.60	30.49561	-22.93241
H20-0541	5.30	13.80			8.00	3.00	0.001	0.60	30.48279	-22.79962
H20-0542	0.29	2.70			2.00	0.50	0.001	0.15	30.61199	-22.84386
H20-0544	9.17	19.90			12.00	0.40	0.001	0.90	30.35025	-23.05862
H20-0548	0.55	34.00			28.00	0.30	0.001	1.00	30.64044	-22.84446
H20-0582	19.80	8.60			5.00	2.30	0.001	0.60	30.52004	-22.79838
H20-0590	20.74	38.80			25.00	0.40	0.001	0.70	30.38278	-23.09527
H20-0592	17.75	36.20			13.00	5.00	0.001	1.00	30.38389	-23.12392
H20-0594	9.69	5.10			3.00	3.00	0.001	0.30	30.44157	-23.13237
H20-0595	6.57	66.00			32.00	0.80	0.001	0.70	30.44881	-23.21798
H20-0596	8.70	13.90			7.00	3.00	0.001	0.30	30.43587	-23.23989
H20-0600	11.79	0.80			1.00	0.40	0.001	0.04	30.42115	-23.22955
H20-0611	2.37	99.70			36.00	3.00	0.001	3.00	30.35920	-23.46960
H20-0617	2.79	16.90			13.00	10.00	0.001	1.30	30.36701	-22.99967
H20-0622	4.94	15.60			11.00	2.60	0.001	0.60	30.65276	-22.88112
H20-0623	1.57	101.80			55.00	6.80	0.001	2.00	30.66745	-22.87517
H20-0624	34.93	9.90			5.00	6.10	0.001	0.25	30.33341	-23.00938
H20-0733	4.75	54.60			44.00	0.80	0.001	0.30	30.65759	-22.73691



H-No	swl (m)	T (m ² /d)				Re (step)	S (step)	Sust Q (l/s per 24h)	Long	Lat
		Logan	Theis	C-J	B-S					
H20-0734	4.14	7.20			5.00	0.40	0.001	0.40	30.61722	-22.85028
H20-0735	3.31	13.50			9.00	0.70	0.001	0.60	30.62966	-22.85469
H20-0737	6.30	257.50			174.00	9.00	0.001	5.00	30.43980	-23.19470
H20-0738	6.99	53.90			52.00	0.20	0.001	2.60	30.40295	-23.08803
H20-0792	6.57	5.10			3.00	1.10	0.001	0.12	30.71323	-22.81246
H20-0827	20.16	14.70			11.00	1.90	0.001	0.60	30.70313	-22.80963
H20-0868	33.20	10.50			5.00	0.50	0.001	0.15	30.42944	-22.90167
H20-0932	11.29				7.00	3.40	0.001	0.30	30.55861	-22.98993
H20-0957	26.80	1.40					0.001	0.02	30.34011	-22.99128
H20-0962	26.00	2.40			1.00	0.40	0.001	0.25	30.63632	-22.74795
H20-1037	2.30	1.70			1.00	5.10	0.001	0.25	30.64908	-22.73218
H20-1041	5.71	3.60			2.00	0.10	0.001	0.10	30.39804	-22.99772
H20-1100	8.40	2.30			1.00	4.90	0.001	0.20	30.84390	-22.73272
H20-1113	10.14	2.00			1.00	2.20	0.001	0.07	30.72911	-22.71897
H20-1116	12.80	8.10			4.00	0.50	0.001	0.20	30.70267	-22.71461
H20-1132	14.50	1.60					0.001	0.05	30.84743	-22.66212
H20-1133	18.60	22.10			11.00	2.00	0.001	1.70	30.84612	-22.66322
H20-1136	16.93	58.10			23.00	3.00	0.001	2.00	30.81607	-22.66492
H20-1144	0.32	2.40			1.00	3.40	0.001	0.30	30.75772	-22.66345
H20-1170	21.40	3.20			2.00	0.20	0.001	0.12	30.86549	-22.60240
H20-1176	21.41	7.10			3.00	1.00	0.001	0.20	30.84016	-22.64064
H20-1182	15.96	12.00			5.00	2.30	0.001	0.20	30.78104	-22.63645
H20-1196	6.08	48.10			30.00	8.00	0.001	2.00	30.90078	-22.59514
H20-1204	10.99	20.60			10.00	1.20	0.001	0.20	30.87284	-22.48667
H20-1206	8.75	2.00			1.00	2.30	0.001	0.13	31.03153	-22.42003
H20-1212	5.40	5.80			3.00	0.70	0.001	0.20	30.89746	-22.47941
H20-1450	24.75	34.40			14.00	4.00	0.001	2.00	30.78689	-22.69580
H22-0152	29.70	36.30			29.00	0.30	0.001	2.00	30.67997	-22.46745

Table B-2: Constant discharge data for high T scenario: borehole H04-0306

	<i>Constant Discharge</i>	<i>Recovery Test</i>
<i>Time, t (s)</i>	<i>Drawdown, s (m)</i>	<i>Drawdown, s (m)</i>
1	2.13	2.53
2	2.46	2.01
3	2.62	1.81
5	3.01	1.59
7	3.29	1.49
10	3.58	1.39
15	4.21	1.33
20	4.39	1.3
30	4.51	1.23
40	4.6	1.19
60	4.7	1.14
90	4.83	1.06
120	4.93	1.02
150	4.99	0.98
180	5.03	0.94
210	5.05	0.93
240	5.05	0.9
300	5.06	0.85
360	5.06	0.82
420	5.06	0.78
480	5.06	0.75
540	5.06	0.72
600	5.06	0.7
660	5.07	0.68
720	5.08	0.65
780	5.1	0.65
840	5.12	0.63
900	5.15	0.62
960	5.16	0.61
1020	5.16	0.59
1080	5.17	0.57
1140	5.17	0.56
1200	5.17	0.54
1250	5.17	0.53
1320	5.18	0.52
1380	5.18	0.51
1440	5.18	0.5

Table B-3: Constant discharge data for intermediate T scenario: borehole H10-0084

<i>Time, t (s)</i>	<i>Constant Discharge</i>	<i>Recovery Test</i>
	<i>Drawdown, s (m)</i>	<i>Drawdown, s (m)</i>
1	1.26	3.16
2	1.58	2.3
3	1.99	2.25
5	2.16	2.24
7	2.41	2.23
10	2.73	2.22
15	2.97	2.2
20	3.34	2.19
30	3.65	2.18
40	3.86	2.16
60	4.13	2.12
90	4.3	2.09
120	4.51	2.06
150	4.69	2.04
180	4.87	2.03
210	5.09	2.02
240	5.16	2
300	5.22	1.99
360	5.31	1.96
420	5.64	1.94
480	5.92	1.87
540	6.04	1.85
600	6.14	1.83
720	6.2	1.78
840	6.4	1.75
960	6.88	1.73
1080	7.01	1.71
1200	7.13	1.69
1320	7.21	1.67
1440	7.46	1.65

Table B-4: Constant discharge data for low T scenario: borehole H07-0841

	<i>Constant Discharge</i>	<i>Recovery Test</i>
<i>Time, t (s)</i>	<i>Drawdown, s (m)</i>	<i>Drawdown, s (m)</i>
1	2.89	28.16
2	3.47	25.44
3	4.01	22.56
5	4.8	15.91
7	5.61	10.44
10	7.01	7.44
15	7.89	4.3
20	8.24	2.8
30	8.47	1.64
40	8.61	1.36
60	8.86	1.16
90	8.86	1.09
120	9.51	1.01
150	9.95	0.95
180	10.01	0.89
210	10.18	0.84
240	10.26	0.81
300	10.83	0.74
360	11.81	0.68
420	12.6	0.62
480	13.76	0.57
540	14.23	0.48
600	14.82	0.42
720	15.09	0.36
840	16.42	0.33
960	19.69	0.29
1080	24.6	0.26
1200	26.63	0.22
1320	31.75	0.17
1440	32.13	0.12

Table B-5: Step-drawdown data for high T scenario: borehole H04-0306

<i>Time, t (s)</i>	<i>Drawdown, s (m)</i>	<i>Abstraction rate, Q (l/s)</i>	<i>Time, t (s)</i>	<i>Drawdown, s (m)</i>	<i>Abstraction rate, Q (l/s)</i>
1	0.71	5	201	3.46	16
2	0.82	5	202	3.7	16
3	0.87	5	203	4.06	16
5	1.08	5	205	4.16	16
7	1.18	5	207	4.23	16
10	1.21	5	210	4.3	16
15	1.25	5	215	4.36	16
20	1.26	5	220	4.37	16
30	1.28	5	230	4.41	16
40	1.31	5	240	4.46	16
50	1.33	5	250	4.5	16
60	1.33	5	260	4.56	16
70	1.34	5	270	4.6	16
80	1.35	5	280	4.63	16
90	1.36	5	290	4.63	16
100	1.37	5	300	4.63	16
101	1.65	10	301	5.37	20
102	1.71	10	302	5.59	20
103	1.9	10	303	5.68	20
105	2.04	10	305	5.7	20
107	2.25	10	307	5.7	20
110	2.36	10	310	5.71	20
115	2.43	10	315	5.71	20
120	2.489	10	320	5.73	20
130	2.5	10	330	5.73	20
140	2.53	10	340	5.73	20
150	2.56	10	350	5.74	20
160	2.56	10	360	5.74	20
170	2.56	10	370	5.74	20
180	2.57	10	380	5.74	20
190	2.58	10	390	5.74	20
200	2.59	10	400	5.74	20

Table B-6: Step-drawdown data for intermediate T scenario: borehole H10-0084

<i>Time, t (s)</i>	<i>Drawdown, s (m)</i>	<i>Abstraction rate, Q (l/s)</i>	<i>Time, t (s)</i>	<i>Drawdown, s (m)</i>	<i>Abstraction rate, Q (l/s)</i>
1	0.8	0.84	75	3.96	1.64
2	1.1	0.84	80	4.04	1.64
3	1.34	0.84	90	4.67	1.64
5	1.67	0.84	100	4.72	1.64
7	1.77	0.84	110	4.89	1.64
10	1.86	0.84	120	5.12	1.64
15	1.9	0.84	121	7.11	2.61
20	2.12	0.84	122	8.14	2.61
30	2.15	0.84	123	9.77	3.44
40	2.2	0.84	125	10.13	3.44
50	2.25	0.84	127	10.96	3.78
60	2.29	0.84	130	11.16	3.86
61	2.6	0.84	135	11.76	3.86
62	2.9	1.64	140	11.94	3.85
63	3.14	1.64	150	12.13	3.85
65	3.68	1.64	160	12.4	3.84
67	3.71	1.64	170	12.66	3.86
70	3.8	1.64	180	12.87	3.81

Table B-7: Step-drawdown data for low T scenario: borehole H17-0841

<i>Time, t (s)</i>	<i>Drawdown, s (m)</i>	<i>Abstraction rate, Q (l/s)</i>	<i>Time, t (s)</i>	<i>Drawdown, s (m)</i>	<i>Abstraction rate, Q (l/s)</i>
1	0.95	0.3	75	4.75	0.65
2	1.42	0.3	80	4.95	0.65
3	1.8	0.3	90	5.1	0.65
5	2.03	0.3	100	5.2	0.65
7	2.2	0.3	110	5.25	0.65
10	2	0.3	120	5.3	0.65
15	2.06	0.3	121	5.85	0.65
20	2.1	0.3	122	6.3	0.65
30	2.2	0.3	123	6.55	1.03
40	2.28	0.3	125	7.3	1.03
50	2.29	0.3	127	7.72	1.03
60	2.32	0.3	130	8.18	1.03
61	2.69	0.65	135	8.63	1.03
62	3.3	0.65	140	8.85	1.03
63	3.55	0.65	150	8.86	1.03
65	4.06	0.65	160	8.92	1.03
64	4.66	0.65	170	9.1	1.03
70	4.66	0.65	180	9.24	1.03